ABSTRACT

Title of Thesis: **INVESTIGATION INTO THE SYSTEM DYNAMICS OF A WETLAND SOIL TECHNOECOSYSTEM USING REDOX POTENTIAL AS A METABOLIC INDICATOR AND FEEDBACK CONTROL PARAMETER**

David Michael Blersch
Master of Science, 2004

Thesis Directed By: **Dr. Patrick Kangas**
Department of Biological Resources Engineering

The engineering of technoecosystems (technological-ecological hybrids) was investigated, focusing specifically on novel behavior exhibited by an ecosystem when given control over its own energy sources via artificial feedback control circuits. A technoecosystem was constructed based upon wetland soil microcosms using redox potential as an indicator of system metabolism and as the controlled parameter. Two types of experiments were performed to elucidate system dynamics. Results of the carbon addition experiments exhibited an increase in the rate of decline of redox potential over time as a result of the feedback control system, indicating increased metabolism in the microcosms. Results of the carbon/nitrate selection experiments showed oscillatory redox potential over time, trending towards regulation of redox potential within a set range. Simple computational models of ecological limiting factors are developed to explain the results. A classification system for technoecosystems is proposed, and implications into technoecosystem intelligence and energetic autonomy are discussed.

INVESTIGATION INTO THE SYSTEM DYNAMICS OF A WETLAND SOIL TECHNOECOSYSTEM USING REDOX POTENTIAL AS A METABOLIC INDICATOR AND FEEDBACK CONTROL PARAMETER

By

David Michael Blersch

Thesis submitted to the Faculty of the Graduate School of the
University of Maryland, College Park, in partial fulfillment
of the requirements for the degree of
Master of Science
2004

Advisory Committee:
Associate Professor Patrick Kangas, Chair
Assistant Professor Paul D. Schreuders
Professor Fredrick W. Wheaton

Dedication

To Dan.

Acknowledgements

I would like to thank those who were instrumental in helping me to complete this work. Special appreciation and heartfelt thanks go to my advisor, Patrick Kangas, whose vision and encouragement inspired this work. I would also like to thank my committee members, Fred Wheaton and Paul Schreuders, for their interest, support, and ideas that helped to make this research document possible. I issue many thanks to my friends and colleagues of the Biological Resources Engineering Department at the University of Maryland, from whom I've derived tremendous support through common trials. Thanks also go to Gary Seibel in the shop for his assistance with some of the controls design.

Even more thanks go to my family, both immediate and extended, and friends, all of who have extended to me tremendous patience, understanding, and love through this time to prepare this document.

Most of all, I owe endless gratitude to my wife, Stacey, whose encouragement, help, patience, and love all these years made this work possible.

TABLE OF CONTENTS

Dedication ii

Acknowledgements iii

LIST OF TABLES xi

LIST OF FIGURES xiv

LIST OF SYMBOLS xxi

1.0 INTRODUCTION 1

1.1 Technoecosystems 2

1.2 Motivation for Study 5

1.3 Problem Statement 7

2.0 OBJECTIVES AND STUDY APPROACH 9

2.1 Objectives 9

2.2 Study Approach 9

3.0 REVIEW OF LITERATURE 11

3.1 Technoecosystem Research 11

3.2 Feedback Control Systems 14

3.3 Energy Sources for Wetland Soil Technoecosystem 17

3.4 Redox Potential in Wetland Soils 18

3.5 Examples of Redox Potential as a Control Parameter 23

4.0 EQUIPMENT 25

4.1 System Overview 25

4.2 Data Acquisition System 27

4.2.1 Computer Hardware 27

4.2.2 Computer Software 28
4.2.3 Redox Electrodes 32
4.2.4 Calomel Reference Probe 32
4.2.5 Salt Bridge 33
4.3 Nutrient Delivery System 34
4.3.1 Pumps 34
4.3.2 Pump Control Relays 35
4.4 Wetland Soil Microcosms 36
4.4.1 Soil and Site Description 36
4.4.2 Microcosm Construction 38
5.0 PROCEDURES 40
5.1 Experimental Design 40
5.1.1 Carbon addition experiments 41
5.1.2 Carbon/Nitrate addition experiments 41
5.2 General Procedures 42
5.3 Specific Procedures According to Experiment Type 45
5.3.1 Carbon Addition Experiments 45
5.3.2 Carbon/Nitrate Selection Experiments 48
6.0 RESULTS 52
6.1 Carbon Addition Experiments 52
6.1.1 Trial 1: Methanol Addition to Wetland Soil Microcosm 52
6.1.2 Trial 5: Repeat of Trial 1. 53
6.1.3 Trial 6: Repeat of Trial 1. 55

6.1.4 Trial 7: Carbon Addition to USDA soil with two different thresholds..... 57
6.1.5 Trial 8: Repeat of Trial 7. 59
6.1.6 Trial 9: Repeat of Trial 7. 61
6.1.7 Trial 10: Experiment with different carbon sources. 63
6.1.8 Trial 11: Experiment with different carbon sources (repeat of Trial 10).. 65
6.1.9 Trial 12: Modified repeat of Trial 10. 67
6.1.10 Trial 19: Modified repeat of Trial 10. 69
6.1.11 Trial 30: Test the effect of dissolved oxygen in carbon solution additions. 71
6.1.12 Carbons Summary Analysis..... 73
6.1.12.1 Qualitative Analyses 73
6.1.12.2 Analyses of Changes in Redox 78
6.1.12.3 Analysis of Redox Values..... 79
6.1.12.4 Analysis of Redox Slopes 87
6.2 Carbon/Nitrate Selection Experiments 96
6.2.1 Trial 13: Carbon/Nitrate Selection..... 96
6.2.2 Trial 14: Carbon/Nitrate Selection with more narrow threshold range 98
6.2.3 Trial 15: Repeat of Trial 14. 100
6.2.4 Trial 16: Carbon/Nitrate Selection with narrow threshold range and more concentrated nutrient reservoirs (modified repeat of Trial 14). 103
6.2.5 Trial 20: Carbon/Nitrate Selection with narrow threshold range (repeat of Trial 14). 105

6.2.6 Trial 21: Carbon/Nitrate Selection with more narrow threshold range and slower nutrient delivery rate (modified repeat of Trial 14). 106
6.2.7 Trial 22: Carbon/Nitrate Selection with more narrow threshold range and normal nutrient delivery rate (modified repeat of Trial 15)..... 109
6.2.8 Trial 25: Carbon/Nitrate Selection with identical upper/lower thresholds (modified repeat of Trial 15)..... 111
6.2.9 Trial 26: Carbon/Nitrate Selection with identical upper/lower thresholds (repeat of Trial 25 with de-oxygenated reservoirs)..... 113
6.2.10 Trial 27: Carbon/Nitrate Selection with identical upper/lower thresholds and de-oxygenated reservoirs (repeat of Trial 26). 118
6.2.11 Trial 28: Carbon/Nitrate Selection with identical upper/lower thresholds and de-oxygenated reservoirs (repeat of Trial 26). 122
6.2.12 Trial 29: Carbon/Nitrate Selection with identical upper/lower thresholds (repeat of Trial 25). 125
6.2.13 Trial 31: Test the effect of dissolved oxygen in nitrate solution additions. 128
6.2.14 Carbon/Nitrate Summary 130
6.2.14.1 Qualitative Analyses 130
6.2.14.2 Analysis of Redox Values 135
7.0 DISCUSSION 137
7.1 Experiment Controls 137
7.2 Carbon Addition Experiments 138
7.2.1 Effect of Feedback Mechanism 138

7.2.2 Proposed Statistical Modeling 141
7.3 Carbon/Nitrate Selection Experiments 146
7.3.1 Effect of Feedback Mechanisms 146
7.4 Conceptual Models of Limiting Factors 149
7.4.1 Minimodel 1: Simple microbial degradation microcosm with one limiting reservoir. 151
7.4.2 Minimodel 2: Microbial degradation microcosm with two limiting reservoirs. 154
7.4.3 Minimodel 3: Microbial degradation microcosm with two limiting reservoirs and artificial feedback control of organic matter availability. 158
7.4.4 Minimodel 4: Microbial degradation microcosm with two limiting reservoirs and artificial feedback control of the availability of both organic matter and the electron acceptor 164
7.4.5 Summary 180
8.0 CONCLUSIONS 183
9.0 IMPLICATIONS 185
9.1 Role of Redox Potential as a Control Parameter 185
9.2 Role of Artificial Feedback in the Technoecosystem 187
9.3 Proposed classification system for Technoecosystems 189
9.3.1 Ecological Prosthetics 189
9.3.2 “True” Technoecosystems 190
9.3.2.1 Physical coupling 191
9.3.2.2 Virtual coupling 193

9.3.3 Intelligent Technoecosystems 195
9.3.4 Summary 199
9.4 Research in Analogous Systems 200
10.0 RECOMMENDATIONS 202
APPENDIX A. DATA ACQUISITION SYSTEM AND PROGRAM 203
A.1 Data Acquisition Hardware 203
A.2 Data Acquisition Software 204
A.2.1 Front Panel 204
A.2.2 Wiring Diagram Program 207
APPENDIX B. STELLA SIMULATION MINIMODELS 210
B.1 Minimodel 1: Microbial Degradation with one limiting reservoir 211
B.2 Minimodel 2: Microbial Degradation with two limiting reservoirs 212
B.3 Minimodel 3: Microbial Degradation with control over organic inputs 214
B.4 Minimodel 4: Microbial Degradation over all limiting inputs 216
B.5 User Control Panel 218
APPENDIX C. DERIVATION AND TESTING OF EQUATION FOR PROPOSED STATISTICAL MODEL 220
C.1 Derivation of General Equation Form 220
C.2 Derivation of the Specific Equation Form 222
C.3 Preliminary regression analysis 224
C.4 Subjective Optimization results 226
APPENDIX D. EXPERIMENTAL PROTOCOLS 230
D.1 Redox Probe Calibration 230

D.1.1 Probe Cleaning 230
D.1.2 Calibration Solution Composition 230
D.1.3 Calibration 231
D.2 Nutrient Reservoir Mixing 232
D.2.1 Carbon Solution 232
D.2.2 Nitrate Solution 232
D.3 Salt Bridge Construction 233
D.3.1 KCl Reservoir Mixing 233
D.3.2 Salt Bridge Manufacture 233
REFERENCES 234

LIST OF TABLES

Table 1. 1. Definitions of ecological/technological hybrids found in the literature. 3

Table 1. 2. Common and not-so-common examples of technoecosystems. 4

Table 3. 1. Range of redox potentials required to reduce oxidized forms of the various redox couples in soil and wetland environments. 22

Table 4. 1. Physical and chemical parameters of the USDA ARS forest wetland soil, sampled for analysis in July 2001. Analysis performed by the Cornell University Nutrient Analysis Laboratory..... 38

Table 5. 1. Trial configurations for carbon addition experiments. 46

Table 5. 2. Trial configurations for carbon/nitrate selection experiments. 49

Table 6. 1. Results for methanol addition experimental units. 74

Table 6. 2. Results for control units that accompanied the methanol experiment trials. .. 75

Table 6. 3. Results for acetate addition experimental units. 76

Table 6. 4. Results for control units that accompanied the acetate experiment trials. 76

Table 6. 5. Results for carbon addition experimental units using either synthetic sewage or tryptic soy. 77

Table 6. 6. Results for control units that accompanied the experiment trials receiving various carbon inputs. 77

Table 6. 7. Mean and standard deviation of the initial and total changes in redox potential for each of the groups of experimental carbon addition trials and for all the controls. 79

Table 6. 8. Results of statistical t-test comparing means of the various treatment groups to the mean of the controls group. A "-" indicates no statistical difference between the means, whereas a "@" indicates that the mean of the treatment group is less than the mean of the control group at the respective level of significance. 79

Table 6. 9. Results of t-test comparing the means of the value of redox potential of each treatment group to the controls group at each time step at two different significance levels. A "-" indicates no statistical difference between the groups, and a "@" indicates a statistical difference does exist. Blank spaces indicate time steps for which no data were present. 86

Table 6. 10. Results of t-test comparing the means of the slopes of redox potential of each treatment group to the controls group at each time step at two different significance levels. A "-" indicates no statistical difference between the groups, and a "@" indicates a statistical difference does exist. Blank spaces indicate time steps for which no data were present. 94

Table 6. 11. Nutrient concentrations in the water column of the soil microcosms at various times before and after nutrient additions. Note that the nutrient addition pump was turned off after hour 40. 117

Table 6. 12. Total nitrate and ammonia nitrogen present in the experiment microcosm for Trial 26 at various times before and after nutrient addition, expressed as total moles N. 117

Table 6. 13. Nutrient concentrations in the water column of the soil microcosms of Trial 27 at various times before and after nutrient additions. Note that the nutrient addition pump was turned off after hour 69. 121

Table 6. 14. Total nitrate and ammonia nitrogen present in the experiment microcosm for Trial 27 at various times before and after nutrient addition, expressed as total moles N. 121

Table 6. 15. Nutrient concentrations in the water column of the soil microcosms of Trial 29 at the beginning and end of the trial. 127

Table 6. 16. Total nitrate and ammonia nitrogen present in the experiment microcosm for Trial 29 at various times before and after nutrient addition, expressed as total moles N. 127

Table 6. 17. Results for control units that accompanied the carbon/nitrate experiment trials. 131

Table 6. 18. Results for carbon/nitrate selection experiments. 132

Table 6. 19. Statistics of variation of results for carbon/nitrate addition experiments. .. 134

Table 7. 1. Parameters and their values used in the STELLA simulation of a simple microbial degradation microcosm with an initial organic matter stock. 153

Table 7. 2. Parameters and their values used in the STELLA simulation of a microbial degradation microcosm with an initial organic matter stock and an initial electron acceptor stock controlling the availability of the organic matter to the consumer population. 157

Table 7. 3. Parameters and their values used in the STELLA simulation of a microbial degradation microcosm with an initial organic matter stock, an initial electron acceptor stock, and a control feedback loop controlling the input of organic matter from outside the system based upon the sensed value of N. 161

Table 7. 4. Parameters and their values used in the STELLA simulation of a microbial degradation microcosm with an initial organic matter stock, an initial electron acceptor stock, and a control feedback loop controlling the input *of* both organic matter and electron acceptor from outside the system based upon the sensed value of N. 168

Table 9. 1. Parameters of computational abilities according to categories of complexity (from Clark, et al., 1999). 196

Table 9. 2. Parameters of computational ability and intelligence evaluated for the wetland soil technoecosystems. 197

Table 9. 3. Summary of technoecosystem classes and their descriptive qualities. 200

LIST OF FIGURES

Figure 3. 1. General block diagram for an automatic control system (from Calow, 1976). 16

Figure 4. 1. Schematic diagram of the system setup for carbon delivery experiments. ... 25

Figure 4. 2. Schematic diagram of the system setup for carbon/nitrate selection experiments. 26

Figure 4. 3. Photograph of microcosm experiment setup, here shown for nitrate/carbon addition scenario. 26

Figure 4. 4. Flow chart for redox potential control program for carbon addition..... 30

Figure 4. 5. Flow chart for redox potential control program with nitrate/carbon source selection. 31

Figure 4. 6. Wiring schematic for relay-controlled power outlet for nutrient pumps..... 35

Figure 4. 7. View of the soil collection site in the USDA's ARS forested wetland in Beltsville, Maryland. 37

Figure 4. 8. Picture of standard wetland soil suspension microcosm in a 1-L jar. 39

Figure 6. 1. Results for Trial 1. Redox potential vs. time for soil microcosm with methanol solution added by controlling computer. 53

Figure 6. 2. Results for Trial 5: Redox potential vs. time for soil microcosms with pure methanol solution added by controlling computer (repeat of Trial 1). 55

Figure 6. 3. Results for Trial 6. Redox potential vs. time for soil microcosms with pure methanol solution added by controlling computer (repeat of Trial 1). 57

Figure 6. 4. Results for Trial 7: Redox potential vs. time for soil microcosms, each with a different threshold, with pure methanol solution added by controlling computer.... 59

Figure 6. 5. Results forTrial 8: Redox potential vs. time for USDA soil microcosms, each with a different threshold, with pure methanol solution added by controlling computer. 61

Figure 6. 6. Results for Trial 9: Redox potential vs. time for soil microcosms, each with a different threshold, with pure methanol solution added by controlling computer (repeat of Trial 7). 63

Figure 6. 7. Results for Trial 10: Redox potential vs. time for soil microcosms, each with different carbon sources than used previously. 65

Figure 6. 8. Results for Trial 11: Redox potential vs. time for soil microcosms, each with a different carbons source than used previously (repeat of Trial 10)..... 67

Figure 6. 9. Results for Trial 12: Redox potential vs. time for soil microcosms, each with different carbon sources than used previously (modified repeat of Trial 10). 69

Figure 6. 10. Results for Trial 19: Redox potential vs. time for soil microcosms with different carbon sources than used previously (modified repeat of Trial 10). 71

Figure 6. 11. Results for Trial 30: Redox potential vs. time for wetland soil microcosms testing the influence of dissolved oxygen in the carbon solution additions..... 73

Figure 6. 12. Mean values of redox potential averaged for each time step for all controls vs. time. Error bars represent standard error. 81

Figure 6. 13. Mean values of redox potential averaged for each time step for controls group and methanol addition groups vs. time. Error bars represent standard error. There is no standard error for the methanols beyond hour 47 as the sample population is 1. 82

Figure 6. 14. Mean values of redox potential averaged for each time step for controls group and acetate addition groups vs. time. Error bars represent standard error. There is no standard error for the acetate group beyond hour 40 as the sample population is 1. 84

Figure 6. 15. Mean values of redox potential averaged for each time step for controls and synthetic sewage addition groups vs. time. Error bars represent standard error. 85

Figure 6. 16. Mean values of the slope of redox potential averaged for each time step for all controls vs. time. Error bars represent standard error. 89

Figure 6. 17. Mean values of the slope of redox potential averaged for each time step for controls and methanol addition groups vs. time. Error bars represent standard error. 90

Figure 6. 18. Mean values of the slope of redox potential averaged for each time step for controls and acetate addition groups vs. time. Error bars represent standard error. . 91

Figure 6. 19. Mean values of the slope of redox potential averaged for each time step for controls and synthetic sewage addition groups vs. time. Error bars represent standard error. 92

Figure 6. 20. Results for Trial 13: Redox potential vs. time for USDA soil microcosms. Experiment received 1.0 M sodium acetate solution and 1.0 M potassium nitrate solution, added via controlling computer. 98

Figure 6. 21. Results for Trial 14: Redox potential vs. time for USDA soil microcosms. Experiment received 2.0 M sodium acetate solution and 1.0 M potassium nitrate solution, added via controlling computer. 100

Figure 6. 22. Results for Trial 15: Redox potential vs. time for USDA soil microcosms. Experiment received 2.0 M sodium acetate solution and 1.0 M potassium nitrate solution, added via controlling computer. 102

Figure 6. 23. Results for Trial 16: Redox potential vs. time for USDA soil microcosms. Experiment received 2.5 M sodium acetate solution and 2.5 M potassium nitrate solution, added via controlling computer. 104

Figure 6. 24. Results for Trial 20: Redox potential vs. time for USDA soil microcosms. Experiment received 2.0 M sodium acetate solution and 1.0 M potassium nitrate solution, added via controlling computer. 106

Figure 6. 25. Results for Trial 21: Redox potential vs. time for USDA soil microcosms. Experiment received 2.0 M sodium acetate solution and 1.0 M potassium nitrate solution, added via controlling computer, every other sample period. 108

Figure 6. 26. Results for Trial 22: Redox potential vs. time for USDA soil microcosms. Experiment received 2.0 M sodium acetate solution and 1.0 M potassium nitrate solution, added via controlling computer, every sample period. 110

Figure 6. 27. Results for Trial 25: Redox potential vs. time for USDA soil microcosms with identical thresholds. Experiment received 2.0 M sodium acetate solution and 1.0 M potassium nitrate solution, added via controlling computer, every sample period. 112

Figure 6. 28. Additional results for Trial 25 after nutrient pumps were turned off. 113

Figure 6. 29. Results for Trial 26: Redox potential vs. time for USDA soil microcosms with identical thresholds. Experiment received 2.0 M sodium acetate solution and 1.0 M potassium nitrate solution, both stripped of oxygen prior to additions. 115

Figure 6. 30. Additional results for Trial 26 after nutrient pumps were turned off. 116

Figure 6. 31. Results for Trial 27: Redox potential vs. time for USDA soil microcosms with identical thresholds. Experiment received 2.0 M sodium acetate solution and 1.0 M potassium nitrate solution, both stripped of oxygen prior to additions. 119

Figure 6. 32. Additional results for Trial 27 after nutrient pumps were turned off. 120

Figure 6. 33. Results for Trial 28: Redox potential vs. time for USDA soil microcosms with identical thresholds. Experiment received 2.0 M sodium acetate solution and 1.0 M potassium nitrate solution, both stripped of oxygen. 123

Figure 6. 34. Additional results for Trial 28 after nutrient pumps were turned off. 124

Figure 6. 35. Results for Trial 29: Redox potential vs. time for USDA soil microcosms with identical thresholds. Experiment received 2.0 M sodium acetate solution and 1.0 M potassium nitrate solution. Solutions were not stripped of oxygen. 126

Figure 6. 36. Results for Trial 31: Redox potential vs. time for USDA soil microcosms testing the influence of dissolved oxygen in the nitrate solution additions. 129

Figure 6. 37. Redox potential vs. time for all nitrate/carbon experiment trials, showing the variability of results among the set of trials. 134

Figure 6. 38. Mean values of redox potential averaged for each time step for controls group and methanol addition groups vs. time. Error bars represent standard error. 136

Figure 7. 1. Results of regression curve-fitting for the mean of the redox potential over time for the controls of all trials, yielding a relatively good fit (R^2 = 0.945). 144

Figure 7. 2. Results of regression curve-fitting for experimental trial 1-01 receiving methanol addition, yielding a relatively poor fit (R^2 = -0.855). 144

Figure 7. 3. Common symbolic elements used in the energy circuit language as developed by Odum (1994). 150

Figure 7. 4. Simple minimodel of a soil microbial decomposition microcosm with an initial organic matter stock included within the microcosm boundaries (adapted from Beyers and Odum, 1993). 151

Figure 7. 5. Results from the STELLA simulation of a simple microbial degradation microcosm with an initial organic matter stock. 154

Figure 7. 6. Minimodel of a soil microbial decomposition microcosm with an initial organic matter stock (E) and an initial electron acceptor stock (N) controlling the availability of E to the consumer population Q. 155

Figure 7. 7. Results from the STELLA simulation of a microcosm with an initial organic matter stock (E) and an initial electron acceptor stock (N) controlling the availability of E to the consumer population Q. 157

Figure 7. 8. Results from the same STELLA simulation with the initial value of N twice as large. 158

Figure 7. 9. Minimodel of a soil microbial decomposition microcosm with an initial organic matter stock (E), an initial electron acceptor stock (N), and a control feedback loop controlling the input of organic matter (J_E) from outside the system based upon the sensed value of N. 159

Figure 7. 10. Results from the STELLA simulation of a microbial degradation microcosm with an initial organic matter stock, an initial electron acceptor stock, and a control feedback loop controlling the input of organic matter from outside the system based upon the sensed value of N. 161

Figure 7. 11. Organic matter E vs. time from the simulation of a microbial decomposition ecosystem. Curve A: Feedback control of organic matter input, with J_E=100 and N_{hi}=2. Curve B: No feedback control. 162

Figure 7. 12. Electron acceptor N vs. time from the simulation of a microbial decomposition ecosystem. Curve A: Feedback control of organic matter input, with J_E=100 and N_{hi}=2. Curve B: No feedback control. 163

Figure 7. 13. Microbial consumer population Q vs. time from the simulation of a microbial decomposition ecosystem. Curve A: Feedback control of organic matter input, with J_E=100 and N_{hi}=2. Curve B: No feedback control..... 164

Figure 7. 14. Minimodel of a soil microbial decomposition microcosm with an initial organic matter stock (E), an initial electron acceptor stock (N), and control feedback loops controlling the input of organic matter (J_E) and electron acceptor (J_N) from outside the system based upon the sensed value of N. 165

Figure 7. 15. Results from the STELLA simulation of a microbial degradation microcosm with an initial organic matter stock, an initial electron acceptor stock, and control feedback loops controlling the input of organic matter and electron acceptor from outside the system based upon the sensed value of N sensed continuously. 169

Figure 7. 16. Organic matter E vs. time from the simulation of a microbial decomposition ecosystem with feedback control over E and N and with J_E varied. Curve A: J_E=20. Curve B: J_E=100. Curve C: J_E=200..... 171

Figure 7. 17. Electron acceptor N vs. time from the simulation of a microbial decomposition ecosystem with feedback control over E and N and with J_E varied. Curve A: J_E=20. Curve B: J_E=100. Curve C: J_E=200. 171

Figure 7. 18. Microbial consumer population Q vs. time from the simulation of a microbial decomposition ecosystem with feedback control over E and N and with J_E varied. Curve A: J_E=20. Curve B: J_E=100. Curve C: J_E=200. 172

Figure 7. 19. Organic matter E vs. time from the simulation of a microbial decomposition ecosystem with feedback control over E and N and with J_N varied. Curve A: J_N=100. Curve B: J_N=500. Curve C: J_N=1000. 173

Figure 7. 20. Electron acceptor N vs. time from the simulation of a microbial decomposition ecosystem with feedback control over E and N and with J_N varied. Curve A: J_N=100. Curve B: J_N=500. Curve C: J_N=1000..... 174

Figure 7. 21. Microbial consumer population Q vs. time from the simulation of a microbial decomposition ecosystem with feedback control over E and N and with J_N varied. Curve A: J_N=100. Curve B: J_N=500. Curve C: J_N=1000. 174

Figure 7. 22. Organic matter E vs. time from the simulation of a microbial decomposition ecosystem with feedback control over E and N, and with N_{hi} constant at 50 and N_{lo} varied. Curve A: ΔN=0. Curve B: ΔN=20. Curve C: ΔN=40..... 176

Figure 7. 23. Electron acceptor N vs. time from the simulation of a microbial decomposition ecosystem with feedback control over E and N, and with N_{hi} constant at 50 and N_{lo} varied. Curve A: ΔN=0. Curve B: ΔN=20. Curve C: ΔN=40. 176

Figure 7. 24. Microbial consumer population Q vs. time from the simulation of a microbial decomposition ecosystem with feedback control over E and N, and with N_{hi} constant at 50 and N_{lo} varied. Curve A: ΔN=0. Curve B: ΔN=20. Curve C: ΔN=40. 177

Figure 7. 25. Organic matter E vs. time from the simulation of a microbial decomposition ecosystem with feedback control over E and N, and with sampling frequency F varied. Curve A: F=20 (continuous). Curve B: F=10. Curve C: F=1. 179

Figure 7. 26. Electron acceptor N vs. time from the simulation of a microbial decomposition ecosystem with feedback control over E and N, and with sampling frequency F varied. Curve A: F=20 (continuous). Curve B: F=10. Curve C: F=1. 179

Figure 7. 27. Microbial consumer population Q vs. time from the simulation of a microbial decomposition ecosystem with feedback control over E and N, and with sampling frequency F varied. Curve A: F=20 (continuous). Curve B: F=10. Curve C: F=1. 180

Figure 9. 1. Translation of energy sources by the addition of artificial feedback: (A) original microcosm functioning off internal energy reservoirs; (B) microcosm accessing previously external energy sources, now internalized. 187

Figure 9. 2. Idealized systems diagram of a physically-coupled true technoecosystem in which the technological components derive electrical power from the ecological components, which in turn access chemical power via the technological components. 191

Figure 9. 3. Idealized systems diagram of a virtually-coupled true technoecosystem in which the virtual ecosystem, a simulation program on a computer, affects the availability of energy to a physical microcosm, which in turn affects the availability of a virtual energy source to the virtual ecosystem..... 194

LIST OF SYMBOLS

α	Level of significance for t-test
A, B, C	Regression constants
C_E	Quantity of organic matter added in pulse in computer minimodels
C_N	Quantity of electron acceptor added in pulse in computer minimodels
DAQ	Data acquisition
ΔEh	Change in redox potential
$\Delta Eh/\Delta t$	Slope of redox curve
ΔG^0_f	Gibbs free energy
ΔN	Difference between high and low setpoints ($N_{hi} - N_{lo}$) in computer minimodels
E	Organic matter state variable in computer minimodels
e^-	Electrons
E_0	Initial value of *E* at time 0 in computer minimodels
E^0	Standard potential for reduction half-cell
Eh	Redox potential
Eh_0	Initial value of redox potential at time 0
Eh_{hi}	Upper threshold *Eh* for control program
Eh_{lo}	Lower threshold *Eh* for control program
e_i	Statistical residuals
F	Faraday constant (9.65×10^4 K mol^{-1})
F	Frequency of data acquisition and control in computer minimodels
f(N)	Control algorithm in computer minimodels

H^+	Protons
J	Joules
J_E	Controlled input pulse of organic matter in computer minimodels
J_N	Controlled input pulse of electron acceptor in computer minimodels
k	First-order degradation rate constant
K	Reduction reaction equilibrium constant
K	Kelvin
$K_1, K_2,\ldots,K_6$	Rate constants for computer minimodels
m, m_i	Number of protons transferred in a redox reaction
M	Molar
mol	Moles
mV	Millivolts
n	Sample population size
n, n_i	Number of electrons transferred in a redox reaction
N	Electron acceptor state variable in computer minimodels
N_0	Initial value of N at time 0 in computer minimodels
N_{hi}	Upper threshold for N in computer minimodels
N_{lo}	Lower threshold for N in computer minimodels
Ox	Oxidized component (electron acceptor) in a reduction/oxidation reaction
Ox^0	Initial concentration of Ox at time 0
Q	Microbial population state variable in computer minimodels
Q_0	Initial value of Q at time 0 in computer minimodels
R	Ideal gas constant (8.31 J K^{-1} mol^{-1})

R^2	Coefficient of determination
Rd	Reduced component (electron donor) in a reduction/oxidation reaction
Rd^0	Initial concentration of Rd at time 0
S_e	Standard error
S_y	Standard deviation
T	Temperature
T	Sample period for control program
t	Time length of pump actuation for control program
V	Volts
W	Watts
y	Measured data
y_{mean}	Mean of measured data
y_p	Predicted data

1.0 INTRODUCTION

Humans have significantly altered ecosystems since first evolving as a species. Indeed, the capacity of humans to reason and think, directly resulting in manipulation of the surrounding environment to increase chances for species survival, is the fundamental basis for the definition of the species designation *Homo sapiens.* Until a few centuries ago, human population was small and spatially diffuse relative to the global environment, and the effects of human action on ecosystems were localized and at a small scale relative to the global biosphere. As human population and technological development has increased, so has its influence and effects on the development and organization of natural ecological systems (Goudie, 1984). This realization by many has led to recent interest in trying to understand how to engineer ecosystems that provide for human survival but within which humans are an integral and contributing component. To do this, it is important to understand how complex hierarchical systems of components, biological and non-biological, organize, and what the effects of humans might be in such a system.

One of the roles of humans in ecosystems is as a processor and creator of information. Through the study and understanding of the world around them, humans create a reservoir of information that may feed back on the natural systems. In addition, humans build persistent structures that convey information long into the future. Finally, humans act as a feedback pathway for entrainment of additional energy into the global ecosystem. Through all of these actions, humans may be seen as acting as a control gate on future states of natural ecosystems. To what extent can an understanding of this role as an ecological control be useful for the developing field of ecological engineering?

Human technological development has progressed to the extent where this conceptual ecological role of humanity developed above—that of a processor and transmitter of information that encourages entrainment of additional energy into ecosystems—may be supplanted by information technology—that is, electromechanical structures created by humans for the detection, processing, storage, and transmission of information. Electronic devices devoted to information processing may be used to add additional feedback loops to otherwise natural systems. A feedback loop in a system may be defined as any flow of information from a system's output that in some way regulates or affects system input (DeAngelis, et al., 1980). In ecological systems, a feedback mechanism can be either natural or artificial. A natural feedback mechanism in an ecosystem is merely the information in the current state of the system that influences future states of the system (Margalef, 1968) and are thus inherent to the system itself. An artificial feedback mechanism, however, is one that is added to the natural system through the action of human presence or intelligence.

1.1 Technoecosystems

It is now possible to add artificial feedback mechanisms to biologically-based ecosystems using human-created technology at a variety of scales, thereby creating new systems that are hybrids of biological and technological components. An array of electronic sensors and computerized control programming can be used to create artificial information feedback loops to an ecosystem, possibly allowing new pathways for energy utilization within the ecosystem. In the literature, systems combining technological and

ecological components have been called technoecosystems (Odum, 1993) or, alternately, ecocyborgs (Clark, et al., 1999), the specific definitions for which are given in Table 1.1.

Table 1. 1. Definitions of ecological/technological hybrids found in the literature.

Term (Authors)	Definition
Technoecosystem (Odum, 1993)	"Systems in which formerly wild components of ecosystems are incorporated into technological systems as hybrids of living units and hardware homeostatically coupled."
Technoecosystem (Duffield, 1976)	"Large, complex, spatially or functionally distinguishable… industrial systems under conscious human control viewed as ecosystems."
Ecocyborg (Clark, et al., 1999)	"Systems that consist of both biological and technological components that interact at the scale of an ecosystem, where the latter is defined as a community of organisms together with their abiotic surroundings."

The definition from Duffield (1976), important as one of the earliest published definitions of technoecosystem, was developed from concepts in Odum (1971) and is more akin to what is currently called industrial ecology. The definition of technoecosystem given by Odum (1993) leaves open the question as to the relative hierarchy of the technological and biological components, thus possibly including systems in which the organization of the biological system is subject to the constraints and controls dictated by the technological environment but not so the converse. The definition of ecocyborg given by Clark, et al. (1999), however, seems to allow the possibility of technological components interacting with biological components at similar hierarchical levels and more subject to the organization and energy utilization of the entire system. Common to these definitions is the concept of some combination of

technological and biological components interacting together, and thus organizing, as a system. In this thesis, the term technoecosystem will be used to designate any system that combines technological and biological components such that the technology provides additional feedback mechanisms. Using these definitions as a guide, it is possible to construct a list of systems that might be categorized as technoecosystems, displaying the fact that technoecosystems are not as exotic as one might first think (Table 1.2).

Table 1. 2. Common and not-so-common examples of technoecosystems.

Bioreactor for waste treatment • Microbial: Wastewater treatment plant • Ecological: Living Machines (Todd and Josephson, 1996)	Ecological systems for life support • NASA Biological Life Support System • Biosphere 2 (Zabel, et al., 1999)
Automated aquaculture tank	Mechanically-tended Agricultural field
Automated greenhouse	

Any discussion of feedback and ecosystems recalls a classic debate of ecological theorists—that of the cybernetic nature of ecosystems. *Cybernetics* is the science of communication and control within systems, where the forcing signals (input) of a system are determined in part by system responses (output) (Weiner, 1948; Phillips and Harbor, 2000). The theoretical consideration and development of cybernetics throughout the 20th Century has led to an entire field of engineering devoted to the design of feedback control systems, resulting in numerous successful designs for electromechanical automated control in countless industries and technologies (Phillips and Harbor, 2000). Many attempts have been made to apply the concepts of engineering control theory to describe the organization of ecosystems (e.g. Lowes and Blackwell, 1975; Boling and Van Sickle,

1975; Hannon and Bentsman, 1991; Hannon, 1986). Typical application focuses on describing the homeostatic nature of complex ecosystems in terms of controlling feedback mechanisms and using the mathematics of engineering control theory. While these efforts have met with mixed success, the maturation of control technology and the advancement of new concepts in ecological engineering yield new opportunities for the testing of feedback mechanisms in ecosystems. For example, Patten and Odum (1981) propose that ecosystem feedback networks are instrumental in forming ecosystem resiliency to perturbations. An experiment might be designed to test this hypothesis using technoecosystems, focusing on the impact of artificial feedback loops on ecosystem resiliency. The addition of new and artificial feedback to ecosystems and their subsequent response in development might also offer insight into the self-organizational capability of complex systems (Petersen, 1998).

1.2 Motivation for Study

Motivation for this avenue of study comes from interest in developing an understanding of the way complex hierarchical systems comprising biological and technological subsystems organize (or fail to organize) over time. The study of technoecosystems will yield new insights and information regarding their development and organization at all scales, from the smallest tended garden plot to the entire global biosphere and emerging technosphere. Additionally, many fields of scientific inquiry and engineering design stand to benefit from a better understanding of techno-ecological organizational processes. One field in particular that stands to benefit is the emerging

discipline of ecological engineering. Ecological engineering has been defined as the use of "ecological processes within natural or constructed imitations of natural systems to achieve engineering goals" (Teal, 1991). An ecologically-engineered system typically contains some proportion of technological and ecological components and thus might be considered a technoecosystem to some degree. While the ratio of technological to ecological components may differ from system to system, all ecologically engineered systems can be considered to fall somewhere in between all biological and all technological. Understanding how the technological components act with feedback control on the ecological components may yield information about the trajectory of system organization, which might then be used to develop design constraints and expected outcomes, vital information for any design process.

Specific motivation for this study results from the recent implementation of a residential-sized wastewater treatment system in rural Virginia. The system is a closed-loop wastewater treatment system that recycles septic tank effluent to the toilets of a small community lodge (Ives-Halperin and Kangas, 2000). The basic design concept for the waste treatment system is a greenhouse-based "living machine" (Todd and Josephson, 1996), a series of ecologically-engineered unit processes that rely on natural processes of aquatic and wetland ecosystems to accomplish secondary and tertiary treatment of the wastewater. Because of the remote location of the system, a low-cost automated monitoring and control system is desired to track and influence the performance of the constructed wetland unit process for nitrogen removal. Pursuit of this design question leads immediately to the larger questions concerning the addition of technological components to complex ecosystems.

1.3 Problem Statement

Constructing a technoecosystem by adding an artificial feedback loop to a naturally-occurring ecosystem results in the creation of a new system that does not exist in nature. For example, an artificial feedback loop may be installed that allows an ecosystem control over its energy source. One might expect that the resulting technoecosystem organizes differently from its natural analog. What describes or predicts how such a system will react or utilize the artificial feedbacks? How will the biological components of the system organize given a new feedback loop, and in what way will it organize differently? The organization of any complex system is dictated by the constraints of thermodynamic laws; thus the development and organization of technoecosystems might be analyzed using principles of systems ecology.

The research presented here focuses upon the design, construction, and operational dynamics of technoecosystems. The technoecosystem studied is based upon a wetland soil microcosm, simulating automated control of a wastewater treatment wetland for optimization of the denitrification process. Using this technoecosystem as a platform, this research explores the basic self-organizing characteristics of technoecosystems in which an artificial feedback loop is added. The question guiding this research is: What happens if an ecosystem, in the form of an ecological microcosm, is given control over its own source of energy? The hypothesis tested here is that if technological components are used to construct information feedback pathways that are artificial to the natural analog of the ecological microcosm, that ecological microcosm internally self-organizes such

that those ecosystem components that can take advantage of the new feedback pathways are favored. If the feedback pathways are designed to allow access to additional sources of energy, the result is an increased use of energy from the source by the microcosm as the loop of positive feedback is established. The evidence of this result is an increase in the ecosystem metabolism.

2.0 OBJECTIVES AND STUDY APPROACH

2.1 Objectives

The objectives of this research are as follows:

1. Construct a technoecosystem using wetland soil microcosms in which feedback control is implemented using redox potential as the monitored variable and which controls inputs of carbon and nitrate as additional sources of energy.
2. Investigate the effects of the feedback control system on the metabolism of the soil microcosm by monitoring the trend in redox potential over time.
3. Begin development of a computational model based upon concepts of limiting factors to assist in understanding the self-organization processes occurring in the soil microcosms with and without feedback control.
4. Propose directions for further research, development, and contextual understanding of technoecosystems.

2.2 Study Approach

The approach to meet these objectives as presented in this document is as follows:

- Following a literature review, the experimental set-up for laboratory experiments on a feedback-controlled wetland soil microcosm is presented.
- Results from the two types of laboratory experiments are presented and discussed.

- A series of simple computational models that represents phenomena observed in the physical experiments is developed and discussed.
- Conclusionary ideas are presented and recommendations are made for further research and development.

3.0 REVIEW OF LITERATURE

3.1 Technoecosystem Research

Designing technoecosystems for study relies upon the construction of ecological microcosms. An ecological microcosm is a scaled miniature ecosystem constructed within a container, maintaining some of the complexity of interactions that occur in natural ecosystem analogs (Beyers and Odum, 1993). Crucial to the definition of a microcosm is a container—some material that exists as an artificial boundary between the microcosm and its surroundings that limits or excludes transfer of energy and/or matter. Typically an ecological microcosm is derived from a natural ecosystem and contains natural mixed populations of organisms. Artificial microcosms can be and have been constructed of any size, ranging from a small flask to a large greenhouse (Beyers and Odum, 1993).

While microcosms have been built for ecological research and education for decades (Beyers and Odum, 1993; Taub, 1974), few have been constructed with feedback control pathways that afford control over the primary energy source driving the ecosystem. One of the earliest examples of this type of construction is the turbidostat, a device that controls the density of the population of a suspended-growth algal culture (Myers and Clark, 1944; Brock, 1966). The device was originally constructed for the continuous culture of the alga *Chlorella.* The culture is contained in a glass tube through which light rays from a fluorescent light source pass. A photocell on the opposite side of

the glass tube intercepts these rays, and another photocell not behind the glass tube is balanced to the first with a light filter. As the algal culture grows, the light through the glass tube is blocked and the two photocells become out of balance. This imbalance triggers the opening of a solenoid valve, adding fresh growth medium solution and diluting the algal suspension to the point where light again passes through and the photocells are balanced. Over time the system establishes a steady-state condition in which cell density, light availability, and nutrient availability is constant (Fogg, 1975). Because all sources of energy are in excess and not limiting, algal growth becomes limited only by factors internal to the alga. Additionally, cell characteristics such as growth rate and photosynthetic rate were shown to have little variation across culture populations (Fogg, 1975).

Patrick (1966) reports on a simple system for controlling the redox potential in soil suspension microcosms used for researching nitrate, iron, and sulfate reduction at constant redox potentials. In this system, a soil sample and an equal amount of water are sealed in a glass test tube. A platinum probe is sealed in the tube, and a calomel reference cell is connected to the suspension by an agar-potassium chloride salt bridge passed through the stopper. These probes are wired to the control unit of an automatic titrator modified to deliver an oxygen-nitrogen gas mixture. Once the tube is sealed, the redox potential decreases over time, due to the activity of the soil microbes, until the set point is reached, activating a solenoid valve and injecting the oxygen mixture. This raises the redox potential until the set point is again reached and the solenoid valve closes. Precise control of redox potential to ±5 mV is reported (Patrick, 1966). The system was later modified and expanded with a pH meter and solenoid controlling flow from an acid or

alkali solution reservoir (Patrick, et al., 1973). This system allows simultaneous control of both redox potential and pH in waterlogged soil suspensions.

Beyers (1974) constructed an aquatic photosynthetic microcosm in which the lights for ecosystem primary production was controlled by measurement of the pH of the solution, which would fluctuate inversely to the concentration of carbon dioxide in the water column. Dissolved carbon dioxide rises or falls because of release or uptake during respiration or photosynthesis, respectively, affecting the pH of the solution. The changes in pH, an indirect measure of the ecosystem metabolism, were monitored with a pH probe and used to automatically switch on and off a light source for the microcosm itself. In unpublished results, Beyers reported that the system exhibited oscillatory behavior, alternating between periods of light and dark. In two of three replicate systems of this configuration, the light phase of the light-dark cycle was longer than the dark phase and gradually increased over time until, eventually, the light remained on constantly. Odum (1993) contends that this indicates the systems gradually organized to maximize photosynthetic power. In the third system, the dark phase was consistently longer that the light phase, and the length of the light phase gradually decreased over time.

Petersen (2001) reported on another photosynthetic technoecosystem in which an artificial feedback loop was added to aquatic planktonic ecosystem microcosms using dissolved oxygen sensors and a data-logging computer. When dissolved oxygen in the water column fell below a lower setpoint because of ecosystem respiration, a fluorescent light was turned on to stimulate photosynthesis. The oxygen created in community photosynthesis increased the dissolved oxygen content of the water until it reached an upper setpoint, at which time the light was turned off. The nutrient uptake, primary

productivity, and duration of light and dark periods were measured for all microcosms. While the overall development of the microcosm ecosystems were not seen to change much compared to fixed lighting conditions, similar patterns in energy demand and oscillatory primary productivity patterns were observed between replicate microcosms. It was found that the artificial feedback induced a poor coupling between productivity and respiration in the planktonic community. Petersen also suggested that the novel character of the oscillations between the light and dark period was controlled by the feedback structure and amounted to emergent behavior at the level of the system.

3.2 Feedback Control Systems

The construction of technoecosystem microcosms with artificial pathways of information falls under the subject of feedback control theory. Concepts of engineering control theory arose as a result of the need for design of automatic control of parameters or variables. The term cybernetics, first suggested by Weiner (1948), has often been applied to describe engineered mechanisms that are automatically controlled. While initially developed as a descriptor of engineered systems, control theory concepts have been used by biologists to describe various physiological and ecological processes, from organism thermoregulation to population dynamics. In a way, these attempts stem from a long tradition in biological science of finding mechanical analogs for descriptive characterization of key biological processes (Calow, 1976).

Feedback control and cybernetic theory rests upon the concept that a physical variable is to be controlled and maintained at a desirable level or within desirable bounds.

In machine or mechanical systems, the mechanism of control is through the measurement of the variable parameter by some sort of sensor. The measured value is then compared to a reference setpoint, and if the difference is greater than a predefined tolerance, the variable is manipulated as necessary by means of an actuator. Cybernetic machines can therefore be conceived as being composed of three main component subsystems, organized into a classic block diagram as shown in Figure 3. 1 (Calow, 1976). The program for operation—that is, the program for the behavior of the variable to be controlled and the establishment of the desired setpoints—is programmed into the motivator. The regulation of the variable is accomplished by some mechanism called the effector, the goal of which is to keep the machine, variable, or system on the desired, predetermined course. Information pathways, which include one or many sensors, transfer feedback information regarding the response of the effector and the effect on the variable back to the motivator. The comparator—often a component of the motivator—compares the output (that is, the information about the response of the effector) with the input (information about the desired response programmed in as setpoints) and undertakes action according to its program and the difference determined by the comparator. Should the variable fall within the tolerance limits established by the setpoints, no action is taken. A disturbance on the system—say on the variable being controlled and measured—is sensed via the feedback signal and produces a dynamic response by the entire system. A classic simple mechanical example of a control system is a thermostat system for temperature control (Calow, 1976).

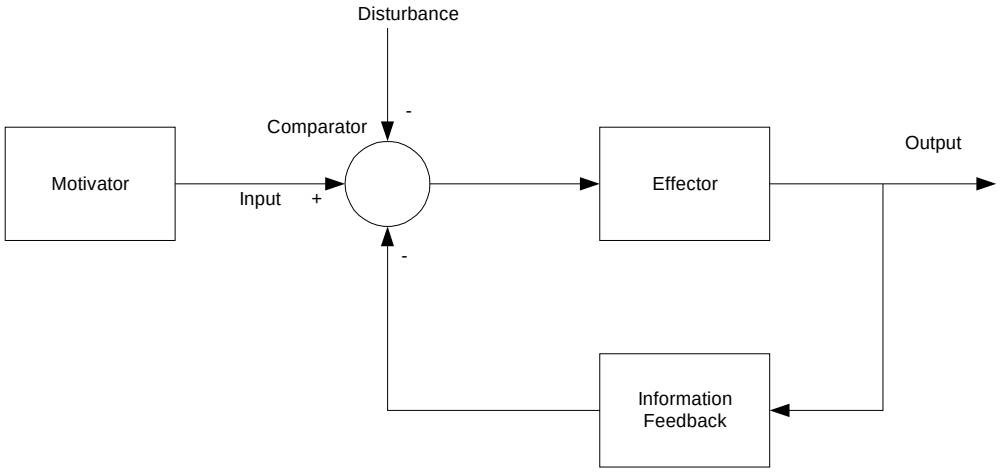

Figure 3. 1. General block diagram for an automatic control system (from Calow, 1976).

Control in ecosystems is the maintenance of that system's state variables within certain bounds (Kitching, 1983). Feedback control implies that certain forcing functions on the ecosystem are determined by certain responses of the system (Phillips and Harbor, 1999). It is important here to make the distinction between two types of systems in relation to feedback mechanisms: those that are open loop systems versus those that are closed loop systems (Phillips and Harbor, 2000). In open loop systems, a process occurs in which the controller of the process is not influenced by information flowing back to the controller from the receiving variable of the process. In closed loop systems, however, the controller of the process receives information concerning the variable being influenced and adjusts its mechanism accordingly (DeAngelis, et al., 1986). Herein lies the potentially critical difference that can be incorporated into technoecosystem microcosms versus their natural analogs. While subsystems within an ecosystem might fit the definition of a closed-loop system, with information feedback readily occurring between components, the entire ecosystem itself can be defined as an open-loop system

in relation to its source of energy. No ecosystem in nature has control over all the inputs of energy that serve as the forcing functions of the system and that influence the structure and functioning of the ecosystem. This is particularly true for ecosystems in which energy is received by light and captured through photosynthesis, where the light source in nature is the sun (to which no pathways of information feedback from the ecosystems on earth are known to exist). Based upon this reasoning, the entire planet itself can be considered an open-loop system (DeAngelis, 1986).

The construction of technoecosystem microcosms thus allows the creation of closed-loop ecosystems by incorporating feedback control pathways that give the ecosystem control over its energy source. The energy source of an ecosystem can be light, mechanical, or chemical energy, and the sum of these sources typically defines that ecosystem's energy signature (Kangas, 2004). When the source of energy for an ecosystem is chemical, as in the case of some microbial ecosystems, the energy is released when organic or inorganic compounds are oxidized. The free energy of this oxidation reaction is the energy that is released and available to do useful work (Brock, et al., 1994).

3.3 Energy Sources for Wetland Soil Technoecosystem

The energy sources for the metabolism occurring in wetland soils are primarily chemical. Organic matter is typically the energy source for soil microbial metabolism, as it is oxidized by various species of aerobic and anaerobic bacteria (Vepraskas and Faulkner, 2001). A common reaction in the anaerobic environment of wetland soils is denitrification, the microbial metabolic conversion of nitrate to gaseous nitrogen. In

denitrification, a carbon source is required to support the denitrification process, in the amounts equivalent to 2.47 g of methanol (CH_3OH) for 1 g of nitrate (Kadlec and Knight, 1996). Both the carbon and the nitrate serve as energy sources for the metabolism of the denitrifying microbial community. Without the availability of either, denitrification may be limited or not occur at all. Thus, in the design of the laboratory wetland soil microcosms with feedback control, the energy source whose availability might be controlled may be a carbon source, such as a methanol solution, or an electron acceptor, such as a nitrate solution. In studies of denitrification and redox potential in anaerobic bioreactors, Koch and Oldham (1985) used a solution of sodium acetate for the carbon source and sodium nitrate as the nitrate source.

3.4 Redox Potential in Wetland Soils

Because of the ease of measurement, low cost for probes, and adequate precedence in wastewater process control, redox potential was selected for this study as the measured parameter for automated control of the chemical additions to a wetland soil microcosm. The long history of the use of redox potential to characterize the reduction state of wetland soils makes it a desirable candidate parameter for this study. A majority of the biological and chemical transformations in wetland soils are characterized by oxidation-reduction or redox chemical reactions (Mitsch and Gosselink, 1993). A redox reaction describes the transfer of electrons between a reductant and oxidant chemical species, as described by the following general reduction half-cell reaction equation (Patrick, et al., 1996):

$$Ox + mH^+ + ne^- \rightarrow Rd \qquad (3.1)$$

where *Ox* is the oxidized component or electron acceptor, *Rd* is the reduced component, *n* is the number of electrons, and *m* is the number of protons involved in the reaction. Because electrons cannot exist alone in a soil or aquatic environment, this half-cell reaction is paired with an accompanying half-cell oxidation reaction that serves as the electron donor for the entire reaction. In treatment wetlands, highly reduced organic matter is the primary electron donor (Patrick, et al., 1996). Thus the oxidation of organic matter through the reduction of nitrate (denitrification) can be written as the summation of two half-cell reactions (Mitsch and Gosselink, 1993):

$$4NO_3^- + 24H^+ + 20e^- \rightarrow 2N_2 + 12H_2O \text{ (reduction)} \quad (3.2)$$

$$5CH_2O + 5H_2O \rightarrow 5CO_2 + 20H^+ + 20e^- \text{ (oxidation)} \quad (3.3)$$

yields the overall reaction

$$4NO_3^- + 5CH_2O + 4H^+ \rightarrow 5CO_2 + 2N_2 + 7H_2O \qquad (3.4)$$

In this reaction, nitrate (NO_3^-) is the electron acceptor, and organic matter (CH_2O) is the electron donor.

Measurement of soil redox potential has commonly been used in soil science to characterize the intensity of the metabolism occurring in flooded or wetland soils (Patrick, et al., 1996). The metabolism of a cell is the sum of all the chemical processes occurring within a cell and is generally considered in two components: anabolism, the processes by which a cell is built up and maintained by materials from the environment; and catabolism, the process by which materials are broken down and energy is released (Brock, et al., 1994). Another term for this catabolic pathway is respiration, which encompasses all the biochemical pathways for the breakdown of organic compounds via

oxidation-reduction reactions. In respiration, organic matter is oxidized by the release of an electron, releasing energy in the process that the cell can use. For the release of this electron to occur, however, molecular oxygen or some other molecule is required to be the terminal electron acceptor (Brock, et al., 1994).

The magnitude of the measured redox potential gives an indication of the strength of the reaction to transfer the electrons, and this is a measure of the availability of electrons for metabolism within the aqueous chemical system (Patrick, et al., 1996). The larger the positive magnitude of the potential, the stronger and more abundant the oxidant is to gain electrons (Jorgensen, 1989). Using expressions for the change in Gibbs free energy and the equivalent reaction expressed as electrochemical energy (volts), Patrick, et al. (1996) derive the following expression for the redox potential *Eh* of one pair of oxidation/reduction half-cell reactions in an aqueous system in equilibrium:

$$Eh = E^o - \frac{RT}{nF}\ln\frac{(Rd)}{(Ox)} + \frac{mRT}{nF}\ln H^+ \quad (3.5)$$

where E^o is the standard potential for the reduction half-cell under consideration, R is the ideal gas constant (8.31 J K^{-1} mol^{-1}), T is the absolute temperature (in degrees Kelvin), F is the Faraday constant (9.65 x 10^4 K mol^{-1}), n is the number of electrons exchanged in the half-cell reaction, m is the number of protons exchanged in the half-cell reaction, and *Rd* and *Ox* represent the aqueous concentrations of the individual reduced or oxidized component of the half-cell reaction. Equation (3.5) shows that the redox potential increases with increasing concentration of the oxidized component, decreases with increasing concentration of the reduced component, and increases with decreasing pH (increased H^+ concentration). Additionally, the standard potential E^o varies for individual chemical species, depending upon the chemical activity as determined by the valence

electron configuration and concentration in solution (Latimer, 1952). Values for E^o for a number of half-cell reduction reactions have been determined experimentally in the laboratory and are tabulated in the literature. The value of E^o for the presence of molecular oxygen as it occurs in the microbial oxidation of organic matter has been determined to be relatively high compared to most other chemical species available in the environment (Latimer, 1952). Thus, the redox potential is strongly related to the presence of oxygen, so much so that it has been used in the past to monitor the cyclical flooding and draining (thus aeration) of a soil (Patrick and Wyatt, 1964).

Critical threshold redox potential values for the reduction of oxidized forms of several inorganic redox systems relevant for organic wetland soils have been measured in a number of experiments (Patrick and Delaune, 1977). The critical value for the reduction of a particular oxidized chemical compound is determined by that compound's respective E^o and *m* and *n* in the respective reduction reaction. Therefore, as organic matter is oxidized in submerged wetland soils, the reduction of the various oxidizers commonly available in wetlands theoretically follows a predictable sequence. Oxygen is the first chemical constituent to be reduced in a soil, and it becomes undetectable at a redox potential of about +350 millivolts. Nitrate follows oxygen as the next substance to be reduced, occurring at a redox potential around +250 mV. Nitrate reduction will only occur once the concentration of oxygen is at or near zero (Patrick and Delaune, 1977). Various biochemical reactions of this sort have been correlated with their associated redox potentials in a saturated wetland soil or aquatic environment, which can be organized according to decreasing potential gradient, as shown in Table 3. 1 (Patrick, et al., 1996).

Table 3. 1. Range of redox potentials required to reduce oxidized forms of the various redox couples in soil and wetland environments.

Redox Couple in Wetland Soils (*Ox* → *Red*)	Range of Measured Redox Potential (mV)
$O_2 \rightarrow H_2O$	+400 to +350
$NO_3^- \rightarrow N_2$	+250 to +200
$Mn^{4+} \rightarrow Mn^{2+}$	+200 to +150
$Fe^{3+} \rightarrow Fe^{2+}$	-25 to -75
$SO_4^{2-} \rightarrow S^{2-}$	-125 to -175
$CO_2 \rightarrow CH_4$	-200 to -250

It should be noted that this sequence is, in theory, predictable. The quantitative value of Equation (3.5) to predict the reduction of a specific chemical species is valid for conditions of chemical equilibrium, typically produced in pure solutions in the laboratory (Patrick, et al., 1996). Chemical equilibrium is rarely found in wetland soils because of fluctuating water tables, soil heterogeneities in the concentration of organic matter or electron acceptors, and differences in the reduction rates of the available electron acceptors (Vepraskas and Faulkner, 2001). It is generally accepted, however, that redox potential is valuable for general quantification of the intensity of the microbial metabolism occurring in a soil, and can be useful for indicating the onset of reducing conditions when oxygen and nitrate have been depleted (Patrick, et al., 1996; Kim and Hao, 2001).

Measurement of the redox potential in wetland soils is typically performed with a platinum electrode. Platinum wire is used because it readily transfers electrons to or from the soils but does not chemically react with it (Patrick, et al., 1996). The platinum electrode is coupled with a half-cell of known potential, so that reducing soils transfer electrons to the electrode and oxidizing soils take electrons from the electrode. The potential between the platinum electrode and the known reference electrode can then be

measured as a voltage with a suitable potentiometer or data-logger. The reference electrode typically employed in field measurements is either a saturated calomel or a silver/silver chloride reference electrode (Patrick, et al., 1996). Because all of the half-cell reduction reactions shown in Table 3. 1 are occurring in wetland soils contemporaneously to some degree, the redox potential readings obtained from platinum redox electrodes is an integrative measurement, representing the weighted average of the potential of all the redox couples occurring simultaneously, and not the potential of any single redox couple (Bohn, 1971; Austin and Huddleston, 1999).

3.5 Examples of Redox Potential as a Control Parameter

A number of precedents for the use of redox potential as a measured parameter for automated monitoring and control exist in the literature on process control in conventional wastewater treatment. Isaacs, et al. (1998) investigated a real-time automated monitoring system for denitrification in a wastewater treatment plant based on measurement of either fluorescence or redox potential of the activated sludge mixture. An apparatus containing both a redox electrode and a fluorescence sensor was designed to perform measurements *in situ* in the anoxic zone of a wastewater plant reactor. It was found that readings from the redox electrode were closely correlated with those from the fluorescence sensor that directly indicated the metabolic state of the denitrifying microorganisms. Al-Ghusain, et al. (1994), investigating real-time automatic monitoring of nitrification and denitrification rates in wastewater treatment plants, used a simple pH probe in a small reactor to monitor the rate of nitrate consumption and to track the shift

from anoxic to anaerobic conditions. Results of the pH probe were accurately correlated with parallel measurement of redox potential and dissolved oxygen from samples. Ginot, et al. (1987), in developing a remote monitoring system for aquaculture, used a suite of instruments to measure and correlate temperature, dissolved oxygen concentration, pH, conductivity, and redox potential to track changes in the aquatic environment of the raised stock. Kim and Hao (2001) successfully used pH and redox potential to initiate and terminate anaerobic conditions in an alternating aerobic and anoxic system for rapid nitrification/denitrification. Specifically, a continuously monitoring data acquisition computer was used to determine the end of denitrification by monitoring for a rapid and sudden change in the slope of the redox potential curve over time, at which time the computer would initiate an aerobic sequence in the reactor.

In summary, therefore, redox potential was used in this study as a control parameter because of the following reasons: (1) its value is an indicator of metabolism in wetland soil microcosms; (2) it is easy and inexpensive to measure; and (3) there is an established practice of using it both as an index in wetland soil systems and as a control parameter in conventional wastewater treatment systems.

4.0 EQUIPMENT

4.1 System Overview

The equipment used for this research included a data acquisition computer that monitored the redox potential measured in wetland soil microcosms via platinum electrodes. The data acquisition computer could manipulate the activity of nutrient delivery pumps by activating a relay with a digital pulse. The nutrient delivery pumps delivered nutrient solution to the soil microcoms. The overall configuration of these elements for the two control scenario types studied (carbon addition and carbon/nitrate selection) are shown in the system schematics (Figure 4. 1 and Figure 4. 2) and accompanying photograph (Figure 4. 3).

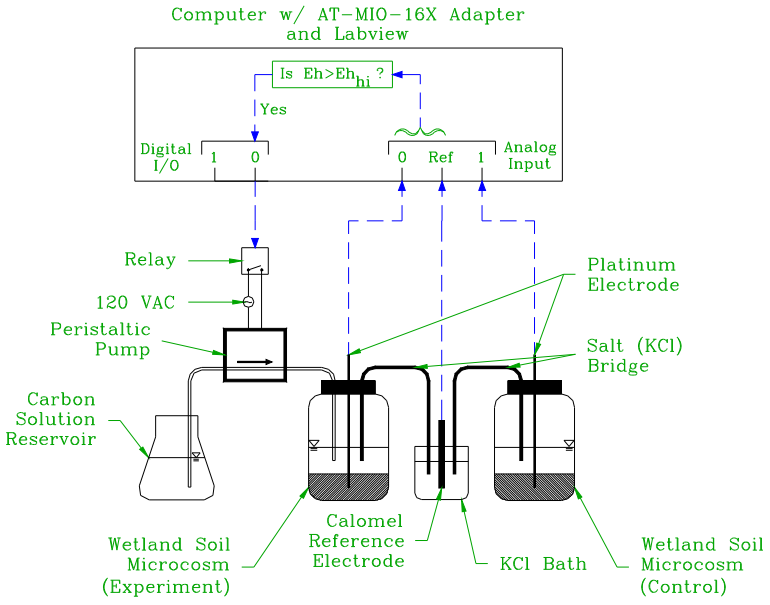

Figure 4. 1. Schematic diagram of the system setup for carbon delivery experiments.

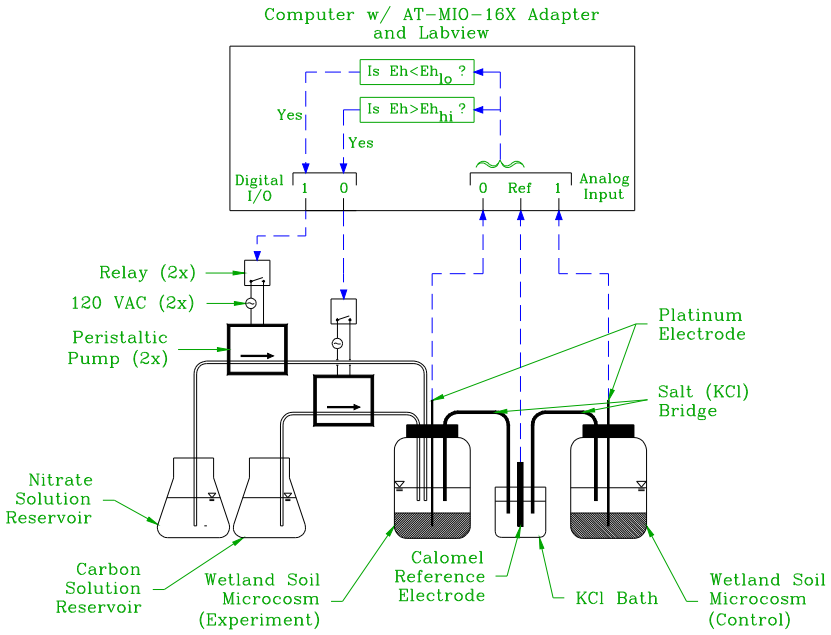

Figure 4. 2. Schematic diagram of the system setup for carbon/nitrate selection experiments.

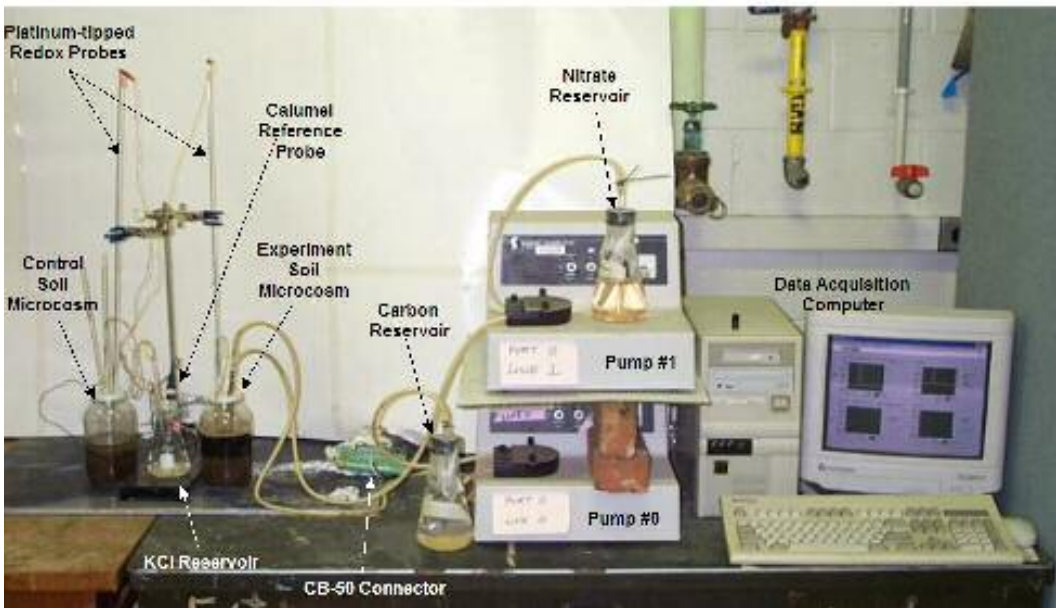

Figure 4. 3. Photograph of microcosm experiment setup, here shown for nitrate/carbon addition scenario.

The equipment configuration may be considered as consisting of three main subsystems: the data acquisition system, consisting of the computer and the probes used for measuring redox potential; the nutrient delivery system, consisting of the pumps, tubing, and controlling switches; and the wetland soil microcosms themselves. Each is discussed here separately.

4.2 Data Acquisition System

Initially, a standard I-486 DX2-66 MHz personal computer (Optiplex Model 466/MX, s/n 3672K, Dell Computers, Round Rock, Texas) was used for data acquisition and control. This computer was used until the 23rd experiment trial, at which point a hardware failure forced a switch to a Pentium-75 MHz (custom built) personal computer. This second computer was used for data acquisition and control in the remaining experimental trials. Both computers used Microsoft® Windows 98 (Microsoft Corporation, Redmond, Washington) as the operating system. At the time of the switch, all hardware and software required to run the data acquisition program were copied from the first computer to the second.

4.2.1 Computer Hardware

The computer was modified with an available adapter card to create the data acquisition system. The card used for data acquisition was the National Instruments AT - MIO-16X (s/n 001297, National Instruments Corp., Austin, Texas), a multifunction analog, digital, and timing input/output (I/O) board for a PC (National Instruments, 1993). A description of the board is given in Appendix A. The board has a 50-pin I/O

connector, to which was attached the ribbon cable (1.0 m type NB1) for the National Instruments CB-50 I/O connector block with 50 screw terminals. The 50-channel pin assignment configuration for the AT-MIO-16X is shown in Appendix A.

4.2.2 Computer Software

For the data acquisition software, the computer was loaded with LabVIEW (version 4.1, 1994, National Instruments Corp., Austin, Texas), a graphical programming language that allows the user to build virtual instruments (VIs) to control equipment and sample data. LabVIEW programs have two components: a front panel display that serves as the user interface, and a block diagram that is a graphical representation of the source code construction. For this set of experiments, a control program was coded using the LabVIEW block diagram and graphical user interface utility.

The control program incorporates an on/off control scenario. This was chosen because it was the simplest to program and incorporate into a control scenario. The control program monitors the redox potential *Eh* in the soil microcosms over time at a user-prescribed frequency. If the *Eh* is outside the bounds of the user-prescribed threshold values, the control program takes action adding a nutrient intended to bring the *Eh* back within bounds. In this way, the control program acts like a simple on/off thermostat system, which, for example, may turn on a heat source to maintain temperature above a certain level. The nutrient delivered to the soil microcosms depends upon the type of experiment chosen by the user. Two scenario types were studied in this set of experiments: carbon addition to minimize *Eh*, and carbon/nitrate selection to maintain *Eh* within certain bounds.

The carbon addition scenario assumes that the availability of carbon is inadequate and thus limiting the microbial metabolism in the soil microcosms. A flow chart of the control program logic for the carbon addition scenarios is given in Figure 4. 4. The program begins by taking an *Eh* reading from the microcosm, recording it and the elapsed time to the computer hard drive, and comparing this reading to a user-defined threshold *Eh*. If the *Eh* reading is above the threshold *Eh* (Eh_{hi}), a pump is turned on fora user - prescribed time *t* delivering a carbon nutrient solution to the microcosm, under the assumption that carbon is limiting the microbial metabolism. If the measured *Eh* is below the threshold *Eh*, the program takes no action. The program then waits a user-defined time *T*, and takes another *Eh* reading, compares it to the threshold, and decides whether or not to take pump action. This sequence is repeated until the measured *Eh* is below the threshold *Eh*.

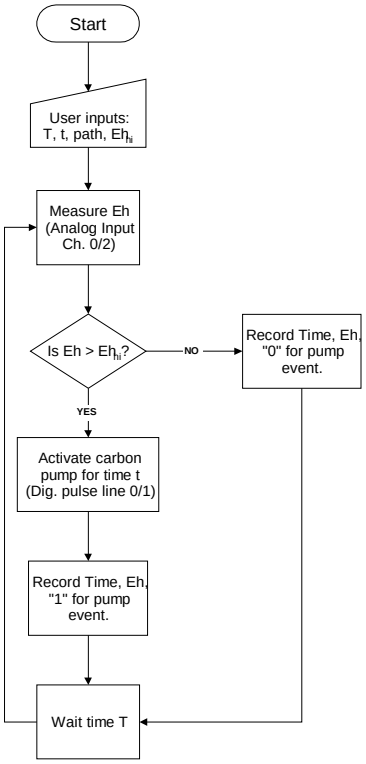

Figure 4. 4. Flow chart for redox potential control program for carbon addition.

The carbon/nitrate selection scenario assumes that either carbon or nitrate is limiting to microbial metabolism. A flow chart of the control program logic is given in Figure 4. 5. Again, this program begins by taking an Eh reading from the microcosm, recording it and the elapsed time to the computer hard drive, and comparing this reading to a user-defined upper threshold. If the *Eh* reading is above the upper threshold (Eh_{hi}), a pump is turned on for a prescribed time *t* delivering a pulse of carbon nutrient solution to the microcosm, under the assumption that carbon is limiting to the microbial metabolism. If the measured *Eh* is below the upper threshold, the program then compares it to the lower threshold (Eh_{lo}). If it is below the lower threshold, a second pump is turned on for a prescribed time *t* delivering a pulse of nitrate nutrient solution to the microcosm, under

the assumption that nitrate is limiting to the denitrifying microbial metabolism. If the measured *Eh* is between the upper and lower threshold values, no action is taken. The program then waits a user-defined time *T*, takes another *Eh* reading, compares it to the thresholds, and decides whether or not to take pump action. This sequence is repeated indefinitely until intervened by the user.

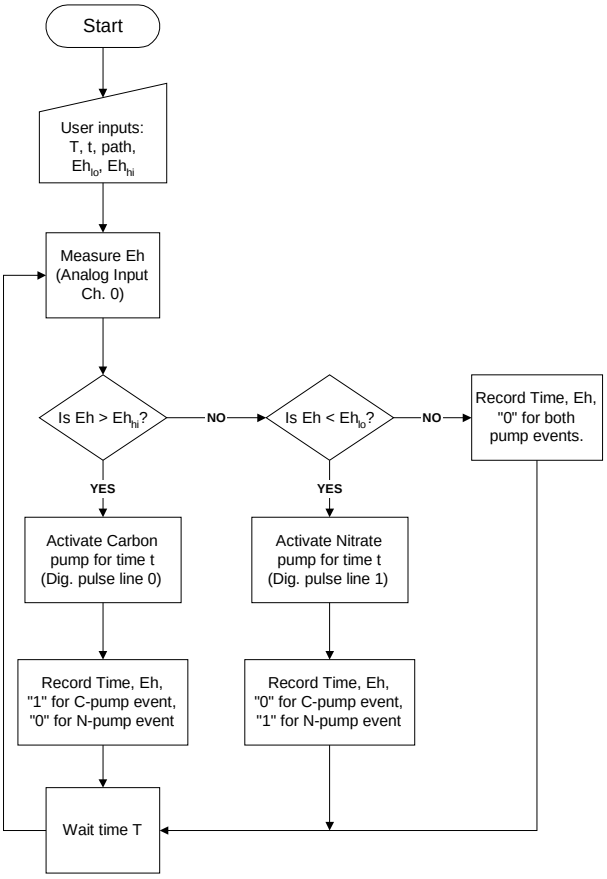

Figure 4. 5. Flow chart for redox potential control program with nitrate/carbon source selection.

A detailed view of the LabVIEW programming, including a discussion on the design and use of the front panel user interface, is included in Appendix A.

4.2.3 Redox Electrodes

The measurement of redox potential is performed with a platinum-tipped electrode and a reference cell electrode. The platinum-tipped electrodes used in this experiment were manufactured by Jensen Instruments (Tacoma, Washington) by special order. Each electrode (model S75.0) is made from a 0.75 m long stainless steel shaft surrounding an insulated copper wire. On one end of each electrode, a removable ceramic tip with an embedded length of platinum wire (model E0) is screwed on such that the platinum wire contacts the inner copper wire. A rubber O-ring gasket between the ceramic tip and the stainless steel shaft seals and protects the platinum/copper junction. A brass electrode tip is permanently installed on the other end of the shaft, to which connectors or alligator clips from a voltmeter or other measuring device can be attached. The brass end of each probe was connected to the respective analog input channel (Channels 0-3 on pins 3, 5, 7, and 9) on the CB-50 connector block using 14-AWG copper wire and alligator clips.

Over time and after repeated use, the platinum tips of the redox probes may build up organics and oxidized compounds, thus affecting their calibration (Patrick et al. 1996). To mitigate this as a potential problem, the platinum tips of the redox probes were periodically cleaned with Ajax cleanser, washed thoroughly, and calibrated using a pH-buffered quinhydrone solution, according to guidelines detailed in Patrick et al. (1996). Detailed description of these methods are included in Appendix D.

4.2.4 Calomel Reference Probe

For all redox potential measurements in this experiment, a saturated calomel electrode was used as the reference electrode. The electrode used was an Accumet

standard size glass body calomel reference electrode (number 13-620-51, s/n 2294019, Fisher Scientific, Hampton, New Hampshire) filled with a saturated KCl solution provided by the manufacturer. This probe was connected to the analog input channels 8-11 (pins 4, 6, 8, and 10) on the CB-50 connector block to allow differential measurement of the redox potential.

4.2.5 Salt Bridge

In all experiment trials, redox potential was measured from at least two and sometimes three soil microcosms simultaneously. In order to reduce the error that might be introduced from using multiple reference electrodes, all redox measurements for each trial were made using the same reference electrode described above. This was accomplished by immersing the tip of the reference electrode in a 1 M KCl solution bath in a beaker and installing a flexible agar salt bridge between this KCl bath and each microcosm. An agar salt bridge is often used to create an electrochemical connection between two separate containers while minimizing the transfer of ions between them (Warner Instruments, 1999). The salt bridges were constructed in the lab using disposable 1.0-mL plastic pipettes attached end-to-end with 0.25 m of 1/8” diameter vinyl tubing. An ionic agar solution was prepared using 3 g of agar in 100 mL of 1M KCl solution. The solution was heated on a hot plate until the agar dissolved, at which point a suction pump was used to draw the liquid agar into the length of the salt bridge tubing. Once cooled, each salt bridge was tested during redox probe calibration to ensure ionic continuity.

4.3 Nutrient Delivery System

A system was designed to deliver the nutrient solutions (either carbon or nitrate) to the soil microcosms based upon the outcome of the algorithm performed by the data acquisition computer. This system consists of two pumps (one for each type of nutrient) powered by relays activated by a digital pulse from the computer's data acquisition and control board.

4.3.1 Pumps

The pumps used for nutrient delivery are Manostat Varistaltic peristaltic pumps (p/n 72-335-000). Two separate pumps were used: one pump (s/n 3424) installed on digital line 0 and used for carbon delivery in all experiments; and the second pump (s/n 3425) installed on digital line 1 and used for either carbon or nitrate solution delivery, depending upon the type of experimental trial. Each pump has an adjustable flow rate controlled by a potentiometer dial on its front face. Each pump potentiometer was initially calibrated using a stopwatch and graduated cylinder to deliver at the minimum rate possible for the pump (approximately 2 ml sec-1 for each pump). After the pumps were connected to the computer, they were recalibrated again by programming the computer to repeatedly send a 1-second digital pulse to activate each pump separately, interspersed with a 10-second stop period; the volume of fluid pumped during each of these 1-s pulse activations was collected and measured in a 10-ml graduated cylinder.

Throughout the course of all trials, the pumps were periodically adjusted and recalibrated to approximately 2±0.4 ml sec-1.

4.3.2 Pump Control Relays

Each pump was plugged into a separate 120-VAC switched outlet controlled by a solid-state relay (Potter & Brumfield, Series SSRT). Each relay, in turn, was hard-wired into the respective digital I/O line (lines 0 and 1) on the CB-50 connector block. When the data acquisition system decides to take action based upon an *Eh* measurement, it sends a 5V digital signal of user-defined length *t* to the proper digital line, activating the relay and switching on 120-VAC power to the electrical outlet for the respective pump. A wiring diagram for the outlet switch relay is shown in Figure 4. 6.

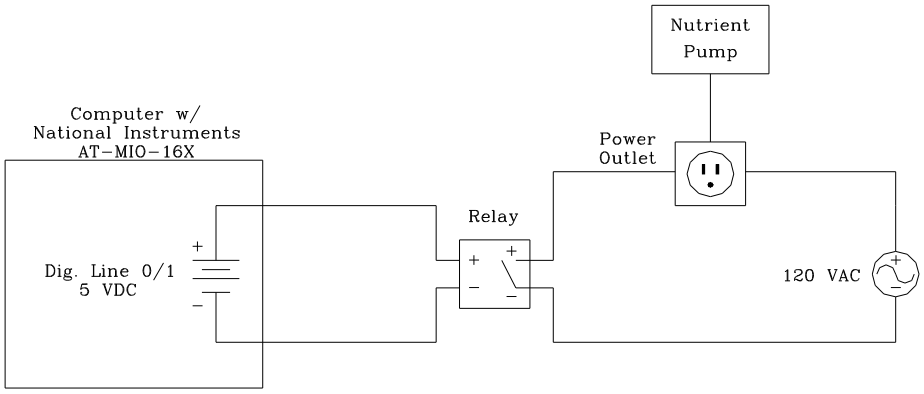

Figure 4. 6. Wiring schematic for relay-controlled power outlet for nutrient pumps.

4.4 Wetland Soil Microcosms

After some trial and error in early experimental trials with different substrates and with different procedures for microcosm construction, all microcosms in later trials were set up using the same soil substrate and the same standardized procedure. Only those microcosm experiments that used the standardized substrate and setup procedure are reported on in this document.

4.4.1 Soil and Site Description

The soil used for all microcosms following standardization of procedures was collected periodically from a site in the U.S. Department of Agriculture's Agricultural Research Center in Beltsville, Maryland. The site is a forested wetland area surrounded by agricultural fields of primarily corn and soybeans. A view of the site from which soil was collected for this series of experiments is shown in Figure 4. 7.

Figure 4. 7. View of the soil collection site in the USDA's ARS forested wetland in Beltsville, Maryland.

A sample of the soil was sent to the Soil Analysis Laboratory at Cornell University for a suite of physical and chemical analyses, the results of which are given in Table 4. 1.

Table 4. 1. Physical and chemical parameters of the USDA ARS forest wetland soil, sampled for analysis in July 2001. Analysis performed by the Cornell University Nutrient Analysis Laboratory.

Parameter	Units	ARS Value
Moisture content	%	1.301
P, available	mg/kg	5.8
K, available	mg/kg	38
Mg, available	mg/kg	315.3
Ca, available	mg/kg	1074
Fe, available	mg/kg	54.5
Al, available	mg/kg	87.2
Mn, available	mg/kg	17.1
Zn, available	mg/kg	10.59
Cu, available	mg/kg	1.5
pH in water	pH	5.53
Exchange Acidity	cmol/kg	16.47
Organic matter (loss on ignition)	%	10.41
NO_3, available	mg/kg	0.00
P, $Mg(NO_3)_2$ Ash	%	0.10
N, total N	%	0.33

4.4.2 Microcosm Construction

Once standardized set-up procedures were determined and established, all microcosms for all experiments were set up following these procedures. First, wetland soil was harvested from approximately 20 cm depth from the USDA ARS site with a shovel and bucket. The soil was brought back to the lab, and all large woody debris (sticks and roots) was removed. A sample of soil was then removed from the bucket by hand, and 300 g (±1 g) was measured using a tared balance. This 300 g sample was then transferred to a 1.0-L jar (Figure 4. 8). Following this, 300 mL of distilled water was

added to each microcosm, and each was swirled gently to facilitate rapid settling. A lid was tightly screwed onto each microcosm. Each lid had four holes punched into it: one for a redox electrode, one for the salt bridge capillary hose, and two for capillary hoses from the nutrient pumps. If a particular microcosm was not to receive nutrients from the pumps, the extra holes were plugged with parafilm for that particular experimental trial.

Figure 4. 8. Picture of standard wetland soil suspension microcosm in a 1-L jar.

5.0 PROCEDURES

5.1 Experimental Design

The physical microcosm experiments were undertaken specifically to investigate the effects of the addition of energy source feedback control on the metabolism of wetland soil microcosms as indicated by the controlled variable of redox potential. Two general types of experiments were performed: carbon addition experiments, and carbon/nitrate selection experiments.

All trials for both carbon addition and carbon/nitrate selection experiments were performed sequentially over time. Overall, various treatment were implemented in the successive trials. Some trials were performed with the same treatments as those previously in attempts to replicate results for that particular treatment. Other trials received treatments that were different from previous trials in attempts to explore the range of resulting system behavior. Each trial was set up according to the general procedures described below and typically allowed to proceed from one to seven days. Each trial comprised an experimental microcosm that received the selected treatment and a control microcosm that received no treatment. The data recorded were redox potential over time for both the experiment and control microcosms at the selected sampling rate (typically once every 30 minutes). Additional nutrient concentration data were collected for certain trials of the nitrate/carbon selection experiments.

5.1.1 Carbon addition experiments

Data analysis for the carbon addition experiments entailed the analysis of the time-based curves of redox potential, evaluated for the effect of the various treatment for each trial on redox potential compared to the respective control. The analysis entails the following:

- A qualitative analysis of the predominant characteristics of the redox potential curves, summarizing each trial for total run time, time length of carbon pump activation, initial (first 10 hours) and total change in redox potential, trend in redox curve over time, and relation of the redox potential curve to that of the control for the same trial;
- An analysis of the means initial and total change in redox potential over time for all experimental trials;
- An analysis of the mean value and rate of change of redox potential at each time step for all trials, comparing each with the controls group via a t-test at each time step.

5.1.2 Carbon/Nitrate addition experiments

Data analysis for the nitrate/carbon selection experiments entailed the analysis of the time-based curves of redox potential, evaluated for the effect of the various treatment for each trial on redox potential compared to the respective control. The analysis entails a qualitative analysis of the predominant characteristics of the redox potential curves, a

semi-quantitative analysis of the predominant trend of the redox curves, and a quantitative mass-balance analysis on the amount of nitrogen added to the microcosms.

5.2 General Procedures

The experiments performed may be classified as two general types: carbon addition (trials 1-12, 19, and 30), and carbon/nitrate selection (trials 13-18, 20-29, and 31). Both types of experimental trials followed the same general procedure. All trials were performed in sequence through time, and care was taken to replicate each trial as much as possible when appropriate. However, there exists some variation in procedure as different combinations of nutrient type and control system settings were tried.

The generalized procedure followed for all trials is as follows:

- Soil was freshly harvested from the USDA ARS forested wetland, brought back to the lab, and prepared as described previously.
- The soil suspension microcosms were prepared as described previously, covered, placed at the experiment station close to the data acquisition computer, and allowed to sit at least 30 minutes to allow fine soil particulates to settle. At least two microcosms were prepared at one time—one (or more) to serve as the experimental unit or units, and one to serve as the control.
- Water samples for nutrient analyses (performed for trials 26, 27, and 29 only) were taken as necessary using a syringe.

- While the microcosms were settling, the nutrient reservoirs were prepared in 0.25 or 0.5 L batches by mixing a measured amount of dry chemicals with a measured volume of distilled water to create the desired concentration.
- In some trials (trials 26, 27, and 28), when available, nitrogen gas was bubbled through the nutrient solution reservoirs for at least 15 minutes to remove dissolved oxygen. As a check, dissolved oxygen was confirmed to be below 0.1 mg/L measured with a dissolved oxygen meter (model 85D combination meter, s/n 01G0076-AC, YSI Corp., Yellow Springs, Ohio). Once a low dissolved oxygen concentration was confirmed, the reservoirs were covered with a sheet of paraffin film paper.
- The pump hoses were flushed with clean distilled water to remove old solution from previous trials. This was performed by first running the pumps until the hoses were dry, then running the pumps until clear distilled water from a water reservoir was observed flowing from the hose outlet. The pumps was then run until the hoses were dry again, the reservoirs were filled with nutrient solution, and the pumps run again until nutrient solution was observed flowing from the hose outlet. The pump rate calibration was checked and adjusted at this time, if necessary.
- The redox probe tips were cleaned, rinsed thoroughly, and calibrated using the data acquisition computer and a pH-buffered quinhydrone solution, as described above. The probes closest to the ideal calibration values (usually two probes, but some trials used four) were selected to use in the trial.

- A redox probe was inserted into each microcosm through a hole in the microcosm cap such that the platinum tip of the probe was deep in the soil layer and nearly touching the bottom of the microcosm jar.
- The redox probes were connected to their respective data acquisition channels using wire and alligator clips.
- The calomel reference probe remained connected to its data acquisition channels for all experiments. Its connection was visually inspected to ensure a solid connection. Also, the level of KCl solution in the reservoir was visually inspected, and 1.0 M KCl solution was replaced if the level was low.
- A salt bridge was inserted into each microcosm such that its tip was below the water level in the microcosm. The other end of the salt bridge was submerged in the KCl reservoir.
- The computer data acquisition program was activated for a short time to check that redox potential readings were being taken from all the connected probes. If any reading looked suspicious (e.g. rapidly changing values with a high variability), all connections were rechecked and reseated until consistent readings were observed.
- Hose ends from the nutrient pump or pumps were inserted through holes in the cap of the experimental microcosm such that the tip of the hose was below the level of the soil. Any remaining holes in the caps to the microcosms were then plugged with paraffin film.
- The required user inputs to the data acquisition program were entered. These inputs included the Eh threshold values, the time between samples, the pump

activation time interval, the pump period respective to the sampling period, and the path and file names for recording data.

- The program was activated and the start time recorded. The program was allowed to run unimpeded for a length of time, usually at least for 24 hours, but sometimes for up to 2 weeks.

5.3 Specific Procedures According to Experiment Type

Two types of experimental trials were performed: carbon addition (trials 1-12, 19, and 30), and carbon/nitrate selection (trials 13-18, 20-29, and 31). Replication was attempted at various times to provide a basis for statistical analyses to elucidate trends. However, because soil was harvested at different times of the year as the experiments progressed, replication can only be loosely assumed. The specific procedures and trial configurations for all experiment trials are presented here, organized by general experiment type (carbon addition or carbon/nitrate selection).

5.3.1 Carbon Addition Experiments

The carbon addition experiments were the first series of experiments to be performed. The intention was to explore the effects of carbon addition on the change in redox potential over time. The basic assumption underlying the automatic addition of carbon was that it was limiting to the metabolism of the soil microbial community, reflected by a high redox potential. Thus, if the redox potential is above a certain threshold value, carbon could be accessed by the microcosm via computer control

system, spurring additional metabolism until the redox potential falls below the threshold value. This logic sequence was presented earlier in the carbon addition flow chart in section 4. In all, 11 separate carbon injection experimental trials were performed using USDA ARS soil as the substrate. These trial configurations are summarized in Table 5. 1.

Table 5. 1. Trial configurations for carbon addition experiments.

Trial No.	Date started	Trial Length (hr)	Age of Soil[1] (d)	Micro-cosm No.	Thresh-holds[2] (mV)	Nutrient Reservoirs	Nutr. Pump No.	Pump flow rate (mL/sec)[3]
01	6/27/01	98.5	0	01-01	+45	100% Methanol	0	2.2(±0.03)
				01-02	control			
05	7/25/01	40.5	0	05-01	+45	100% Methanol	0	1.6(±0.09)
				05-02	control			
06	7/27/01	40.5	2	06-01	+45	100% Methanol	0	1.6
				06-02	Control--Data lost			
07	7/31/01	23.5	0	07-01	+45	100% Methanol	0	1.6
				07-02	control			
				07-03	-755	100% Methanol	1	1.4(±0.14)
08	8/1/01	23.5	1	08-01	+45	100% Methanol	0	1.6
				08-02	control			
				08-03	-755	100% Methanol	1	1.4
09	8/2/01	23.5	0	09-01	+45	100% Methanol	0	1.6
				09-02	control			
				09-03	-755	100% Methanol	1	1.4
10	8/3/01	47.5	1	10-01	-55	50% Methanol	0	1.6
				10-02	control			
				10-03	-55	Synth. Sewage	1	1.4
11	8/6/01	47.0	0	11-01	-55	100% Methanol	0	1.6
				11-02	control			
				11-03	-55	Synth. Sewage	1	1.4
12	8/8/01	40.0	2	12-01	-55	100% Methanol	0	1.6
				12-02	-55	1M CH_3COONa	1	1.4
				12-03	Control			
19	2/4/02	100.0	5	19-01	-155	Tryp. Soy Broth	0	1.6
				19-02	Control			
30	6/10/03	50.0	0	30-01	-5	2M CH_3COONa	0	2.0
				30-02	Control			
				30-03	-5	Water	1	2.0

NOTES:

[1]Length of time (days) between soil harvest and start of trial.

[2]Threshold setpoint for the DAQ computer, above which the nutrient pump was turned on.

[3]Mean and standard deviation (in parentheses) based upon measurement with a 10-mL graduated. cylinder. For those trials without s.d. reported, flow rates were assumed from previous trials.

The trials were undertaken as experimental exploration to elucidate variations in system behavior resulting from different initial conditions and trial configurations. Some continuity of procedure was maintained between all trials making them rough replicates of each other. Most trials were performed over the summer of 2001. The length of each trial varied, although all were allowed to continue for at least one day. The age of the soil varied for all trials too; while it was generally desirable to have fresh soil for each trial, outdoor conditions and vehicle availability often prevented the collection of fresh soil samples. Each time soil was harvested, it was stored in a covered bucket in the laboratory for possible use in the next trial (hence, for some trials, the age of soil is greater than zero). Each microcosm was given a number, where the 01/03 units were the experiments and 02 were the controls. For each experiment trial, the control unit was a sealed microcosm in which redox potential was measured and recorded and no nutrient addition was made, and the experiment unit was another sealed microcosm into which carbon nutrient solution was injected automatically by the computer control system. The thresholds for activating nutrient injection for each trial were set at an arbitrary level close to the level of reducing conditions. In some trials (for example, numbers 7, 8, and 9), a second experimental unit was set up feeding from the same nutrient source but with a lower threshold. The nutrient reservoir used in most cases was a pure methanol solution, although other carbon sources (1.0 M sodium acetate solution, synthetic sewage, and tryptic soy broth) were tried in later trials. Generally, the nutrient pump flow rates were held constant between trials, although periodic equipment failures necessitated recalibration. In some trials, the data were lost because of equipment failures or were unusable because of procedural variation. For example, equipment failure on trial 6

caused a loss of data for the control unit. Data for all other trials were collected without incident and are reported as results.

5.3.2 Carbon/Nitrate Selection Experiments

The carbon/nitrate selection experiment trials generally followed completion of the series of carbon addition experiments. The intention was to explore the possibility of engineering a system that controls access to its own limiting factors. This was set up experimentally by allowing it to maintain the redox potential within a certain zone, in this case, the zone ideal for denitrification (+200 to +250 mV) as reported in Patrick, et al. (1996). The basic assumption underlying this set of experiments was that, if the redox potential remained high, carbon was limiting to the metabolism of the soil microbial community, and thus should be added if redox is above a certain threshold value. If redox potential fell too low (particularly, if it fell below the theoretical range indicating nitrate reduction), then nitrate was limiting to the metabolism of the soil denitrifiers and should be added. This logic sequence was presented earlier in the nitrate/carbon selection flow chart in section 4. In all, 13 separate carbon/nitrate selection experimental trials were performed using USDA ARS soil as the substrate. These trial configurations are summarized in Table 5. 2.

Table 5. 2. Trial configurations for carbon/nitrate selection experiments.

Trial No.	Date started	Trial Length (hr)	Age of Soil[1] (d)	Micro-cosm No.	Thresh-holds[2] (mV)	Nutrient Reservoirs	De-Aerate Nutrients?[3]	Pump No.	Pump flow rate (mL/sec)[4]
13	8/13/01	49.0	7	13-01	+300 (upper)	1M CH_3COONa	No	0	1.6
					+150 (lower)	1M KNO_3	No	1	1.4
				13-02	control				
14	8/15/01	80.0	9	14-01	+250 (upper)	2M CH_3COONa	No	0	1.6
					+200 (lower)	1M KNO_3	No	1	1.4
				14-02	control				
15	9/1/01	250.0	0	15-01	+250 (upper)	2M CH_3COONa	No	0	1.6
					+200 (lower)	1M KNO_3	No	1	1.4
				15-02	control				
16	9/19/01	120.0	19	16-01	+250 (upper)	2.5M CH_3COONa	No	0	1.6
					+200 (lower)	2.5M KNO_3	No	1	1.4
				16-02	control				
20	4/12/02	118.0	0	20-01	+250 (upper)	2M CH_3COONa	No	0	2.0(±0.11)
					+200 (lower)	1M KNO_3	No	1	2.0(±0.00)
				20-02	control				
21	4/17/02	350.0	5	21-01	+205 (upper)	2M CH_3COONa	No	0	2.0
					+195 (lower)	1M KNO_3	No	1	2.0
				21-02	control				
22	5/7/02	57.0	0	22-01	+205 (upper)	2M CH_3COONa	No	0	2.0
					+195 (lower)	1M KNO_3	No	1	2.0
				22-02	control				
23	COMPUTER CRASH--DATA LOST								
24	COMPUTER CRASH--DATA LOST								
25	5/24/02	310.0	0	25-01	+200 (upper)	2M CH_3COONa	No	0	2.0
					+200 (lower)	1M KNO_3	No	1	2.0
				25-02	control				
26	6/6/02	300.0	0	26-01	+200 (upper)	2M CH_3COONa	Yes	0	2.0
					+200 (lower)	1M KNO_3	Yes	1	2.0
				26-02	control				
27	6/20/02	150.0	0	27-01	+200 (upper)	2M CH_3COONa	Yes	0	2.0
					+200 (lower)	1M KNO_3	Yes	1	2.0
				27-02	control				
28	7/22/02	98.0	0	28-01	+200 (upper)	2M CH_3COONa	Yes	0	2.0
					+200 (lower)	1M KNO_3	Yes	1	2.0
				28-02	control				
29	5/27/03	233.0	0	29-01	+200 (upper)	2M CH_3COONa	No	0	2.0
					+200 (lower)	1M KNO_3	No	1	2.0
				29-02	control				
31	7/25/03	70.0	0	31-01	+200 (lower)	1M KNO_3	No	0	2.0
				31-02	control				
				31-03	+200 (lower)	Dist. Water	No	1	2.0

NOTES:

[1]Length of time (days) between soil harvest and start of trial.

[2]Threshold setpoints for the DAQ computer, above or below which the nutrient pumps were turned on.

[3]In some trials, N_2(gas) was bubbled through the nutrient solution before the trial began to remove dissolved O_2.

[4]Mean and standard deviation (in parentheses) based upon measurement with a 10-mL graduated cylinder. For those trials without s.d. reported, flow rates from previous trials were assumed.

As with the carbon addition experiments, the nitrate/carbon selection experiments were conducted as experimental exploration to elucidate variations in system behavior resulting from different initial conditions and trial configurations. Some continuity of procedure was maintained between all trials making them rough replicates of each other. Generally, the nitrate/carbon selection scenario trials were commenced following carbon addition trials in the summer of 2001 and continued through much of 2002. The length of each trial varied, although all were allowed to continue for at least two days, and some were allowed to continue extensively for weeks. Also, the age of the soil varied for all trials; as with the carbon experiments, while it was generally desirable to have fresh soil for each trial, conditions often prevented the collection of fresh soil samples. Again, each time soil was harvested, it was stored in a covered bucket in the laboratory for possible use in the next trial (hence, for some trials, the age of soil is greater than zero). Each microcosm was given a number, where the 01 units were the experiments and 02 were the controls. As with the carbon addition experiments, the controls were sealed microcosms in which redox potential was measured and recorded and no nutrient addition was made. The thresholds for the experimental unit of each trial were set at levels generally in the range defining nitrate reduction in wetland soils (approximately +200 to +250 mV) as reported in Patrick, et al. (1996), although this range was narrowed in later trials. The nutrient reservoirs used was in most cases a 2.0 M sodium acetate solution for the carbon source, and a 1.0 M potassium nitrate solution for the nitrate source (Koch and Oldham, 1985), although different concentrations were tested in two trials (trials 13 and 16). Removal of dissolved oxygen from the nutrient reservoirs prior to the trial was attempted for three trials (nos. 26, 27, and 28). The nutrient pump flow rates were recalibrated only

once during the sequence of trials and was held constant for all trials before and after this calibration. The flow rates for each nutrient of each trial are indicated in the table.

As in the carbon experiments, the data from some trials were lost because of equipment failures. A computer hard-drive failure occurred on Trial 23, and repeated on Trial 24. All data from these trials were lost as a result. Data for all other trials were collected without incident and are reported as results. In addition, in three trials (trials 26, 27, and 29), samples were taken from the microcosm water column and analyzed for nitrate and ammonia concentration for mass-balance analyses on nitrogen.

6.0 RESULTS

6.1 Carbon Addition Experiments

Following is a summary discussion of each of the experimental trials for the carbon addition scenario experiments. Accompanying the discussion for each trial is a chart showing redox potential versus time for the microcosm units in each trial. Each chart compares the change in redox potential for the experimental microcosm (the one receiving carbon addition) with that of the control microcosm (one receiving no addition).

6.1.1 Trial 1: Methanol Addition to Wetland Soil Microcosm

The first experiment was commenced in the laboratory on 27 June 2001. Fresh soil was collected from the USDA ARS forest. Two microcosms were constructed (units 01-01 and 01-02). The units were constructed following the general procedures outlined in the Procedures section and allowed to sit overnight. Each was connected to the DAQ computer via platinum redox probe and calomel probe, and the experimental unit receiving treatment (unit 01) was connected to the hose of the nutrient delivery pump. The carbon solution reservoir for the nutrient pump was filled with methanol (CH_3OH) solution (pure concentration), and the pump calibrated to deliver a flow rate of 2.2 (±0.03) $ml \cdot s^{-1}$. The sample period was set to 1800 s (1/2 hour), and pump time was set to 1 s, and the threshold *Eh* voltage (above which carbon solution was added) was set to +45 mV. The experiment was initiated and allowed to proceed for 98.5 hours.

Results were immediately obvious within the first 6 hours. As expected, all units showed a decrease in redox potential over time as soil microbial metabolism created more reducing conditions (Figure 6. 1). For the experimental unit, the controlled addition of carbon solution occurred for the first 4.5 hours, driving the redox potential down at a faster rate than the control unit not receiving any addition, as was expected (Figure 6. 1). The experimental unit then remained more highly reduced for the remainder of the trial length. In total, the carbon injection pump was activated for 9 events.

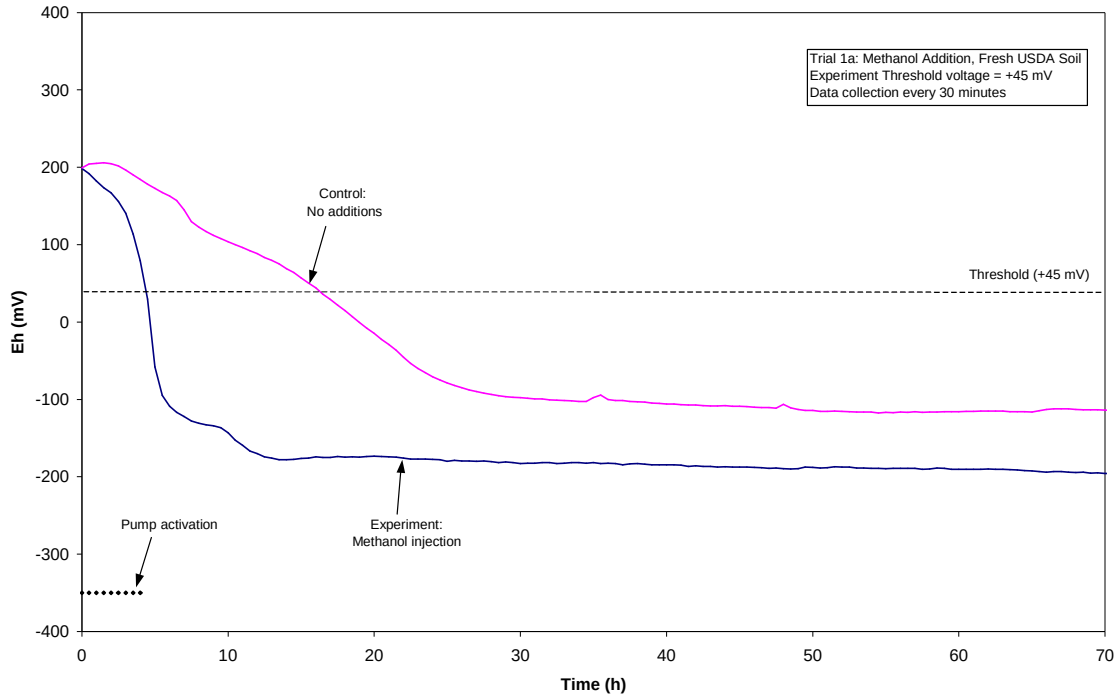

Figure 6. 1. Results for Trial 1. Redox potential vs. time for soil microcosm with methanol solution added by controlling computer.

6.1.2 Trial 5: Repeat of Trial 1.

The next experiment was commenced in the laboratory on 25 July 2001 as an attempt to repeat Trial 1. Fresh soil was collected from the USDA ARS forest site, and

two soil microcosms were constructed (units 05-01 and 05-02). The units were constructed and sealed following the general procedure outlined above and allowed to sit for 1 hour. Each was connected to the DAQ computer via platinum redox probe and calomel probe, and the experimental unit receiving treatment (unit 01) was connected to the hose of the methanol delivery pump. The pump reservoir was filled with fresh methanol (CH_3OH) solution (pure concentration). The pump was checked and recalibrated for a lower flow rate at 1.6 (±0.09) $ml \cdot s^{-1}$. The sample period was set to 1800 s (1/2 hour), and pump time was set to 1 s. The threshold *Eh* voltage (above which carbon solution was added) was set to +45 mV for unit 01. The experiment was initiated and proceeded for 40.5 hours.

Results for Trial 5 were similar to Trial 1. Initially, both the experimental unit (05-01) and the control unit (05-02) showed an increase in redox potential before decreasing again, possibly due to oxygen introduced during construction of the microcosms (Figure 6. 2). The redox potential in the experimental unit, however, peaked approximately 3 hours earlier than the control, due likely to the automatic addition of carbon. Both the experiment and the control showed the expected decrease in redox potential over time. The experimental unit, however, showed a greater rate of decrease within the first 10 hours, presumably because of the carbon addition. The experimental unit also exhibited oscillation of the redox potential beyond hour 20, a phenomenon as yet unexplained. The controlled addition of carbon occurred for all 40.5 hours of the trial, driving down the redox potential in the experimental unit but not below the control program threshold setpoint. In total, the carbon solution injection pump was activated for 82 events.

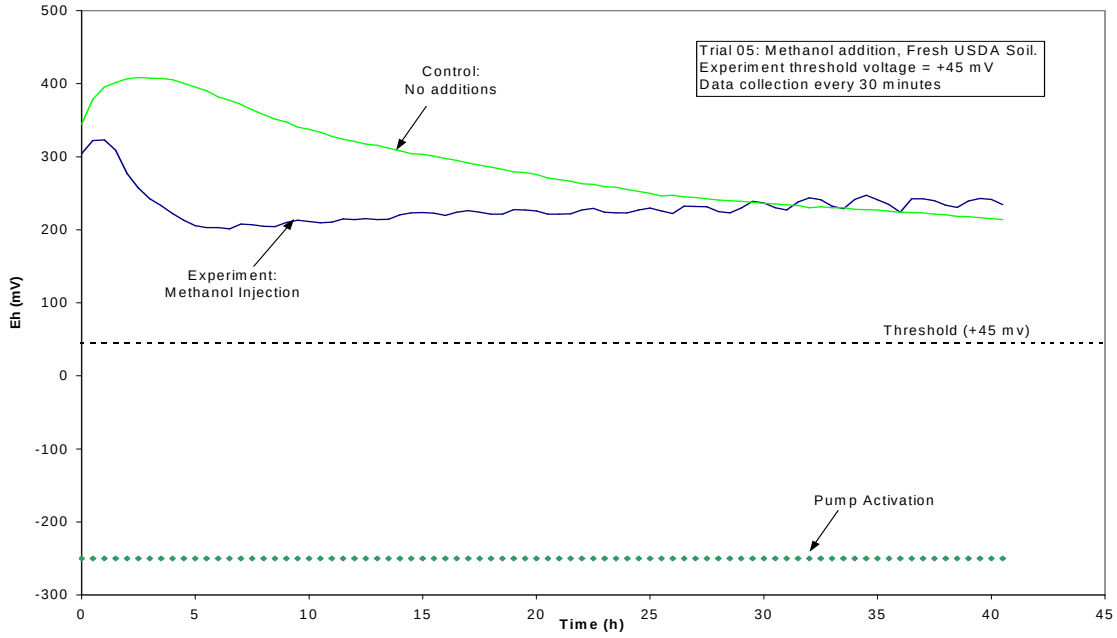

Figure 6. 2. Results for Trial 5: Redox potential vs. time for soil microcosms with pure methanol solution added by controlling computer (repeat of Trial 1).

6.1.3 Trial 6: Repeat of Trial 1.

The next experiment was commenced in the laboratory on 27 July 2001 as another attempt to repeat Trial 1. The same USDA ARS forest soil collected for Trial 5 was used after storage for two days at 4°C. From this soil, two new microcosms were constructed (units 06-01 and 06-02). The units were constructed and sealed following the general procedure outlined above and allowed to sit for 1 hour. Each was connected to the DAQ computer via platinum redox probe and calomel probe, and the experimental unit receiving treatment was connected to the hose of the methanol delivery pump. The pump reservoir was filled with fresh methanol (CH_3OH) solution (pure concentration). The pump delivery rate was kept at 1.6 (±0.09) $ml \cdot s^{-1}$. The sample period was set to 1800 s (1/2 hour), and pump time was set to 1 s. The threshold *Eh* voltage (above which carbon

solution was added) was set to +45 mV for the experimental unit. The experiment was initiated and proceeded for 40.5 hours.

A computer malfunction prevented the recording of redox potential data for the control unit. However, results for the experimental unit of Trial 6 were similar to Trial 5. Initially, the experimental unit showed an increase in redox potential before decreasing again, again possibly due to oxygen introduced during construction of the microcosms (Figure 6. 3). The redox potential in the experimental unit peaked at approximately hour 3.5, later than the peak in trial 5. The experiment showed the expected decrease in redox potential over time, but the overall rate and magnitude of the drop were less than that exhibited in Trial 5. This may be due to effects of the cold 2-day storage on the soil microbial community, which may have reduced the overall bacterial count and thus the respiratory potential of the soil microcosm. The controlled addition of carbon occurred for the all 40.5 hours of the trial, driving down the redox potential only a little and not at all below the threshold setpoint. In total, the carbon injection pump was activated for 82 events.

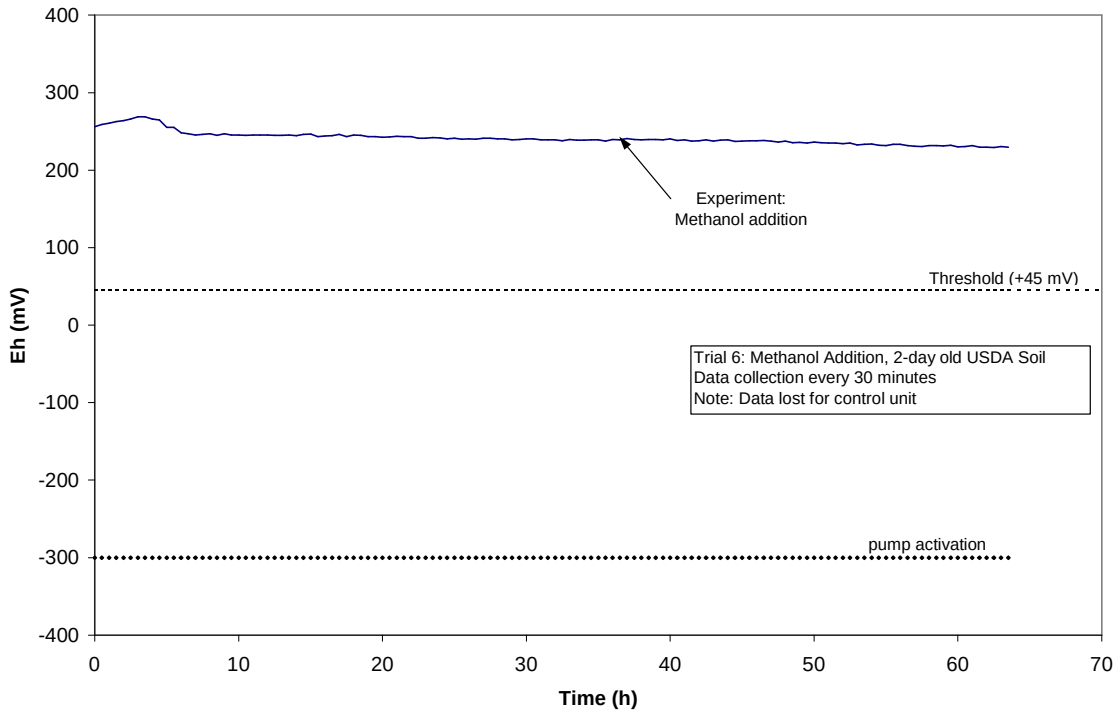

Figure 6. 3. Results for Trial 6. Redox potential vs. time for soil microcosms with pure methanol solution added by controlling computer (repeat of Trial 1).

6.1.4 Trial 7: Carbon Addition to USDA soil with two different thresholds.

Trial 7 was started in the laboratory on 31 July 2001, in part as an attempt to repeat Trial 1 and to investigate the effect of setting a lower threshold setpoint. Fresh soil was collected from the USDA ARS forest site, and three soil microcosms were constructed (units 07-01, 07-02, and 07-03). The units were constructed and sealed following the general procedure outlined above and allowed to sit for 1 hour. Each was connected to the DAQ computer via platinum redox probe and calomel probe, and the experimental units receiving treatment (units 01 and 03) were connected to the hoses of the methanol delivery pumps. The pump reservoir was filled with fresh methanol (CH_3OH) solution (pure concentration). The pump flow rate for the pump for

experimental unit 1 was kept at 1.6 (±0.09) $ml \cdot s^{-1}$, and the pump for experimental unit 2 was calibrated as closely as possible to the first pump to 1.4 (±0.14) $ml \cdot s^{-1}$. The sample period was set to 1800 s (1/2 hour), and pump time was set to 1 s. The threshold *Eh* voltage (above which carbon solution was added) was set to +45 mV for experimental unit 1 and –755 mV for experimental unit 2. The experiment was initiated and allowed to proceed for 23.5 hours.

Results for Trial 7 were unexpectedly contrary to previous results (Figure 6. 4). The control unit showed a gradual decrease in redox potential from an initial oxidized state, as in previous trials. The experimental units, however, despite an initial state more reduced than the control, showed an immediate increase in redox potential. Within 5 hours, the redox potential in both experimental units had reached a maximum around or above +300 mV, showing no indication of decreasing. The methanol pump was activated for both experimental units for the entire duration of the trial, as the redox potential never fell below the threshold setpoint. One explanation for this behavior might be that oxygen dissolved in the methanol solution was a sufficient enough quantity to maintain the microcosm in an aerobic state, reflected by the relatively high values of redox potential. In total, each of the carbon injection pumps was activated for 48 events.

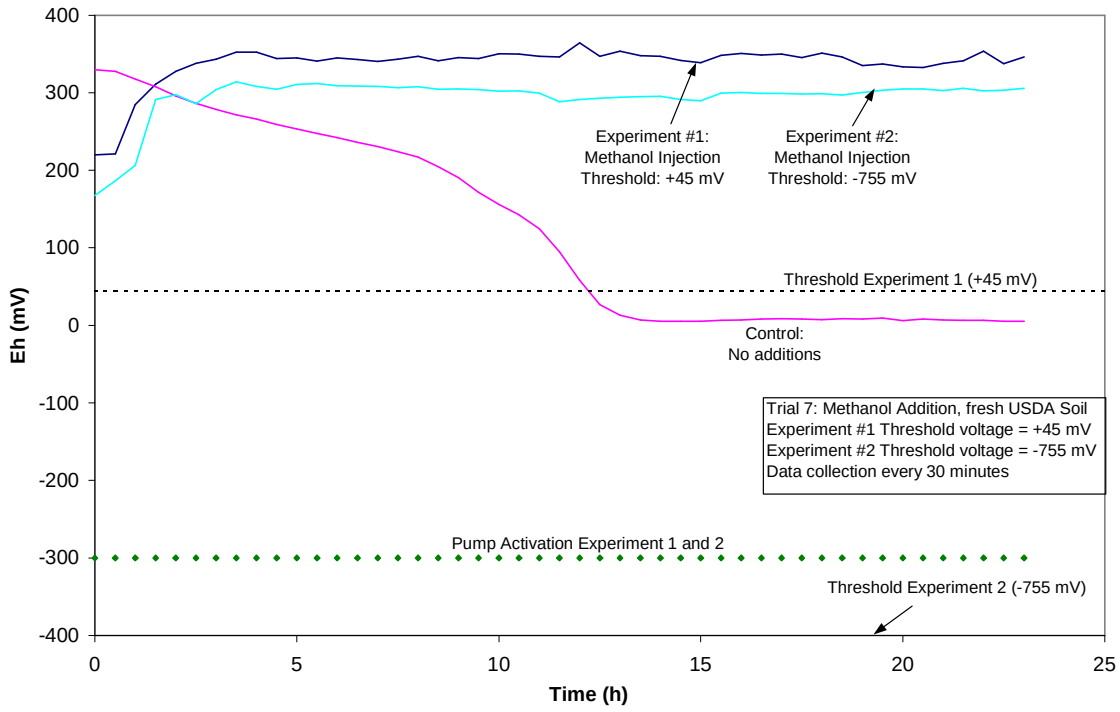

Figure 6. 4. Results for Trial 7: Redox potential vs. time for soil microcosms, each with a different threshold, with pure methanol solution added by controlling computer.

6.1.5 Trial 8: Repeat of Trial 7.

Trial 8 was started in the laboratory on 1 August 2001 as an attempt to repeat Trial 7, investigating the effect of setting a lower threshold setpoint. The same soil sample was used as in Trial 7 (24 hours old at this point), and three soil microcosms were constructed and sealed following the general procedure and allowed to sit for 1 hour. Each was connected to the DAQ computer via platinum redox probe and calomel probe, and the experimental units receiving treatment were connected to the hoses of the methanol delivery pumps. The pump reservoir was filled with fresh methanol (CH_3OH) solution (pure concentration). The pump flow rates were checked and kept at 1.6 (±0.09)

$ml \cdot s^{-1}$ for experimental unit number 1 and 1.4 (±0.14) $ml \cdot s^{-1}$ for experimental unit number 2. The sample period was set to 1800 s (1/2 hour), and pump time was set to 1 s. The threshold *Eh* voltage (above which carbon solution was added) was set to +45 mV for experimental unit 1 and –755 mV for experimental unit 2. The experiment was initiated and allowed to proceed for 23.5 hours.

Results for Trial 8 were similar to Trial 7 in that they were unexpectedly contrary to all other previous results (Figure 6. 5). The most noticeable aspect of the redox curves is the disparate initial conditions, where the control unit starts off nearly 150 mV below experiment no. 2 and over 200 mV below experiment no. 1. This points to either a problem with the calibration of the redox probes, or exemplifies the variability that might be expected due to biological and chemical heterogeneities in the wetland soil. Observing the relative change in redox potential over time for the three units, the control unit showed the greatest rate of decrease in redox potential, although the absolute change in redox potential is little more than 50 mV from its highest to its lowest value. Both experimental units showed a more gradual decrease in redox potential from the onset, the redox potential vs. time curves for each following parallel tracks. However, whereas the rate of change in redox potential for the control unit went from negative to zero (and then slightly positive) within the first 3 hours, the two experimental unit showed a negative rate of decrease in redox potential for the entire length of the trial. The redox values for both experimental units remained well above the threshold setpoint for the duration of the trial, and thus the methanol pump was activated every sample period for the entire trial length. In total, each of the carbon injection pumps was activated for 48 events.

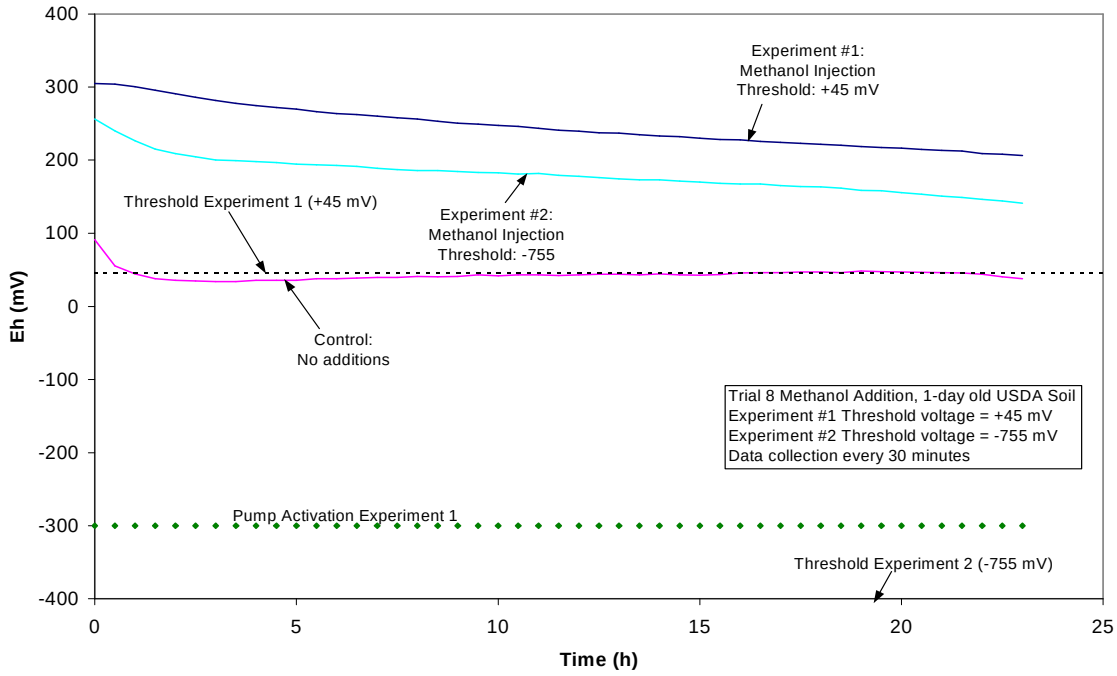

Figure 6. 5. Results forTrial 8: Redox potential vs. time for USDA soil microcosms, each with a different threshold, with pure methanol solution added by controlling computer.

6.1.6 Trial 9: Repeat of Trial 7.

Trial 9 was started in the laboratory on 2 August 2001 as another attempt to repeat Trial 7, investigating the effect of setting a lower threshold setpoint. Freshly harvested USDA ARS soil was used to construct three new soil microcosms following the general procedure. Each was connected to the DAQ computer via platinum redox probe and calomel probe via salt bridge, and the experimental units receiving treatment were connected to the hoses of the methanol delivery pumps. The pump reservoir was filled with fresh methanol (CH_3OH) solution (pure concentration). The pump flow rates were checked and kept at 1.6 (±0.09) $ml \cdot s^{-1}$ for experimental unit number 1 and 1.4 (±0.14) $ml \cdot s^{-1}$ for experimental unit number 2. The sample period was set to 1800 s (1/2 hour),

and pump time was set to 1 s. The threshold *Eh* voltage (above which carbon solution was added) was set to +45 mV for experimental unit 1 and –755 mV for experimental unit 2. The experiment was initiated and allowed to proceed for 23.5 hours.

Results for Trial 9 were again mixed (Figure 6. 6). In this trial, the initial conditions of all the replicates were relatively close to each other (within 25 mV). Again, the control unit unexpectedly showed the greatest rate of decrease in redox potential initially, dropping from around 195 mV to around 55 mV within the first two hours but showing little change after that. Experiment 1 likewise showed a rapid drop in redox potential, although not so great as the control. The state of redox decrease was maintained for a longer period of time, however, as the redox potential for experiment 1 fell below that of the control. Experiment 2, however, showed little total change in redox potential for the entire trial despite regular methanol addition for the entire length of the trial. This again points to the biological heterogeneities in the soil microcosms. The carbon injection pump was activated for experiment 1 for 9 events, whereas it was activated for experiment 2 for 48 events, the entire length of the trial.

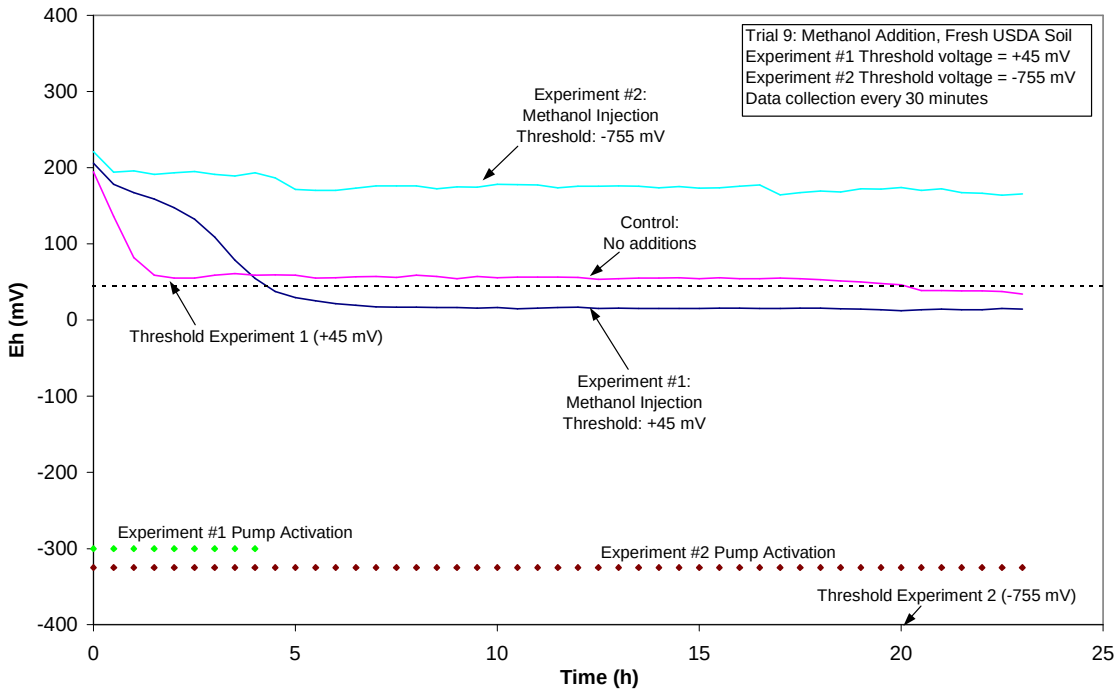

Figure 6. 6. Results for Trial 9: Redox potential vs. time for soil microcosms, each with a different threshold, with pure methanol solution added by controlling computer (repeat of Trial 7).

6.1.7 Trial 10: Experiment with different carbon sources.

Trial 10 was started in the laboratory on 3 August 2001 to test different carbon sources other than the pure methanol solution used. Results from previous trials seemed to indicate that the methanol solution might be inhibiting the microbial respiration in the microcosms. Two different carbon source reservoirs were thus made: one carbon solution was made from diluting the pure methanol solution with equal parts water, yielding a 50% methanol solution; and the second reservoir solution was made following a standard recipe for synthetic sewage (OECD, 1981). One-day old USDA ARS soil (the same soil sample used for Trial 9) was used to construct three new soil microcosms following the

general procedure. Each was connected to the DAQ computer via platinum redox probe and calomel probe via salt bridge. Experimental unit 1 was connected to the hose of the pump delivering the diluted methanol solution; experimental unit 2 was connected to the hose of the pump delivering the synthetic sewage solution. The pump flow rates were checked and kept at 1.6 (±0.09) $ml \cdot s^{-1}$ for experimental unit number 1 and 1.4 (±0.14) $ml \cdot s^{-1}$ for experimental unit number 2. The sample period was set to 1800 s (1/2 hour), and pump time was set to 1 s. The threshold *Eh* voltage (above which carbon solution was added) was set to -55 mV for both experimental units. The trial was initiated and allowed to proceed for 47.5 hours.

Results for Trial 10 were again mixed (Figure 6. 7). In this trial, while the initial conditions of the experimental units were relatively close to each other (within 10 mV), the initial redox state of the control was approximately 100 mV greater, due either to probe miscalibration or to microsite heterogeneities in the soil. The control unit exhibited the typical decreasing trend in redox potential at an average rate of decrease until approximately hour 37, when redox potential took a sudden sharp increase. This may possibly be due to oxygen leaking in to the microcosm. Experiment 1, receiving the methanol solution, had the greatest rate of decrease in redox potential, dropping approximately 100 mV within the first 3 hours before stabilizing out at approximately +30 mV. Experiment 2 likewise showed a decrease in redox potential over time, though at a slower rate than experiment 1. The redox potential in experiment 2, however, continued to decrease for the duration of the trial, possibly indicating that the synthetic sewage is a more appropriate carbon source. The pump delivering methanol solution to Experiment 1 was activated for 95 events (the entire length of the trial), whereas the

pump delivering synthetic sewage to experiment 2 was activated for 82 events (the first 40.5 hours of the trial).

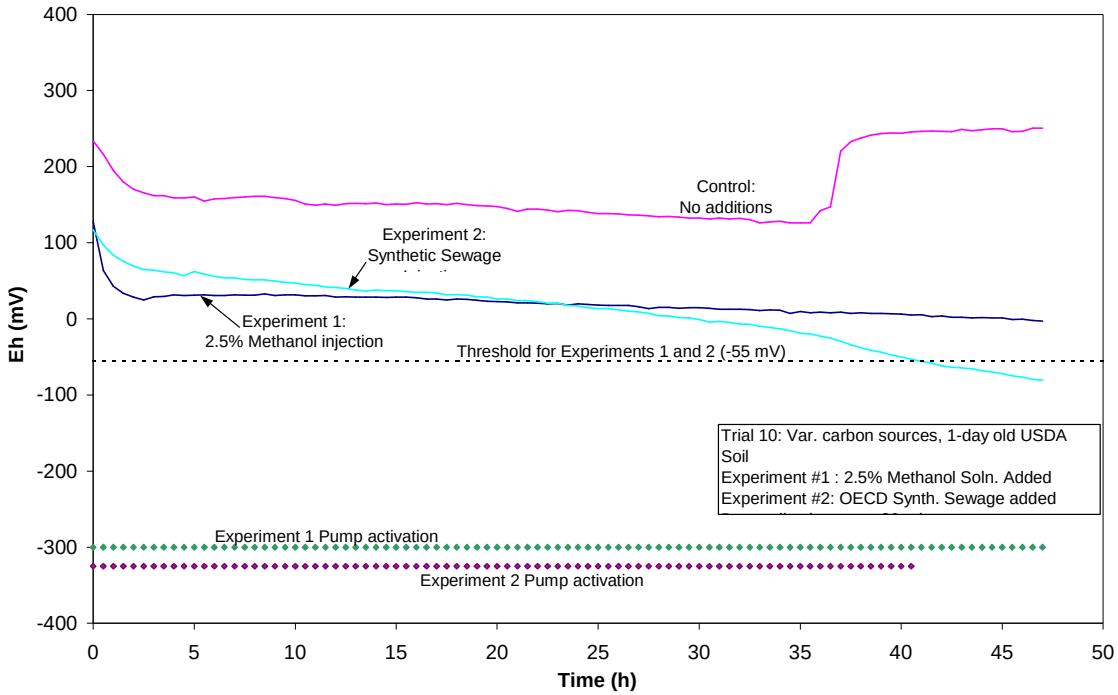

Figure 6. 7. Results for Trial 10: Redox potential vs. time for soil microcosms, each with different carbon sources than used previously.

6.1.8 Trial 11: Experiment with different carbon sources (repeat of Trial 10).

Trial 11 was started in the laboratory on 6 August 2001 to test the OECD synthetic sewage again as a source of carbon. Fresh USDA ARS soil was used to construct three new soil microcosms following the general procedure. Each was connected to the DAQ computer via platinum redox probe and calomel probe via salt bridge. Experimental unit 1 was connected to the hose of the pump delivering pure methanol solution, while experimental unit 2 was connected to the hose of the pump delivering the synthetic sewage solution. The pump flow rates were checked and kept at

1.6 (±0.09) $ml \cdot s^{-1}$ for experimental unit number 1 and 1.4 (±0.14) $ml \cdot s^{-1}$ for experimental unit number 2. The sample period was set to 1800 s (1/2 hour), and pump time was set to 1 s. The threshold *Eh* voltage (above which carbon solution was added) was set to -55 mV for both experimental units. The trial was initiated and allowed to proceed for 47.0 hours.

Results for Trial 11 were similar to Trial 10 (Figure 6. 8). Again, while the initial conditions of the experimental units were relatively close to each other (within 10 mV), the initial redox state of the control was almost 200 mV greater, due either to probe miscalibration or to microsite heterogeneities in the soil. The control unit showed appreciable decrease in redox potential over time, calling into question the possibility of measurement error due to calibration. Both experimental units showed a decrease in redox potential over time, as expected. The redox potential in the unit receiving methanol decreased at a faster rate than that of the unit receiving sewage, similar to Trial 10. The pump delivering methanol solution to experiment 1 was activated for 53 events (the first 25.5 hours of the trial), whereas the pump delivering synthetic sewage to experiment 2 was activated for 95 events (the entire length of the trial).

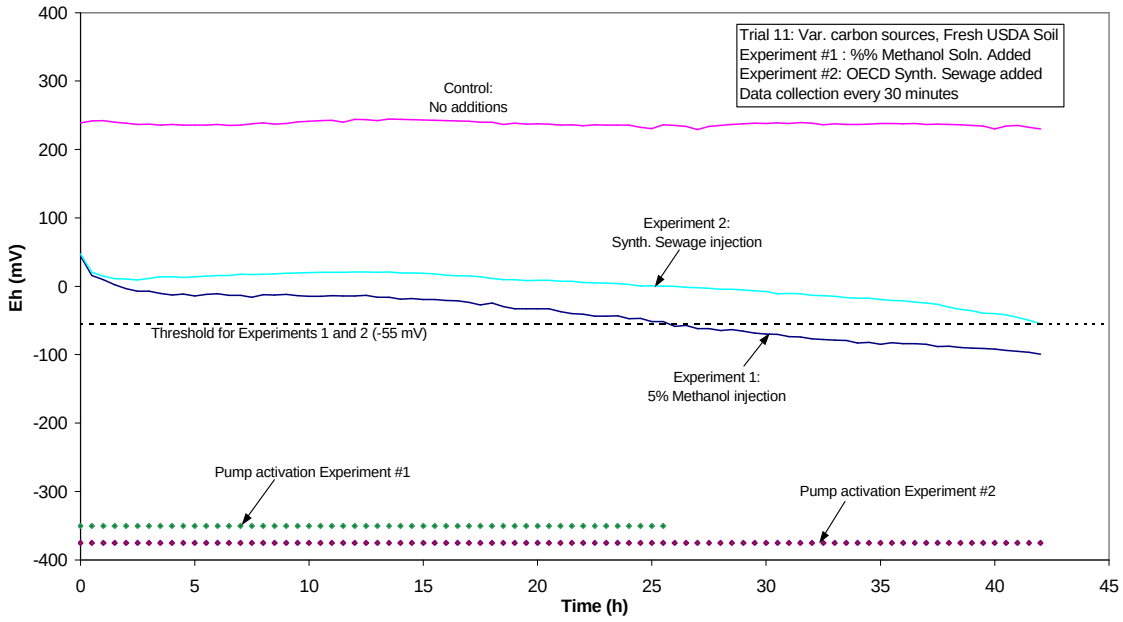

Figure 6. 8. Results for Trial 11: Redox potential vs. time for soil microcosms, each with a different carbons source than used previously (repeat of Trial 10).

6.1.9 Trial 12: Modified repeat of Trial 10.

Trial 12 was started in the laboratory on 8 August 2001 to test an acetate solution as another potential source of carbon. Previous researchers have used a sodium acetate solution as a source of carbon for increasing the rate of denitrification in wastewater engineering applications (Koch and Oldham, 1985). Two-day old USDA ARS soil (from the same sample used for Trial 11) was used to construct three new soil microcosms following the general procedure. Each was connected to the DAQ computer via platinum redox probe and calomel probe via salt bridge. Experimental unit 1 was connected to the hose of the pump delivering pure methanol solution. Experimental unit 2 was connected to the hose of the pump delivering a 1.0 M sodium acetate solution. The pump flow rates were checked and kept at 1.6 (±0.09) $ml \cdot s^{-1}$ for experimental unit number 1 and 1.4 (±0.14) $ml \cdot s^{-1}$ for experimental unit number 2. The sample period was set to 1800 s (1/2

hour), and pump time was set to 1 s. The threshold *Eh* voltage (above which carbon solution was added) was set to -55 mV for both experimental units. The trial was initiated and allowed to proceed for 40.0 hours.

Results for Trial 12 showed that the sodium acetate solution was as good a carbon source as methanol (Figure 6. 9). For this trial, the initial conditions of all units were widely separated by approximately 100 mV each, due likely to soil hetereogenieties. Results for the control unit showed considerable noise, as yet unexplained but possibly due to some interaction between the monitoring system and the microcosms previously unaccounted for. However, a general downward trend in redox potential over time can be seen. Both experimental units showed a substantial decrease in redox potential over time, as expected. The redox potential in the unit receiving methanol decreased at a slightly faster rate than that of the unit receiving acetate. Both exhibited a drop in redox potential to around -30 mV, although the unit receiving acetate showed a slight increase later on. The pumps for both experimental units were each activated for 81 events (the entire length of the trial).

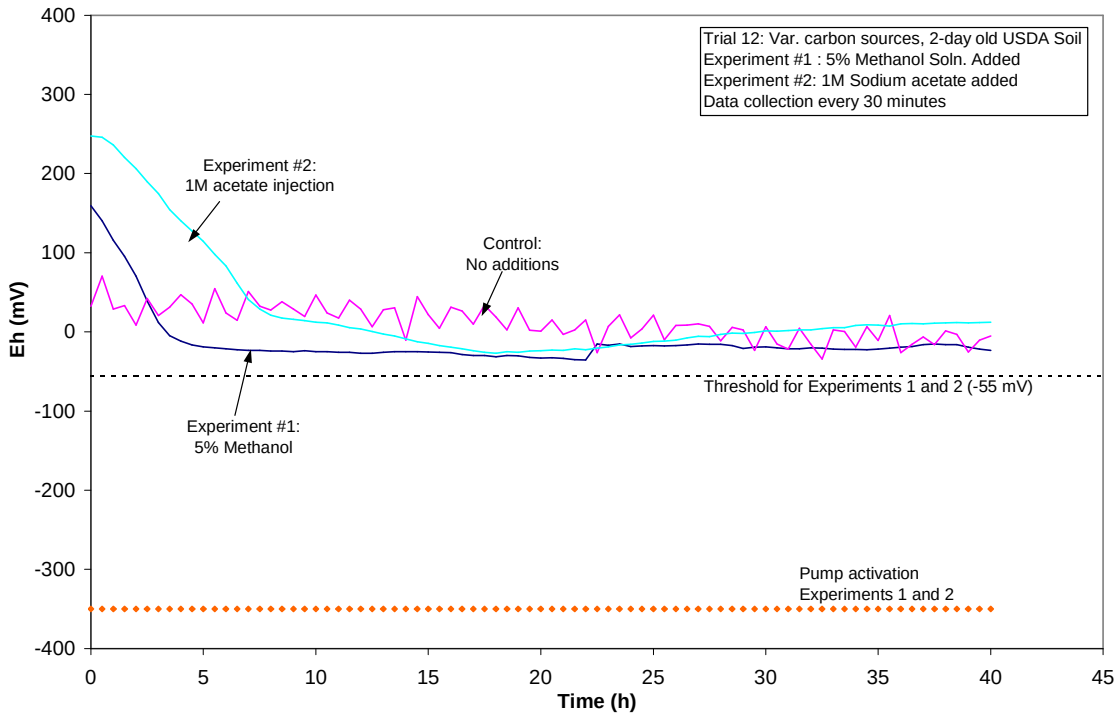

Figure 6. 9. Results for Trial 12: Redox potential vs. time for soil microcosms, each with different carbon sources than used previously (modified repeat of Trial 10).

6.1.10 Trial 19: Modified repeat of Trial 10.

Trial 19 was started in the laboratory on 4 February 2002 to test tryptic soy broth as a carbon source. Soy broth was mixed at and autoclaved for sterilization. Five-day old USDA ARS soil was used to construct two new soil microcosms following the general procedure. Each was connected to the DAQ computer via platinum redox probe and calomel probe via salt bridge. The experimental unit was connected to the hose of the pump delivering the soy broth solution. The pump flow rate was checked and kept at 1.6 (±0.09) $ml \cdot s^{-1}$. The sample period was set to 900 s (1/4 hour), and pump time was set to 1 s. The threshold *Eh* voltage for the experimental unit (above which carbon solution was

added) was set to a value of -155 mV for both experimental units. The trial was initiated and allowed to proceed for 100.0 hours.

Results for Trial 19 were difficult to interpret (Figure 6. 10). First, one notices that the initial conditions of the experimental and control units were rather widely separated by approximately 100 mV, due likely to soil hetereogenieties. One also immediately notices a considerable amount of noise in the redox potential signal, due possibly to some sort of interference in the data collection signal. However, a general downward trend in redox potential over time can be seen for both units. The control unit showed a very gradual decrease in redox potential over time, as expected. The redox potential in the experimental unit showed extremely variable behavior: first, there was a substantial decrease in redox potential over time within the first 5 hours, followed by a leveling out for a while, and then a rapid decrease into highly reduced conditions around a time of 26 hours, and finally an increase and return to moderately reduced conditions for the remainder to the trial. The rapid decreases into reducing conditions may indicate that soy broth is a good source of carbon for the reduction processes occurring in the soil. The various periods of leveling out and rapid decreases may be an indication of the microbial processes passing through the various reduction stages, using different primary electron acceptors as others are used up. The pump for the experimental unit was activated for nearly the entire length of the trial because of the excessively low setpoint. Note that the noise in the redox potential measurements at times caused the pump to activate when likely it should not have. For example, around hour 28, the trend in the redox potential curve would suggest that potential measurement was below the threshold setpoint and thus no carbon would be added. Measurement noise, however, gave a false

reading of redox potential well above this threshold, thus adding carbon solution when likely none should have been added. In total, the carbon injection pump was activated for 365 events.

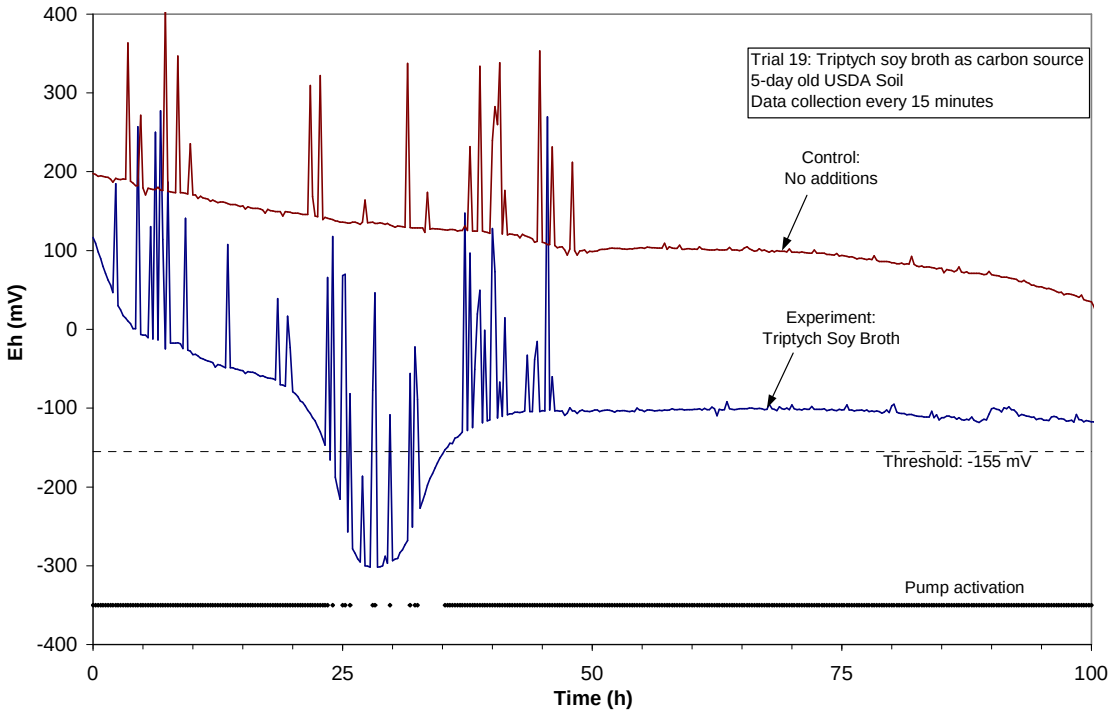

Figure 6. 10. Results for Trial 19: Redox potential vs. time for soil microcosms with different carbon sources than used previously (modified repeat of Trial 10).

6.1.11 Trial 30: Test the effect of dissolved oxygen in carbon solution additions.

Trial 30 was initiated to test whether or not the presence of dissolved oxygen in the carbon solution might be affecting the redox potential measurements in the experimental units. While it was expected that carbon addition would drive down the redox potential into lower reducing ranges more quickly, some trials exhibited the exact opposite behavior, showing an increase in redox potential as carbon solution was added. The cause of this was suspected to be the presence of oxygen in the carbon solution

additions, generally kept at atmospheric conditions and thus an average concentration of 8 to 9 mg/L. Trial 30 was started in the laboratory on 10 June 2003. Fresh USDA ARS soil was used to construct three new soil microcosms following the general procedure. Each was connected to the DAQ computer via platinum redox probe and calomel probe via salt bridge. Control 1 received no additions. Control 2 was connected to the hose of a pump delivering distilled water. The experimental unit was connected to the hose of a pump delivering 1.0 M sodium acetate solution. The dissolved oxygen concentration of the two reservoirs was checked with a YSI-85 combination meter (s/n 01G0076-AC) and found to be 8.4 mg/L, The pump flow rates were checked and both calibrated at a value of 2.0 $ml \cdot s^{-1}$ (± 0.11 $ml \cdot s^{-1}$ for the experimental unit and ± 0.00 $ml \cdot s^{-1}$ for control 2). The sample period was set to 1800 s (1/4 hour), and pump time was set to 1 s. The threshold *Eh* voltage for the experimental unit (above which carbon solution was added) was set to -5 mV for both experimental units. The trial was initiated and allowed to proceed for 50.0 hours.

Results for Trial 30 were contrary to what was expected (Figure 6. 11). First, one notices that the initial conditions of the experimental and control no.1 units were very close to each other, whereas that of control unit 2 was approximately 100 mV greater. Control unit 1, receiving no additions, showed a gradual decrease in redox potential as in other trials. Control unit 2, receiving distilled water, likewise showed a gradual decrease in redox potential. The rate of decrease in control 2 was not as great as in control 1, presumably because of the dissolved oxygen present in the additions of water. The experimental unit, however, showed an unexpected increase in redox potential for the entire length of the trial despite the consistent addition of carbon. These results possibly

point to other biochemical reactions occurring as a result of acetate addition that cause an increase in redox potential that have not been accounted for in this series of trials. Note that pump additions occurred for the entire length of the trial for both control 2 and the experiment for a total of 100 events each.

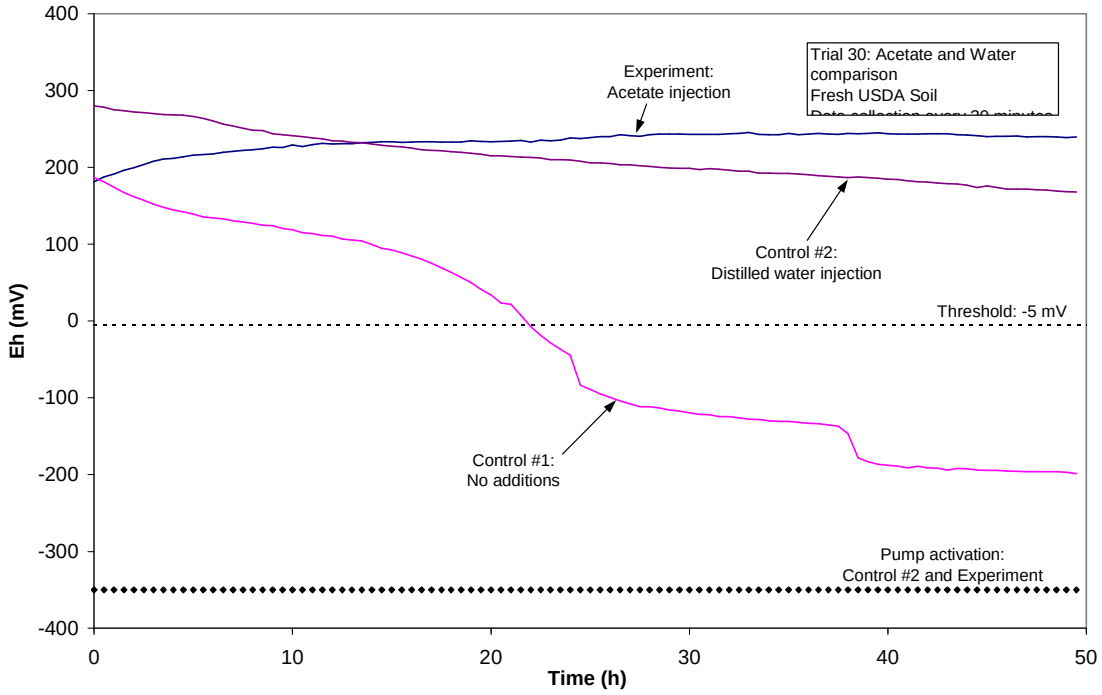

Figure 6. 11. Results for Trial 30: Redox potential vs. time for wetland soil microcosms testing the influence of dissolved oxygen in the carbon solution additions.

6.1.12 Carbons Summary Analysis

6.1.12.1 Qualitative Analyses

Results for all carbon addition trials are summarized in the following set of tables. Each experiment of each trial was analyzed for total run time, length of time the carbon pump was activated, overall number of pump events, total moles of carbon added, initial

change in redox potential (arbitrarily defined here as the change in redox in the first 10 hours), total change in redox potential over the entire length of the trial, qualitative assessment of the trend in redox potential, and the relation of the redox potential to the control of the same trial. Such results for methanol addition experiments are summarized in Table 6. 1, and similar results for the accompanying controls are summarized in Table 6. 2.

Table 6. 1. Results for methanol addition experimental units.

Trial	Total Run Time (hr)	Length of Pump Action (hr)	No. of Pump Events	Total Carbon Added (mol C)	Initial Change in *Eh*[1] (mV)	Total Change in *Eh*[2] (mV)	General Redox Pattern	Relation to Control
1-01	98.0	4.0	9	0.49	-342	-394	Steep initial decline	Lower
5-01	40.5	40.5	82	3.24	-93	-70	Steep initial decline, then gradual increase	Similar
6-01	63.5	63.5	82	3.24	-10	-27	Small decline	__
7-01	23.0	23.0	48	1.90	+130	+126	Steep initial increase	Higher
7-03	23.0	23.0	48	1.66	+135	+138	Steep initial increase	Higher
8-01	23.0	23.0	48	1.90	-57	-99	Gradual decline	Higher
8-03	23.0	23.0	48	1.66	-74	-115	Gradual decline	Higher
9-01	23.0	4.0	9	0.36	-190	-192	Steep initial decline	Similar
9-03	23.0	23.0	48	1.66	-43	-55	Gradual decline	Higher
10-01[3]	47.0	47.0	95	1.88	-96	-131	Steep initial decline	Lower
11-01	42.0	25.5	53	2.10	-59	-143	Gradual decline	Lower
12-01	40.0	40.0	81	3.20	-185	-183	Steep initial decline	Similar

[1]The change in redox potential from time t=0 to time t=10 hr.
[2]The change in redox potential from time t=0 until the end of the trial.
[3]A diluted methanol solution (1:1 methanol:water) added instead of pure methanol.

Table 6. 2. Results for control units that accompanied the methanol experiment trials.

Trial	Total Run Time (hr)	Initial Change in *Eh*[1] (mV)	Total Change in *Eh*[2] (mV)	General Redox Pattern	General Trend of Slope
1-02	98.0	-96	-313	Gradual decline	-
5-02	40.5	-77	-125	Gradual decline	-
6-02[3]	--	--	--	--	--
7-02	23.0	-174	-324	Gradual, then steep decline	-
8-02	23.0	-49	-53	Steep initial decline	-
9-02	23.0	-139	-161	Steep initial decline	-
10-02	47.0	-78	+17	Steep initial decline, steep end incline	-
11-02	42.0	+2	-9	No change	0
12-03	40.0	+14	-38	Oscillating; no overall trend	0

[1]The change in redox potential from time t=0 to time t=10 hr.
[2]The change in redox potential from time t=0 until the end of the trial.
[3]Some data were lost in trial 6 due to computer error.

Table 6. 1 and Table 6. 2 show the variability of results obtained from the experiments. As shown by the total change in redox, most experimental units in Table 6. 1 experienced a decline in redox potential; only those from Trial 7 experienced a redox increase. Many trials exhibited a steep initial decline in redox potential, evidenced by a large magnitude in the initial change in redox potential. Five of the experiment trials had higher redox potentials than their accompanying controls, whereas four had lower redox potentials, and three had similar redox potentials. Also, for most experiment trials, the pump was activated for the entire run time; only in three trials was the pump activation for a time period shorter than the entire trial run time. Most of the controls listed in Table 6. 2 show a decline in redox, either gradual or steep; only two show no slope, and none show an increase in redox.

Not all trials in the carbon addition experiments received methanol. Other carbon sources were tried for some of the trials in the carbon addition experiments. Table 6. 3 summarizes results for those trials receiving sodium acetate, with results for their accompanying controls summarized in Table 6. 4.

Table 6. 3. Results for acetate addition experimental units.

Trial	Total Run Time (hr)	Length of Pump Action (hr)	No. of Pump Events	Total Carbon Added (mol C)	Initial Change in *Eh* (mV)[1]	Total Change in *Eh* (mV)[2]	General Redox Pattern	Relation to Control
12-02	40.0	40.0	81	0.227	-235	-235	Steep initial decline	Similar
30-01	49.5	49.5	100	0.800	+48	+55	Gradual increase	Higher

[1]The change in redox potential from time t=0 to time t=10 hr.
[2]The change in redox potential from time t=0 until the end of the trial.

Table 6. 4. Results for control units that accompanied the acetate experiment trials.

Trial	Total Run Time (hr)	Initial Change in *Eh*[1] (mV)	Total Change in *Eh*[2] (mV)	General Redox Pattern	General Trend of Slope
12-03	40.0	+14	-38	Oscillating	Variable
30-02	49.5	-67	-385	Gradual decline	-

[1]The change in redox potential from time t=0 to time t=10 hr.
[2]The change in redox potential from time t=0 until the end of the trial.

Table 6. 3 and Table 6. 4 again show the variability of results obtained from the experiments. As shown by the total change in redox, one experimental unit in Table 6. 3 experienced a significant and steep decline in redox potential, while the other experienced a gradual increase. Neither of the experiment trials had higher redox potentials than their accompanying controls, although one was similar. For both experiment trials, the pump was activated for the entire run time. Only one of the controls

listed in Table 6. 4 showed a decline in redox; the other showed oscillatory behavior, the redox potential cycling up and down around a constant value.

Other carbon sources besides methanol and acetate were used in a few of the trials. Results for these trials are summarized in Table 6. 5, with results from their accompanying controls summarized in Table 6. 6.

Table 6. 5. Results for carbon addition experimental units using either synthetic sewage or tryptic soy.

Trial	Total Run Time (hr)	Length of Pump Activation (hr)	No. of Pump Events	Initial Change in *Eh*[1] (mV)	Total Change in *Eh*[2] (mV)	General Redox Pattern	Relation to Control
10-03[3]	47.0	40.5	82	-70	-197	Moderate decline	Lower
11-03[3]	42.0	42.0	95	-27	-102	Gradual decline	Lower
19-01[4]	100.0	--[5]	365	-149	-234	Steep initial decline, then increase	Lower

[1]The change in redox potential from time t=0 to time t=10 hr.
[2]The change in redox potential from time t=0 until the end of the trial.
[3]Synthetic sewage used as carbon source.
[4]Tryptic soy used as carbon source.
[5]Pump was activated at sporadic times.

Table 6. 6. Results for control units that accompanied the experiment trials receiving various carbon inputs.

Trial	Total Run Time (hr)	Initial Change in *Eh*[1] (mV)	Total Change in *Eh*[2] (mV)	General Redox Pattern	General Trend of Slope
10-02	47.0	-78	+17	Steep initial decline; Steep incline at end	-
11-02	42.0	+2	-9	No change	0
19-02	100.0	-27	-163	Gradual decline	-

[1]The change in redox potential from time t=0 to time t=10 hr.
[2]The change in redox potential from time t=0 until the end of the trial.

Table 6. 5 and Table 6. 6 show some variability of results. As shown by the total change in redox, all experimental units in Table 6. 5 experienced a decline in redox potential, although only one had a steep decline. Also, all of the experiment trials had

lower redox potentials than their accompanying controls. For one experiment trial (10-03), the pump was activated for less than the entire run time. Two of the three controls listed in Table 6. 6 showed a decline in redox; the other showed no overall change.

6.1.12.2 Analyses of Changes in Redox

Because of the different conditions under which each trial was performed, a statistical comparison among the trials can yield limited information. However, taking the mean of the change in redox potential for all trials gives a general indication of the trends experienced by each treatment. Table 6. 7 shows the mean and standard deviation of the initial and total changes in redox potential for each of the groups of trials and for the controls, which were all analyzed together as all controls were treated approximately in the same manner. Comparing the means for the various carbon input trial groups with the controls group (bottom row), it can be seen that all carbon addition groups exhibited a greater initial decline than the controls group. However, only the miscellaneous carbon addition group (the sewage/soy broth addition group) exhibited a total redox decline greater than the controls. Note, however, that the large standard deviations may render any difference between the experiment and control groups insignificant. This is confirmed by the results of a one-sided t-test (McCuen, 1984) comparing the means of the various treatment groups with the means of the controls group (Table 6. 8). The t-testing shows that no treatment group exhibited either an initial or a total change in redox potential that is statistically different than the controls group at a level of significance of 0.05 and 0.10.

Table 6. 7. Mean and standard deviation of the initial and total changes in redox potential for each of the groups of experimental carbon addition trials and for all the controls.

Group	Initial Change in *Eh* (mV)		Total Change in *Eh* (mV)	
	Mean	Std Dev	Mean	Std Dev
Methanol Input (n=12)	-73.7	131.2	-95.4	141.6
Acetate Input (n=2)	-93.5	--	-90.0	--
Misc Input (n=3)	-82.0	61.9	-177.7	68.1
All Controls (n=13)	-57.9	58.7	-121.8	139.9

Table 6. 8. Results of statistical t-test comparing means of the various treatment groups to the mean of the controls group. A "-" indicates no statistical difference between the means, whereas a "@" indicates that the mean of the treatment group is less than the mean of the control group at the respective level of significance.

Group	Initial Change in *Eh* (mV)		Total Change in *Eh* (mV)	
Test Level of Significance	α=0.05	α=0.10	α=0.05	α=0.10
Methanol Input (n=12)	-	-	-	-
Acetate Input (n=2)	-	-	-	-
Misc Input (n=3)	-	-	-	-
All Controls (n=13)	-	-	-	-

6.1.12.3 Analysis of Redox Values

An analysis was performed on the values of the redox potential curves at each time step for the controls and all of the treatments. This analysis assumes that the procedure was uniform for each treatment group and for all the controls. The data obtained from these analyses are then used to perform comparative tests between the various treatment groups and the control group.

Controls Group. The controls were analyzed for each time step. Controls from almost all trials (including those from the carbon/nitrate selection trials) were used; the data from trials 12 and 19 were omitted because of excessive noise. For this group of trials, the length of time each trial was performed ranged from 23 hours to over 100 hours, and thus the number of sample population *n* varies from 21 to 9 as the time step proceeds from 0 to 100 hours. For each time step, the data were averaged and the standard error calculated for the respective sample population *n*. Results from this analysis are plotted in Figure 6. 12 and show the averaged redox potential over time. As expected, there is an obvious downward trend that is slightly steeper within the first 10 hours. Discontinuities in the otherwise smooth curve occur at time steps when data from one of the trials in the group ends and the value of *n* changes. Error bars on the plot represent standard error.

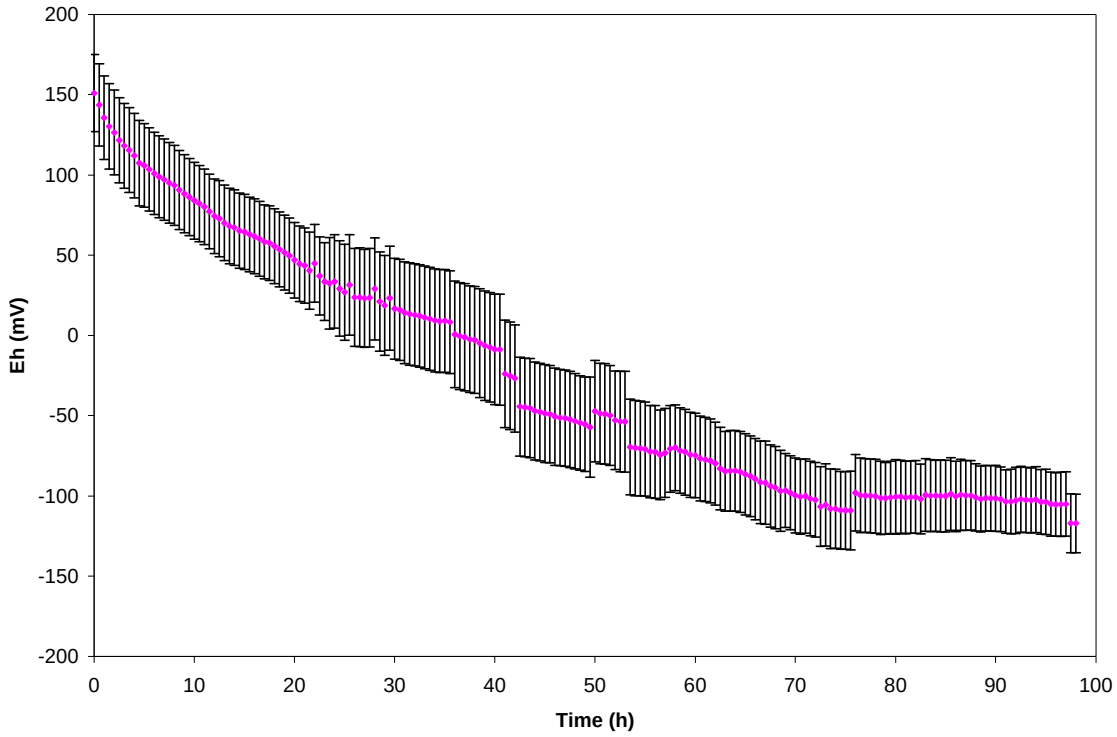

Figure 6. 12. Mean values of redox potential averaged for each time step for all controls vs. time. Error bars represent standard error.

Methanol Addition Group. All trials in which methanol was added (except Trial 7) were analyzed for each time step. Trial 7 was omitted from this analysis as an outlier because both replicates showed an increase in redox potential over time. As in the controls group, the length of time for each methanol trial ranged from 23 hours to 100 hours, and thus the number of sample population *n* varies from 11 to 1 as the time step proceeds from 0 to 100 hours. For each time step, the data were averaged and the standard error calculated for the respective sample population *n*. Results from this analysis are plotted in Figure 6. 13 and show the averaged redox potential over time for the methanol group compared to the controls group. This comparison shows that the

values for redox in the methanols group are generally higher than the controls group in the early stages (up to 5 hours), about the same between 5 and 25 hours, and generally lower beyond a time of 25 hours. As in the controls group, discontinuities in the otherwise smooth curve occur at time steps when data from one of the trials in the group ends and the value of *n* changes. Error bars on the plot represent standard error. There is considerable overlap between the standard error for the two sets of data. There are no error bars on the plot for the methanols group beyond a time of 47.0 hours since *n*=1 beyond this point.

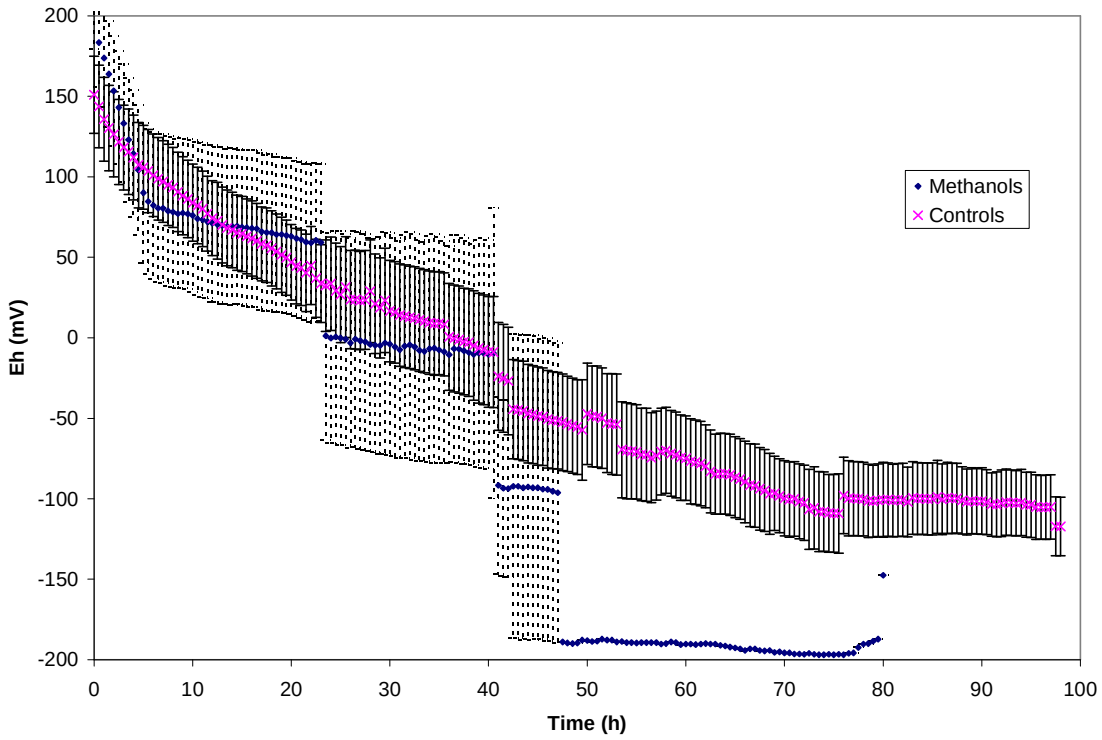

Figure 6. 13. Mean values of redox potential averaged for each time step for controls group and methanol addition groups vs. time. Error bars represent standard error. There is no standard error for the methanols beyond hour 47 as the sample population is 1.

Acetate Addition Group. Both trials in which acetate was added were analyzed for each time step. Only two trials were performed in which acetate was added, one for 40 hours and one for 49 hours. Thus the sample population *n* is 2 for most of the analysis, not enough for a robust statistical treatment. However, the same analysis was attempted, in which, for each time step, the data were averaged and the standard error calculated. Results from this analysis are plotted in Figure 6. 14 and show the averaged redox potential over time for the acetate group compared to the controls group. This comparison shows that the values for redox in the acetate group are higher than the controls at all time steps. There is a discontinuity in the otherwise smooth curve at time t=40 hr. when data from one of the trials in the group ends. Error bars on the plot represent standard error. There is considerable overlap between the standard error for the two sets of data, as the error for the acetate group is large because of a small sample number. There are no error bars on the plot for the acetate group beyond a time of 40.0 hours since *n*=1 beyond this point.

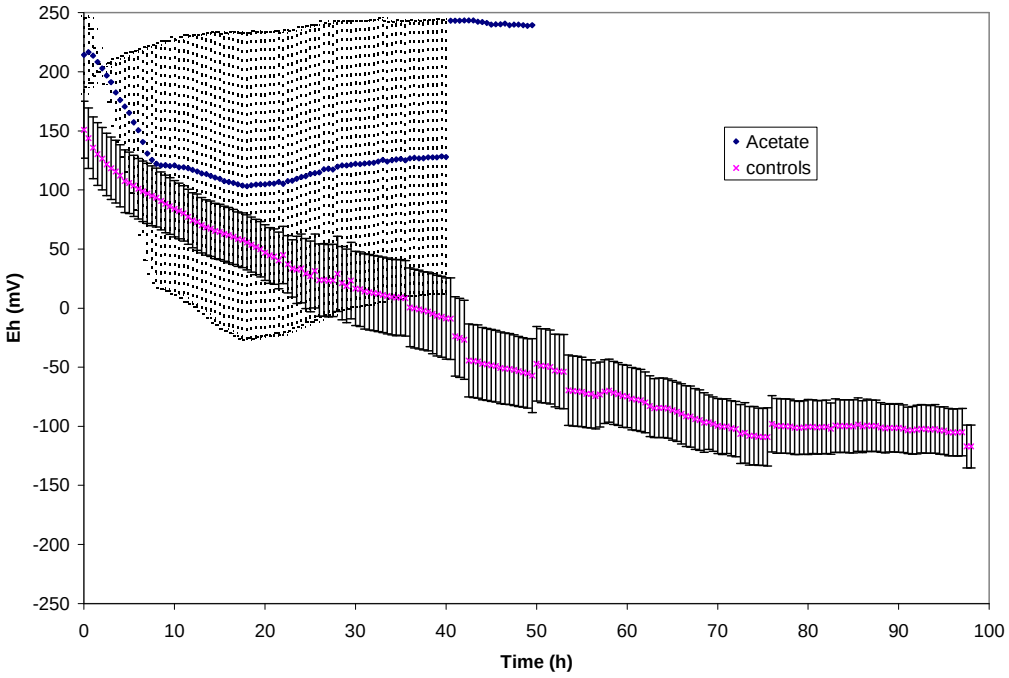

Figure 6. 14. Mean values of redox potential averaged for each time step for controls group and acetate addition groups vs. time. Error bars represent standard error. There is no standard error for the acetate group beyond hour 40 as the sample population is 1.

Synthetic Sewage Addition Group. Both trials in which synthetic sewage was added were analyzed for each time step. Only two trials were performed in which synthetic sewage was added, one for 42 hours and one for 47 hours. Thus the sample population *n* is 2 for most of the analysis, not enough for a robust statistical treatment. However, the same analysis was attempted, in which, for each time step, the data were averaged and the standard error calculated. Results from this analysis are plotted in Figure 6. 15 and show the averaged redox potential over time for the synthetic sewage group compared to the controls group. This comparison shows that the values for redox in the synthetic sewage group are lower than the controls at all time steps, and the synthetic sewage group shows a considerably steeper slope in the first two hours. Error

bars on the plot represent standard error. There is not much overlap between the standard error for the two sets of data in the first 20 hours, despite the small sample number for the synthetic sewage group.

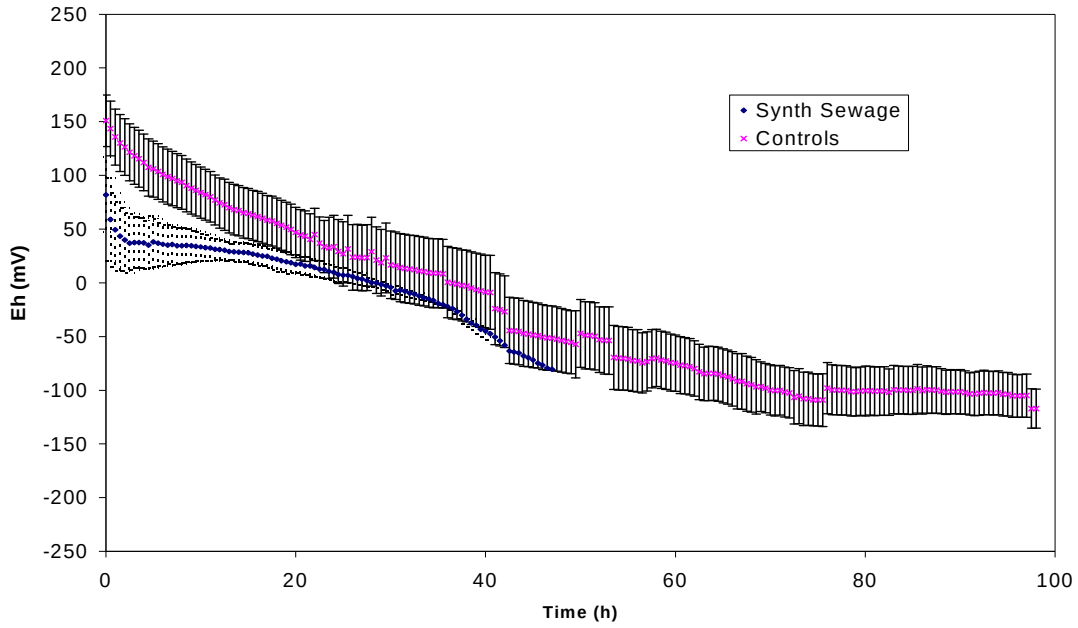

Figure 6. 15. Mean values of redox potential averaged for each time step for controls and synthetic sewage addition groups vs. time. Error bars represent standard error.

Statistical Testing on Redox Values. To test whether or not the mean values of redox potential for each treatment group were statistically different than the controls group, a t-test was performed comparing the means of the treatment and controls group at each time step. The test was performed at significance levels of 0.05 and 0.10 up to a time of 47.0 hours (beyond which the sample populations of the treatment groups are too small). The results presented in Table 6. 9 show that there is no statistical difference between the treatments and controls groups at either level of significance at any time step.

Table 6. 9. Results of t-test comparing the means of the value of redox potential of each treatment group to the controls group at each time step at two different significance levels. A "-" indicates no statistical difference between the groups, and a "@" indicates a statistical difference does exist. Blank spaces indicate time steps for which no data were present.

Eh Values						
	α = 0.05			α = 0.10		
Time (h)	Methanol Trials (n=9)	Acetate Trials (n=2)	Synth. Sewage Trials (n=2)	Methanol Trials (n=9)	Acetate Trials (n=2)	Synth. Sewage Trials (n=2)
0	-	-	-	-	-	-
0.5	-	-	-	-	-	-
1.0	-	-	-	-	-	-
1.5	-	-	-	-	-	-
2.0	-	-	-	-	-	-
2.5	-	-	-	-	-	-
3.0	-	-	-	-	-	-
3.5	-	-	-	-	-	-
4.0	-	-	-	-	-	-
4.5	-	-	-	-	-	-
5.0	-	-	-	-	-	-
5.5	-	-	-	-	-	-
6.0	-	-	-	-	-	-
6.5	-	-	-	-	-	-
7.0	-	-	-	-	-	-
7.5	-	-	-	-	-	-
8.0	-	-	-	-	-	-
8.5	-	-	-	-	-	-
9.0	-	-	-	-	-	-
9.5	-	-	-	-	-	-
10.0	-	-	-	-	-	-
10.5	-	-	-	-	-	-
11.0	-	-	-	-	-	-
11.5	-	-	-	-	-	-
12.0	-	-	-	-	-	-
12.5	-	-	-	-	-	-
13.0	-	-	-	-	-	-
13.5	-	-	-	-	-	-
14.0	-	-	-	-	-	-
14.5	-	-	-	-	-	-
15.0	-	-	-	-	-	-
15.5	-	-	-	-	-	-
16.0	-	-	-	-	-	-
16.5	-	-	-	-	-	-
17.0	-	-	-	-	-	-
17.5	-	-	-	-	-	-
18.0	-	-	-	-	-	-
18.5	-	-	-	-	-	-
19.0	-	-	-	-	-	-
19.5	-	-	-	-	-	-
20.0	-	-	-	-	-	-
20.5	-	-	-	-	-	-
21.0	-	-	-	-	-	-
21.5	-	-	-	-	-	-
22.0	-	-	-	-	-	-
22.5	-	-	-	-	-	-
23.0	-	-	-	-	-	-
23.5	-	-	-	-	-	-
24.0	-	-	-	-	-	-
24.5	-	-	-	-	-	-

Table 6. 9. (Continued).

Eh Values (continued)						
	α = 0.05			α = 0.10		
Time (h)	Methanol Trials (n=9)	Acetate Trials (n=2)	Synth. Sewage Trials (n=2)	Methanol Trials (n=9)	Acetate Trials (n=2)	Synth. Sewage Trials (n=2)
25.0	-	-	-	-	-	-
25.5	-	-	-	-	-	-
26.0	-	-	-	-	-	-
26.5	-	-	-	-	-	-
27.0	-	-	-	-	-	-
27.5	-	-	-	-	-	-
28.0	-	-	-	-	-	-
28.5	-	-	-	-	-	-
29.0	-	-	-	-	-	-
29.5	-	-	-	-	-	-
30.0	-	-	-	-	-	-
30.5	-	-	-	-	-	-
31.0	-	-	-	-	-	-
31.5	-	-	-	-	-	-
32.0	-	-	-	-	-	-
32.5	-	-	-	-	-	-
33.0	-	-	-	-	-	-
33.5	-	-	-	-	-	-
34.0	-	-	-	-	-	-
34.5	-	-	-	-	-	-
35.0	-	-	-	-	-	-
35.5	-	-	-	-	-	-
36.0	-	-	-	-	-	-
36.5	-	-	-	-	-	-
37.0	-	-	-	-	-	-
37.5	-	-	-	-	-	-
38.0	-	-	-	-	-	-
38.5	-	-	-	-	-	-
39.0	-	-	-	-	-	-
39.5	-	-	-	-	-	-
40.0	-	-	-	-	-	-
40.5	-			-		
41.0	-			-		
41.5	-			-		
42.0	-			-		
42.5	-			-		
43.0	-			-		
43.5	-			-		
44.0	-			-		
44.5	-			-		
45.0	-			-		
45.5	-			-		
46.0	-			-		
46.5	-			-		
47.0	-			-		

6.1.12.4 Analysis of Redox Slopes

An analysis was performed on the slopes of the redox potential curves at each time step for the controls and all of the treatments. This analysis assumes that the procedure was uniform for each treatment group and for all the controls. The data

obtained from these analyses are then used to perform comparative tests between the various treatment groups and the control group. The slope, $\Delta Eh/\Delta t$, was calculated for each trial at each time step i as the change in redox potential at time step $i+1$ minus the redox potential at time step i, divided by the change in time (the sample period of 0.5 hr). Then, for each time interval, the mean and standard error was calculated for each trial group.

Controls Group. As in the previous analysis, controls from almost all trials (including those from the carbon/nitrate selection trials) were used; the data from trials 12 and 19 were omitted because of excessive noise. For this group of trials, the length of time each trial was performed ranged from 23 hours to over 100 hours, and thus the number of sample population n varies from 21 to 9 as the time step proceeds from 0 to 100 hours. For each time step, the slope was calculated for each trial, and then data from all trials were averaged and the standard error calculated for the respective sample population n for each time step. Results from this analysis are plotted in Figure 6. 16. The mean slope is generally negative early on between time 0 and 10, and closer to zero beyond that. This shows the rapid decline of redox potential early in the trials, followed by a leveling off. Interestingly, there is considerably large standard errors for the data between time 20 and 30 due to noise in the individual data sets.

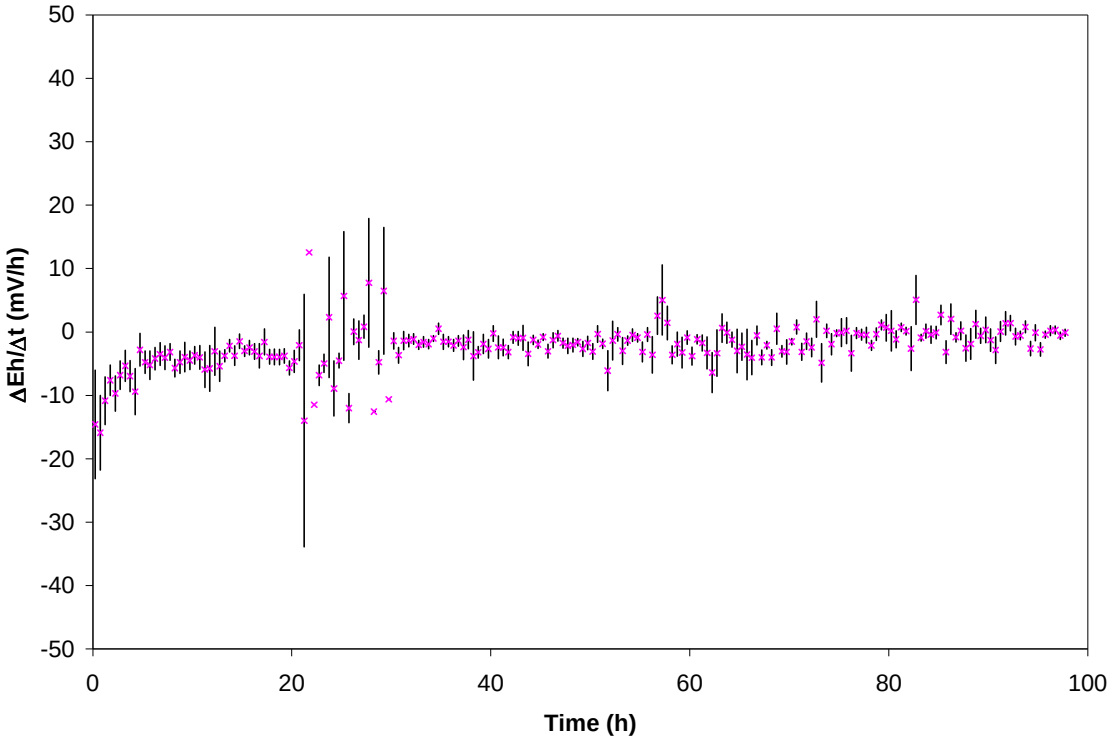

Figure 6. 16. Mean values of the slope of redox potential averaged for each time step for all controls vs. time. Error bars represent standard error.

Methanol Addition Group. All trials in which methanol was added (except Trial 7) were analyzed for each time step. Again, Trial 7 was omitted from this analysis as an outlier because both experimental replicates showed an increase in redox potential over time. As in the controls group, the length of time for each methanol trial ranged from 23 hours to 100 hours, and thus the number of sample population *n* varies from 11 to 1 as the time step proceeds from 0 to 100 hours. For each time step, the slope was calculated for each trial, and then data from all trials were averaged and the standard error calculated for the respective sample population *n* for each time step. Results from this analysis are plotted in Figure 6. 17 showing the averaged redox slope at each time step. This comparison shows that the redox slopes of the methanols group are lower than the controls group in the early stages (up to 5 hours) and about the same thereafter. This

shows that the methanols group declined more rapidly than the controls in the early stages. Error bars on the plot represent standard error, and there is considerable overlap between the standard error for the two sets of data. There are no error bars on the plot for the methanols group beyond a time of 47.0 hours since *n*=1 beyond this point.

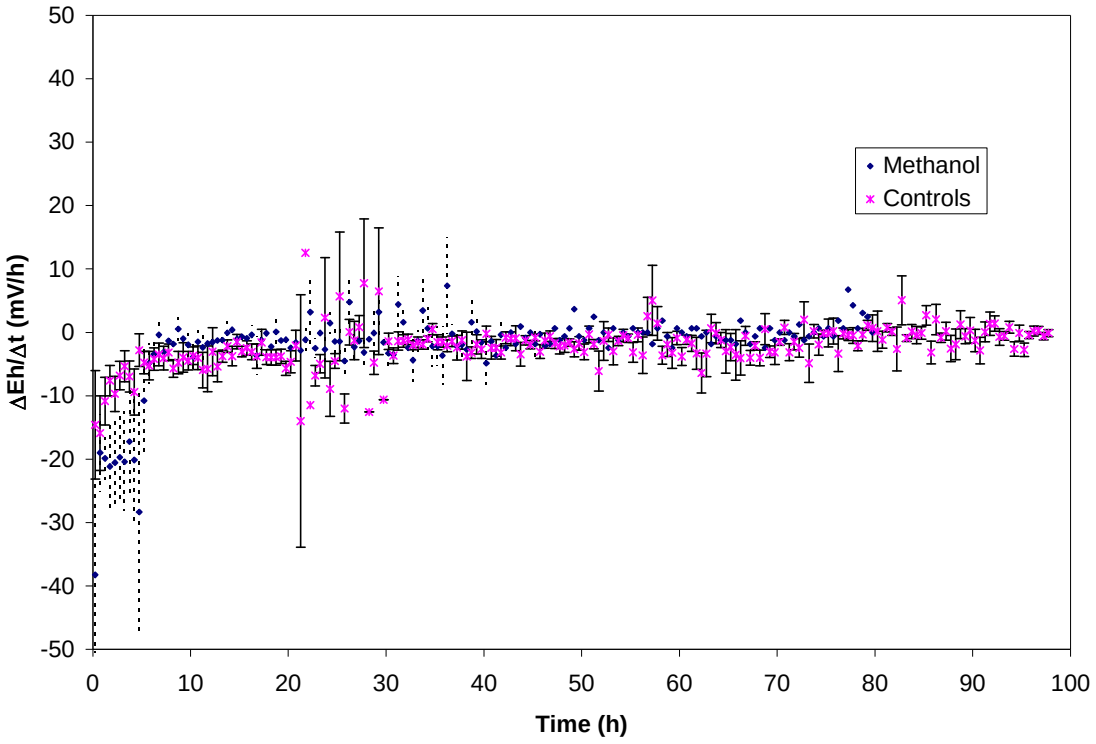

Figure 6. 17. Mean values of the slope of redox potential averaged for each time step for controls and methanol addition groups vs. time. Error bars represent standard error.

Acetate Addition Group. Both trials in which acetate was added were analyzed for each time step. For each time step, the slope was calculated for each trial, and then data from all trials were averaged and the standard error calculated for the respective sample population *n=2* for each time step. Results from this analysis are plotted in Figure 6. 18 showing the average slope of redox potential at each time step for the acetate group

compared to the controls group. This comparison shows that the redox slopes of the acetate group are generally lower than the controls group in the early stages (up to 5 hours) and about the same thereafter. This is suspect to uncertainty, however, because the sample population is small (n=2) for the acetate group and the error is large. This possibly shows that the acetate group at times declined more rapidly than the controls in the early stages. Error bars on the plot represent standard error, and there is considerable overlap between the standard error for the two sets of data. There are no error bars on the plot for the acetate group beyond a time of 40.0 hours since *n*=1 beyond this point.

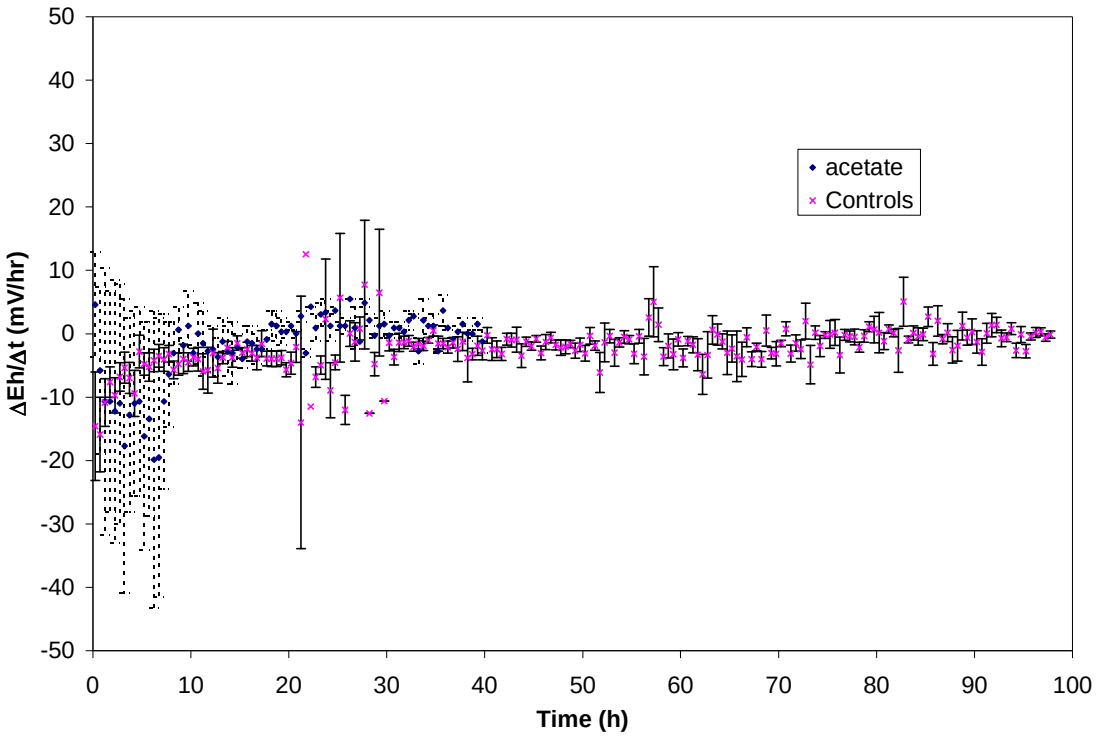

Figure 6. 18. Mean values of the slope of redox potential averaged for each time step for controls and acetate addition groups vs. time. Error bars represent standard error.

Synthetic Sewage Addition Group. Both trials in which synthetic sewage was added were analyzed for each time step. For each time step, the slope was calculated for each trial, and then data from all trials were averaged and the standard error calculated for the respective sample population *n=2* for each time step. Results from this analysis are plotted in Figure 6. 19 showing the averaged slope of redox potential at each time step for the synthetic sewage group compared to the controls group. This comparison shows that the values for redox in the synthetic sewage group, compared to the controls, are about the same in the first few hours, slightly higher from time 5 to 15 hours, nearly the same from 15 to 30 hours, and slightly lower after that. Error bars on the plot represent standard error. There is considerable overlap between the standard error for the two sets of data for most of the time period.

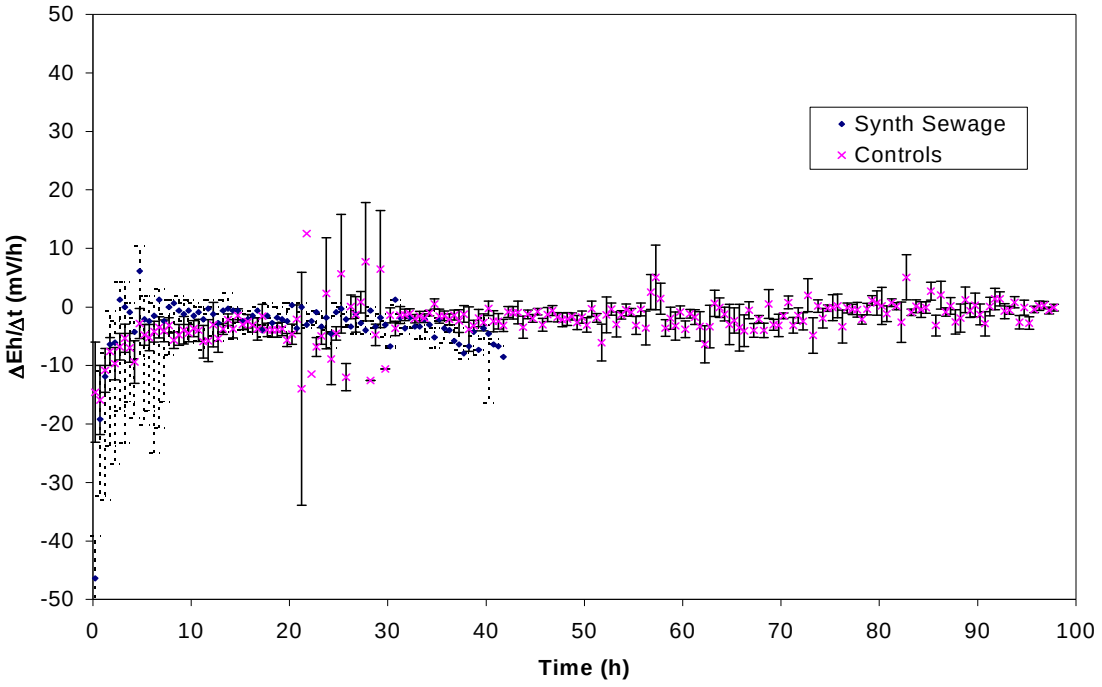

Figure 6. 19. Mean values of the slope of redox potential averaged for each time step for controls and synthetic sewage addition groups vs. time. Error bars represent standard error.

Statistical Testing on Redox Slopes. To test whether or not the mean slopes of redox potential for each treatment group were statistically different than the controls group, a t-test was performed comparing the means of the slopes of the treatment and controls group at each time step. The test was performed at significance levels of 0.05 and 0.10 up to a time of 47.0 hours (beyond which the sample populations of the treatment groups are too small). The results are presented in Table 6. 10. There is a clear signal that, for the methanols group, the slope is different than the controls group at both levels of significance (0.10 and 0.05). The results of the t-test are such that the methanols group is statistically shown to have a steeper slope than those replicates receiving no treatment. Likewise, for the acetate additions group, there is a difference in slope around hour 6.5, again shown by the test to be steeper than that of the controls. For the synthetic sewage additions, there is no clear difference in slope until later in the trials, beyond hour 30. Whereas the difference in slopes appears clustered within a short time frame for the methanols and acetate addition group, for the synthetic sewage group the clustering is more spread out, occurring intermittently over a broader time period. Also, it should be noted again that the veracity of results from the acetate and synthetic sewage groups is subject to question because of the small sizes of the sample population.

Table 6. 10. Results of t-test comparing the means of the slopes of redox potential of each treatment group to the controls group at each time step at two different significance levels. A "-" indicates no statistical difference between the groups, and a "@" indicates a statistical difference does exist. Blank spaces indicate time steps for which no data were present.

Eh Slopes						
	α = 0.05			α = 0.10		
Timestep (h)	Methanol Trials (n=9)	Acetate Trials (n=2)	Synth. Sewage Trials (n=2)	Methanol Trials (n=9)	Acetate Trials (n=2)	Synth. Sewage Trials (n=2)
0 - 0.5	-	-	-	@	-	-
0.5 - 1.0	-	-	-	-	-	-
1.0 - 1.5	-	-	-	@	-	-
1.5 - 2.0	@	-	-	@	-	-
2.0 - 2.5	@	-	-	@	-	-
2.5 - 3.0	@	-	-	@	-	-
3.0 - 3.5	@	-	-	@	-	-
3.5 - 4.0	-	-	-	@	-	-
4.0 - 4.5	-	-	-	-	-	-
4.5 - 5.0	@	-	-	@	-	-
5.0 - 5.5	-	-	-	-	@	-
5.5 - 6.0	-	-	-	-	-	-
6.0 - 6.5	-	@	-	-	@	-
6.5 - 7.0	-	@	-	-	@	-
7.0 - 7.5	-	-	-	-	-	-
7.5 - 8.0	-	-	-	-	-	-
8.0 - 8.5	-	-	-	-	-	-
8.5 - 9.0	-	-	-	-	-	-
9.0 - 9.5	-	-	-	-	-	-
9.5 - 10.0	-	-	-	-	-	-
10.0 - 10.5	-	-	-	-	-	-
10.5 - 11.0	-	-	-	-	-	-
11.0 - 11.5	-	-	-	-	-	-
11.5 - 12.0	-	-	-	-	-	-
12.0 - 12.5	-	-	-	-	-	-
12.5 - 13.0	-	-	-	-	-	-
13.0 - 13.5	-	-	-	-	-	-
13.5 - 14.0	-	-	-	-	-	-
14.0 - 14.5	-	-	-	-	-	-
14.5 - 15.0	-	-	-	-	-	-
15.0 - 15.5	-	-	-	-	-	-
15.5 - 16.0	-	-	-	-	-	-
16.0 - 16.5	-	-	-	-	-	-
16.5 - 17.0	-	-	-	-	-	-
17.0 - 17.5	-	-	-	-	-	-
17.5 - 18.0	-	-	-	-	-	-
18.0 - 18.5	-	-	-	-	-	-
18.5 - 19.0	-	-	-	-	-	-
19.0 - 19.5	-	-	-	-	-	-
19.5 - 20.0	-	-	-	-	-	-
20.0 - 20.5	-	-	-	-	-	-
20.5 - 21.0	-	-	-	-	-	-
21.0 - 21.5	-	-	-	-	-	-
21.5 - 22.0			-			-
22.0 - 22.5	-		-	-		-
22.5 - 23.0	-	-	-	-	-	-
23.0 - 23.5	-	-	-	-	-	-
23.5 - 24.0	-	-	-	-	-	-
24.0 - 24.5	-	-	-	-	-	-
24.5 - 25.0	-	-	-	-	-	-

Table 6. 10. (Continued).

Eh Slopes (continued)						
	α = 0.05			α = 0.10		
Timestep (h)	Methanol Trials (n=9)	Acetate Trials (n=2)	Synth. Sewage Trials (n=2)	Methanol Trials (n=9)	Acetate Trials (n=2)	Synth. Sewage Trials (n=2)
25.0 - 25.5	-	-	-	-	-	-
25.5 - 26.0	-	-	-	-	-	-
26.0 - 26.5	-	-	-	-	-	-
26.5 - 27.0	-	-	-	-	-	-
27.0 - 27.5	-	-	-	-	-	-
27.5 - 28.0	-	-	-	-	-	-
28.0 - 28.5			-			-
28.5 - 29.0	-	-	-	-	-	-
29.0 - 29.5	-	-	-	-	-	-
29.5 - 30.0			-			-
30.0 - 30.5	-	-	-	-	-	@
30.5 - 31.0	-	-	-	-	-	-
31.0 - 31.5	-	-	-	-	-	-
31.5 - 32.0	-	-	-	-	-	-
32.0 - 32.5	-	-	-	-	-	-
32.5 - 33.0	-	-	-	-	-	-
33.0 - 33.5	-	-	-	-	-	-
33.5 - 34.0	-	-	-	-	-	-
34.0 - 34.5	-	-	-	-	-	-
34.5 - 35.0	-	-	@	-	-	@
35.0 - 35.5	-	-	-	-	-	-
35.5 - 36.0	-	-	-	-	-	-
36.0 - 36.5	-	-	-	-	-	-
36.5 - 37.0	-	-	-	-	-	@
37.0 - 37.5	-	-	-	-	-	-
37.5 - 38.0	-	-	-	-	-	@
38.0 - 38.5	-	-	-	-	-	-
38.5 - 39.0	-	-	-	-	-	-
39.0 - 39.5	-	-	-	-	-	-
39.5 - 40.0	-	-	-	-	-	-
40.0 - 40.5	-			@		
40.5 - 41.0	-			-		
41.0 - 41.5	-			-		
41.5 - 42.0	-			-		
42.0 - 42.5	-			-		
42.5 - 43.0	-			-		
43.0 - 43.5	-			-		
43.5 - 44.0	-			-		
44.0 - 44.5	-			-		
44.5 - 45.0	-			-		
45.0 - 45.5	-			-		
45.5 - 46.0	-			-		
46.0 - 46.5	-			-		
46.5 - 47.0	-			-		

6.2 Carbon/Nitrate Selection Experiments

Following is a summary discussion of each of the experiment trials for the carbon/nitrate selection scenario experiments. Accompanying the discussion for each trial is a chart showing redox potential versus time for the microcosm units in each trial for the maximum time the trial was allowed to proceed. Each chart compares the change in redox potential for the experimental microcosm (the one receiving carbon addition) with that of the control microcosm (one receiving no addition).

6.2.1 Trial 13: Carbon/Nitrate Selection

The first of the carbon/nitrate selection experiments was commenced in the laboratory on 13 August 2001. Two microcosms were constructed using USDA ARS soil harvested 7 days earlier for a previous trial. The units were constructed and sealed following the same general procedure used for the carbon addition trials. Both were allowed to sit for approximately 1 hour, after which each was connected to the DAQ computer via redox probe and calomel probe via a salt bridge. The experimental unit was connected to the delivery hoses from both nutrient delivery pumps. The reservoir for pump number 0 (carbon delivery pump) was filled with fresh 1.0 M sodium acetate solution, and the reservoir for pump number 1 (nitrate delivery pump) was filled with fresh 1.0 M potassium nitrate solution. The pump flow rates were checked and kept at 1.6 (±0.09) and 1.4 (±0.14) $ml \cdot s^{-1}$ for pumps 0 and 1, respectively. For both experiment and control units, the sample period was set to 900 s (1/4 hour), and pump time was set to 1 s

to be activated every other sample event. For the experimental unit, the upper threshold (above which carbon would be added) was set to +300 mV, and the lower threshold (below which nitrate would be added) was set to +150 mV. The experiment was initiated and allowed to proceed for 49.0 hours.

Results for Trial 13 conformed well to expected results (Figure 6. 20). Both the experimental and control units showed an initial decrease in redox potential over time. The initial state of the experimental unit, however, was significantly more reduced (by approximately 150 mV) than the control as well as being below the lower threshold. Thus the nitrate pump was activated from the start and continued for the first 16 hours. While *Eh* in the control continued to decrease for the extent of the trial as reducing metabolism continued, the *Eh* in the experimental unit first stabilized around 0 mV at hour 4, then effected a drastic increase after hour 13, presumably as a result of anaerobic nitrate respiration. The *Eh* in the experiment then continued to increase at an ever-slower rate for the entire length of the trial, approaching but never reaching the upper threshold setpoint. In total, the carbon injection pump was never activated, and the nitrate injection pump was activated for 33 events.

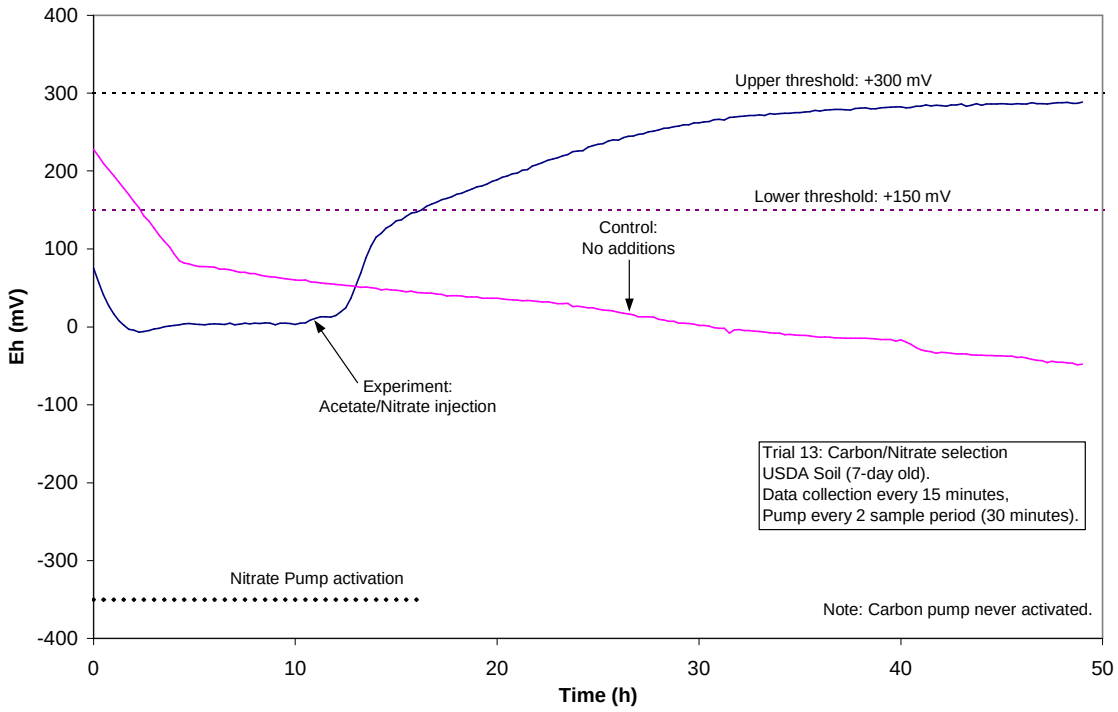

Figure 6. 20. Results for Trial 13: Redox potential vs. time for USDA soil microcosms. Experiment received 1.0 M sodium acetate solution and 1.0 M potassium nitrate solution, added via controlling computer.

6.2.2 Trial 14: Carbon/Nitrate Selection with more narrow threshold range

Trial 14 was started in the laboratory on 15 August 2001 to attempt to repeat the results of Trial 13 using a smaller range between the upper and lower threshold setpoints. Two microcosms units were constructed using the same USDA ARS soil used in Trial 13. The units were constructed and sealed following the same general procedure used previously and were allowed to sit for approximately 1 hour. Each unit was then connected to the DAQ computer via redox probe and calomel probe via a salt bridge. The experimental unit was connected to the delivery hoses from both nutrient delivery pumps. The reservoir for pump number 0 (carbon delivery pump) was filled with fresh 2.0 M

sodium acetate solution, and the reservoir for pump number 1 (nitrate delivery pump) was filled with fresh 1.0 M potassium nitrate solution. The pump flow rates were checked again at 1.6 (±0.09) and 1.4 (±0.14) $ml \cdot s^{-1}$ for pumps 0 and 1, respectively. For both experiment and control units, the sample period was set to 900 s (1/4 hour), and pump time was set to 1 s to be activated every other sample event. For the experimental unit, the upper threshold (above which carbon would be added) was set to +250 mV, and the lower threshold (below which nitrate would be added) was set to +200 mV. The experiment was initiated and allowed to proceed for over 100 hours.

Results for Trial 14 were consistent with those of the previous trial (Figure 6. 21). After a slight initial increase in redox potential, the control unit exhibited the expected continuous decrease in redox potential for the entire trial length. The experiment showed an initial decrease in redox potential, continuing to decrease for the first 14 hours, during which time nitrate solution was added. After hour 14, however, the redox potential in the experimental unit began to increase drastically, presumably as a result of increased anaerobic nitrate respiration. Redox potential continued to rise, climbing first above the lower threshold at hour 20, thus turning off the nitrate pump, and then continuing above the upper threshold by hour 28, thus turning on the carbon pump. Redox potential continued to rise until approximately hour 50 when it began to decrease again, presumably because of the increased availability of carbon. The carbon pump continued to be activated until hour 76, after which the redox potential fell again below the upper threshold. Although the trial continued beyond 100 hours, the carbon reservoir was empty some time around hour 73; thus only the first 80 hours of data are reported here. In total,

the carbon injection pump was activated for 96 events, and the nitrate pump was activated for 40 events.

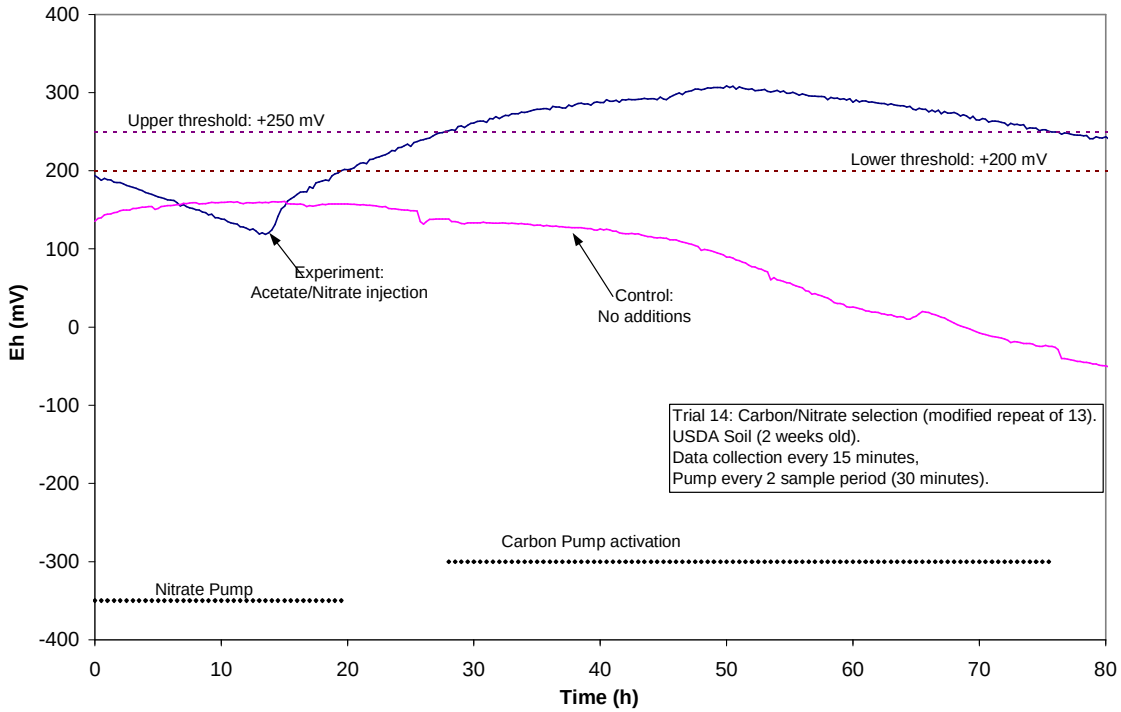

Figure 6. 21. Results for Trial 14: Redox potential vs. time for USDA soil microcosms. Experiment received 2.0 M sodium acetate solution and 1.0 M potassium nitrate solution, added via controlling computer.

6.2.3 Trial 15: Repeat of Trial 14.

Trial 15 was started in the laboratory on 1 September 2001 as a repeat of Trial 14. Two microcosms units were constructed using freshly-harvested USDA ARS soil. The units were constructed and sealed following the same general procedure used previously and were allowed to sit for approximately 1 hour. Each unit was then connected to the DAQ computer via redox probe and calomel probe via a salt bridge. The experimental unit was connected to the delivery hoses from both nutrient delivery pumps. The

reservoir for pump number 0 (carbon delivery pump) was filled with fresh 2.0 M sodium acetate solution, and the reservoir for pump number 1 (nitrate delivery pump) was filled with fresh 1.0 M potassium nitrate solution. Larger reservoir containers were used to prevent them from going empty as in Trial 14. The pump flow rates were checked again and verified at 1.6 (±0.09) and 1.4 (±0.14) $ml \cdot s^{-1}$ for pumps 0 and 1, respectively. For both experiment and control units, the sample period was set to 900 s (1/4 hour), and pump time was set to 1 s to be activated every other sample event. For the experimental unit, the upper threshold (above which carbon would be added) was set to +250 mV, and the lower threshold (below which nitrate would be added) was set to +200 mV. The experiment was initiated and allowed to proceed for over 250 hours.

Results for Trial 15 were consistent with those of the Trial 14 (Figure 6. 22). The control unit again exhibited a continuous decline in redox potential for the entire trial length. The experiment likewise showed a decrease in redox potential from the start, continuing to decrease for the first 15 hours, during which time nitrate solution was added. After hour 15, however, the redox potential in the experimental unit began to increase again, presumably as a result of increased anaerobic nitrate respiration. Redox potential continued to rise, climbing first above the lower threshold at hour 30, thus turning off the nitrate pump, and then continuing above the upper threshold by hour 34, thus turning on the carbon pump. Redox potential continued to rise until peaking at approximately hour 45 when it began to decrease again, presumably because of the increased availability of carbon. The carbon pump continued to be activated until hour 54, after which the redox potential fell again. It continued to decrease until dropping below the lower threshold again at hour 68, activating the nitrate pump again. The rate of

decrease in redox potential then slowed and the redox potential leveled off to around 100 mV, activating the nitrate pump for the remainder of the trial. The nitrate pump was activated for the first 30 hours, followed by the carbon pump for 20 hours, and then finally the nitrate pump again for the last 182 hours of the trial. In total, the carbon pump was activated for 42 events, and the nitrate pump was activated for 414 events. Note that sporadic signal noise between hours 100 and 130 occasionally and unexpectedly activated the carbon pump.

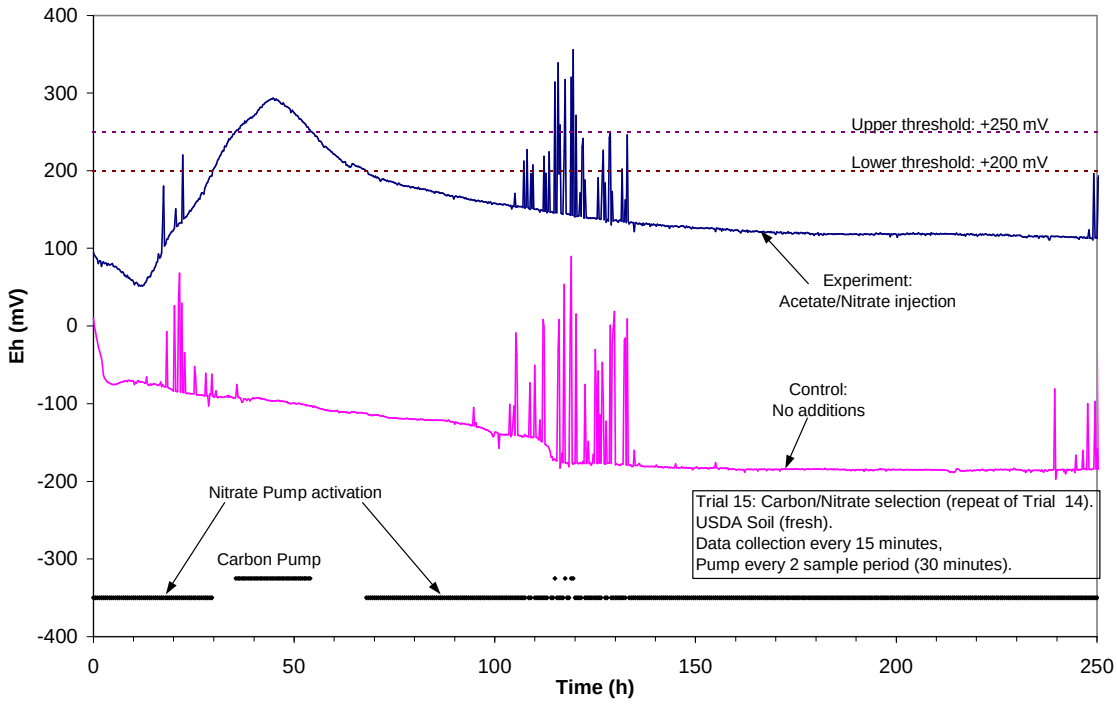

Figure 6. 22. Results for Trial 15: Redox potential vs. time for USDA soil microcosms. Experiment received 2.0 M sodium acetate solution and 1.0 M potassium nitrate solution, added via controlling computer.

6.2.4 Trial 16: Carbon/Nitrate Selection with narrow threshold range and more concentrated nutrient reservoirs (modified repeat of Trial 14).

Trial 16 was started in the laboratory on 19 September 2001 as a modified repeat of Trial 14 to test the effect of stronger nutrient solutions. Two microcosms units were constructed using the same USDA ARS soil as used in Trial 15 (thus 19 days old). The units were constructed and sealed following the same general procedure used previously and were allowed to sit for approximately 1 hour. Each unit was then connected to the DAQ computer via redox probe and calomel probe via a salt bridge. The experimental unit was connected to the delivery hoses from both nutrient delivery pumps. The reservoir for pump number 0 (carbon delivery pump) was filled with fresh 2.5 M sodium acetate solution, and the reservoir for pump number 1 (nitrate delivery pump) was filled with fresh 2.5 M potassium nitrate solution. The pump flow rates were checked again and verified at 1.6 (±0.09) and 1.4 (±0.14) $ml \cdot s^{-1}$ for pumps 0 and 1, respectively. For both experiment and control units, the sample period was set to 900 s (1/4 hour), and pump time was set to 1 s to be activated every other sample event. For the experimental unit, the upper threshold (above which carbon would be added) was set to +250 mV, and the lower threshold (below which nitrate would be added) was set to +200 mV. The experiment was initiated and allowed to proceed for over 120 hours.

Results for Trial 16 were different than those in previous trials (Figure 6. 23). Right away, the redox states of the control and experimental units were widely disparate. The control unit started off in a highly reduced state (around –80 mV) and exhibited a gradual yet continuous decline in redox potential for the entire trial length. The experiment, however, started off in a more oxidized state (around +175 mV), yet below the lower threshold setpoint, thus activating the nitrate pump form the start. Nitrate was

added for only the first 2.5 hours until the redox potential increased above the lower threshold. Redox potential peaked some time around hour 18, although never climbing above the upper threshold to activate the carbon pump. After hour 18, redox potential decreased again, dropping below the lower threshold by hour 29 and again activating the nitrate pump. Despite nitrate addition for the remainder of the trial, redox potential continued to gradually decrease, possibly locked in a cycle of continuing anaerobic nitrate respiration. However, redox potential made a steep decline into reducing conditions around hour 95, possibly indicating the initiation of another anaerobic metabolic pathway despite the strong availability of nitrate. The nitrate pump was activated for the first 2.5 hours, and again for the last 94 hours of the trial. In total, the carbon pump was never activated, and the nitrate pump was activated for 189 events.

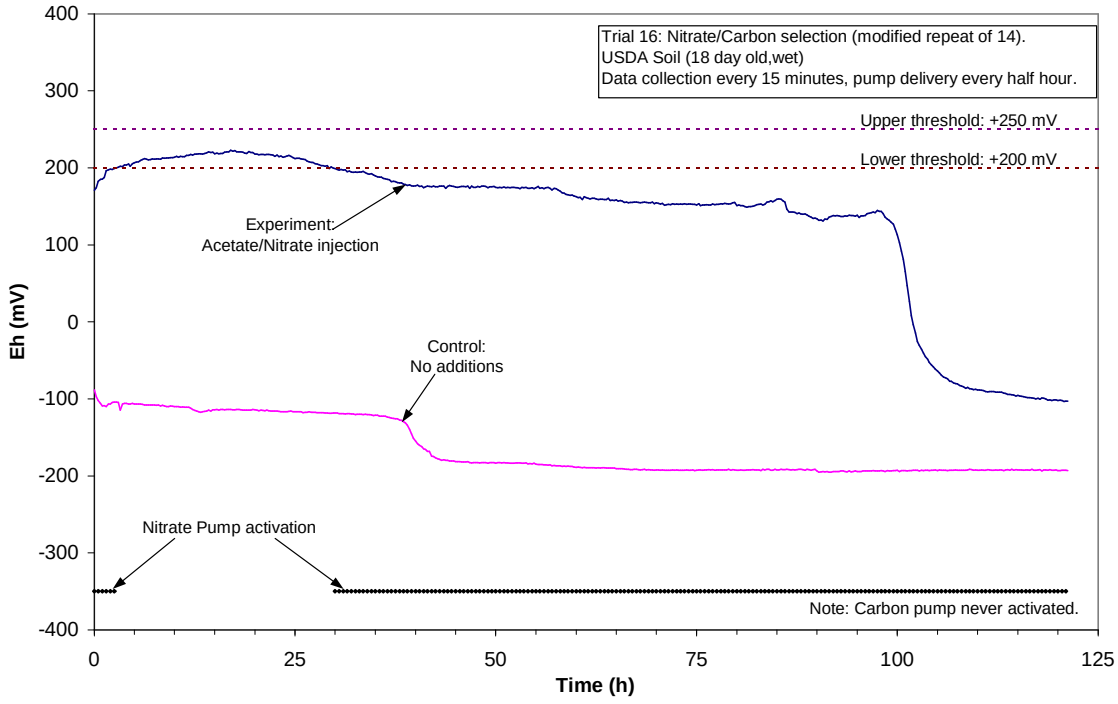

Figure 6. 23. Results for Trial 16: Redox potential vs. time for USDA soil microcosms. Experiment received 2.5 M sodium acetate solution and 2.5 M potassium nitrate solution, added via controlling computer.

6.2.5 Trial 20: Carbon/Nitrate Selection with narrow threshold range (repeat of Trial 14).

Trial 20 was started in the laboratory on 12 April 2002 to attempt to repeat the results of Trial 14. Two microcosms units were constructed using freshly-harvested USDA ARS soil. The units were constructed and sealed following the same general procedure used previously and were allowed to sit for approximately 1 hour. Each unit was then connected to the DAQ computer via redox probe and calomel probe via a salt bridge. The experimental unit was connected to the delivery hoses from both nutrient delivery pumps. The reservoir for pump number 0 (carbon delivery pump) was filled with fresh 2.0 M sodium acetate solution, and the reservoir for pump number 1 (nitrate delivery pump) was filled with fresh 1.0 M potassium nitrate solution. The pump flow rates were recalibrated at 2.0 $ml \cdot s^{-1}$ (± 0.11 $ml \cdot s^{-1}$ for pump 0 and ± 0.00 $ml \cdot s^{-1}$ for pump 1). For both experiment and control units, the sample period was set to 1800 s (1/2 hour), and pump time was set to 1 s to be activated every sample event. For the experimental unit, the upper threshold (above which carbon would be added) was set to +250 mV, and the lower threshold (below which nitrate would be added) was set to +200 mV. The experiment was initiated and allowed to proceed for over 118 hours.

Results for Trial 20 were inconsistent with those of the previous trials (Figure 6. 24). The control unit exhibited the expected continuous and gradual decrease in redox potential for the entire trial length, except for a sudden increase around hour 72, possibly indicating the inception of one of the anaerobic respiratory metabolic pathways. The experiment showed an initial steep decrease in redox potential within the first half-hour,

immediately activating the nitrate delivery pump. The experiment then exhibited an immediate and steep increase in redox potential, increasing rapidly for the next 2 hours, and then more gradually for the remainder of the trial. The redox potential climbed above the lower threshold by hour 54, turning off the nitrate pump. Redox potential never climbed above the upper threshold, and the carbon pump was never activated. In total, the nitrate pump was activated for 108 events, and the carbon pump was never activated.

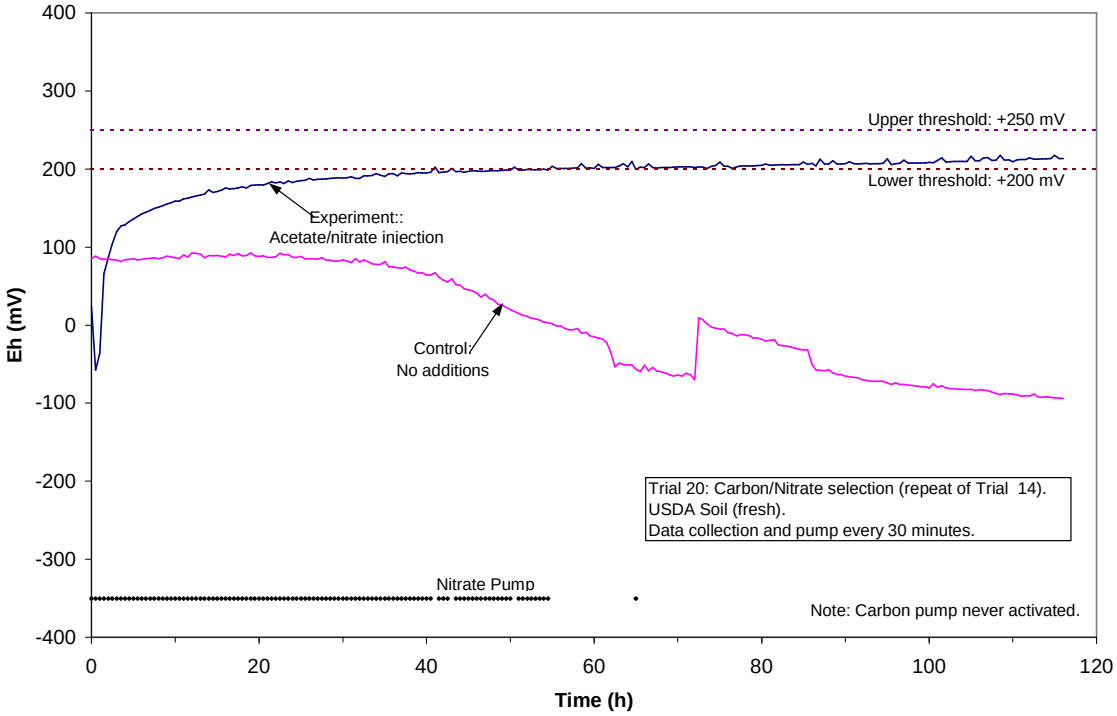

Figure 6. 24. Results for Trial 20: Redox potential vs. time for USDA soil microcosms. Experiment received 2.0 M sodium acetate solution and 1.0 M potassium nitrate solution, added via controlling computer.

6.2.6 Trial 21: Carbon/Nitrate Selection with more narrow threshold range and slower nutrient delivery rate (modified repeat of Trial 14).

Trial 21 was started in the laboratory on 17 April 2002 to investigate the effect of narrowing the range between the thresholds even further. Two microcosms units were

constructed using the same batch of USDA ARS soil used in Trial 20. The units were constructed and sealed following the same general procedure used previously and were allowed to sit for approximately 1 hour. Each unit was then connected to the DAQ computer via redox probe and calomel probe via a salt bridge. The experimental unit was connected to the delivery hoses from both nutrient delivery pumps. The reservoir for pump number 0 (carbon delivery pump) was filled with fresh 2.0 M sodium acetate solution, and the reservoir for pump number 1 (nitrate delivery pump) was filled with fresh 1.0 M potassium nitrate solution. The pump flow rates were checked at 2.0 $ml \cdot s^{-1}$ (± 0.11 $ml \cdot s^{-1}$ for pump 0 and ± 0.00 $ml \cdot s^{-1}$ for pump 1). For both experiment and control units, the sample period was set to 1800 s (1/2 hour), and pump time was set to 1 s to be activated every other sample event (thus the maximum possible delivery rate would be once an hour). For the experimental unit, the upper threshold (above which carbon would be added) was set to +205 mV, and the lower threshold (below which nitrate would be added) was set to +195 mV. The experiment was initiated and allowed to proceed for over 350 hours.

Results for Trial 21 were somewhat similar to those of previous trials (Figure 6. 25). The control unit exhibited the expected continuous and gradual decrease in redox potential for the entire trial length, except for a gradual increase around hour 30, again possibly indicating the inception of one of the anaerobic respiratory metabolic pathways. The experiment started in a more oxidized state (+170 mV) than in previous trials, although this was lower than the lower threshold setpoint, thus immediately activating the nitrate delivery pump. The experiment then exhibited an immediate and steep increase in redox potential, increasing rapidly for the next 2 hours, and then more gradually for the

next 12 hours. After this, the redox potential generally remained between the threshold setpoints, occasionally dropping below the lower threshold and activating the nitrate pump. Redox potential climbed above the upper threshold only once, immediately activating the carbon pump for one event, following which the redox potential precipitously dropped over 50 mV. After this, the redox potential fluctuated up and down, but always below the lower setpoint, and the nitrate pump was activated every other sample period until the end of the trial. In total, the nitrate pump was activated for 262 events, and the carbon pump was activated for 1 event.

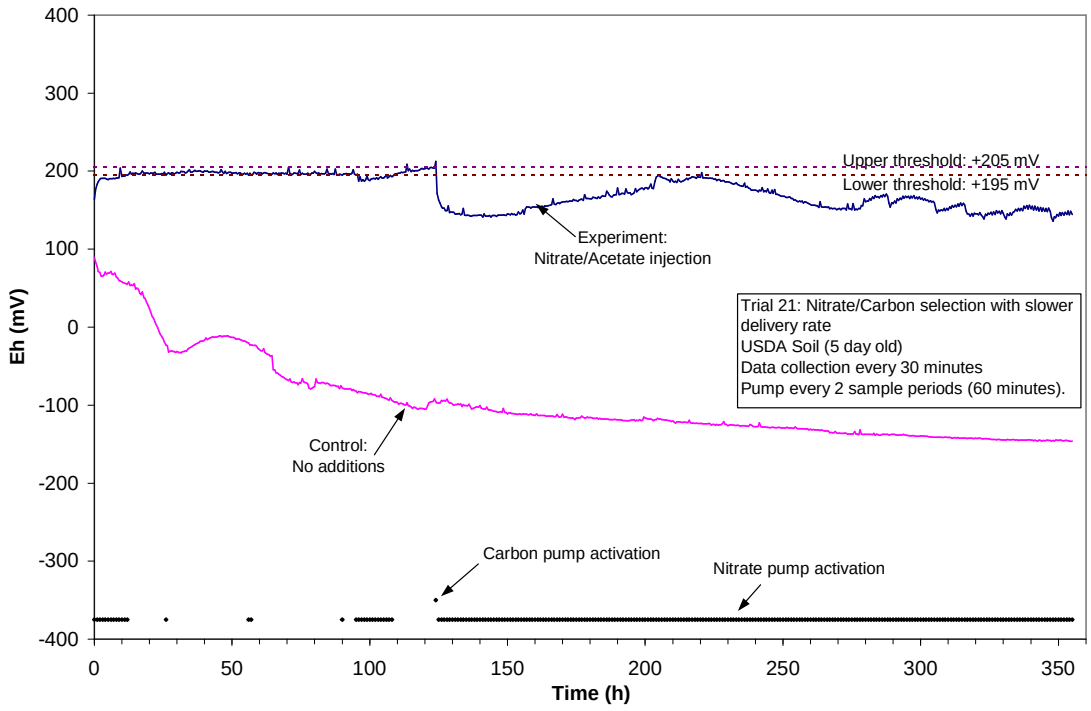

Figure 6. 25. Results for Trial 21: Redox potential vs. time for USDA soil microcosms. Experiment received 2.0 M sodium acetate solution and 1.0 M potassium nitrate solution, added via controlling computer, every other sample period.

6.2.7 Trial 22: Carbon/Nitrate Selection with more narrow threshold range and normal nutrient delivery rate (modified repeat of Trial 15).

Trial 22 was started in the laboratory on 7 May 2002 to attempt to replicate the results of Trial 15 with a narrower threshold range. Two microcosms units were constructed using freshly-harvested USDA ARS soil and following the same general procedure used previously. Each unit was then connected to the DAQ computer via redox probe and calomel probe via a salt bridge. The experimental unit was connected to the delivery hoses from both nutrient delivery pumps. The reservoir for pump number 0 (carbon delivery pump) was filled with fresh 2.0 M sodium acetate solution, and the reservoir for pump number 1 (nitrate delivery pump) was filled with fresh 1.0 M potassium nitrate solution. The pump flow rates were checked again at 2.0 $ml \cdot s^{-1}$ for both pumps (±0.11 $ml \cdot s^{-1}$ for pump 0 and ±0.00 $ml \cdot s^{-1}$ for pump 1). For both experiment and control units, the sample period was set to 1800 s (1/2 hour), and pump time was set to 1 s to be activated every sample event. For the experimental unit, the upper threshold (above which carbon would be added) was set to +205 mV, and the lower threshold (below which nitrate would be added) was set to +195 mV. The experiment was initiated and allowed to proceed for 57 hours.

Results for Trial 22 conformed very closely to expected results (Figure 6. 26). The control unit exhibited the expected continuous and gradual decrease in redox potential for the first 20 hours, but then showed a slight increase at hour 21 and an even sharper increase at hour 25. Again, this possibly indicates the inception of one of the anaerobic respiratory metabolic pathways. The experiment started in a slightly more oxidized state than the control, but because this was lower than the lower threshold setpoint, the nitrate delivery pump was immediately activated. Despite the addition of

nitrate, the redox potential in the experimental unit continued to decrease for 5.5 hours, showing a rapid increase by hour 6. A more gradual increase in redox potential then occurred, climbing above the lower threshold by hour 12 and shortly thereafter activating the carbon delivery pump. Following addition of carbon, redox potential peaked by hour 17, gradually decreasing again below the lower threshold by hour 21 and remaining below for the remainder of the trial. Interestingly, redox potential in both the experimental unit and the control unit ended at nearly the same value of +117 mV. In total, the nitrate pump was activated for 174 events, and the carbon pump was activated for 15 events.

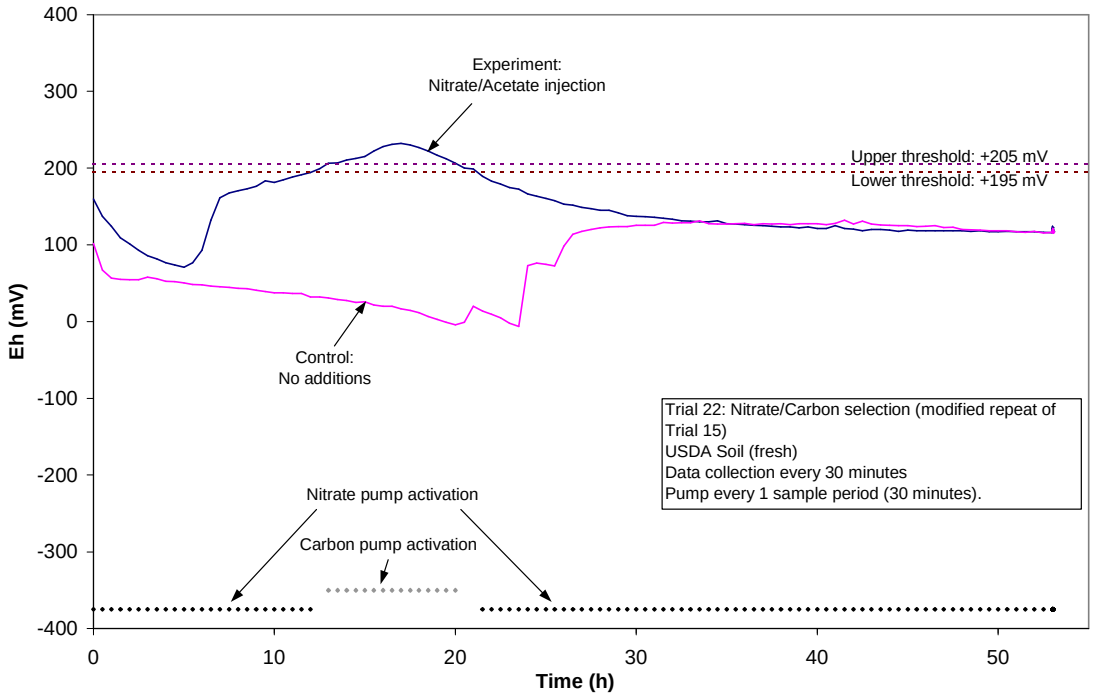

Figure 6. 26. Results for Trial 22: Redox potential vs. time for USDA soil microcosms. Experiment received 2.0 M sodium acetate solution and 1.0 M potassium nitrate solution, added via controlling computer, every sample period.

6.2.8 Trial 25: Carbon/Nitrate Selection with identical upper/lower thresholds (modified repeat of Trial 15).

Trial 25 was started in the laboratory on 24 May 2002 to attempt to replicate the results of Trial 15 with no range between the threshold setpoints (that is, identical upper and lower threshold setpoints). Two microcosms units were constructed using freshly-harvested USDA ARS soil and following the same general procedure used previously. Each unit was then connected to the DAQ computer via redox probe and calomel probe via a salt bridge. The experimental unit was connected to the delivery hoses from both nutrient delivery pumps. The reservoir for pump number 0 (carbon delivery pump) was filled with fresh 2.0 M sodium acetate solution, and the reservoir for pump number 1 (nitrate delivery pump) was filled with fresh 1.0 M potassium nitrate solution. The pump flow rates were checked again at 2.0 $ml \cdot s^{-1}$ for both pumps (± 0.11 $ml \cdot s^{-1}$ for pump 0 and ± 0.00 $ml \cdot s^{-1}$ for pump 1). For both experiment and control units, the sample period was set to 1800 s (1/2 hour), and pump time was set to 1 s to be activated every sample event. For the experimental unit, both the upper threshold (above which carbon would be added) and the lower threshold (below which nitrate would be added) were set to +200 mV. The experiment was initiated and allowed to proceed for 120 hours.

Results for Trial 25 were similar to those obtained in Trial 20 (Figure 6. 27). The control unit exhibited the expected continuous and gradual decrease in redox potential for the entire trial length without any sudden increases. The experiment started off in somewhat reduced conditions, immediately activating the nitrate delivery pump. The experiment then exhibited an immediate and steep increase in redox potential, increasing rapidly for the next two hours, and then more gradually for the next 45 hours. After that, the redox potential was maintained around the threshold value, periodically climbing

above it or below and alternately activating the carbon or nitrate delivery pump. In total, the nitrate pump was activated for 197 events, and the carbon pump was activated for 44 events.

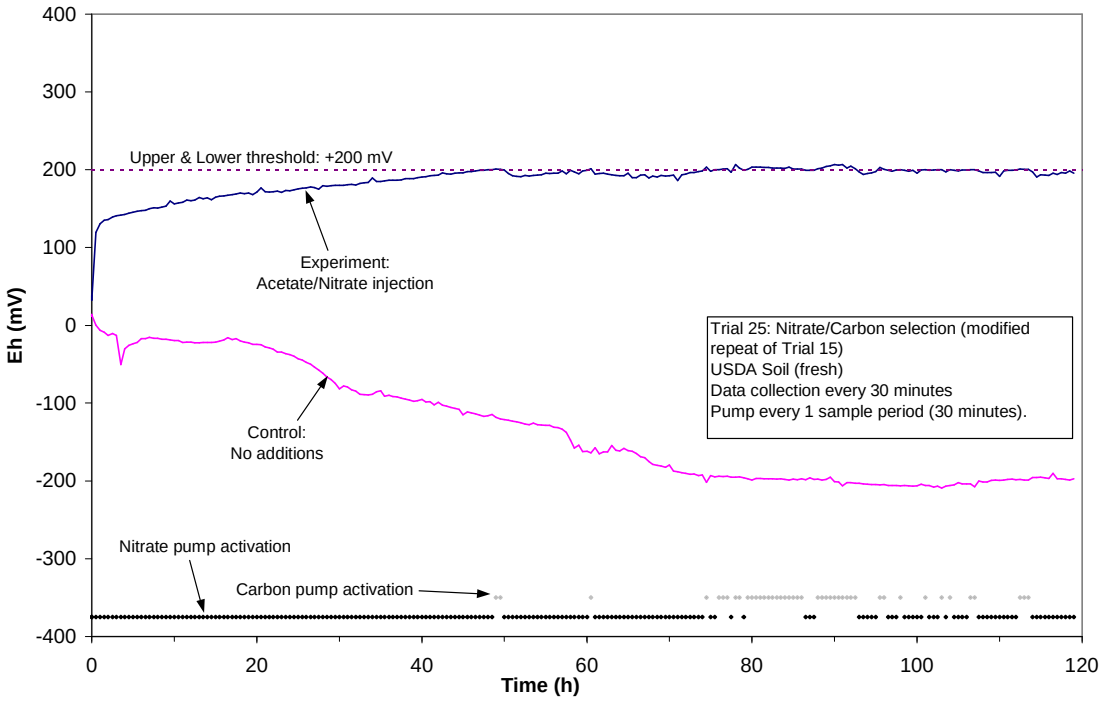

Figure 6. 27. Results for Trial 25: Redox potential vs. time for USDA soil microcosms with identical thresholds. Experiment received 2.0 M sodium acetate solution and 1.0 M potassium nitrate solution, added via controlling computer, every sample period.

It was thought that possibly too much nitrate and/or carbon was being added to the experiment microcosm, such that it was negatively affecting the microbial community in the soil and thus causing the redox potential curve to go flat. To investigate this hypothesis, the nutrient delivery pumps were turned off at hour 120 of Trial 25 and data recording continued, the results of which are shown in Figure 6. 28. Immediately after pumps are turned off, the redox potential in the experimental unit began a gradual decline lasting for approximately 50 hours. After this, redox potential began to gradually increase

again until approximately hour 240, when it began a steep decline of almost 250 mV in 40 hours, possibly indicating the shift of the soil microbial metabolism into other anaerobic respiration pathways. Interestingly, the redox potential for the control unit remains in highly reduced conditions for much of the trial, yet increases drastically around hour 220, a phenomenon similar to that seen in previous trials.

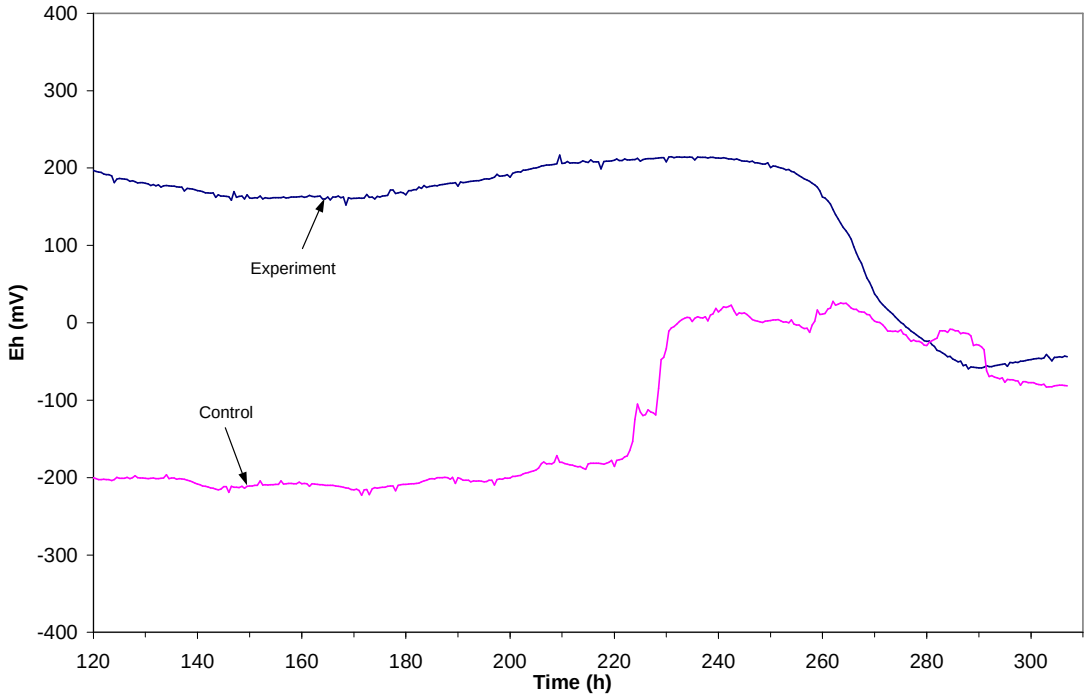

Figure 6. 28. Additional results for Trial 25 after nutrient pumps were turned off.

6.2.9 Trial 26: Carbon/Nitrate Selection with identical upper/lower thresholds (repeat of Trial 25 with de-oxygenated reservoirs).

Trial 26 was started in the laboratory on 6 June 2002 to attempt to replicate the results of Trial 25. Two microcosms units were constructed using freshly-harvested USDA ARS soil and following the same general procedure used previously, and each unit was then connected to the DAQ computer via the probes. The experimental unit was

connected to the delivery hoses from both nutrient delivery pumps. The reservoir for pump number 0 (carbon delivery pump) was filled with fresh 2.0 M sodium acetate solution, and the reservoir for pump number 1 (nitrate delivery pump) was filled with fresh 1.0 M potassium nitrate solution. Nitrogen gas was bubbled through each of the reservoir solutions for at least ½ hour to remove all dissolved oxygen. The pump flow rates were checked again at 2.0 $ml \cdot s^{-1}$ for both pumps (±0.11 $ml \cdot s^{-1}$ for pump 0 and ±0.00 $ml \cdot s^{-1}$ for pump 1). For both experiment and control units, the sample period was set to 1800 s (1/2 hour), and pump time was set to 1 s to be activated every sample event. For the experimental unit, both the upper threshold (above which carbon would be added) and the lower threshold (below which nitrate would be added) were set to +200 mV. The experiment was initiated and allowed to proceed for 40 hours.

Results for Trial 26 were similar to those obtained in previous trials (Figure 6. 29). The control unit exhibited the expected continuous and gradual decrease in redox potential for most of the trial length, except for a small increase around hour 27. The experiment started off in somewhat reduced conditions, immediately activating the nitrate delivery pump. The experiment then exhibited a slight, gradual increase in redox potential, peaking by hour 5, and then gradually decreasing to a low by hour 17. Following this, a rapid increase was observed until the redox potential leveled off near the threshold, varying above and below it for the remainder of the trial. Due to this variation, alternation back and forth between carbon and nitrate pump activation was observed. In total, the nitrate pump was activated for 67 events, and the carbon pump was activated for 14 events.

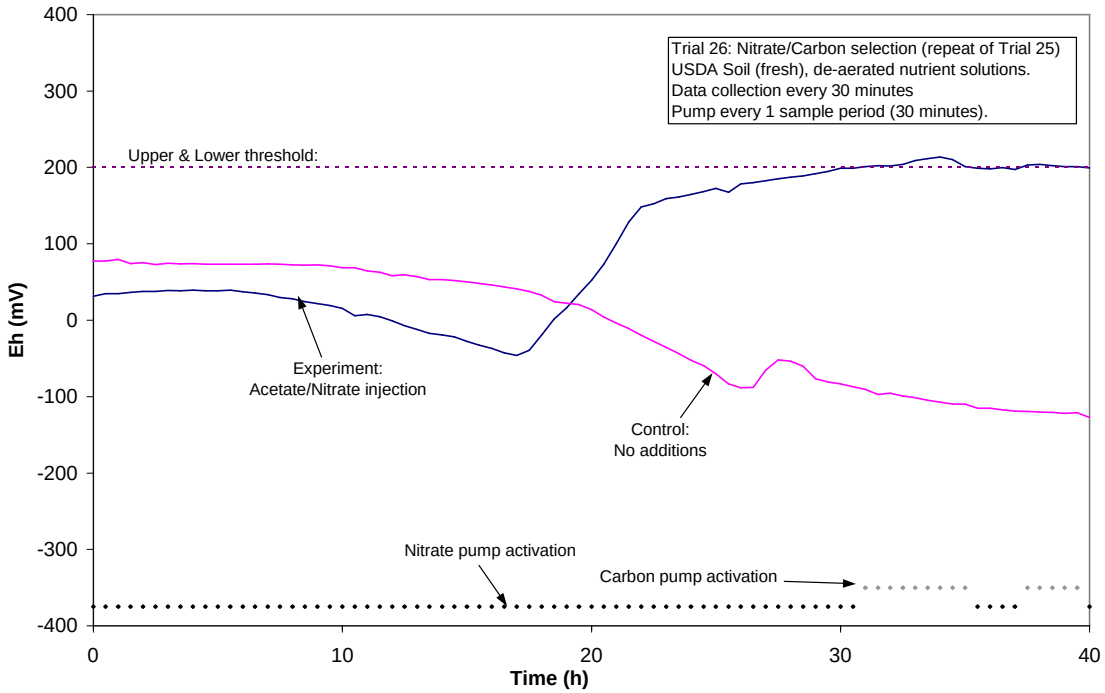

Figure 6. 29. Results for Trial 26: Redox potential vs. time for USDA soil microcosms with identical thresholds. Experiment received 2.0 M sodium acetate solution and 1.0 M potassium nitrate solution, both stripped of oxygen prior to additions.

As in Trial 25, the nutrient delivery pumps were turned off after a certain time to observe the change in redox potential as an indication of continuing microbial metabolism. For this trial, the pumps were turned off at hour 40 and data were recording continued, the results of which are shown in Figure 6. 30. Immediately after pumps were turned off, the redox potential in the experimental unit began a gradual decline lasting for the entire length of the trial (300 hours), possibly indicating continued anaerobic respiration in the soil microcosm. Again, the redox potential for the control unit remained in highly reduced conditions for much of the trial, yet increasing around hour 80.

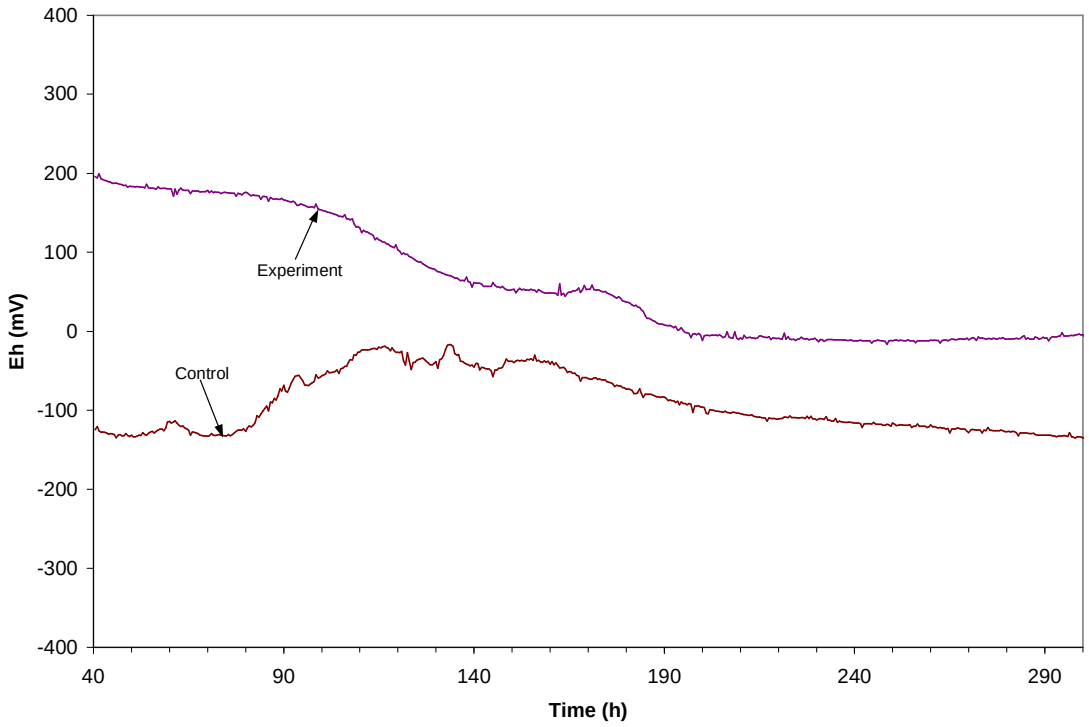

Figure 6. 30. Additional results for Trial 26 after nutrient pumps were turned off.

Nutrient analyses were also performed on samples taken from the water column of both units in Trial 26 as an indicator of the rate of denitrification. Samples were taken through one of the ports in each of the microcosm lids using a syringe. The samples were analyzed for nitrate and ammonia using a Hach DR2000 spectrophotometer, the samples were analyzed for nitrate and ammonia at a 1/25 dilution following the methods outlined in the Hach user manual. The results of this analysis are shown in Table 6. 11.

Table 6. 11. Nutrient concentrations in the water column of the soil microcosms at various times before and after nutrient additions. Note that the nutrient addition pump was turned off after hour 40.

Unit	Nutrient	Time		
		0 hr.	40 hr.	300 hr.
Experiment	NO_3 (mg/l)	0.0	575	660
	NH_3 (mg/l)	6.7	3.9	25.8
Control	NO_3 (mg/l)	0.0	8.0	11.0
	NH_3 (mg/l)	1.7	1.9	2.3

The rate of anaerobic nitrate respiration can be inferred by tracking the total moles of nitrogen present in the water column at the various time steps. Focusing on the experimental unit, the concentrations in Table 6. 11 can be converted to equivalent moles of nitrogen by multiplying by the total water volume at each time step (correcting for additions due to nutrient pump activations and subtractions due to sampling removals) and dividing by the molecular weight of the chemical species. These results are presented in Table 6. 12.

Table 6. 12. Total nitrate and ammonia nitrogen present in the experiment microcosm for Trial 26 at various times before and after nutrient addition, expressed as total moles N.

Nutrient	Time		
	0 hr.	40 hr.	300 hr.
NO_3 (mol-N)	0.0	0.0043	0.0039
NH_3 (mol-N)	0.0012	0.00011	0.00055
TOTAL (mol-N)	0.0012	0.00441	0.00445

As shown in the table, the total ammonia and nitrate nitrogen present increases between 0 and 40 hours, a true signal of the nutrient additions via automatic pump. However, the total nitrogen does not change significantly from 40 hours to 300 hours, possibly indicating a shift in microcosm metabolism away from denitrification. The

proportion of ammonia to nitrogen does change from 40 hours to 300 hours: at 40 hours, ammonia is 2.5% of the total, whereas at 300 hours, ammonia is 12.4% of the total. Most interestingly, the expected moles of nitrogen present, based upon the number of pumping events (67) of a known volume (2 ml) and know concentration (1.0 M potassium nitrate), is at least 0.13 mol NO_3-N. Thus, approximately 0.125 mol NO_3-N is unaccounted for in this analysis.

6.2.10 Trial 27: Carbon/Nitrate Selection with identical upper/lower thresholds and de-oxygenated reservoirs (repeat of Trial 26).

Trial 27 was started in the laboratory on 20 June 2002 to attempt to replicate the results of Trial 26. Two microcosms units were constructed using freshly-harvested USDA ARS soil and following the same general procedure used previously, and each unit was then connected to the DAQ computer via the probes. The experimental unit was connected to the delivery hoses from both nutrient delivery pumps. The reservoir for pump number 0 (carbon delivery pump) was filled with fresh 2.0 M sodium acetate solution, and the reservoir for pump number 1 (nitrate delivery pump) was filled with fresh 1.0 M potassium nitrate solution. Nitrogen gas was bubbled through each of the reservoir solutions for ½ hour to remove any dissolved oxygen. The pump flow rates were checked again at 2.0 $ml \cdot s^{-1}$ for both pumps (±0.11 $ml \cdot s^{-1}$ for pump 0 and ±0.00 $ml \cdot s^{-1}$ for pump 1). For both experiment and control units, the sample period was set to 1800 s (1/2 hour), and pump time was set to 1 s to be activated every sample event. For the experimental unit, both the upper threshold (above which carbon would be added) and the lower threshold (below which nitrate would be added) were set to +200 mV. The experiment was initiated and allowed to proceed for 68.5 hours.

Results for Trial 27 were similar to those obtained in previous trials (Figure 6. 31). The control unit exhibited the expected continuous and gradual decrease in redox potential for the entire trial length. The experiment started off in reduced conditions, immediately activating the nitrate delivery pump. The experiment then continued to decline gradually until exhibiting a sudden increase around hour 7. Redox potential continued to increase somewhat gradually until reaching the threshold by hour 28, at which point the nitrate pump turned off and the carbon pump turned on. After this, the rate of increase continued to slow, and redox potential peaked by hour 42, slowly declining after that but never falling below the threshold again. In total, the nitrate pump was activated for 57 events, and the carbon pump was activated for 81 events.

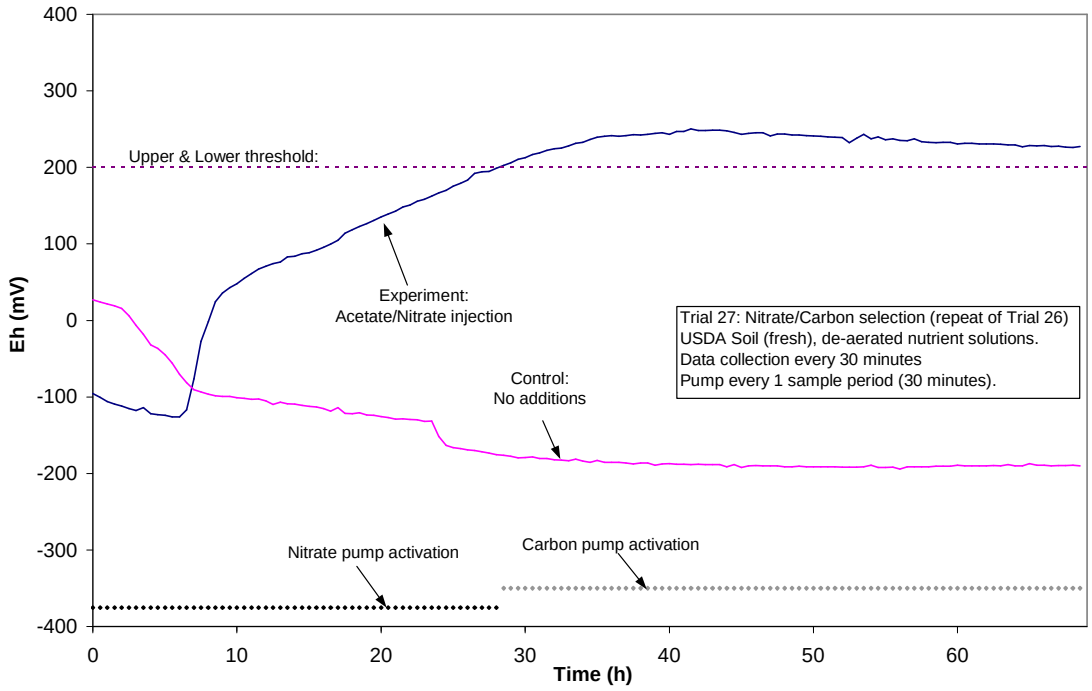

Figure 6. 31. Results for Trial 27: Redox potential vs. time for USDA soil microcosms with identical thresholds. Experiment received 2.0 M sodium acetate solution and 1.0 M potassium nitrate solution, both stripped of oxygen prior to additions.

As in the previous two trials, the nutrient delivery pumps were turned off after a certain time to observe the change in redox potential as an indication of continuing microbial metabolism. For this trial, the pumps were turned off at hour 69 and data recording continued, the results of which are shown in Figure 6. 32. Shortly after pumps are turned off, the redox potential in the experimental unit began a short, rapid decline, followed by a much more gradual decline lasting for most of the trial length (150 hours), possibly indicating continued anaerobic respiration in the soil microcosm. The redox potential for the control unit remained in highly reduced conditions for the remainder of the trial.

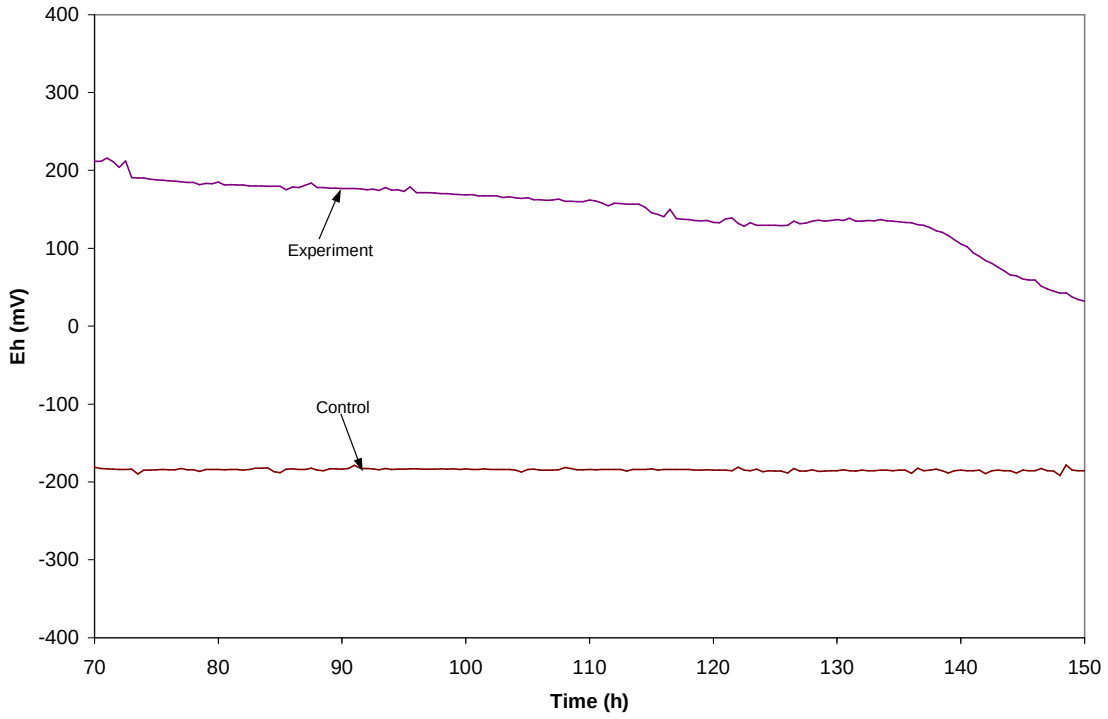

Figure 6. 32. Additional results for Trial 27 after nutrient pumps were turned off.

Nutrient analyses were also performed on samples taken from the water column of both units in Trial 27 as an indicator of the rate of denitrification. Samples were taken and analyzed via the procedure outlined in the previous section. The results of this analysis are shown in Table 6. 13.

Table 6. 13. Nutrient concentrations in the water column of the soil microcosms of Trial 27 at various times before and after nutrient additions. Note that the nutrient addition pump was turned off after hour 69.

Unit	Nutrient	Time		
		0 hr.	69 hr.	150 hr.
Experiment	NO_3 (mg/l)	0.0	53	10
	NH_3 (mg/l)	4.8	2.5	4.0
Control	NO_3 (mg/l)	0.0	0.3	9
	NH_3 (mg/l)	4.2	1.9	2.9

Again, the rate of anaerobic nitrate respiration can be inferred by tracking the total moles of nitrogen present in the water column at the various time steps. Focusing on the experimental unit, the concentrations in Table 6. 13 can be converted to equivalent moles of nitrogen by multiplying by the total water volume at each time step (correcting for additions due to nutrient pump activations and subtractions due to sampling removals) and dividing by the molecular weight of the chemical species. These results are presented in Table 6. 14.

Table 6. 14. Total nitrate and ammonia nitrogen present in the experiment microcosm for Trial 27 at various times before and after nutrient addition, expressed as total moles N.

Nutrient	Time		
	0 hr.	69 hr.	150 hr.
NO_3 (mol-N)	0.0	0.00049	0.000085
NH_3 (mol-N)	0.000085	0.000085	0.000124
TOTAL (mol-N)	0.000085	0.000575	0.000209

The total ammonia and nitrate nitrogen present in the experiment microcosm increases between 0 and 69 hours, again a signal of the nutrient additions via automatic pump. The total nitrogen decreases rather significantly from 69 hours to 150 hours, possibly indicating continued anaerobic nitrate respiration for the entire time. The proportion of ammonia to nitrogen likewise changes from 69 hours to 150 hours: at 69 hours, ammonia is 15% of the total, whereas at 300 hours, ammonia is 59% of the total. Most interestingly, the expected moles of nitrogen present, based upon the number of pumping events (57) of a known volume (2 ml) and know concentration (1.0 M potassium nitrate), is at least 0.114 mol NO_3-N. Thus, approximately 0.110 mol NO_3-N, or nearly all that was added, is unaccounted for in this analysis.

6.2.11 Trial 28: Carbon/Nitrate Selection with identical upper/lower thresholds and de-oxygenated reservoirs (repeat of Trial 26).

Trial 28 was started in the laboratory on 22 July 2002 to attempt to replicate the results of Trial 26. Two microcosms units were constructed using freshly-harvested USDA ARS soil and following the same general procedure used previously, and each unit was then connected to the DAQ computer via the probes. The experimental unit was connected to the delivery hoses from both nutrient delivery pumps. The reservoir for pump number 0 (carbon delivery pump) was filled with fresh 2.0 M sodium acetate solution, and the reservoir for pump number 1 (nitrate delivery pump) was filled with fresh 1.0 M potassium nitrate solution. Nitrogen gas was bubbled through each of the reservoir solutions for ½ hour to remove any dissolved oxygen. The pump flow rates were checked again at 2.0 $ml \cdot s^{-1}$ for both pumps (±0.11 $ml \cdot s^{-1}$ for pump 0 and ±0.00 $ml \cdot s^{-1}$ for pump 1). For both experiment and control units, the sample period was set to 1800 s

(1/2 hour), and pump time was set to 1 s to be activated every sample event. For the experimental unit, both the upper threshold (above which carbon would be added) and the lower threshold (below which nitrate would be added) were set to +200 mV. The experiment was initiated and allowed to proceed for 68.5 hours.

Results for Trial 28 were different than most other previous trials (Figure 6. 33). The control unit exhibited a very slow rate of decrease in redox potential for the entire trial length. The experiment started off in relatively oxidized conditions, immediately activating the carbon delivery pump. However, carbon addition seemed to have little effect of the redox potential, as it remained above the upper threshold for the entire 21 hours of the trial, showing only minor fluctuation up and down. In total, the nitrate pump was never activated, and the carbon pump was activated for 43 events.

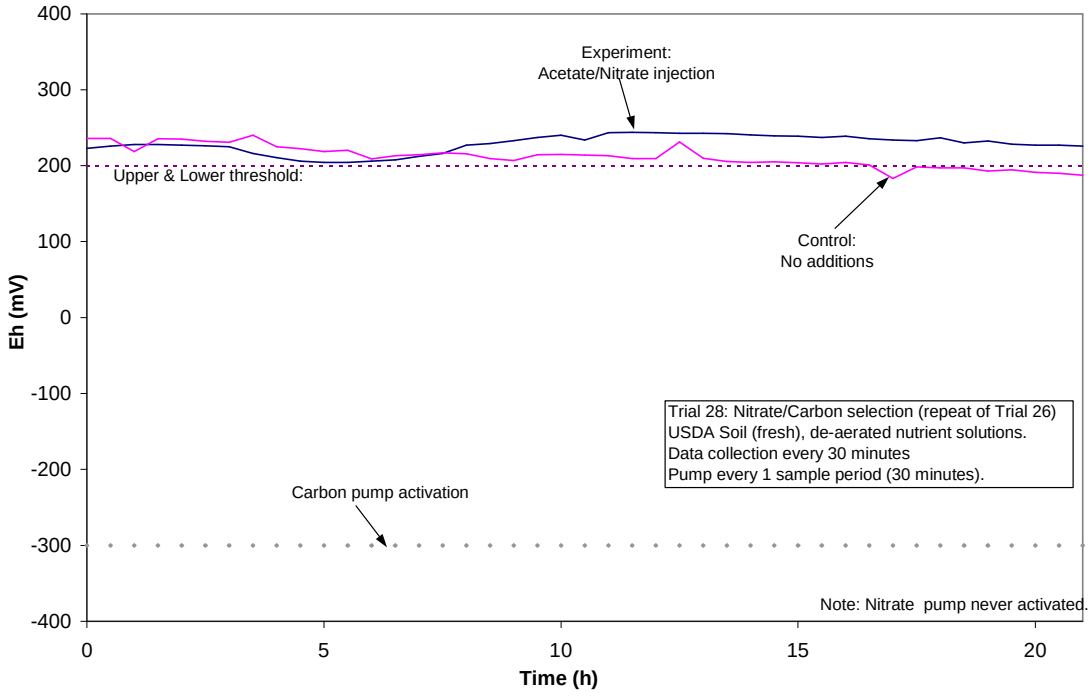

Figure 6. 33. Results for Trial 28: Redox potential vs. time for USDA soil microcosms with identical thresholds. Experiment received 2.0 M sodium acetate solution and 1.0 M potassium nitrate solution, both stripped of oxygen.

As in the previous two trials, the nutrient delivery pumps were turned off after a certain time to observe the change in redox potential as an indication of continuing microbial metabolism. For this trial, the pumps were turned off at hour 21 and data recording continued until hour 96.5, the results of which are shown in Figure 6. 34. After the pumps are deactivated, the redox potential in the experimental unit continued to decline slowly for another 10 hours. Following this, it began to gradually increase again, continuing for the remainder of the trial, a result different from most other trials. The redox potential for the control unit continued to decrease into reduced conditions for the remainder of the trial. Because only carbon was added in the experiment while the pumps were on, nutrient analyses were not performed.

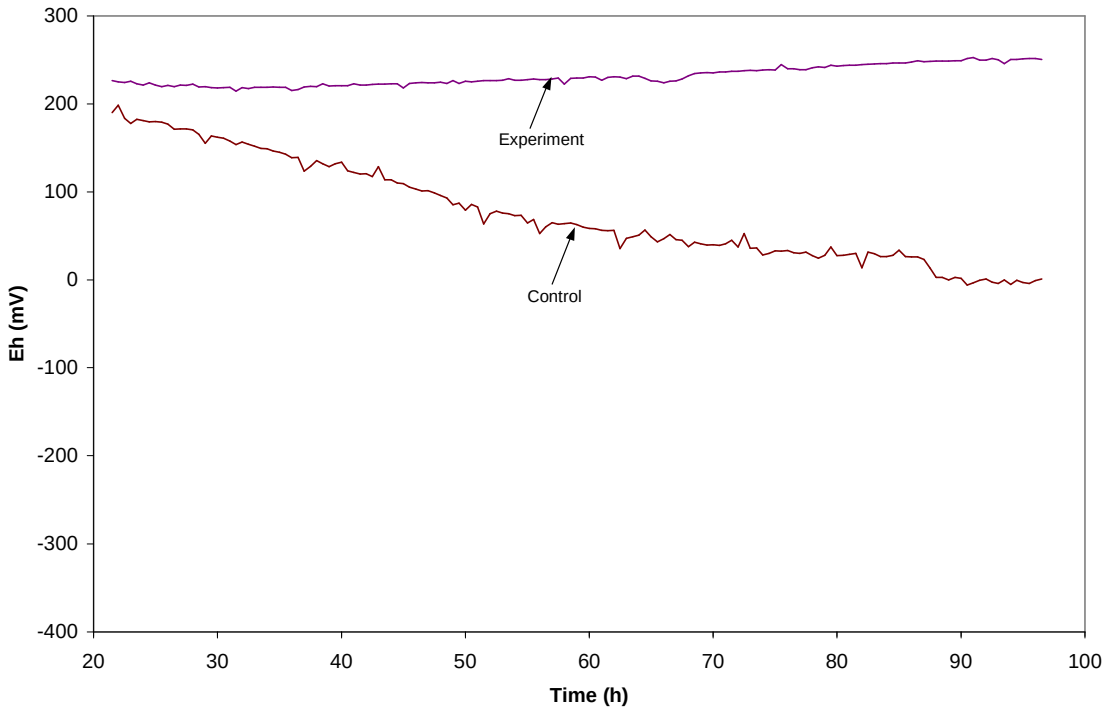

Figure 6. 34. Additional results for Trial 28 after nutrient pumps were turned off.

6.2.12 Trial 29: Carbon/Nitrate Selection with identical upper/lower thresholds (repeat of Trial 25).

Trial 29 was started in the laboratory on 27 May 2003 to attempt to replicate again the results of Trial 25. Two microcosms units were constructed using freshly-harvested USDA ARS soil and following the same general procedure used previously, and each unit was then connected to the DAQ computer via the probes. The experimental unit was connected to the delivery hoses from both nutrient delivery pumps. The reservoir for pump number 0 (carbon delivery pump) was filled with fresh 2.0 M sodium acetate solution, and the reservoir for pump number 1 (nitrate delivery pump) was filled with fresh 1.0 M potassium nitrate solution. This time, no nitrogen gas was bubbled through the reservoirs. The pump flow rates were checked again at 2.0 $ml \cdot s^{-1}$ for both pumps (±0.11 $ml \cdot s^{-1}$ for pump 0 and ±0.00 $ml \cdot s^{-1}$ for pump 1). For both experiment and control units, the sample period was set to 1800 s (1/2 hour), and pump time was set to 1 s to be activated every sample event. For the experimental unit, both the upper threshold (above which carbon would be added) and the lower threshold (below which nitrate would be added) were set to +200 mV. The experiment was initiated and allowed to proceed for 70.0 hours.

Results for Trial 29 conformed to expected results (Figure 6. 35). After a slight initial increase, the redox potential in the control unit exhibited a slow, continuous rate of decrease in redox potential for the entire trial length. The experiment started off in relatively oxidized conditions, immediately activating the carbon delivery pump. The redox potential immediately decreased at a relatively fast rate, falling below the threshold by hour 7 and activating the nitrate pump. Redox potential continued to decrease until hitting a low by around hour 25, at which point it began to increase again. Redox

potential continued to increase for the remainder of the trial, approaching but not reaching the threshold before the trial was terminated. Nitrate continued to be injected the remainder of the trial. The trial was terminated at hour 70 when the nitrate solution reservoir was empty. In total, the nitrate pump was activated for 125 events, and the carbon pump was activated for 14 events.

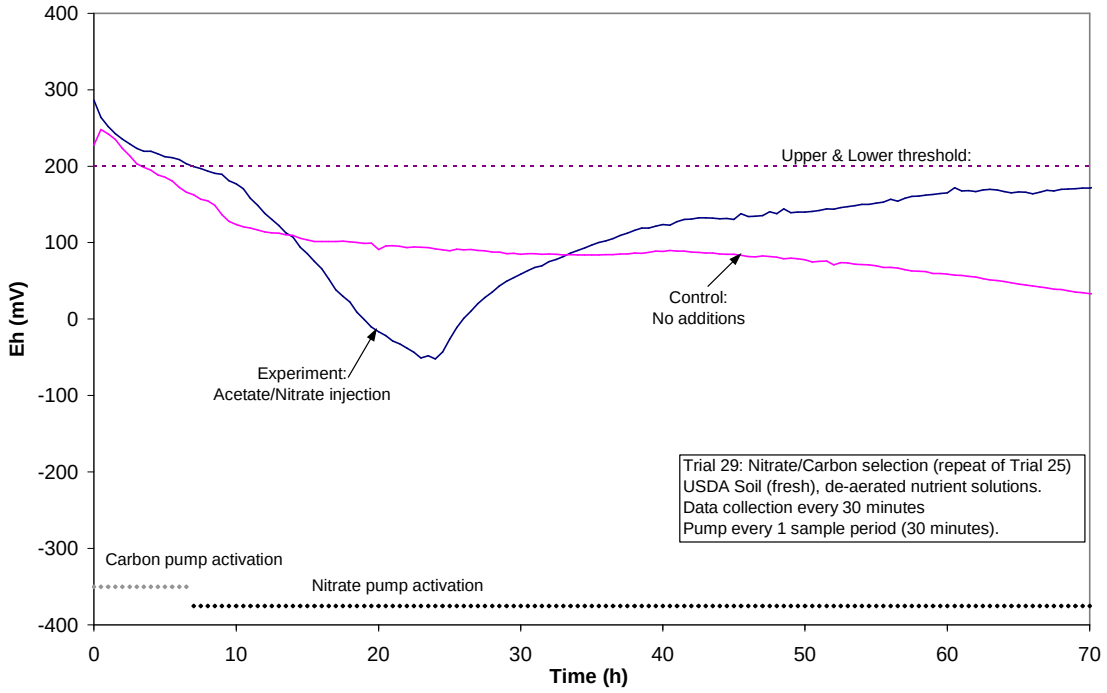

Figure 6. 35. Results for Trial 29: Redox potential vs. time for USDA soil microcosms with identical thresholds. Experiment received 2.0 M sodium acetate solution and 1.0 M potassium nitrate solution. Solutions were not stripped of oxygen.

Nutrient analyses were performed on samples taken from the water column of both units in Trial 29. Samples were taken an analyzed via the procedure outlined in previous sections. Samples were taken at the equivalent time of hour 233 of the trial. The results of this analysis are shown in Table 6. 15.

Table 6. 15. Nutrient concentrations in the water column of the soil microcosms of Trial 29 at the beginning and end of the trial.

Unit	Nutrient	Time	
		0 hr.	233 hr.
Experiment	NO_3 (mg/l)	0.0	5100
	NH_3 (mg/l)	0.24	5.1
Control	NO_3 (mg/l)	0.0	1.0
	NH_3 (mg/l)	0.28	0.20

Again, the rate of anaerobic nitrate respiration can be inferred by tracking the total moles of nitrogen present in the water column at the various time steps. Focusing on the experimental unit, the concentrations in the table can be converted to equivalent moles of nitrogen by multiplying by the total water volume at each time step (correcting for additions due to nutrient pump activations and subtractions due to sampling removals) and dividing by the molecular weight of the chemical species. These results are presented in Table 6. 16.

Table 6. 16. Total nitrate and ammonia nitrogen present in the experiment microcosm for Trial 29 at various times before and after nutrient addition, expressed as total moles N.

Nutrient	Time	
	0 hr.	233 hr.
NO_3 (mol-N)	0.0	0.0627
NH_3 (mol-N)	0.000004	0.00023
TOTAL (mol-N)	0.000004	0.0629

The total ammonia and nitrate nitrogen present in the experiment microcosm increases from beginning to end, again a signal of the nutrient additions via automatic pump. This time, the total nitrate remaining at the end of the trial is an order of magnitude greater than that remaining at the end of Trial 26 and 3 orders of magnitude

greater than that remaining at the end of Trial 27. However, the total moles of ammonia/nitrate nitrogen in solution at the end of the trial is less than that expected. Based upon the number of pumping events (125) of a known volume (2.0 ml) and know concentration (1.0 M potassium nitrate), the expected value of moles nitrogen is at least 0.250 mol NO_3-N. Thus, approximately 0.187 mol NO_3-N is unaccounted for in this analysis.

6.2.13 Trial 31: Test the effect of dissolved oxygen in nitrate solution additions.

Trial 31 was initiated to test whether or not the presence of dissolved oxygen in the nitrate solution might affect the redox potential measurements in the experimental units. While it was expected that nitrate addition would maintain the redox potential in the positive range at which denitrification might occur, one might expect oxygen present in the nutrient solution to induce similar behavior. This trial was undertaken to parse out the effect of nitrate in solution from the effect of dissolved oxygen in the solution. Trial 31 was started in the laboratory on 25 July 2003. Fresh USDA ARS soil was used to construct three new soil microcosms following the general procedure. Each was connected to the DAQ computer via platinum redox probe and calomel probe via salt bridge. Control 1 received no additions. Control 2 was connected to the hose of a pump delivering distilled water. The experimental unit was connected to the hose of a pump delivering 1.0 M potassium nitrate solution. The dissolved oxygen concentration of both reservoirs was checked with a YSI-85 DO probe and found to be 8.6 mg/L, The pump flow rates were checked and both calibrated at 2.0 $ml \cdot s^{-1}$ (± 0.11 $ml \cdot s^{-1}$ for pump 0 and ± 0.00 $ml \cdot s^{-1}$ for pump 1). The sample period was set to 1800 s (1/4 hour), and pump time was set to 1 s. The threshold *Eh* voltage for the experimental unit (below which nitrate

solution was added) was set to +195 mV for both units receiving additions. The trial was initiated and allowed to proceed for 70.0 hours.

Results for Trial 31 are shown in Figure 6. 36. Control 1, receiving no additions, showed a gradual decrease in redox potential as in other trials. Control 2, receiving distilled water, likewise showed a gradual decrease in redox potential. The rate of decrease in control 2 was not as great as in control 1, presumably because of the dissolved oxygen present in the additions of water. The experimental unit receiving nitrate additions showed an initial decrease in redox potential until it dropped below the threshold, at which time the nitrate pump is activated once. This caused an immediate increase in redox potential, which then stayed above the threshold for the remainder of the trial. Redox potential for control 2, however, remained below the threshold for the entire length of the trial, activating the water addition pump throughout.

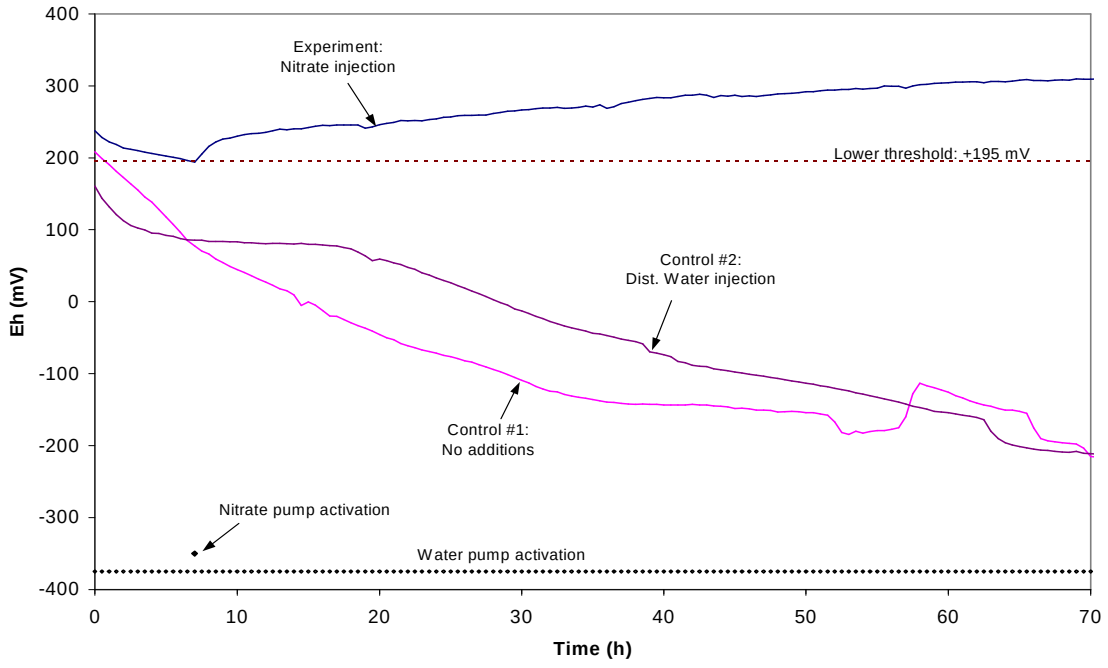

Figure 6. 36. Results for Trial 31: Redox potential vs. time for USDA soil microcosms testing the influence of dissolved oxygen in the nitrate solution additions.

6.2.14 Carbon/Nitrate Summary

6.2.14.1 Qualitative Analyses

Results for all carbon/nitrate addition trials are summarized in the following set of tables. Results for each control of each trial were analyzed for total run time, initial change in redox potential (arbitrarily defined here as the change in redox in the first 10 hours), total change in redox potential over the first 100 hours, qualitative assessment of the trend in redox potential, and the general trend in slope. Results for each experiment of each trial were analyzed for total run time, overall number of carbon pump events, amount of carbon added in moles of carbon, overall number of nitrate pump events, amount of nitrate added in moles, the minimum and maximum *Eh* values, the overall amplitude of the variation in *Eh*, the number of cycles the variation in *Eh* passes through, and the general pattern of redox change over time. Results for the controls that accompany the experimental trials are summarized in Table 6. 17, and the results for the experimental trials themselves are summarized in Table 6. 18.

Table 6. 17. Results for control units that accompanied the carbon/nitrate experiment trials.

Trial	Total Run Time (hr)	Initial Change in *Eh*[1] (mV)	Total Change in *Eh*[2] (mV)	General Redox Pattern	General Trend of Slope
13-02	49.0	-168	-276	Steep initial decline, then gradual decline	-
14-02	80.0	+24	-185	Gradual incline, then gradual decline	+/-
15-02	>100	-82	-147	Steep initial decline, then gradual decline	-
16-02	>100	-22	-105	Gradual decline	-
20-02	>100	+1	-165	No change, then gradual decline	-
21-02	>100	-31	-175	Moderately steep initial decline, then gradual decline	-
22-02	53.0	-64	+15	Steep initial decline, steep midway incline	-/+
25-02	>100	-34	-220	Gradual decline	-
26-03	40.0	-9	-205	Gradual decline	-
27-02	68.5	-128	-217	Gradual decline	-
28-02	21.0	-21	-49	Gradual decline	-
29-02	69.0	-104	-192	Initial incline, then gradual decline	+/-
31-02	70.0	-164.0	-423	Moderately steep decline	-

[1]The change in redox potential from time t=0 to time t=10 hr.
[2]The change in redox potential from time t=0 until time t=100 hr.

Table 6. 18. Results for carbon/nitrate selection experiments.

Trial	Total Run Time (hr)	No. of Carbon Pump Events	Total Carbon Added (mol C)	No. of Nitrate Pump Events	Total Nitrate Added (mol NO_3)	Mini-mum *Eh*[1] (mV)	Maxi-mum *Eh*[2] (mV)	*Eh* Ampli-tude (mV)	No. of Cycles[3] (radians)	Redox Pattern
13-01	49.0	0	0	33	0.046	-7	289	296	1.5π	Sinusoidal with initial steep decline
14-01	80.0	96	0.614	40	0.056	118	309	191	1.75π	Sinusoidal with gradual initial decline
15-01	220.0	42	0.269	357	0.500	52	294	242	1.75π	Sinusoidal with gradual initial decline
16-01[4]	120.0	0	0	189	0.662	-104	223	327	1.5π	Remotely sinusoidal with steep initial incline
20-01	118.0	0	0	108	0.216	-57	218	275	1.5π	Sinusoidal with very steep initial decline
21-01	355.0	1	0.008	262	0.524	136	213	77	2π	Approximate sinusoidal with steep initial incline
22-01	53.0	15	0.120	174	0.348	71	232	161	2π	Sinusoidal with steep initial decline
25-01	119.0	44	0.352	197	0.394	32	207	175	0.5π	Logistic with steep initial incline
26-01	40.0	14	0.112	67	0.134	-46	214	260	2.5π	Sinusoidal with gradual initial decline, then sharp increase
27-01	68.5	81	0.648	57	0.114	-126	250	376	1.5π	Sinusoidal with gradual initial decline, then sharp increase
28-01	21.0	43	0.344	0	0	204	244	40	2π	Shallow sinusoid with gradual initial increase
29-01	69.0	14	0.112	125	0.250	-52	287	339	1π	Sawtooth sinusoid with steep initial decline
31-01[5]	70.0	0	0	1	0.002	194	323	129	1π	Shallow sawtooth sinusoid with gradual initial decline

[1]The lowest value reached by *Eh* within the total run time.
[2]The highest value reached by *Eh* within the total run time.
[3]The number of oscillations through an approximately sinusoidal cycle, where 2π is one full cycle.
[4]Molar concentrations of 2.5 M sodium acetate and 2.5 M KNO_3 used.
[5]Nitrate only used; no carbon reservoir used.

Table 6. 17 and Table 6. 18 show the variability of results obtained from the experiments. For the controls (Table 6. 17) the initial change in redox ranged from +24 to –168 mV, albeit most showed a negative initial change in redox potential. Indeed, five trials exhibited a steep initial decline, whereas only two exhibited an initial incline. The total change in redox ranged from +15 to –423 mV; all but one exhibited at least a gradual decline in redox potential. As for the experiment trials (Table 6. 18), there was a wide range of variability, as indicated by comparing them all on the same set of axes (Figure 6. 37) and as summarized in Table 6. 19. The number of carbon pump events ranged from 0 to 96, adding from 0 to 0.648 mol C. The number of nitrate pump events ranged from 0 to 262, adding from 0 to 0.662 mol NO_3. Redox potential minima ranged from –126 to 204 mV, and maxima ranged from 207 to 323 mV, and the amplitude of *Eh* variation ranged from 40 to 376 mV. Generally, all experiments exhibited sinusoidal variation, most passing through at least ¾ of a full cycle.

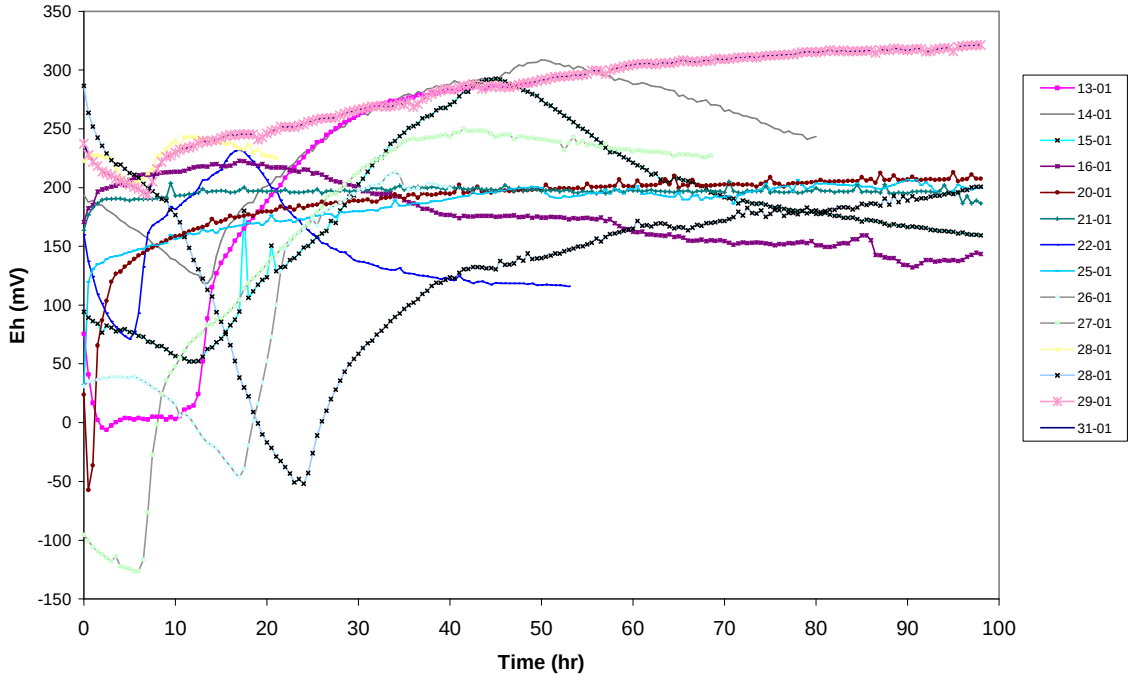

Figure 6. 37. Redox potential vs. time for all nitrate/carbon experiment trials, showing the variability of results among the set of trials.

Table 6. 19. Statistics of variation of results for carbon/nitrate addition experiments.

Parameter	No. of Carbon Pump Events	Total Carbon Added (mol C)	No. of Nitrate Pump Events	Total Nitrate Added (mol NO_3)	Mini-mum *Eh*[1] (mV)	Maxi-mum *Eh*[2] (mV)	*Eh* Ampli-tude (mV)
Mean	27	0.198	124	0.250	32	254	222
Standard Deviation	32	0.231	108	0.219	109	41	103
Minimum	0	0.000	0	0.000	-126	207	40
Maximum	96	0.648	357	0.662	204	323	376

6.2.14.2 Analysis of Redox Values

As with the carbon addition experiments, an analysis was performed on the values of the redox potential curves at each time step for the controls and all of the nitrate/carbon treatments. This analysis assumes that the procedure was uniform for each treatment group and for all the controls. The data obtained from these analyses are then used to perform comparative tests between the various treatment groups and the control group.

Controls Group. The same data set was used as developed previously as the analysis of the controls for each time step (see Figure 6. 12).

Nitrate/Carbon Additions Group. All trials in which nitrate and carbon were added were analyzed for each time step up to 100 hours. The length of time for each replicate in the group ranged from 21 hours to over 100 hours, and thus the number of sample population *n* varies from 13 to 7 as the time step proceeds from 0 to 100 hours. For each time step, the data were averaged and the standard error calculated for the respective sample population *n*. Results from this analysis are plotted in Figure 6. 38 and show the averaged redox potential at each time step for the nitrate/carbon additions group compared to the controls group. This comparison shows that the mean value for redox in the nitrate/carbons group is higher than that of the controls group for the entire time. In addition, the redox potential of the nitrate/carbons additions group generally remains between the maximum and minimum setpoints used in any of the trials, and over time trends towards the lower *Eh* setpoint of +200 mV. As in the controls group, discontinuities in the otherwise smooth curve occur at time steps when data from one of the trials in the group ends and the value of *n* changes. Error bars on the plot represent

standard error. There is considerable overlap between the standard error for the two sets of data within the first 10 hours only.

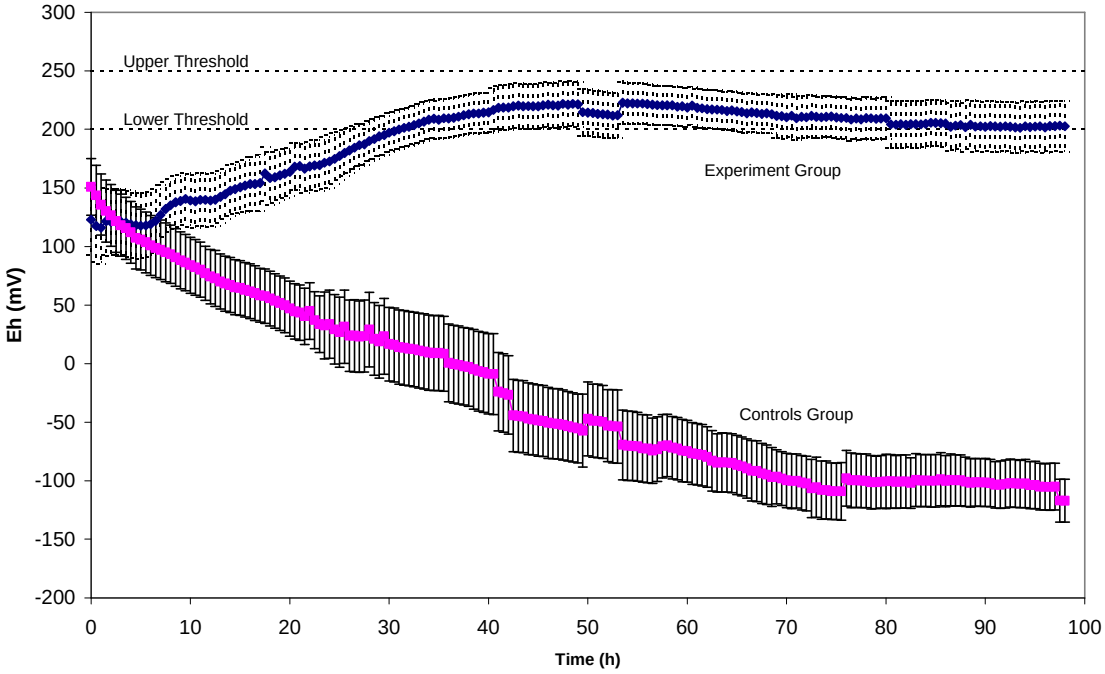

Figure 6. 38. Mean values of redox potential averaged for each time step for controls group and methanol addition groups vs. time. Error bars represent standard error.

7.0 DISCUSSION

7.1 Experiment Controls

As a group, the controls from each of the experiment trials forms a baseline set of data against which data from other treatments can be compared. Of all the treatments, the controls were the most uniform in their setup and implementation from trial to trial, and thus can be considered replicates of each other. After filtering out data sets with excessive measurement noise, the mean of all trials at each time step yields a curve of mean redox potential over time with a definite negative slope (Figure 6.12). As a gross metric of this characteristic curve, the total change in the mean redox potential is approximately –250 mV per 100 hours, or –2.5 mV/hr, averaged over 100 hours. This metric, however, ignores the more rapid decline in redox potential observed within the first 10 hours of measurement, the mean of which was calculated at –57.9 mV, or alternately, at –5.8 mV/hr. This is nearly an order of magnitude less than the rate reported by Koch and Oldham (1985) of –280 mV in 5 hours, or –56 mV/hr, for an anaerobic bioreactor for nitrate removal. This order of magnitude difference is to be expected, as it likely indicates the effect of monitoring redox potential in the static, unmixed submerged soil microcosms used in this experiment versus a well-mixed fluid bioreactor. As an indicator of microbial metabolism in the soil microcosms, redox potential drops as electron acceptors are reduced, the overall rate of which may be restricted by relatively slow diffusion rates through the soil compared to a mixed bioreactor.

7.2 Carbon Addition Experiments

7.2.1 Effect of Feedback Mechanism

It was expected that, by adding the feedback mechanism on redox potential to add carbon to the wetland soil microcosms, the value of the redox potential measured over time would more quickly be driven lower than those not given the feedback mechanism. As an energy source for the microbial metabolism occurring in the soil, the source of carbon is possibly normally limiting in the wetland soil. Making it available through a feedback mechanism in effect removes this limitation, with the expected result that, by allowing the metabolism to occur unhindered and thus at a faster rate, the redox potential over time should be much lower than the non-feedback counterparts. Indeed, this pattern was observed on individual experimental trials (for example, Trial 1, Figure 6.1) in which the redox potential of the experimental unit was considerably lower than that of the associated control for the length of the entire trial. However, as shown in Tables 6.8 and 6.9, when compared as groups, there is no statistical difference between those receiving carbon feedback and those without.

This is not necessarily so when the data are analyzed for the slopes of the redox potential curves. Again, it was expected that the rate of change of redox potential, as an indicator of the metabolism of the soil wetland microcosm, would be greater for those replicates that had the carbon addition feedback control than those without. Indeed, as shown in Table 6.10, there exists a statistical difference between the slopes of the experiments and controls at least some time in the first 47 hours, albeit at different times for different sources of carbon. The strongest signal of this phenomenon comes from those receiving methanol addition, which showed a steeply-declining slope early (less

than 5 hours) in the trials. The next strongest signal was from those receiving acetate, which showed steeper slope later than the methanol trials, but much earlier than those receiving synthetic sewage. While the veracity of the statistical results for the acetate and synthetic sewage trials is suspect because of the low sample population, it does conform to a reasonable pattern. It might be expected that methanol, as the most concentrated carbon source (having the most number of moles of carbon per unit volume) would have the strongest effect on the trend in redox, followed by the less-concentrated acetate and synthetic sewage solutions. It is possible that the less-concentrated carbon sources, input at the same volumetric rate as the methanol, take longer to build up to a high enough concentration in the microcosm water column to have an effect on the redox potential. However, with methanol, the opposite problem may have been a factor in that some replicates (for example, Trial 9, Figure 6.6) may have been rendered biologically inactive by the high methanol concentration. This is the general reason for exploring other carbon sources such as acetate or synthetic sewage, and points to the necessity to optimize the feedback system with a balance between the delivery rate and concentration of the carbon solution.

The failure of the statistical testing to show any significant difference between both the redox values at all time steps and the redox slopes at most is a result of the considerable variability among all the replicates. This is evidenced by the relatively large standard deviations of the means of the initial and total changes in redox (Table 6.7), as well as the large standard errors evident on the plots for the means for each timestep (Figures 6.12 to 6.15). The possible causes of this variability are manifold. It is possible that air occasionally leaked into the microcosms, in which case the oxygen might cause

the redox potential to remain at a higher voltage than it otherwise might (for example, see Figure 6.11 for Trial 30). Also, various trials exhibited considerable noise in the redox data that was collected, likely a result of electrical noise from other nearby laboratory equipment. Even electrical noise on the order of a few millivolts might affect the outcome of the statistical analysis, particularly that of the redox slopes which can be sensitive to small changes in redox over a large timestep. Finally, there is inherent variability in the microcosms because they are biological systems. The design of the carbon addition feedback loop relies upon some fairly broad assumptions about redox potential as it relates to the presumed predominant microbial metabolism occurring in the wetland soil. Compounding this is the fact that wetland soil samples were collected as needed at various times of the year for constructing the microcosms. The possibility of seasonal fluctuations in nutrient and microbial population composition in the wetland soil, while not addressed in this research, may introduce variability such that it effectively overwhelms any statistically rigorous results.

One place where this variability in the results is evident is in the length of pump action, or alternately in the number of pump events, for the experiments. For the methanols addition group, the number of pump events ranges from 9 to 95 (Table 6.1) and is directly related to the rate at which redox potential drops below the threshold setpoint. Most of those trials that exhibited a gradual decline in redox potential had a greater number of pump events. There are at least two interpretations of this fact: one, that the carbon additions were having little or no (or even the reverse) effect on the rate at which redox potential drops; or, alternately, that the microcosm was metabolizing as much of the carbon solution at the fastest additions rate allowed by the feedback. The

conditions for the latter option to occur require a sufficiently dense soil microbial population and large reservoirs of oxidizers in the soil, a fact not altogether substantiated by the soil nutrient analyses. But the question is intriguing: in those cases where the redox potential did not drop below the threshold setpoint that turned off the nutrient pump, might the microcosm have been metabolizing as much of the carbon as could be input as allowed by the feedback loop? Might this be a similar situation to what Petersen (2001) found in the photosynthetic technoecosystems that maximized their light input? This experiment was not designed to answer these specific questions, but it points the way for possible avenues of research on future microcosm studies.

7.2.2 Proposed Statistical Modeling

For the analysis of both the controls and the experimental groups for the carbon addition experiments, a number of attempts were made at using regression analysis to fit model curves to the individual data sets of redox potential over time. This was performed in an attempt to yield regression coefficients that might be analyzed for their goodness of fit to an idealized model and allow comparison between the experimental and control data sets. This analysis met with less than desired results because of limitations with the model assumptions. The deficiencies, however, point to a possible avenue for refining this type of analysis.

The first attempt at this analysis assumed that the trend in redox potential over time can be described by a first-order exponential decay model of the type:

$$Eh(t) = Eh_0 e^{-kt} \qquad (7.1)$$

where Eh_0 is the initial value of redox potential at time zero, k is the first- order rate constant, and t is time. This follows by reflecting upon the expression for redox potential, as derived by Patrick, et al. (1996) and presented in previous sections, which is as follows:

$$Eh = E^o - \frac{RT}{nF}\ln\frac{(Rd)}{(Ox)} + \frac{mRT}{nF}\ln H^+ \qquad (7.2)$$

where E^o is the standard potential for the reduction half-cell under consideration, R is the ideal gas constant (8.31 J K^{-1} mol^{-1}), T is the absolute temperature (in degrees Kelvin), F is the Faraday constant (9.65 x 10^4 K mol^{-1}), n is the number of electrons exchanged in the half-cell reaction, m is the number of protons exchanged in the half-cell reaction, and Rd and Ox represent the aqueous concentrations of the individual reduced or oxidized component of the half-cell reaction. This expression shows that the redox potential Eh is a function of the concentration of the available electron acceptors (the oxidized component or Ox in equation 7.2) in the aquatic environment. Therefore, it might be expected that the redox potential measured over time be correlated with the concentration of electron acceptors in solution. One possible way to model the concentration of electron acceptor over time is as a first-order exponential decay model, which can be used to describe the uptake of a fixed reservoir of nutrients by a growing microbial population (Odum, 1993; Johnson, 1999). Thus, it might be expected that the redox potential measured over time be correlated with a first-order exponential decay model of the type in equation 7.1.

Rudimentary regression analyses were performed using a statistical curve-fitting package provided in Microsoft Excel (version 9.0/2000, Microsoft Corp., Redmond, Washington). To perform a regression analysis to fit an exponential curve to the redox

data collected in this research, certain manipulation of the data was necessary. Because the value of measured redox potential was often negative, the raw data had to be translated upwards such that all values were positive before an exponential curve could be fit. It can be argued that this translation is acceptable, as redox potential is expressed as a voltage relative to a reference redox couple, and thus is translated to different scales depending upon the type of probe used to measure it. In the results reported here, data were translated upward by +250 mV to allow regression curve fitting.

Preliminary results of this regression curve-fitting met were mixed, with some trials exhibiting good correlation and others showing poor correlation. Results for this regression curve-fitting for the mean of redox potential at each time step for the controls group, shown in Figure 7. 1, exhibit a good correlation (R^2 = 0.945). However, results for this regression curve-fitting for one of the methanol addition trials (Trial 1-01), shown in Figure 7. 2, exhibit a poor, even negative, correlation (R^2 = -0.854). In general, the values for Eh_0 and k were found to vary widely for many trials, and generally the values for the correlation coefficient R^2, used as a measure of goodness of fit, were quite poor.

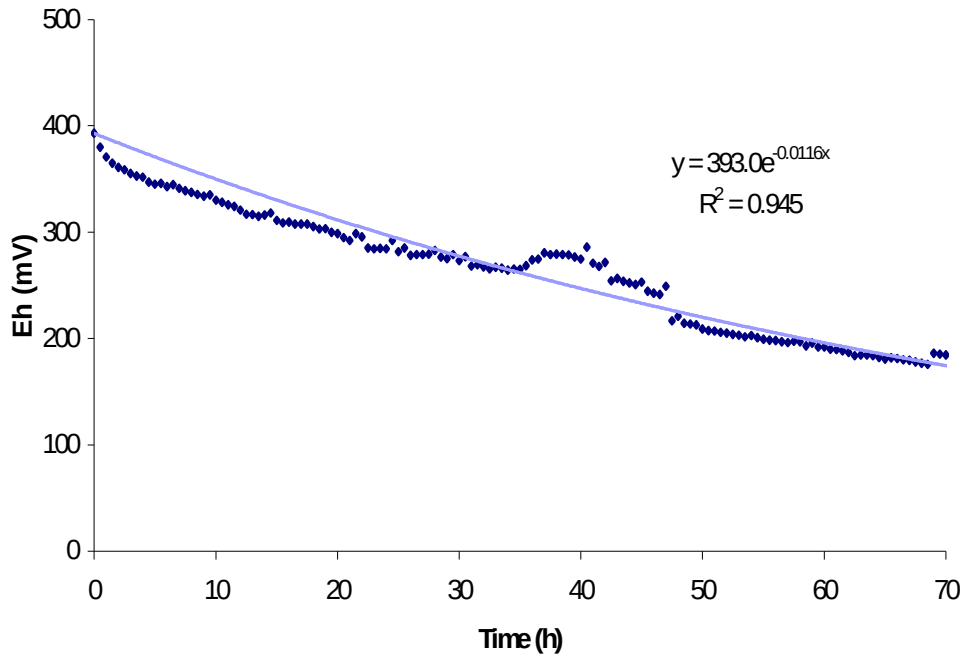

Figure 7. 1. Results of regression curve-fitting for the mean of the redox potential over time for the controls of all trials, yielding a relatively good fit (R^2 = 0.945).

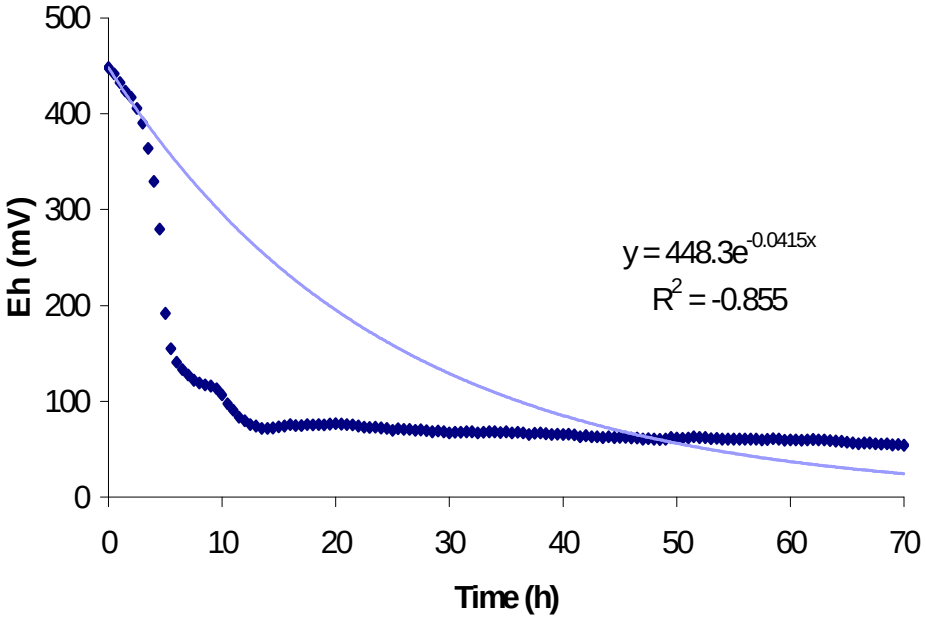

Figure 7. 2. Results of regression curve-fitting for experimental trial 1-01 receiving methanol addition, yielding a relatively poor fit (R^2 = -0.855).

Further refinement of this method comes from a return to equation 7.2. As a first attempt to derive from this a model for the change in *Eh* as a function of time, the following simplifying assumptions can be made:

- The pH remains constant (assuming a well-buffered system);
- The oxidized component of the half cell reaction (*Ox*) decreases as it is reduced in metabolism according to a first-order exponential decay model;
- The reduced component of the half-cell reaction (*Rd*) increases according to a first-order exponential growth as a product of the metabolic reduction of the oxidized component;
- The total measured redox potential in a solution is the weighted average of all the redox pairs present (Bohn 1971).

Following these assumptions, the following expression can be derived for redox potential as a function of time:

$$Eh(t) = C - A\ln\left[\prod_i \left(Be^{k_i t} - 1\right)^{1/n_i}\right] \qquad (7.3)$$

where k_i is the first order reaction constant for redox couple i, n_i is the number of electrons exchanged in the redox reaction i, and C, A, and B are constants. A more detailed discussion of the derivation of this equation is given in Appendix C. If is assumed that five major reduction reactions (oxygen, nitrate, manganese, iron, and carbon dioxide) dominate the overall redox potential in freshwater wetland soils, and that these couples are averaged weighted according to the Gibbs free energy released for support of metabolism and expressed as a fixed ratio of their first-order reaction constants, the resulting equation yields an approximation for redox potential over time

based upon the variation of five quantities decaying exponentially. As a test of this model, preliminary regression analysis was performed using the coefficient of determination R^2 (Kvalseth 1985) and residuals analysis (McCuen 1984) as goodness-of-fit metrics. Results of this analysis, shown in Appendix C, show a relatively good fit with high R^2 (up to 0.996) and low residuals bias (less than 1.0) when fit to data from the controls from various trials. Further development of this method may prove valuable for developing a regression model of redox potential dynamics over time for the microcosm systems studied here.

7.3 Carbon/Nitrate Selection Experiments

7.3.1 Effect of Feedback Mechanisms

Whereas it was expected in the carbon addition experiments that, by adding the feedback mechanism, the value of the redox potential measured over time would be driven lower more quickly than those not given the feedback mechanism, the reverse was expected for a nitrate addition feedback mechanism. As an oxidizer used to metabolize reduced organic matter, nitrate in solution is expected to raise the value of redox potential. Thus the combined effect of having both feedback mechanisms available to the microcosms was expected to be a redox potential fluctuating up and down between the upper and lower threshold setpoints. Generally, this is what was observed on individual experimental trials (for example, Trial 13, Figure 6.20) and likewise in the mean of all trials (Figure 6. 38).

For all trials in this set of experiments, a sodium acetate solution was used as the carbon source. As demonstrated in the carbon only experiments, acetate generally did not produce strong impacts on the redox potential. An exception might be Trial 21 (Figure 6.25) in which one pump event for carbon (at a time of 124 hours) produced a dramatic decrease in redox potential. This impact seems to be an aberration, though, as most trials exhibited a slow change in redox potential over time. The addition of nitrate, on the other hand, usually had dramatic effects on the value of redox potential, usually precipitating a steep rise in redox potential shortly after injection. For example, this was observed at the beginning of Trial 20 (Figure 6.24) and Trial 25 (Figure 6.27), both of which began with sharp inclines in redox potential, and at hour 7 of Trial 31 (Figure 6.36), in which one single pump event of nitrate solution dramatically changed the trajectory of the redox potential changes. Interestingly, other trials exhibited considerable lag between the time when nitrate was first injected to when a dramatic change in redox potential was registered. For example, Trials 13, 14, 26, and 29 (Figures 6.20, 6.21, 6.29, and 6.35, respectively) all showed a characteristic lag of 15 to 20 hours between the start of nitrate injection and the resulting change in the trajectory of the redox potential curve.

Despite an apparent variability amongst all the trials, especially noticeable when all experiments are plotted on the same set of axes (Figure 6.37), the mean of all data at each timestep yields a surprisingly smooth and regular curve with a clear sinusoidal pattern (Figure 6.38). When compared to the mean values of the controls, the effect of nitrate addition in raising the redox potential is clear. Any variability that does exist is due again to issues discussed previously: noise in the data collection electronics, and biological variation between the replicate trials. Indeed, the variability of the number of pump event

for both carbon and nitrate (Table 6.18) attest to the unpredictability of these systems. A correlation analysis between the number of pump events and subsequent changes in redox potential may yield further valuable information to help describe the dynamics of the ecological/technological interface.

Again, the wide range of pump events raises questions. Certain replicates had extremely large inputs of nitrate over the entire time of the test (for example, Trial 21 had 262 nitrate pump events injection a total of 0.524 mol of nitrate). The same issue of interpretation is raised as in the carbon addition experiments: either there exists a lag between the initial time of nitrate injection and its effect on redox potential, during which more than desired nitrate is injected, or alternately, the microcosm is metabolizing as much nitrate as can be injected. In this case, the latter is somewhat supported by the nutrient analyses taken in Trials 26, 27, and 29. In each of these trials, based upon the mass balance on moles of nitrogen, some nitrogen mass is unaccounted for, thus indicating possible denitrification. Most compelling are the nutrient analyses results from Trial 27 (Table 6.14) in which a vast majority of the nitrogen mass actually injected is unaccounted for by what remains in the water column. In that replicate, the microcosm appears to have organized quickly to maximize the metabolic consumption of nitrate, injecting carbon again later on when it as likely become limiting.

Another interesting result of the experiments is the apparent behavior of the redox potential getting ‘stuck’ in the zone between the upper and lower thresholds. This was observed in Trial 20 (Figure 6.24). In this case, it seems possible that much more nitrate was injected than could be metabolized, resulting in a condition of a redox potential dominated by nitrate ions in solution, and where metabolic reduction of the nitrate may or

may not be limited by the availability of carbon. This suggests an improved control scenario in which the triggering threshold is not the value of redox potential but the change in redox potential. Thus the computer could be programmed to track the slope of the redox curves, taking action when the slope has leveled off for some period of time. This is fundamentally different control program than that utilized here, and may result in considerably different system dynamics. Indeed, some researchers have incorporated elements of this type of monitoring into wastewater treatment applications, using a sudden change in slope as an indicator of nitrate limitation in a denitrification process (Kim and Hao, 2001).

7.4 Conceptual Models of Limiting Factors

One method for further exploring the behavior of the addition of technological feedback to a simple microbial soil ecosystem is through modeling. The energy circuit language, as developed by Odum (1971, 1994) is a common and useful language for developing models of energy transformations through ecological systems. Common useful symbolic elements of the energy circuit language are shown in Figure 7. 3.

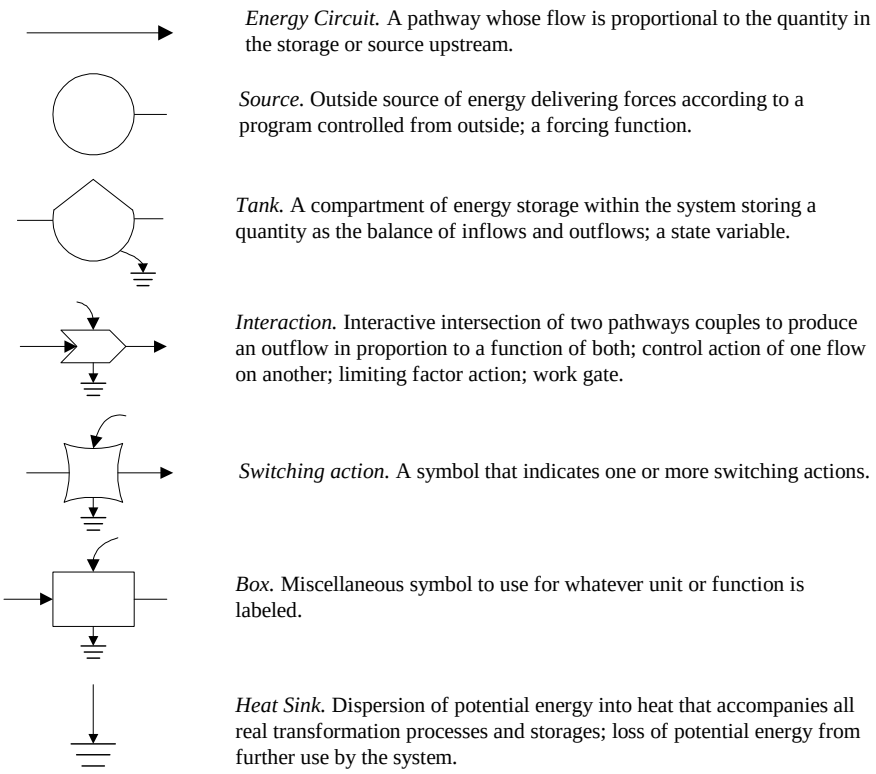

Figure 7. 3. Common symbolic elements used in the energy circuit language as developed by Odum (1994).

Using these symbols, simple minimodels of the soil microbial technoecosystem can be developed, and conditions of the technoecosystem can be simulated over time to show general behavioral characteristics. The goal of this development process is to construct a model that will in general reflect a microbial degradation microcosm to which artificial technological feedback is added via sensors to allow control over its energy source. This modeling sequence was originally undertaken as an independent exercise to elucidate the role of limiting factors in the wetland soil microcosms. As discussed later, certain results from the modeling process reflect some of those obtained from the physical experiments.

7.4.1 Minimodel 1: Simple microbial degradation microcosm with one limiting reservoir.

Beyers and Odum (1993) give a simple minimodel of a soil microbial decomposition system based upon an initial stock of organic matter. A version of this minimodel using the symbols of the energy circuit language and modified to include the organic matter storage within the boundaries of a microcosm is shown in Figure 7. 4.

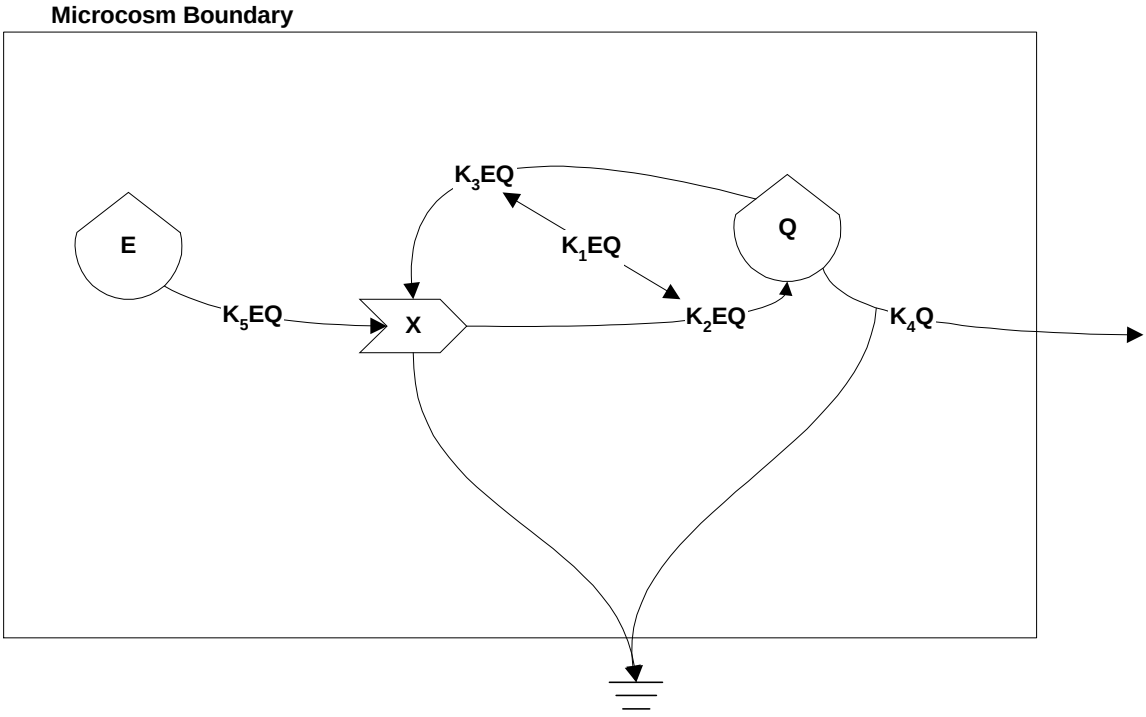

Figure 7. 4. Simple minimodel of a soil microbial decomposition microcosm with an initial organic matter stock included within the microcosm boundaries (adapted from Beyers and Odum, 1993).

In this model, the initial storage of organic matter is represented by the tank symbol *E* (for energy). The microbial population in the soil is represented by the consumer tank symbol *Q*. In the physical system, the microbial ecosystem will self-organize, through means of competition between species and natural selection, to reinforce those pathways (i.e. species) that can utilize the availability of *E* the greatest

and collectively increasing the consumption of the system (Beyers and Odum 1993). This type of loop is often referred to as an autocatalytic loop; the many such autocatalytic loops of the real microbial system is represented here as a single autocatalytic loop. The essence of the autocatalytic loop is that some of the system energy utilized by the consumer population is fed back to upstream energy circuits of the system to entrain more energy in the process (Odum 1993). In the modeling language of energy circuit diagramming, this is represented by the work gate interaction symbol *X* and typically implies a multiplication function.

Once a model of the system is diagrammed using the symbols of the energy circuit language, determining the equations to describe the state of the system through time becomes relatively straightforward, using rules detailed by Odum (1972). Assigning rate constants K_i to the flow pathways to and from the storage tank units, and ignoring the heat sink, the system of differential equations describing the systems diagram of Figure 7. 4 are as follows:

$$\dot{Q} = \frac{dQ}{dt} = K_1 EQ - K_4 Q$$
$$\dot{E} = \frac{dE}{dt} = -K_5 EQ$$
$$K_1 = K_2 - K_3$$

With the describing equations in hand, a model can be constructed using a computer program to numerically solve the system of equations through time, thus exhibiting the behavior of the overall system. In this study, the system of equations was programmed into the modeling program STELLA (version 5.1.1, High Performance Systems, Inc., Hanover, New Hampshire) using methods for translating equations to STELLA elements given in Hannon and Ruth (1997). The STELLA graphical

representation and code constructed to simulate this system of equations is shown in Appendix B.

Model parameters used for the STELLA simulation of Minimodel 1 are shown in Table 7. 1. Values for the parameters were chosen by a process of trial-and-error such that model results generally reflected those found in Beyers and Odum (1993). Results for these parameters are shown graphically in Figure 7. 5. These results show the exponential increase of *Q* over time as a result of the autocatalytic loop. *Q* continues to increase until the amount of *E* is less than that needed to sustain *Q*—that is, until *E* becomes limiting. Beyond this point, *Q* decreases as a result of its death rate determined by the constant K_4, eventually approaching zero. These results conform to logic: as the food source of the microbial system is exhausted, the microbial system begins to die, eventually dying completely. This also conforms to simulation results presented by Beyers and Odum (1993), thus validating the modeling method developed here.

Table 7. 1. Parameters and their values used in the STELLA simulation of a simple microbial degradation microcosm with an initial organic matter stock.

Parameter	**Description**	**Value**
E_0	Initial value of E	100
Q_0	Initial value of Q	0.05
$K_1 = K_2 – K_3$	Rate constant	0.1
K_4	Rate constant	0.5
K_5	Rate Constant	0.1

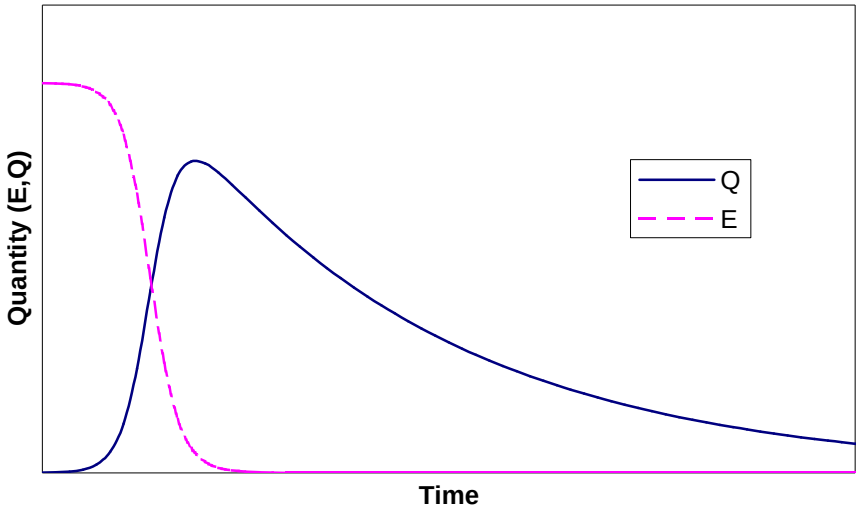

Figure 7. 5. Results from the STELLA simulation of a simple microbial degradation microcosm with an initial organic matter stock.

7.4.2 Minimodel 2: Microbial degradation microcosm with two limiting reservoirs.

A series of models will now be developed using the simple microbial degradation system developed above as a basis and adding elements incrementally to increase the complexity of the modeled system. To continue this process of model development, it is helpful to analyze more completely the processes that might occur in the physical microcosm. The microbial degradation of organic matter is a process of respiration, and thus it is dependent upon the availability of an electron acceptor as well as the organic matter itself. In soils, for example, the molecules typically available as electron acceptors are oxygen in aerobic systems and nitrate or sulfate in anaerobic systems (Vepraskas and Faulkner, 2001). To account for this in the microbial degradation model developed previously, a tank symbol *N* may be added within the microcosm boundary to represent the available reservoir of electron acceptor in the system (Figure 7. 6). The reservoir *N*

interacts with the other components via a work gate interaction, in effect controlling the availability of the organic matter *E* to the consumer population *Q*.

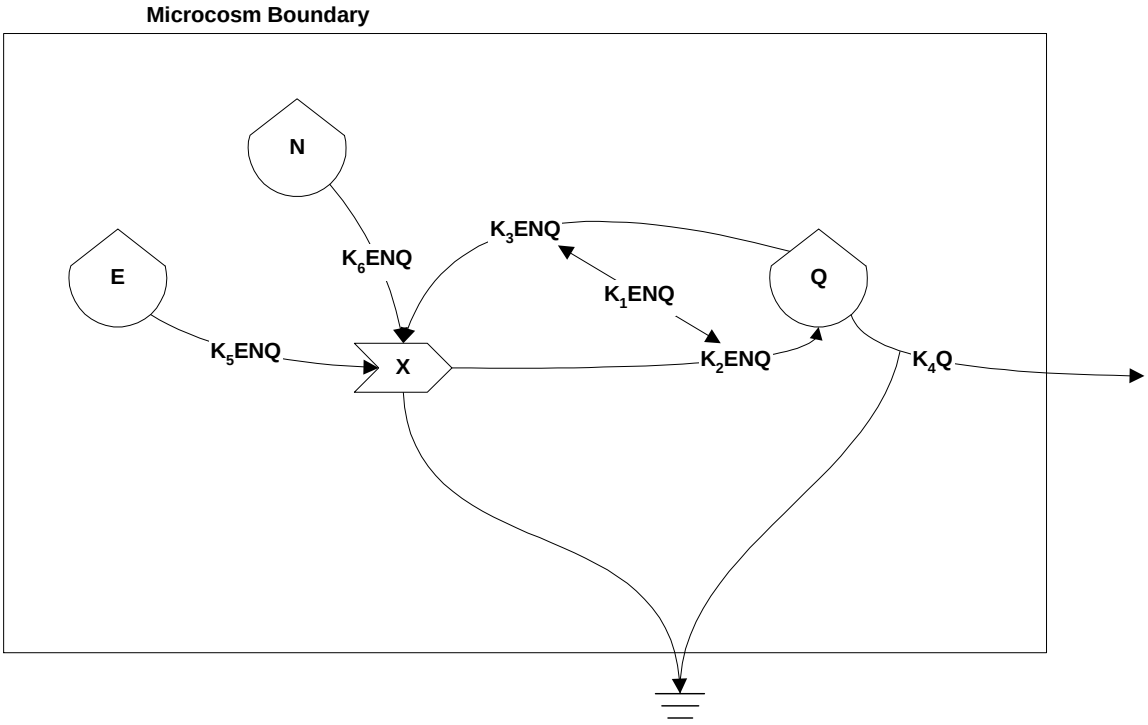

Figure 7. 6. Minimodel of a soil microbial decomposition microcosm with an initial organic matter stock (E) and an initial electron acceptor stock (N) controlling the availability of E to the consumer population Q.

Again, assigning rate constants K_i to the flow pathways to and from the storage tank units, the system of differential equations describing the systems diagram of Figure 7. 6 are as follows:

$$\dot{Q} = \frac{dQ}{dt} = K_1 ENQ - K_4 Q$$

$$\dot{E} = \frac{dE}{dt} = -K_5 ENQ$$

$$\dot{N} = \frac{dN}{dt} = -K_6 ENQ$$

$$K_1 = K_2 - K_3$$

Again, this system of equations was programmed into STELLA; the STELLA graphical representation and code constructed to simulate this system of equations is shown in Appendix B.

Model parameters used for the STELLA simulation of Minimodel 2 are given in Table 7. 2. Values for the parameters were chosen by a process of trial-and-error such that model results were visually discernable and generally reflected those found in Beyers and Odum (1993). Results for simulation with these parameter values are shown graphically in Figure 7. 7. As in Minimodel 1, these results show the exponential increase of *Q* over time as a result of the autocatalytic loop. *Q* continues to increase until *N* becomes limiting. The utilization of *N* relative to *E* is set by the relative values of K_5 and K_6; in this case, *N* is used twice as fast as *E*. Thus, in general, *Q* continues to grow until either *E* or *N* is limiting. Beyond this point, *Q* decreases as a result of its death rate, again approaching zero. As before, these results conform to logic: as either the organic matter or the electron acceptor allowing it to be available as food is exhausted, the microbial system begins to die, eventually dying completely. If the initial amount of *N* is increased, holding all other parameters the same**,** the maximum population reached by *Q* is greater as a result of the greater availability of *E* facilitated by the presence of *N* (Figure 7. 8). The results obtained here also loosely reflect the declining trend in redox potential in the control microcosms from the physical experiments (Figure 6.12), where redox potential should decrease with decreasing availability of the electron acceptor in the microcosm, as predicted by Equation 7.2.

Table 7. 2. Parameters and their values used in the STELLA simulation of a microbial degradation microcosm with an initial organic matter stock and an initial electron acceptor stock controlling the availability of the organic matter to the consumer population.

Parameter	Description	Value
E_0	Initial value of E	100
N_0	Initial value of N	100 (Figure 7. 7)
		200 (Figure 7. 8)
Q_0	Initial value of Q	0.01
$K_1 = K_2 - K_3$	Rate constant	0.001
K_4	Rate constant	0.5
K_5	Rate Constant	0.1
K_6	Rate Constant	0.2

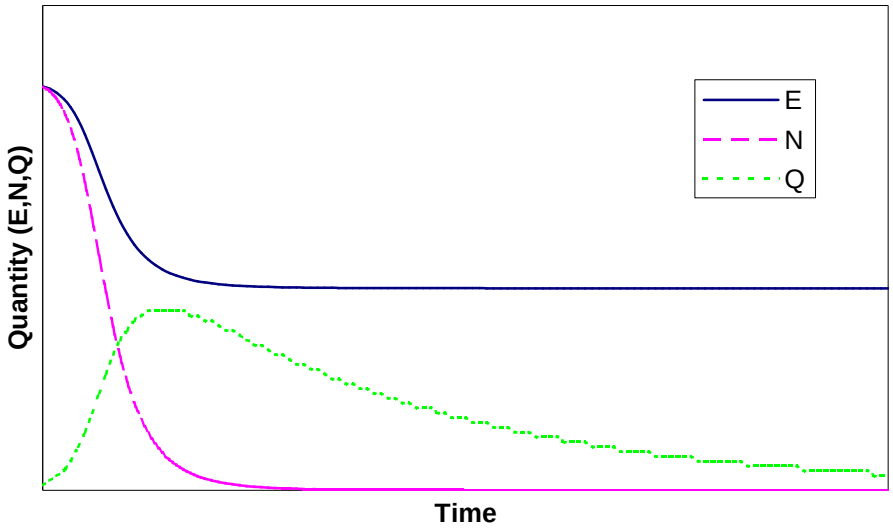

Figure 7. 7. Results from the STELLA simulation of a microcosm with an initial organic matter stock (E) and an initial electron acceptor stock (N) controlling the availability of E to the consumer population Q.

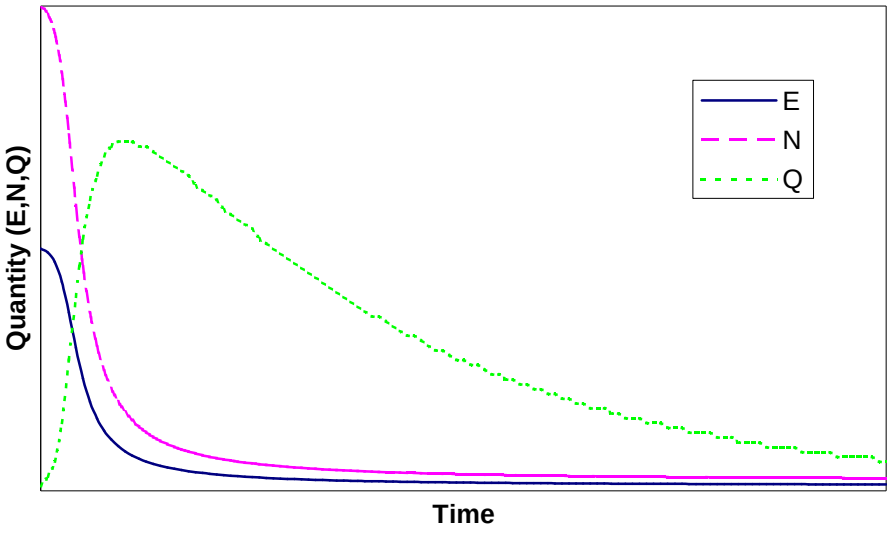

Figure 7. 8. Results from the same STELLA simulation with the initial value of N twice as large.

7.4.3 Minimodel 3: Microbial degradation microcosm with two limiting reservoirs and artificial feedback control of organic matter availability.

Continuing the series of model development, the microbial degradation system with two limiting reservoirs developed above may be modified to include a feedback control loop that controls the availability of the organic matter to the microcosm based upon the measurement of redox potential. Referring again to Equation 7.2, redox potential is in essence a function of the ratio of the reduced form to the oxidized form of an electron acceptor (or acceptors) in a soil, as described by the Nernst equation (Patrick et al. 1996). For the model developed here, this may be simplified as merely the amount of electron acceptor remaining at any time. The feedback control loop may thus be incorporated into Minimodel 2 by adding an information pathway that senses the value of the reservoir *N* at any time, processes this information through a control algorithm *f(N),* and takes action on a switch controlling the input of organic matter J_E from an infinite

source outside the microcosm system. The energy circuit diagram for this control scenario is shown in Figure 7. 9.

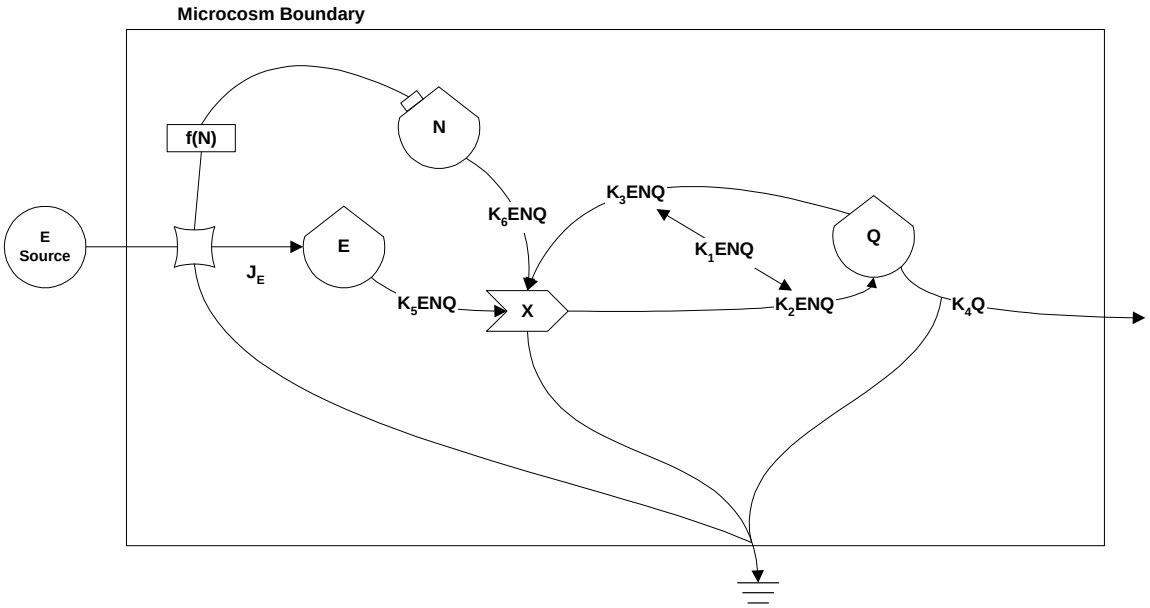

Figure 7. 9. Minimodel of a soil microbial decomposition microcosm with an initial organic matter stock (E), an initial electron acceptor stock (N), and a control feedback loop controlling the input of organic matter (J_E) from outside the system based upon the sensed value of N.

Assigning rate constants K_i to the flow pathways to and from the storage tank units, and setting the control algorithm *f(N)* to reflect the Boolean logic used in the physical microcosm experiments, the system of equations describing the systems diagram of Figure 7. 9 are as follows:

$$\dot{Q} = \frac{dQ}{dt} = K_1 ENQ - K_4 Q$$

$$\dot{E} = \frac{dE}{dt} = J_E - K_5 ENQ$$

$$\dot{N} = \frac{dN}{dt} = -K_6 ENQ$$

$$K_1 = K_2 - K_3$$

$$f(N): \begin{cases} J_E = C \ldots if \ldots N > N_{hi} \\ J_E = 0 \ldots if \ldots N < N_{hi} \end{cases}$$

The algorithm for the control function *f(N)* assumes that, if the redox potential remains high (above the threshold N_{hi}) , system respiration is not occurring because of a limitation of organic matter, and thus should be injected into the system at a flow rate *C*. Again, this system of equations was programmed into STELLA. The STELLA graphical representation and code constructed to simulate this system of equations is shown in Appendix B.

Model parameters used for the STELLA simulation of Minimodel 3 are given in Table 7. 3. Values for the parameters were chosen by a process of trial-and-error such that model results were visually discernable. Results for simulation with these parameter values are shown graphically in Figure 7. 10. Again, these results show the exponential increase of *Q* over time as a result of the autocatalytic loop. *Q* continues to increase until *N* becomes limiting. *E* is not limiting because of its availability provided by the feedback control loop; the amount of *E* plateaus out as *N* becomes too small to support the growth of *Q*.

Table 7. 3. Parameters and their values used in the STELLA simulation of a microbial degradation microcosm with an initial organic matter stock, an initial electron acceptor stock, and a control feedback loop controlling the input of organic matter from outside the system based upon the sensed value of N.

Parameter	Description	Value
E_0	Initial value of E	100
N_0	Initial value of N	200
Q_0	Initial value of Q	0.01
$K_1 = K_2 - K_3$	Rate constant	0.001
K_4	Rate constant	0.5
K_5	Rate Constant	0.1
K_6	Rate Constant	0.2
J_E	Organic matter supply rate	100
N_{hi}	Control function threshold value of N	2

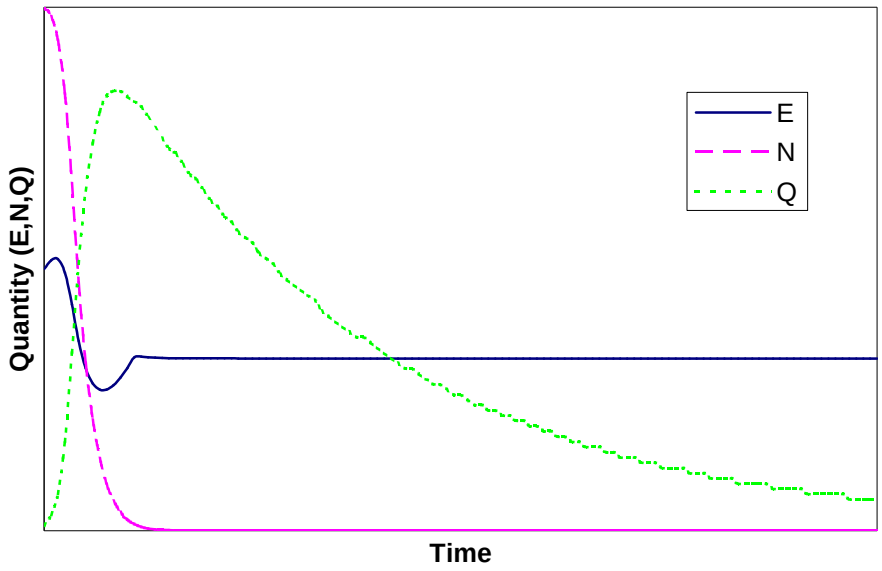

Figure 7. 10. Results from the STELLA simulation of a microbial degradation microcosm with an initial organic matter stock, an initial electron acceptor stock, and a control feedback loop controlling the input of organic matter from outside the system based upon the sensed value of N.

To fully appreciate the effect of the feedback control loop on the system, it is helpful to examine curves that compare the behavior of the system with feedback control to those without. These are provided in the following three figures. In each, one of the state variables is plotted over time resulting from the system both with and without feedback control over organic matter input. Figure 7. 11 shows the amount of organic matter *E* over time. These results show that, with the input of organic matter J_E actively controlled by conditions within the system (curve A*), E* is not limiting to the system growth. When the controlled input of *E* is not provided (curve B), the stock of *E* runs down as in previous models and potentially becomes limiting to the system.

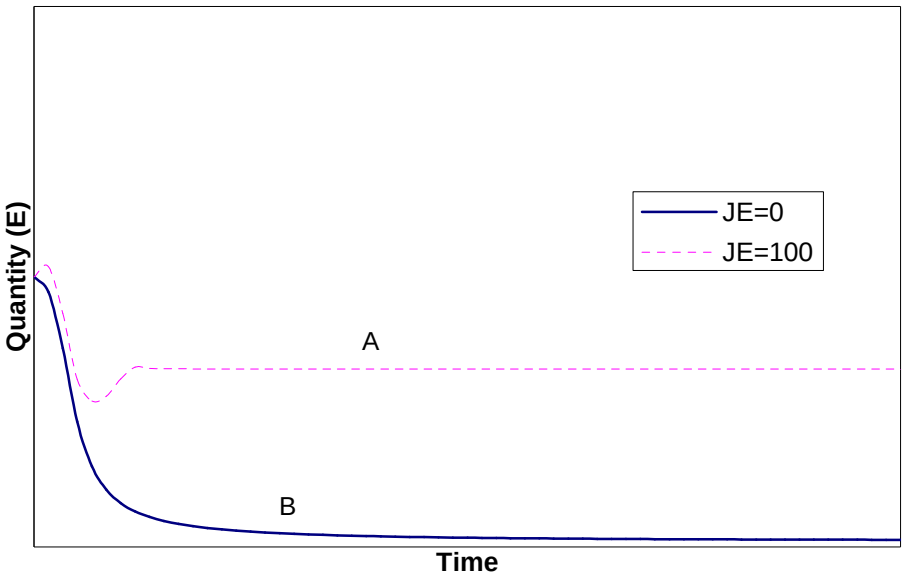

Figure 7. 11. Organic matter E vs. time from the simulation of a microbial decomposition ecosystem. Curve A: Feedback control of organic matter input, with J_E=100 and N_{hi}=2. Curve B: No feedback control.

Figure 7. 12 shows the amount of electron acceptor *N* over time for the same parameters. These results show that, with the input of organic matter J_E actively controlled (curve A), *N* is used up faster than when control is not provided (curve B). In

both cases, for this modeling scenario, *N* is the limiting factor to growth; *N* becomes limiting faster in the feedback control scenario than in the one without feedback control.

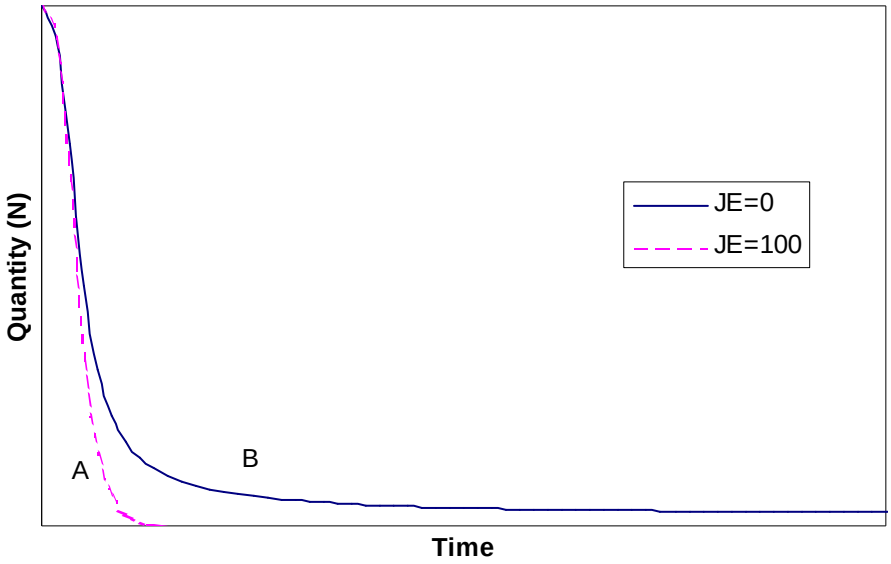

Figure 7. 12. Electron acceptor N vs. time from the simulation of a microbial decomposition ecosystem. Curve A: Feedback control of organic matter input, with J_E=100 and N_{hi}=2. Curve B: No feedback control.

Figure 7. 13 shows the microbial consumer population *Q* over time for the same parameters. These results show that, with the feedback control of organic matter (curve A), the maximum population *Q* is greater than without feedback control (curve B). In addition, the maximum population is reached at an earlier time when feedback control is present, owing in part to the greater availability of *E* and the faster utilization of *N* towards limiting concentrations.

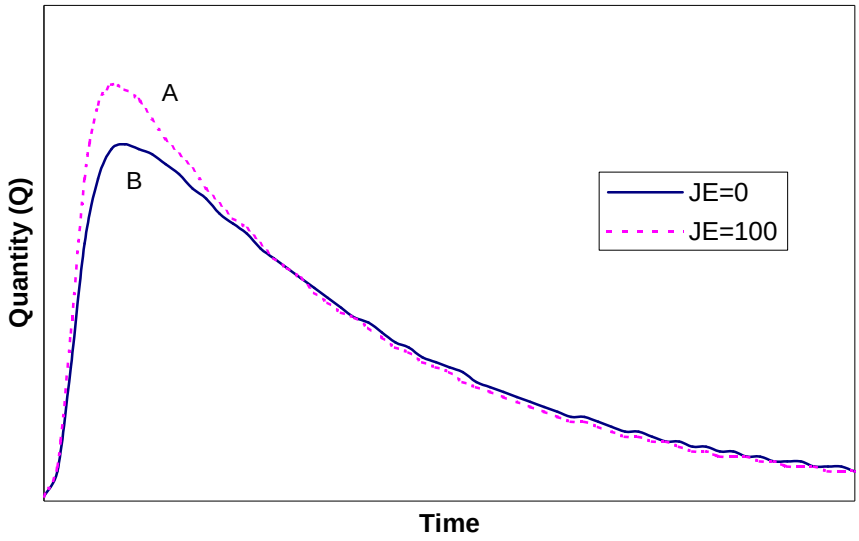

Figure 7. 13. Microbial consumer population Q vs. time from the simulation of a microbial decomposition ecosystem. Curve A: Feedback control of organic matter input, with J_E=100 and N_{hi}=2. Curve B: No feedback control.

These curves show evidence that the addition of active feedback control to a microbial ecosystem allows the system to entrain energy into the system at a faster rate. The greater energy availability is reflected by the more rapid growth rate and greater maximum population of the consumer population *Q*. The faster growth rate in turn drives the system into a limited state more quickly, as other factors necessary for consumer growth (in this case, the electron acceptor *N*)are utilized faster and become limiting sooner. The more rapid use of *N* may be reflected in the physical systems by the more rapid change in the value of the redox potential, as seen in the methanol experiments.

7.4.4 Minimodel 4: Microbial degradation microcosm with two limiting reservoirs and artificial feedback control of the availability of both organic matter and the electron acceptor

The final model in this series is of a microbial degradation system with two limiting reservoirs and feedback control loops that control the availability of both the

organic matter and the electron acceptor to the microcosm. This is a modification of the previous model, using the sensed value of *N* (representing the measurement of redox potential in the physical system) to activate control mechanisms for either the organic matter or the electron acceptor. Whether the addition of organic matter or electron acceptor is performed depends upon the configuration of the control algorithm *f(N)*. This takes action on switches controlling the input of organic matter J_E and the input of electron acceptor J_N from infinite sources outside the microcosm system. The energy circuit diagram for this control scenario is shown in Figure 7. 14.

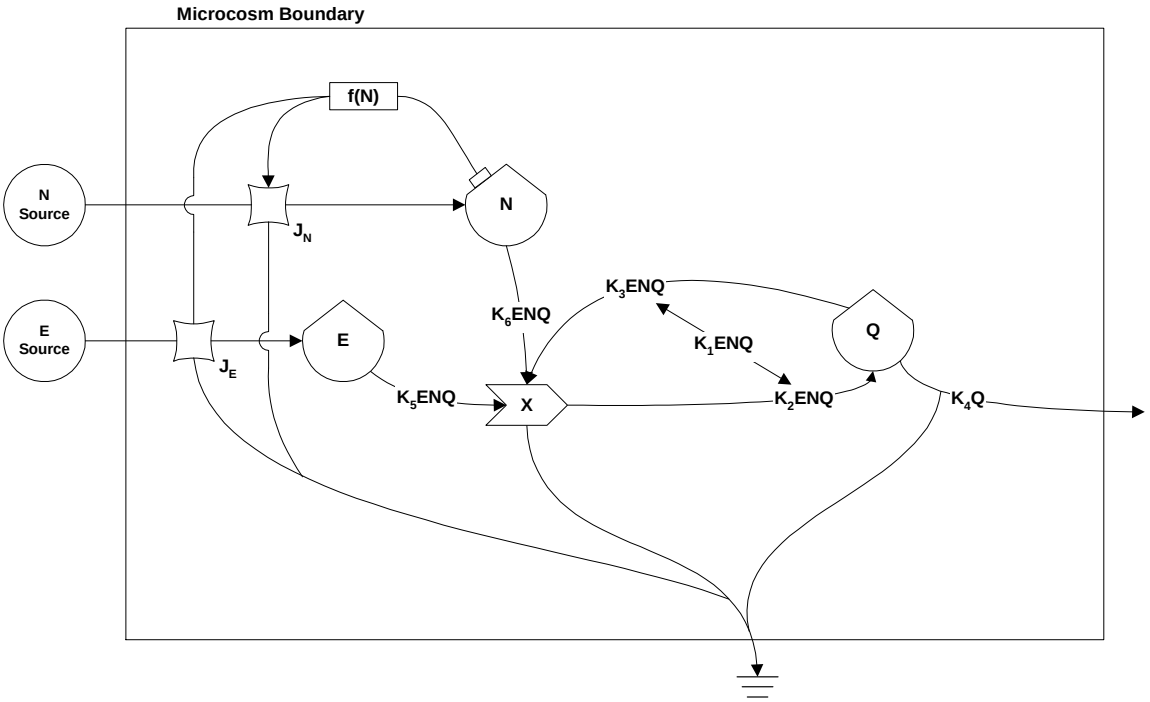

Figure 7. 14. Minimodel of a soil microbial decomposition microcosm with an initial organic matter stock (E), an initial electron acceptor stock (N), and control feedback loops controlling the input of organic matter (J_E) and electron acceptor (J_N) from outside the system based upon the sensed value of N.

Assigning rate constants K_i to the flow pathways to and from the storage tank units, and setting the control algorithm *f(N)* to reflect the Boolean logic used in the

physical microcosm experiments, the system of equations describing the systems diagram of Figure 7. 14 are as follows:

$$\dot{Q} = \frac{dQ}{dt} = K_1 ENQ - K_4 Q$$

$$\dot{E} = \frac{dE}{dt} = J_E - K_5 ENQ$$

$$\dot{N} = \frac{dN}{dt} = J_N - K_6 ENQ$$

$$K_1 = K_2 - K_3$$

$$f(N): \begin{cases} J_E = C_E \ldots if \ldots N > N_{hi} \\ J_E = 0 \ldots if \ldots N < N_{hi} \\ J_N = 0 \ldots if \ldots N > N_{lo} \\ J_N = C_N \ldots if \ldots N < N_{lo} \end{cases}$$

This algorithm for the control function *f(N)* assumes that, as before, if the redox potential remains high, system respiration is not occurring because of a limitation of organic matter, and thus should be injected into the system at a flow rate C_E. In addition, if the redox potential is low, the system growth is limited by the availability of the electron acceptor, and this should be injected into the system at a flow rate C_N. This algorithm roughly approximates the operation of the control program used in the physical microcosm experiments. This system of equations was programmed into STELLA. The STELLA graphical representation and code constructed to simulate this system of equations is shown in Appendix B. In addition, because of the complexity of this model, a user panel was designed for the STELLA interface; this, too, is shown in Appendix B.

A significant modification incorporated into Minimodel 4 is the user control over whether the feedback control loop is performed continuously or at discrete time steps with a defined periodicity. In the physical microcosm experiments, data acquisition and feedback control occurred discretely, usually with a period of 30 minutes. The rate at

which feedback control is activated is as important in determining the availability of the inputs as is the amount of input itself. The frequency of the data acquisition and control per unit time is thus incorporated into this model as the user-defined parameter *F*, the effects of which might then be explored.

Model parameters used for the STELLA simulation of Minimodel 4 are given in Table 7. 4. Values for the parameters were chosen by a process of trial-and-error such that model results were visually discernable. Sample results for simulation with these parameter values are shown graphically in Figure 7. 15. These results show the exponential increase of *Q* early on, again as a result of the autocatalytic loop. *Q* then enters an oscillatory behavior, varying cyclically and maintained within a small range. This results from the alternating addition of *E* and *N* as either becomes limiting based upon the logic for *f(N)* defined previously. The death rate of *Q* is counterbalanced by the continued, cyclic additions of *E* and *N*, maintaining the system indefinitely.

Table 7. 4. Parameters and their values used in the STELLA simulation of a microbial degradation microcosm with an initial organic matter stock, an initial electron acceptor stock, and a control feedback loop controlling the input *of* both organic matter and electron acceptor from outside the system based upon the sensed value of N.

Parameter	Description	Value
E_0	Initial value of E	100
N_0	Initial value of N	200
Q0	Initial value of Q	0.01
$K_1 = K_2 - K_3$	Rate constant	0.001
K_4	Rate constant	0.5
K_5	Rate Constant	0.1
K_6	Rate Constant	0.2
J_E	Organic matter supply rate	100
J_N	Electron acceptor supply rate	500
N_{hi}	Threshold value of N controlling JE	50
N_{lo}	Threshold value of N controlling JN	40
F	Frequency of N-sensing and control	20 (continuous)

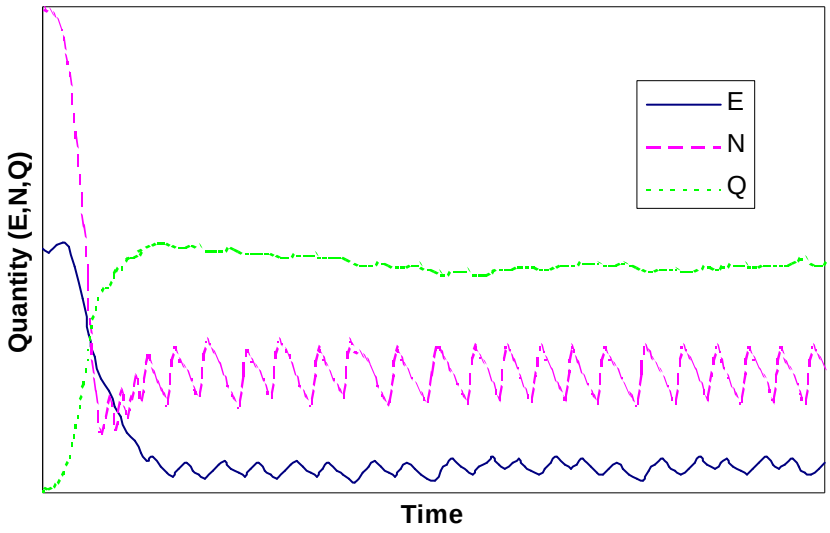

Figure 7. 15. Results from the STELLA simulation of a microbial degradation microcosm with an initial organic matter stock, an initial electron acceptor stock, and control feedback loops controlling the input of organic matter and electron acceptor from outside the system based upon the sensed value of N sensed continuously.

To fully explore the complexity of this model, a number of the parameters may be varied over a range to explore their effect upon the behavior of the system. For the analysis that follows, four parameters were chosen and varied individually, holding all others constant. The four parameters varied were as follows: the organic matter input rate (J_E), the electron acceptor rate (J_N), the difference between the high and low setpoints for the control variable N (i.e., $N_{hi} - N_{lo}$), and the frequency of data acquisition and control (F). All other parameters were held constant at the values presented in Table 7. 4. Results of this analysis are presented in the following twelve figures.

First, the organic matter input rate J_E is varied, and the results are shown in the following three figures. Results are shown for J_E =20 (curve A in each), J_E =100 (curve B), and J_E =200 (curve C). Organic matter E varies cyclically over time as a result of

periodic additions (Figure 7. 16). Comparing curve A to B, the frequency of *E* addition increases as J_E is increased. Curve C shows instability, however, as the frequency of the addition of *E* is at first chaotic and then abruptly drops to zero when time is approximately 2. Likewise, the electron acceptor *N* varies cyclically over time because of periodic additions (Figure 7. 17). Comparing curve A to B, the frequency of *N* addition also increases as J_E is increased. Curve C again shows instability, abruptly changing to a constant value when time is approximately 2. The instability is explained by examining the curves for the microbial consumer population *Q* (Figure 7. 18). For low and intermediate values of J_E (curves A and B), *Q* increases exponentially, overshooting an optimum value around which it varies in the steady state. This steady state value of *Q* is greater for larger values of J_E (compare curve A to B), owing to more energy being entrained into the system. However, at some point the availability of J_E is too much, stimulating the production of *Q* beyond that which can be maintained by the availability of *N*. Over time, the system crashes, stuck in a condition where neither *N* nor *E* can be input to stimulate and maintain the population of *Q*.

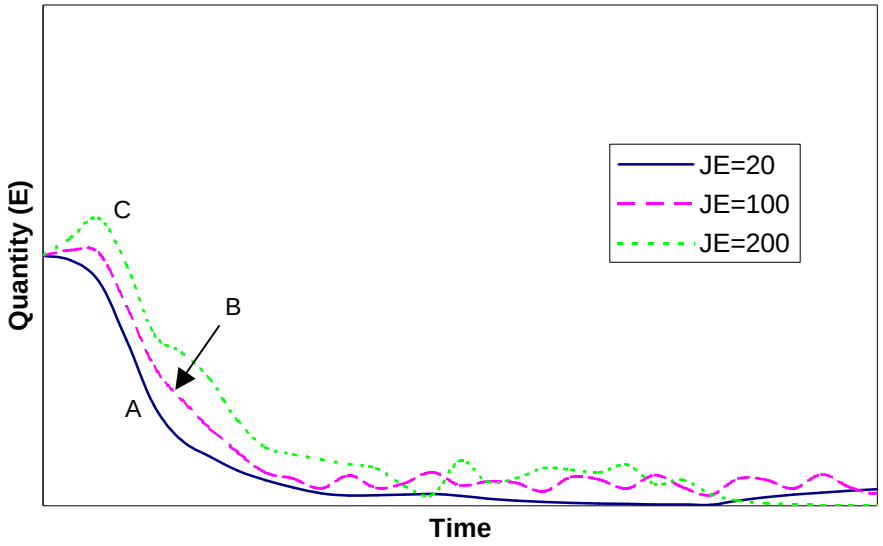

Figure 7. 16. Organic matter E vs. time from the simulation of a microbial decomposition ecosystem with feedback control over E and N and with J_E varied. Curve A: J_E=20. Curve B: J_E=100. Curve C: J_E=200.

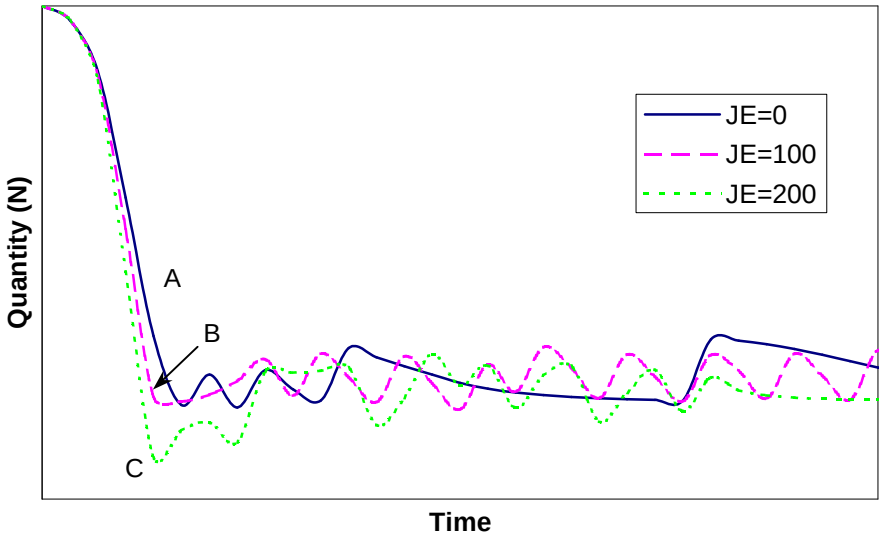

Figure 7. 17. Electron acceptor N vs. time from the simulation of a microbial decomposition ecosystem with feedback control over E and N and with J_E varied. Curve A: J_E=20. Curve B: J_E=100. Curve C: J_E=200.

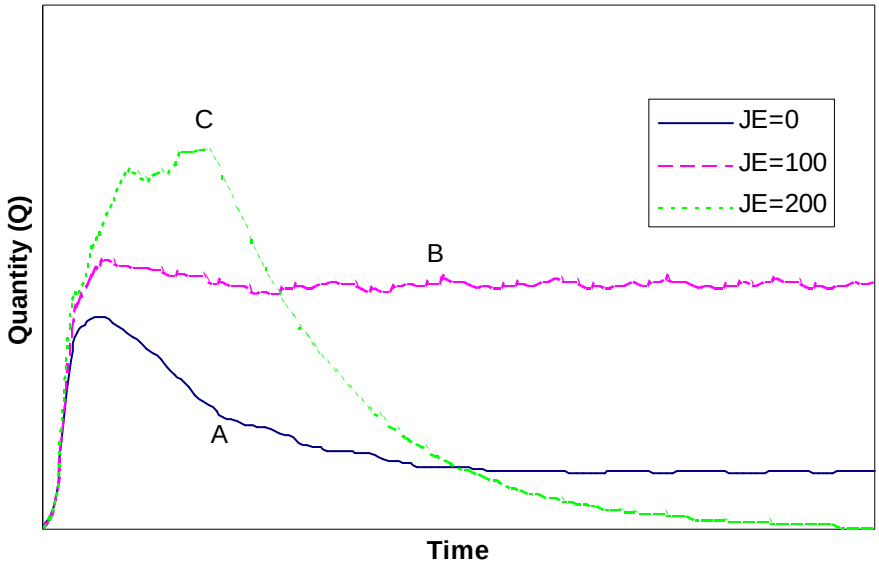

Figure 7. 18. Microbial consumer population Q vs. time from the simulation of a microbial decomposition ecosystem with feedback control over E and N and with J_E varied. Curve A: J_E=20. Curve B: J_E=100. Curve C: J_E=200.

Next, the electron acceptor input rate J_N is varied, and the results are shown in the next three figures. Results are shown for J_N =100 (curve A), J_N =500 (curve B), and J_N =1000 (curve C). Results show that, at low rates of *N* addition, organic matter *E* first increases, and then decreases steadily and rapidly to zero beyond time 1 (curve A, Figure 7. 19). At higher rates of *N* addition (curves B and C), E varies cyclically as it too is periodically added. Likewise, the electron acceptor *N* decreases steadily to a constant for low rates of addition (curve A, Figure 7. 20). For higher values of J_N, *N* varies cyclically over time because of periodic additions (curves B and C). Comparing curve B to C, the frequency of *N* addition decreases as its input amount J_N is increased. Examining the curves for the microbial consumer population *Q* (Figure 7. 21), it is evident that for low values of J_N (curve A), the availability of *N* is not enough to raise *Q* above a threshold to sustain itself. After an initial increase to time t=1, the population *Q* crashes to zero, and

the system is stuck in a condition where neither *E* nor *N* can be input. For intermediate and high values of J_N (curves B and C), *Q* is maintained at or around a quasi-steady state, as the combined availability of *N* and *E* is enough to sustain it. This steady state value of *Q* is greater for larger values of J_N (compare curve B to C), again owing to more energy being entrained into the system.

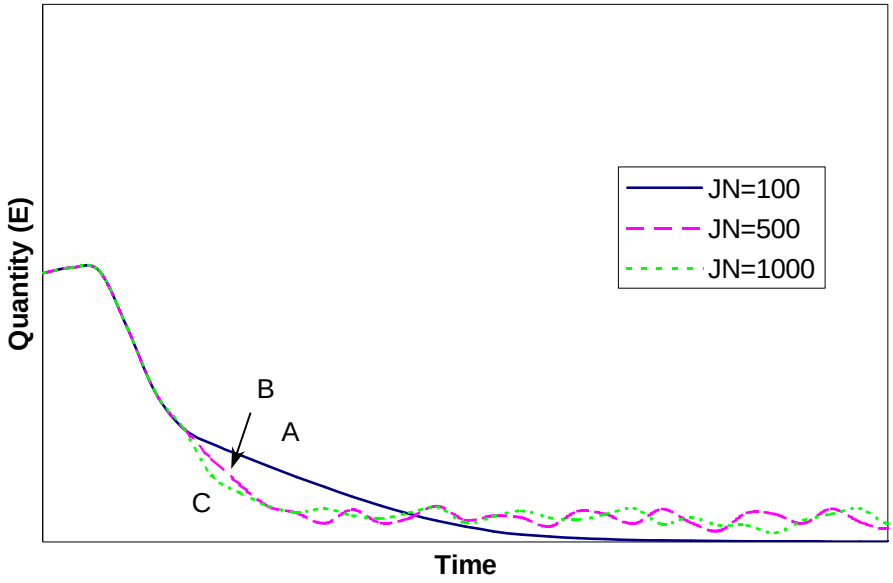

Figure 7. 19. Organic matter E vs. time from the simulation of a microbial decomposition ecosystem with feedback control over E and N and with J_N varied. Curve A: J_N=100. Curve B: J_N=500. Curve C: J_N=1000.

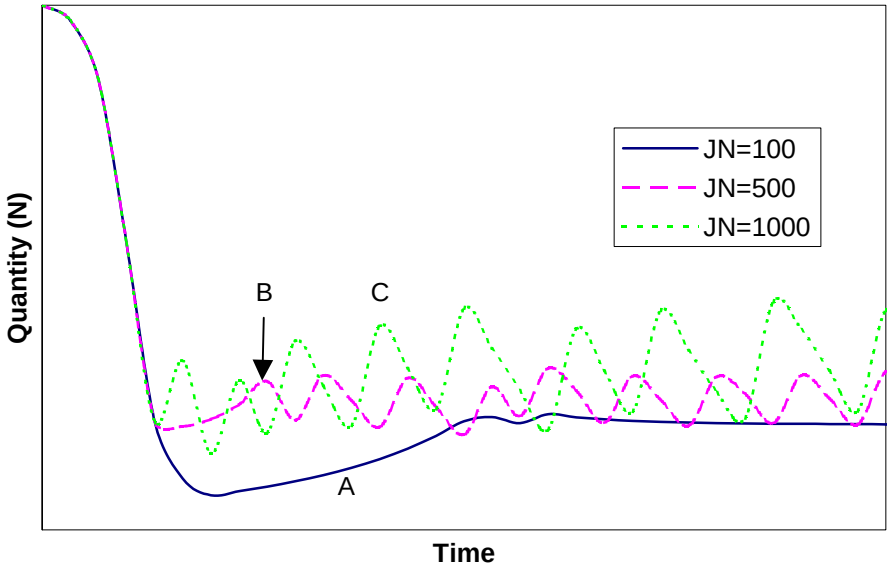

Figure 7. 1. Electron acceptor N vs. time from the simulation of a microbial decomposition ecosystem with feedback control over E and N and with J_N varied. Curve A: J_N=100. Curve B: J_N=500. Curve C: J_N=1000.

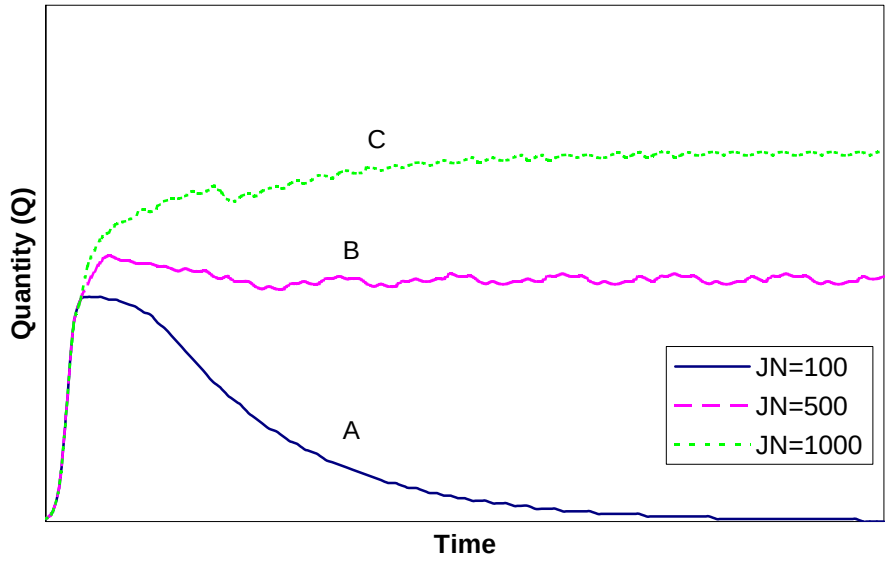

Figure 7. 2. Microbial consumer population Q vs. time from the simulation of a microbial decomposition ecosystem with feedback control over E and N and with J_N varied. Curve A: J_N=100. Curve B: J_N=500. Curve C: J_N=1000.

Next, the difference between the high and low setpoints ($\Delta N = N_{hi}-N_{lo}$) for the control algorithm is varied. This is accomplished by holding the upper setpoint N_{hi} constant at 50, and varying the lower setpoint N_{lo}. The results are shown in the following three figures for ΔN=0 (curve A), ΔN=20 (curve B), and ΔN=40 (curve C). Results show that, when the difference between the high and low setpoints is small, organic matter *E* varies cyclically as it is periodically added (curves A and B, Figure 7. 22). Curve A has a cyclical frequency greater than curve B; thus, the smaller the difference between the setpoints, the greater the frequency of addition of *E.* When the difference between the setpoints is large, the addition of *E* starts initially and then stops, and *E* tends towards zero (curve C). Likewise, the electron acceptor *N* varies cyclically for a smaller difference between the setpoints (curves A and B, Figure 7. 23). As with *E*, the greater the difference between the setpoints, the lower the frequency of *N* addition (compare curve A to curve B). When the difference between the setpoints is large (curve C), the addition of *N* ceases after time t=3, indicating the system is running down. This is confirmed by examining the curves for the microbial consumer population *Q* (Figure 7. 24). For a small difference between the setpoints, *Q* reaches a quasi-steady state level (curves A and B). The smaller the difference between the setpoints, the greater the steady state value of *Q,* since energy is added into the system at a greater frequency. When the setpoint difference is low, however, the population of *Q* first increases and then crashes (curve C). In this case, the greater setpoint difference causes a great enough lag in the addition of *N* such that the growth rate of *Q* cannot be maintained. Beyond this, the system gets stuck in a condition where neither *E* nor *N* can be input.

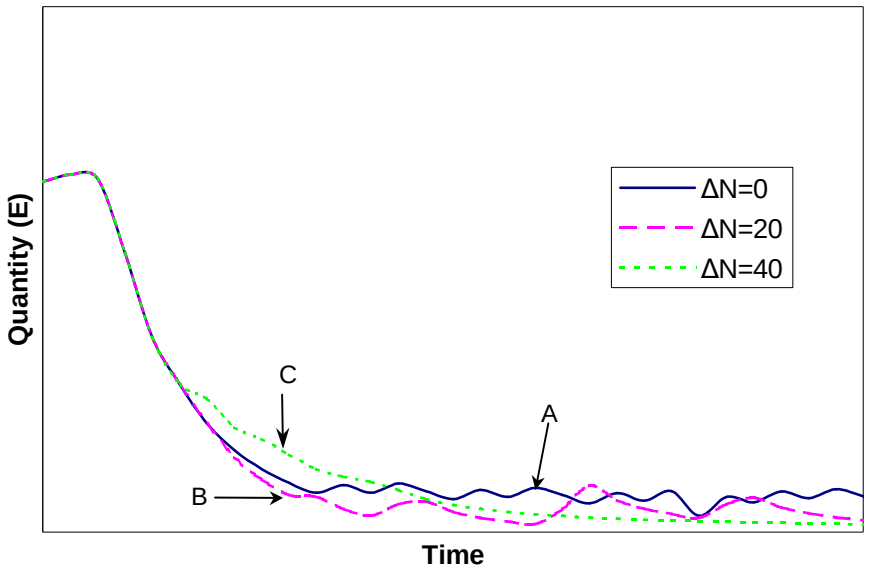

Figure 7. 22. Organic matter E vs. time from the simulation of a microbial decomposition ecosystem with feedback control over E and N, and with N_{hi} constant at 50 and N_{lo} varied. Curve A: ΔN=0. Curve B: ΔN=20. Curve C: ΔN=40.

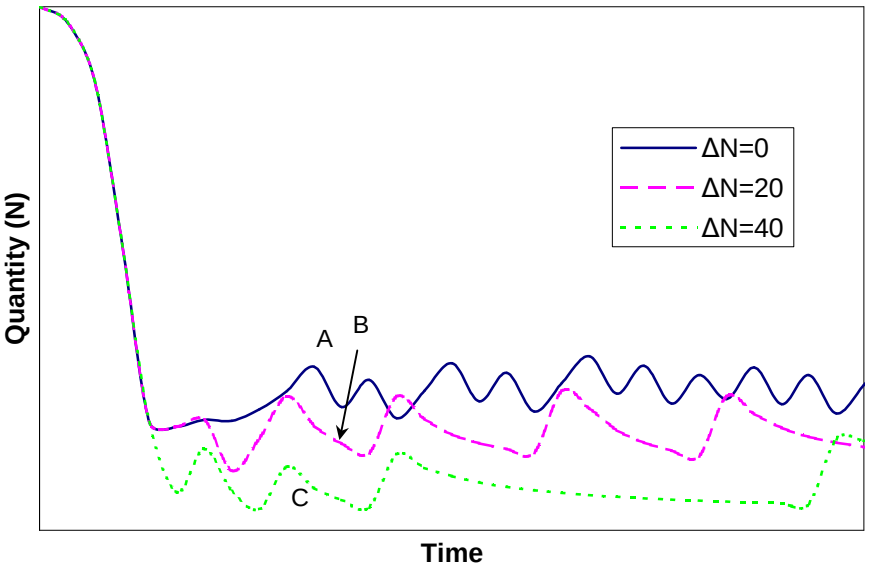

Figure 7. 23. Electron acceptor N vs. time from the simulation of a microbial decomposition ecosystem with feedback control over E and N, and with N_{hi} constant at 50 and N_{lo} varied. Curve A: ΔN=0. Curve B: ΔN=20. Curve C: ΔN=40.

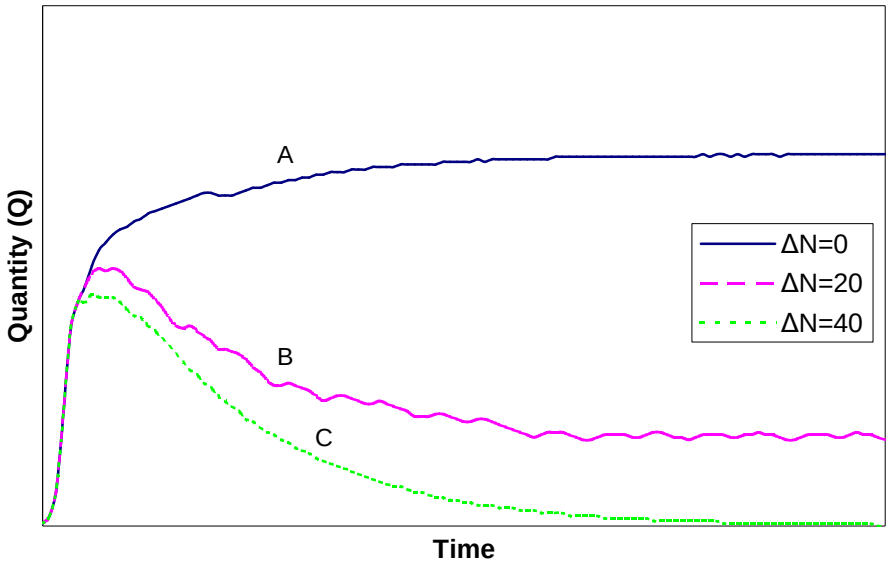

Figure 7. 24. Microbial consumer population Q vs. time from the simulation of a microbial decomposition ecosystem with feedback control over E and N, and with N_{hi} constant at 50 and N_{lo} varied. Curve A: ΔN=0. Curve B: ΔN=20. Curve C: ΔN=40.

Finally, the sampling frequency *F* of the feedback control operation is varied. The results are shown in the following three figures for *F*=20 (curve A), *F*=10 (curve B), and *F*=1 (curve C). Note that an integration time step of 0.05 is used in the simulation model. Therefore, a sampling frequency of 20 means 20 samples per unit time, effectively equivalent to continuous sampling. A sampling frequency of 10 means 10 samples per unit time, or every other integration timestep. Results show that, when the sampling frequency is greater, organic matter *E* varies cyclically as it is periodically added (curves A and B, Figure 7. 25). Curve A has a cyclical frequency greater than curve B; thus, the greater the sampling frequency, the greater the frequency of the addition of *E*. When the sampling frequency is low, the frequency of *E* addition starts initially and then stops, and *E* tends towards zero (curve C). Likewise, the electron acceptor *N* varies cyclically for

greater values of the sampling frequency (curves A and B, Figure 7. 26). As with *E*, the greater the sampling frequency is, the greater the frequency of *N* addition (compare curve A to curve B). When the sampling frequency is low (curve C), the addition of *N* ceases after time t=3, indicating the system is running down. Again, this is confirmed by examining the curves for the microbial consumer population *Q* (Figure 7. 27). For a large sampling frequency, *Q* reaches a quasi-steady state level (curves A and B). Continuous sampling yields the highest possible steady state value of *Q* (curve A), and lower sampling frequencies yields lower steady state values (curve B). When the sampling frequency is too low, however, the population of *Q* first increases and then crashes (curve C). The lower sampling frequency causes a lag in the addition of *N* and *E* such that the growth rate of *Q* cannot be maintained. Beyond this, the system gets stuck in a condition where neither *E* nor *N* can be input. Through trial and error manipulation of the parameter *F*, it was determined that the threshold sampling frequency for this value set of parameters above which *Q* can be maintained at a quasi-steady state is 4.444…. Below this value, the growth of *Q* cannot be maintained and the system crashes.

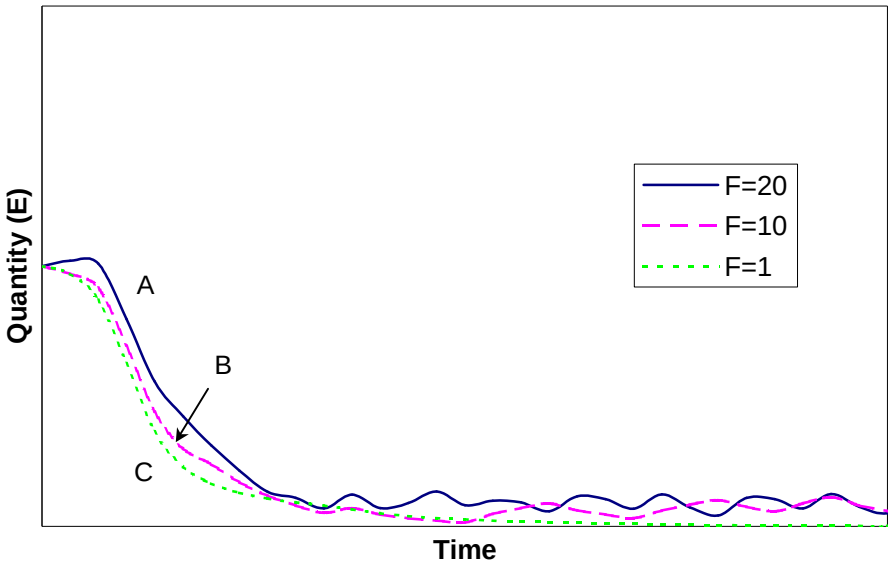

Figure 7. 25. Organic matter E vs. time from the simulation of a microbial decomposition ecosystem with feedback control over E and N, and with sampling frequency F varied. Curve A: F=20 (continuous). Curve B: F=10. Curve C: F=1.

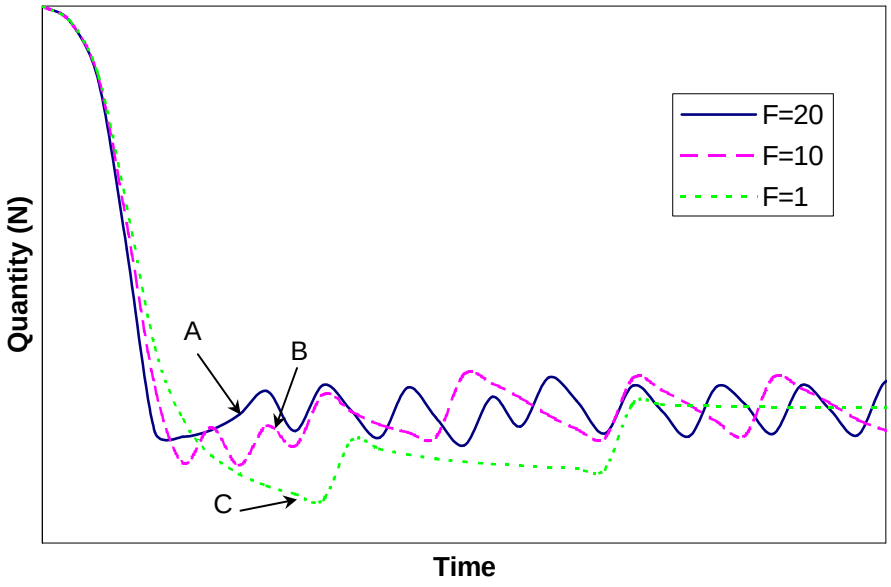

Figure 7. 26. Electron acceptor N vs. time from the simulation of a microbial decomposition ecosystem with feedback control over E and N, and with sampling frequency F varied. Curve A: F=20 (continuous). Curve B: F=10. Curve C: F=1.

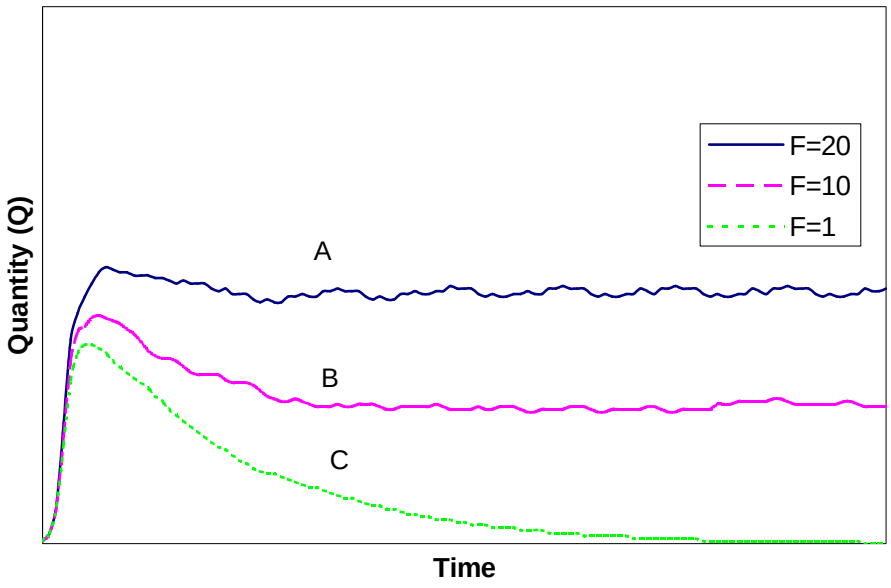

Figure 7. 27. Microbial consumer population Q vs. time from the simulation of a microbial decomposition ecosystem with feedback control over E and N, and with sampling frequency F varied. Curve A: F=20 (continuous). Curve B: F=10. Curve C: F=1.

7.4.5 Summary

What can be concluded from these series of models and curves? First, that the addition of artificial feedback control gives an autocatalytic ecological system the opportunity to entrain more energy at a faster rate, as exemplified by the results of Minimodel 3. While many of the setpoints and parameters of the feedback system are determined externally by the ecological engineer, the self-organizational processes of the microbial ecosystem, represented in these models by the autocatalytic feedback loop, harness the opportunity afforded by the artificial feedback information pathway to access an energy source. Those species in the microbial ecosystem that can harness the energy provided by the technological components under the conditions set by their functional parameters (*f(N)* on the simulation model) are selectively reinforced by a positive feedback. Those elements (in this case, the microbial species whose metabolism

functions at the redox potential established as the thresholds in *f(N))* continue to entrain more energy as long as it is available, thus undergoing more and more growth. Thus the ecological system internally self-organizes in such a way as to maximize the opportunity for access to the energy source. The continued growth is exhibited by increased ecosystem metabolism as represented by the change in redox potential. This matches results obtained from the physical microcosm experiments with carbon input, particularly those receiving methanol.

Second, the parameters that determine the operational details of the artificial feedback control critically affect the rate of interaction with the autocatalytic components of the microbial ecosystem, as shown by Minimodel 4. There exist finite boundaries to these parameters (threshold setpoints, nutrient delivery rates, etc.) within which the microbial ecosystem can harness the energy resources made available by the artificial feedback. In this case, one might expect the state variables in the microcosm to vary indefinitely around the threshold setpoints (for example, as in Trial 25, Figure 6.27). Outside of these parameter boundaries, the feedback control system operates at a rate out of sync with the rate of processes occurring in the microcosm. In this case, the microcosm is handicapped and cannot fully access the energy resources available to it. This may possibly have happened on experiment Trial 20 (Figure 6.24) in which no additional inputs made any affect on the redox potential. One can envision a multi-dimensional set space defined by the boundaries of the human-set parameters of the control system. Outside of this set space, the technological and ecological components of the technoecosystem will likely not be able to adequately interlace. The values of the parameters that will work are determined by the rates of biological metabolism and

material transfer within the ecosystem. The key to successful technoecosystem engineering and design is to calibrate the human-set parameters of the technological components of the system to a similar time constant as the processes being monitored in the biological component.

It is interesting to extrapolate from this experience to the hypothetical situation of a completely autonomous technoecosystem. Given the previous analysis, the design of a system of feedback control for an ecosystem is contingent upon the designer successfully fine-tuning the parameters that affect the rate at which the control system operates with the rates of those processes within the ecosystem deemed important. This means that value judgment is imposed upon the system from the outside; the decision as to which parameters to vary and processes to be sensed lies with the ecological engineer designing the technoecosystem. Is it possible for a technoecosystem to determine its parametric configuration internally? That is, can the interface between the technological feedback components and the biological components be fine-tuned by the processes internal to the system itself? This would entail events such as threshold setpoints and sampling rates being changed over time in response to the effect of their previous values on previous states of the system. How they would be changed might be determined by programming, again a condition imposed externally upon the system. This analysis thus falls into a state of infinite regression. Practically, at some point, a human operator must impose a value judgment as to the desirable state of the system, which the system itself can then use as a model around which to organize.

8.0 CONCLUSIONS

1. A technoecosystem was successfully constructed using wetland soil microcosms in which feedback control was implemented using redox potential as the monitored variable in an on/off control scenario that controlled inputs of carbon and nitrate as additional sources of energy.
2. It was found that the feedback control system affected the metabolism of the soil microcosm by increasing it when additional sources of energy were added. In the carbon addition microcosms, the signature of this increased metabolism was the increased rate of change of redox potential over time. In the nitrate/carbon selection scenario microcosms, the signature was the continued utilization of nitrate from the source reservoir and the maintenance of a high redox potential within the threshold boundaries. These signature changes on metabolic activity are presumably indicative of the microcosms' internal self-organizational processes interacting with the technological components. This did not hold in all cases, however, due likely in part to biological variability.
3. Initial steps were taken towards the development of a computational models based upon concepts of limiting factors. These models generally reflected behavior of trends in redox potential observed in some of the microcosms, supporting the hypothesis that microcosm internal self-organization occurs such that the biological components harness an artificial feedback loop if it allows access to additional energy sources. The modeling process also indicated that the values chosen for the rate-affecting parameters of the technological components of the

feedback control system critically affect the interaction with the biological components. In the design of technoecosystems, attention must be paid to matching the time constants of the technological components with those of the ecological system.

4. Directions for further research, development, and contextual understanding of technoecosystems are proposed in the following sections.

9.0 IMPLICATIONS

9.1 Role of Redox Potential as a Control Parameter

In the series of experiments presented here, the change in redox potential (ΔEh) has been used as an integrating measure of the system metabolism for the soil microbial ecosystem. Redox potential itself represents the aggregate of the chemical potential in the soil that the community of soil bacteria exploits as an acceptor for electrons. As this reservoir of energy is used up by the microbial metabolism, it is reflected by the change in redox potential. This is akin to the measurement of the change in pH by Beyers (1974) and to the measurement of the change in dissolved oxygen by Peterson (2001) as integrative measures of ecosystem metabolism of photosynthetic planktonic microcosms. The nature of these parameters—and, in particular, redox potential—makes them well-suited for easy measurement with electrical sensors and thus useful for an automated measurement and control scenario. The control system studied here is not far from other engineered control systems for wastewater treatment (c.f. Kim and Hao, 2001). However, viewed from the perspective of the ecosystem being controlled, the measurement and control circuitry comprise a new information pathway that, in this case, allows access to an energy source for the ecosystem.

Further considering the relationship between the technological and ecological components of this technoecosystem, it is apparent that the dynamics of this interface depend upon the parameters of the technological components in relation to the rates of physical change in the ecological components. This was shown by the analysis of a simple generalized model of the system presented in the discussion, where it was shown

through simulation modeling that those parameters of the technological components that define the rate or frequency of interaction between the technological and ecological components—such as frequency of data collection and rate of energy source delivery—are most important to the continued functioning of the entire system. Consequently, there exist finite boundaries to these parameters within which the microbial ecosystem can harness the energy resources made available by the artificial feedback. Outside of these boundaries, the technological components operate at rates out of sync with the rates of the metabolic processes in the biological system. This might possibly have been predicted by analysis with engineering control theory if enough information about the physical and biotic parameters in the microcosms could be known.

As for the relationship between the system itself and its energy source, the coupling of the technological components to the ecological system in effect causes a translation of the system boundaries to include inside of it previously external sources of energy. The basis for this translation is shown in Figure 9. 1. In this case, the next most immediate external source of energy becomes the source for the entire system. For example, prior to adding the technological components, the soil ecological microcosms derive their energy from the chemical reservoirs within the soil column (Figure 9. 1A). Adding the technological components in the form of a computer and wiring in effect allow the ecological components to access additional sources of energy in the form of electricity (Figure 9. 1B). This is the source that then becomes the driving force on the entire technoecosystem as other energy sources are internalized in the overall system.

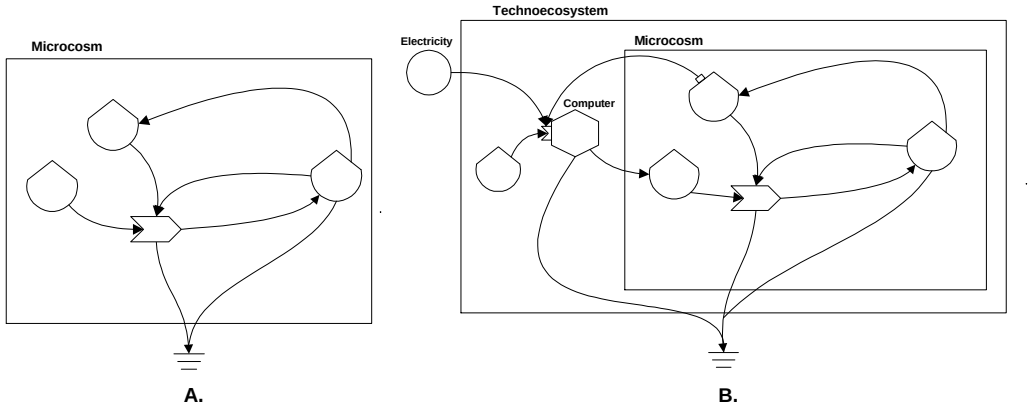

Figure 9. 1. Translation of energy sources by the addition of artificial feedback: (A) original microcosm functioning off internal energy reservoirs; (B) microcosm accessing previously external energy sources, now internalized.

9.2 Role of Artificial Feedback in the Technoecosystem

Reflecting upon the technoecosystem studied in the research presented here, it has been discussed that its design and construction relied upon the addition of pathways of information to an ecological microcosm. These pathways were artificial in that they were constructed of technological components not found in the natural analog of the microcosm. As information feedback pathways, however, they may not necessarily be new to the ecological system. The feedback control system employed in this research used information about the redox potential in a wetland soil microcosm to control access to additional storages of energy (carbon and nitrate). It is possible that redox potential similarly acts as a control in natural wetland settings. For example, in an inundated wetland soil, redox potential drops as the available electron acceptors are used up by soil microbes in their metabolism. The electron acceptors are used up in a predictable sequence: first oxygen, then nitrate, manganese, and iron, etc., each with its own characteristic range of redox potential at which the metabolic reactions occur. When

redox potential drops below the range of denitrification as a result of the depletion of nitrate, it enters the range of iron, sulfate, and finally carbon dioxide reduction, possibly to the detriment of some members of the plant community above. For example, sulfate reduction results can result in hydrogen sulfide (H_2S) that can be toxic to plant roots (Mitsch and Gosselink, 1993). Thus the low redox potential may cause certain wetland plants not adapted to low redox conditions to die off. Indeed, the role of redox potential as a controlling factor on the growth and competition of cattail and sawgrass has been suggested by Kludze and DeLaune (1996). The decomposition of this dead plant material releases a pulse of organic nitrogen that, following mineralization to ammonia and nitrification near the upper layers of the soil, might diffuse and percolate into the lower wetland soils as nitrate, making it available for denitrifiers in the soil and effectively raising the redox potential. Over time, the rates of all processes occurring will balance to a quasi-steady state of redox potential, and major fluctuations then result from seasonal fluctuations.

Thus the feedback control circuit constructed to form the technoecosystem for this series of experiments may be interpreted as a technological substitution of an already existing control mechanism. This is loosely analogous to a prosthetic substitution in individual organisms, where *prosthesis* is defined as the artificial replacement of a functional part (American Heritage, 1985). It is important to recognize, however, that the replacement feedback circuit has the potential to operate at a substantially faster rate than the natural analog, a result of the replacement's reliance upon an outside, high quality energy source (that is, electricity).

It is likewise important to recognize that the substitution in this set of experiments was goal oriented: the decision of what feedback to substitute and the important controlling parameters that affect the ecological role of this feedback were determined by decisions and value judgments made by the human designer. Recognizing the degree of goal-orientation injected into a technoecosystem design may be the key to one possible system of classification of technoecosystems.

9.3 Proposed classification system for Technoecosystems

Overall, technoecosystems may be seen as an entire class of ecologically-engineered systems, each with a natural analog but incorporating technological components as part of its feedback and energy signature. The design and manner of implementation of the technological components is done so with a degree of goal-orientation that determines its classification. Some possible subclass categories may be as follows:

- Ecological prosthetics
- True technoecosystems
- Intelligent technoecosystems

Each of these categories might well serve as avenues for future research beyond this study. Each is discussed briefly in the following sections.

9.3.1 Ecological Prosthetics

Ecological protsthetics or ecoprostheses, as discussed above, is a technoecosystem in which some biological components that serve as regulatory feedback mechanisms within the natural analog are substituted with artificial components.

Typically the artificial components are added for information feedback and control within the system for overall regulation of some process. This regulation and control for a process or product implies moderate to high level of goal-oriented implementation determined by the ecological engineer. Systems like algal turf scrubbers (Adey et al., 1993) might be considered in this class. The technoecosystem presented in this document likewise may be considered in this class.

9.3.2 "True" Technoecosystems

In the technoecosystem described in this research, there is a basic asymmetry in the relationship between the biological and technological components. Whereas the technological components provide the biological components access to additional sources of energy, the energy sources for the technological are not influenced by any feedback from the biological. Thus the class of "true" technoecosystems harkens back to the original definition given by Odum (1993), which defines technoecosystems as "hybrids of living units and hardware homeostatically coupled". The term "homeostatic" refers to the regulation of the system via feedback mechanisms. The term " coupled" implies that the components of the system are completely interdependent as a result of the feedback mechanisms. Thus, in a true technoecosystem, not only is it the activity of the technological components that is regulated by the biological components, but the energy source for the technological components is as well. The regulation of the technological components by feedback from the biological is just as prevalent as the converse, eliminating the typical asymmetry. There are at least two conceivable subcategories of true technoecosystems: those constructed with physical coupling, and those constructed with virtual coupling.

9.3.2.1 Physical coupling

Technoecosystems might be engineered in which the technological components actually derive their source of energy from the biotic components, which, in turn, derive their source of energy from the technological components. An idealized energy circuit diagram of such an arrangement is shown in Figure 9. 2. The energy source for the technological components is imagined in this case to be electrical, where the action of the biological components establishes an electrical potential strong enough to form an electrical current. One might also imagine possible scenarios, however, in which the technological components function off of mechanical or pneumatic energy provided by the biological system. As the energy circuit diagram shows, so long as access to the external chemical energy source is maintained, the system should continue to function.

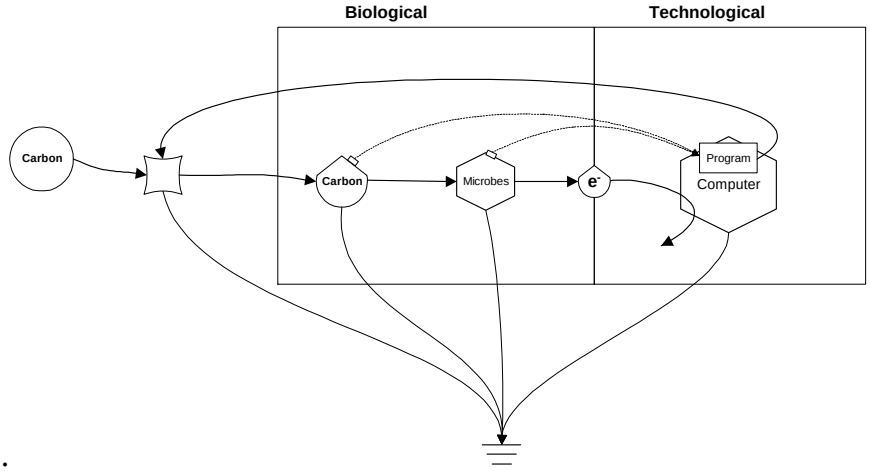

Figure 9. 2. Idealized systems diagram of a physically-coupled true technoecosystem in which the technological components derive electrical power from the ecological components, which in turn access chemical power via the technological components.

There are many possible ways to engineer such a system. An immediately obvious way is to employ technological components designed to harvest useful electricity from a microbial ecosystem. One such method might employ a sediment microbial battery (Reimers, et al., 2001; Bond, et al., 2002) in which a graphite anode placed in the anaerobic zone of marine sediments acts as the electron acceptor for the microbial respiration occurring there when connected to a similar graphite electrode in the overlying aerobic water. In a series of experiments, these microbial batteries obtained a continuous electrical power output of 0.016 W per square meter of electrode (Bond, et al., 2002). Electrical power was especially plentiful when sodium acetate was added to the water column as a supplement to the carbon already available in the sediment. Similar studies conducted years before by Armstrong and Odum (1964) confirmed the development of electrical potentials on the order of 0.4 V from a blue-green algal mat system as a result of photosynthesis. These are electrical power supplies on the order of what might be useful to power logic and control circuitry that might, in turn, control the supply of chemical energy to the biotic components (for example, the circuitry might control the feed source of acetate to the microbial battery system). In this way, both the technological and ecological components ultimately derive their operational energy from the same external source: the reservoir of chemical energy that feeds the biotic components of the system.

One interesting configuration of this type of technoecosystem is to enclose the microbial ecosystem completely within a technological envelope. The electrical potential derived from this microbial ecosystem might then be used to power complex operations of the autonomous electromechanical envelope. Sometimes called “gastrobots”, such

systems are being designed and built as independently mobile units with the ability to seek out sources of organic matter as “food” (Wilkenson, 2000). The organic matter is first broken down in chemical chambers and then used to supply a microbial fuel cell in which an anode acts as the terminal electron acceptor for the microbial degradation reactions occurring there. The electrical power derived from the microbial fuel cell powers sensors and control over motors for motion and searching capabilities of the entire system. This is an interesting arrangement of the mutualistic feedback between technological and ecological components. Power for the entire technoecosystem is derived from the microbial metabolism, but access to the energy source for this metabolism is granted by the sophistication and mobility of the technological components. One can envision a mobile robot that must search, forage, and possibly compete for organic energy sources to power itself. These “ecological robots” may indeed comprise another distinct subclass of technoecosytems that conceivably could take on a bizarre assortment of physical forms.

9.3.2.2 Virtual coupling

Another way to construct a true technoecosystem is to engineer it using virtual coupling between technological and ecological components. This would entail the coupling between a virtual, simulated ecosystem on a computer and a physical microcosm. The coupling is achieved by one or more feedback loops of material (real or virtual) or information between the virtual ecosystem and the physical microcosm (Figure 9. 3). The virtual ecosystem might be programmed as a collection of independent virtual entities that interact according to a rule-based set of code, as explored by Parrot and Kok (2002). In this arrangement, the state of one or more components in the virtual

ecosystem, as output by programmed computer code, affect the availability of an energy source to the physical microcosm. Likewise, the states of various components in the physical microcosm, as sensed by physical sensors, affect the availability of a virtual energy source (in essence, the availability of certain segments of computer code) to the virtual ecosystem. One challenge in making this system work is calibrating the rate of processes within the virtual ecosystem simulation to the real-time process rates of the virtual ecosystem. Engineering these types of systems, however, may be a simpler way to explore the basic ecological principles that govern technoecosystems.

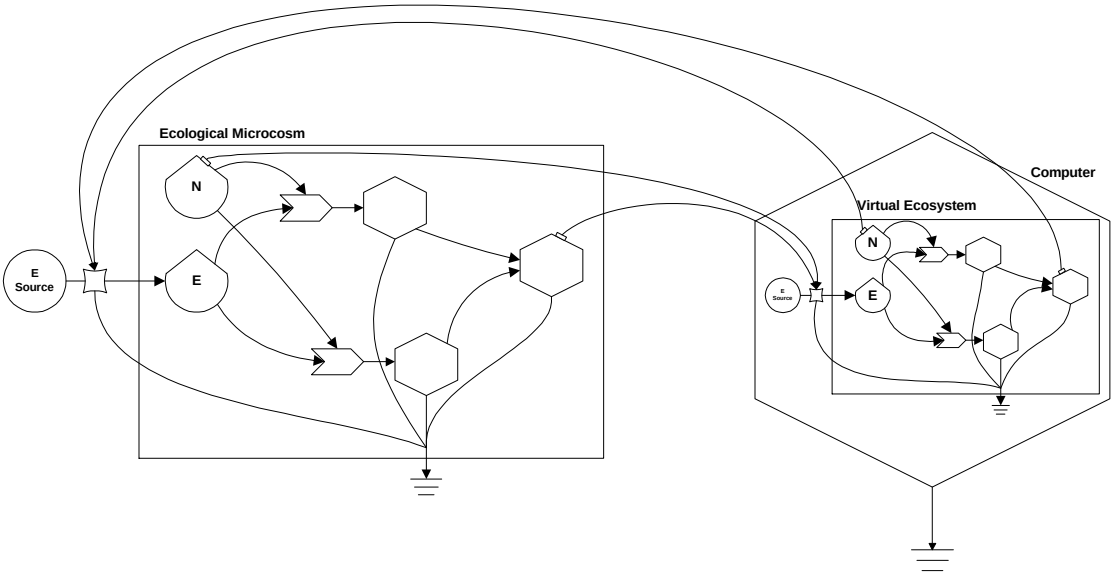

Figure 9. 3. Idealized systems diagram of a virtually-coupled true technoecosystem in which the virtual ecosystem, a simulation program on a computer, affects the availability of energy to a physical microcosm, which in turn affects the availability of a virtual energy source to the virtual ecosystem.

One of the distinguishing characteristics of true technoecosystems is that the goals are completely internal to the system. The feedback circuits are implemented by the ecological engineer to allow self-organization between the technological and ecological

components to occur for the sake of the self-organization itself. In this way there is no overt goal; so long as the primary energy source is available, these systems merely exist and evolve.

9.3.3 Intelligent Technoecosystems

Possibly one of the most extreme possibilities for technoecosystems is the combination of ecological components with technological information networks designed for some measure of artificial intelligence. An intelligent technoecosystem could process information about its internal state and take appropriate and necessary action to maintain a homeostatic state, for example, by accessing additional sources of energy or nutrients or mitigate infestations of unwanted species. Indeed, this type of system has recently been proposed on the greenhouse scale (Clark and Kok, 1998). Within this context of intelligent technoecosytems, a categorization scheme has been proposed by Clark, et al., (1999) that uses nomenclature and concepts from the field of artificial intelligence (Table 9. 1). Each parameter within this system of classification should be present to some degree within the technoecosystem under consideration. That degree determines the level to which the technoecosytem might be considered intelligent.

Table 9. 1. Parameters of computational abilities according to categories of complexity (from Clark, et al., 1999).

Parameter	Description
Perception	Ability to create information from signals. Akin to observation of either the internal or external environment.
Memory	All abilities required to index, retain, and retrieve information along with some ability to detect and compare patterns
Reason	Flexible and high-level formulation of appropriate responses to unanticipated stimuli
Expression	Abilities required for the transformation of mental products into output signals, influencing the external or internal environment
Learning	Abilities allowing the computational center to restructure itself adaptively.
Consciousness	Ability to observe and reason about self, dependent upon the maintenance of a self-referential model.

This classification system might be applied to any technoecosystem as a qualitative measure of its intelligence. For example, the wetland soil microcosm discussed in this research can be analyzed according to each of these intelligence parameters (Table 9. 2). Interestingly, the results of this analysis seem to indicate that even this simple technoecosystem exhibits rudimentary characteristics of artificially intelligent systems.

Table 9. 2. Parameters of computational ability and intelligence evaluated for the wetland soil technoecosystems.

Parameter	Evaluation
Perception?	YES: Redox probe/DAQ system affords the ability to create information from signals. Observation is of the internal environment.
Memory?	NO: Abilities to index and retain only. BUT, information retrieval and pattern analysis might be easily programmed.
Reason?	NO: System is limited to one response based upon expected stimuli. Difficult to foresee how to program.
Expression?	YES: Limited ability to influence internal environment through carbon addition via output signals.
Learning?	NO: No ability for adaptive restructuring. Requires programming akin to neural networks.
Consciousness?	NO: System is self-observational, but has no real ability to reason about self. A simple self-referential model (e.g. soil redox model) might be incorporated into programming.

This analysis also points towards new avenues of research that could be undertaken using the soil microcosm technoecosystems described here. The intelligence of the soil microcosm technoecosystem could be improved with a few steps in development of the control programming with elements that already exist. For example, the system memory (in the context of intelligence as described in Table 9. 1) might easily be improved upon by making past sets of data available to the control program. The control program might compare the current state and trend of the redox potential in a microcosm with past states, in which case the action of the nutrient delivery pumps becomes a function of the change in redox potential over time.

Another way to improve upon the intelligence capabilities of the existing system is to improve the level of consciousness via programming. As stated in Table 9. 1,

consciousness may be considered as the ability of the system to observe and reason about itself. Thus the controlling program of the system must have available to it a model of itself to which it can refer. In a programming sense, this implies a computer simulation model of itself. Combining the simulation models developed previously in this research with the data acquisition program yields an entirely different technoecosystem with a substantially higher level of intelligence. One proposal is to allow the model to act as a virtual replicate in an experiment, serving as an ideal case to which the state of the physical microcosms can be compared and action taken accordingly. It is expected that in such a system the energy utilization, signified by the action of the nutrient delivery pumps, would be significantly different than the simpler microcosms studied here.

The goal orientation of such a system might vary depending upon the sophistication of the intelligence programming. For example, the soil microcosm technoecosystem studied in this research is decidedly goal-oriented. Through the setting of thresholds and logic conditions in the control programming, goals were established along the lines of keeping redox potential within a certain range. However, intelligence programming might be used to decouple the system from dependence upon these specific parametric goals and rely more upon general system-level goals for operational guidance. For example, imagine a system with adequate elements of all the artificial intelligence parameters discussed in Table 9. 1 that includes the ability to learn over time. A generalized goal to the technoecosystem might be to perpetuate survival at a certain level of productivity. This goal would be implicit in the design of the controlling hardware and software in the form of a suite of sensors and actuators to monitor and affect any number of internal parameters of the system that adequately describe the internal state as relates

to productivity. Once allowed to function, the system might follow a trajectory of homeostasis, taking what action as necessary to maintain that state. Imagine additionally that the control program is constructed with the ability to learn, thus allowing the system to learn the results of certain actions given a particular combination of parametric states. The resulting system might be one that can manipulate setpoints and thresholds for the various control actions on its own, possibly converging on local optimum setpoints. The system thus is separated from specific goals for individual parameters, and rather allowed to optimize a set of parameters based upon an internal learning process performed under a small and general set of rules and actions.

9.3.4 Summary

The classification system for technoecosystems proposed here is a first attempt at categorizing the vast range of possibilities of engineered systems. A summary table shows the qualitative differences between the categories discussed here (Table 9. 3). Additional categories are certainly possible and can be determined along the already discussed scales of intelligence and goal-orientation of the systems.

Table 9. 3. Summary of technoecosystem classes and their descriptive qualities.

Class	Role of Technological Components	Role of Ecological Components	Goal-Orientation of Design
Ecoprothetics	• Substitute for feedbacks in natural analog	• Base of system to which technological amendments are made	• Typically yes, to modify some process for a product or service
True Techno-ecosystems	• Feedback control over energy sources for ecological components.	• Feedback control over energy sources for technological components.	• Goals are internal to overall system and implied in design of coupling interface.
Intelligent Ecosystems	• Provide awareness, control, and intelligence via higher mentation abilities.	• Base of system to which technological amendments are made. • Possible feedback control over energy sources to technological components.	• Not necessarily; only as far as to maintain the entire system.

9.4 Research in Analogous Systems

What is the ultimate value of studying technoecosystems? The value in study is that of any microcosm: a small model of a larger analogous system that can be manipulated experimentally from which basic principles might be gleaned. Laboratory-scale technoecosystems might be useful for understanding and predicting the effects of technological amendments to their larger natural analogs. Focusing in on the component description of technoecosystems lends some guidance as to their possible use in research. Technoecosystems are biological systems derived from natural analogs to which technological additions are made to form artificial pathways of information feedback. The information is processed in various ways by a controlling design or program and used to access additional sources of energy. It can be argued that this description is an analog for any ecosystem that contains humans (Petersen 2001), recognizing that humans specialize in processing and reacting to information. Indeed, the global biosphere may

operate in the fashion of a technoecosystem. Humans are an integral and inseparable component of the biosphere. Because of their intelligence, humans have the ability to sense and process information about the state of the biosphere environment. Information is especially prevalent regarding the state of the human component's own metabolism, as represented by the economy (in essence, the summation of all the production and consumption cycles that define the human environment). Moreover, this information is used to activate mechanisms that, in the end, affect the rate of flow of additional sources of energy (for example, through the tapping of fossil fuel reserves) into the overall biospheric system. Might a technoecosystem microcosm be designed such that the pieces and parts represent components of the global biosphere, with technological information pathways representing the role of humans in the biosphere as information processors and controlling actuators that access additional energy sources? What might this tell us about future states of the planet, as influenced by the role of feedback induced by the human presence?

10.0 RECOMMENDATIONS

Recommendations for further research and study of technoecosystems, as determined by the various analyses in this research, are as follows:

- Research the dynamics of a feedback control system using the change in redox potential over time as the measured parameter (as opposed to the value of redox potential);
- Continue with development of the data acquisition system presented here, in particular focusing on additional signal conditioning and filtering;
- Perform additional testing on acetate and synthetic sewage as sources of carbon and their effects on redox potential in the wetland soil microcosms;
- Continue with studies of denitrification in the wetland soil microcosms, investigating the role of the feedback control system in the optimization of the denitrification metabolic pathway;
- Further develop the proposed regression model as developed in the Discussion, focusing upon statistical goodness-of-fit to refine the model;
- Further develop the computer minimodels on limiting factors, calibrating the models to the redox phenomena observed in the physical experiments;
- Develop artificially-intelligent ecosystem based upon the incorporation of a computer model into the existing control system.

APPENDIX A. DATA ACQUISITION SYSTEM AND PROGRAM

A.1 Data Acquisition Hardware

The data acquisition board used to build the data acquisition system was the National Instruments' AT-MIO-16X (s/n 001297, National Instruments Corp., Austin, Texas), a multifunction analog, digital, and timing input/output (I/O) board for a PC (National Instruments, 1993). This board has 16 single-ended or 8 differential analog input channels, two 16-bit analog output channels, eight digital I/O channels, and three 16-bit counter-timers for timing input and output. It has a 10 μsec, 16-bit sampling analog-to-digital converter that can monitor a single input channel or scan through 16 single-ended channels or 8 differential channels. The analog input has a bipolar input range of 20 V (±10 V), with possible gains of 1, 2, 5, 10, 20, 50, and 100. The board has a 50-pin I/O connector, to which was attached the ribbon cable (1.0 m type NB1) for the National Instruments CB-50 I/O connector block with 50 screw terminals. The 50-channel pin assignment configuration for the AT-MIO-16X is shown in Figure A. 1. The probes for redox measurement were wired to the CB-50 connector block for differential analog measurement; up to four probes were used at any one time, allowing *Eh* measurement on four separate analog channels. Control signals (to turn on pumps, for example) were output from the board using digital I/O ports.

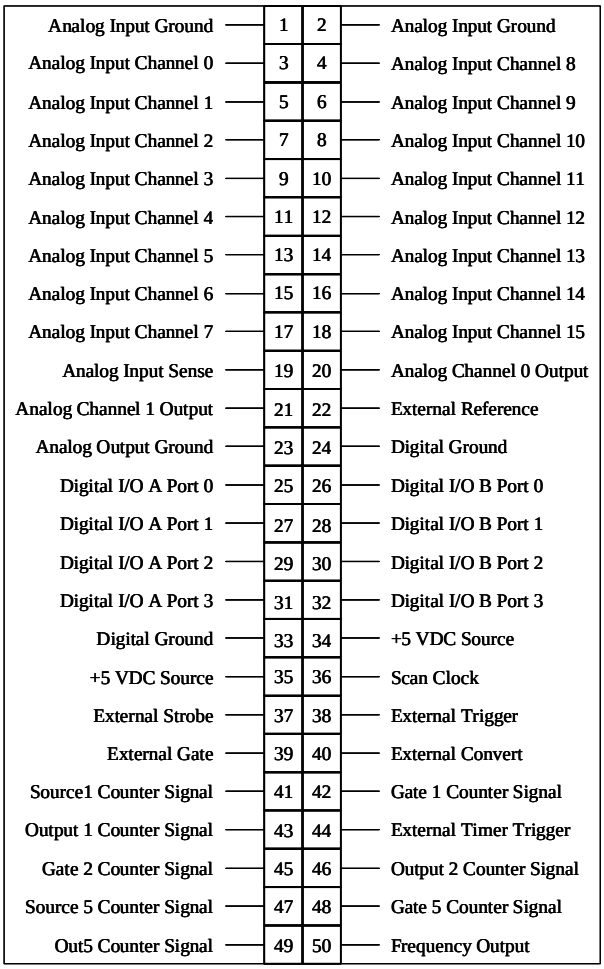

Figure A. 1. Pin assignments for the AT-MIO-16X I/O connector (from National Instruments (1993)).

A.2 Data Acquisition Software

A.2.1 Front Panel

The front panel of the LabVIEW data acquisition program serves as the user interface and affords the user control over the data acquisition and control process (Figure A. 2). The program allows the user to select between one of three control scenarios: carbon addition to minimize *Eh*, oxygen or nitrate addition to maximize *Eh*

(used only once in this research), and nitrate/carbon selection for *Eh* maintenance between high and low setpoints. To use the program, the user is required to select the type of control scenario (field 1. “Logic Control”) and set the program to enable (2. “Overall Enable”). The user is then required to set the desired time (in seconds) between sampling events (3. “Time Between Samples”), the desired time for the nutrient delivery pump to activate (4. “Pump Time”), and the frequency at which pumping is initiated relative to the sampling frequency (5. “Pump every X sample periods”). The user must then type in the path and file name where the measured *Eh* data are to be recorded (6. “Data Control”). Up to four channels of data can be recorded at any one time (Channels 0-3). The user enters the upper and lower setpoints for the nutrient addition pumps (7. “Thresholds”), and activates the pump or pumps by toggling the adjacent on/off panel switches (8. “Pump Activation”). Finally, the user activates the appropriate chart windows at the bottom; the chart for Channel 0 is always on, and those for Channels 1-3 are optional, activated by the accompanying switches. These charts continuously display the resulting measured *Eh* over time. The control program is set up such that Channels 0 and 2 are available for nutrient pump control; Channels 1 and 3 record *Eh* data and initiate no control actions. The program also outputs the start time and date, the elapsed time, the sample loop number, and the state of the pump on that sample period in the appropriate fields.

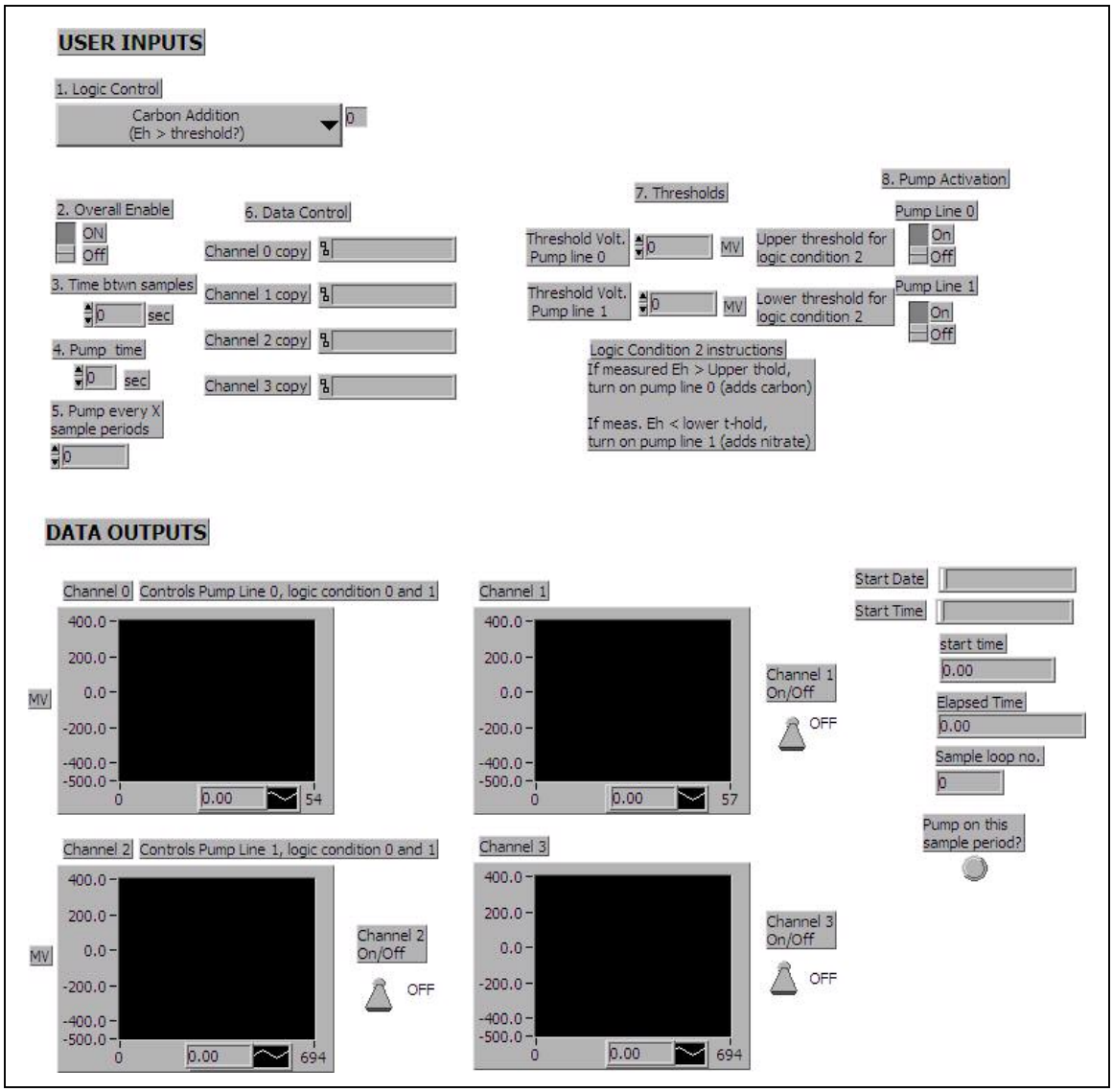

Figure A. 2. Front panel display of the LabVIEW data acquisition program.

A.2.2 Wiring Diagram Program

The wiring diagram for the LabVIEW control program takes the information from the user inputs and runs the data acquisition sequence (Figure A. 3). The program is set up as a large timed loop, repeating itself at a time period ("Time between samples") set by the user. The program allows the anolog input of four *Eh* measurements: two for active control of nutrient pumps (Channels 0 and 2), and two without pump control (Channels 1 and 3). Hence, the LabView wiring diagram program is similar for Channels 0 and 2 and Channels 1 and 3. For all active channels, the program takes an *Eh* reading via the sub-program "AI ONE PT", measuring the analog voltage input at one port. If "Carbon Addition" was selected as the control scenario, the program compares the *Eh* value from analog input Channel 0 and Channel 2, if active, with the user-defined thresholds using simple Boolean logic commands. If the result of the Boolean logic sequence is "True" (i.e., if measured *Eh* is greater than the threshold and all other user-activated switches are set to on), the pump series is activated. This entails using the sub-program "DIG LINE" to activate a 5V signal on a digital line (digital line 0 for Analog Input Channel 0, digital line 1 for Analog Input Channel 2), then waiting for a user-defined time before turning off the digital voltage pulse. If "Carbon/Nitrate selection" was selected by the user as the control scenario, only Analog Input Channel 0 controls both pumps (one for carbon and one for nitrate), and Channels 2 and 3 are not used. The program compares the *Eh* value from analog input Channel 0 with first the upper and then the lower user-defined thresholds using simple Boolean logic commands. If the result of the Boolean logic sequence is "True" for the upper threshold comparison, the sequence for pump 0 (on digital line 0) is activated; if the result for the lower threshold

comparison is “True”, the sequence for pump 1 on digital line 1 is activated. When all control actions are complete, the *Eh* data from all active channels, and indicators for pump activation (“1” if a pump was turned on this time period, “0” if not turned on) are bundled with a time stamp and recorded to an ASCII file (one for each channel) on the hard drive. The program waits for the time specified by the user, and the loop repeats until intervention by the user.

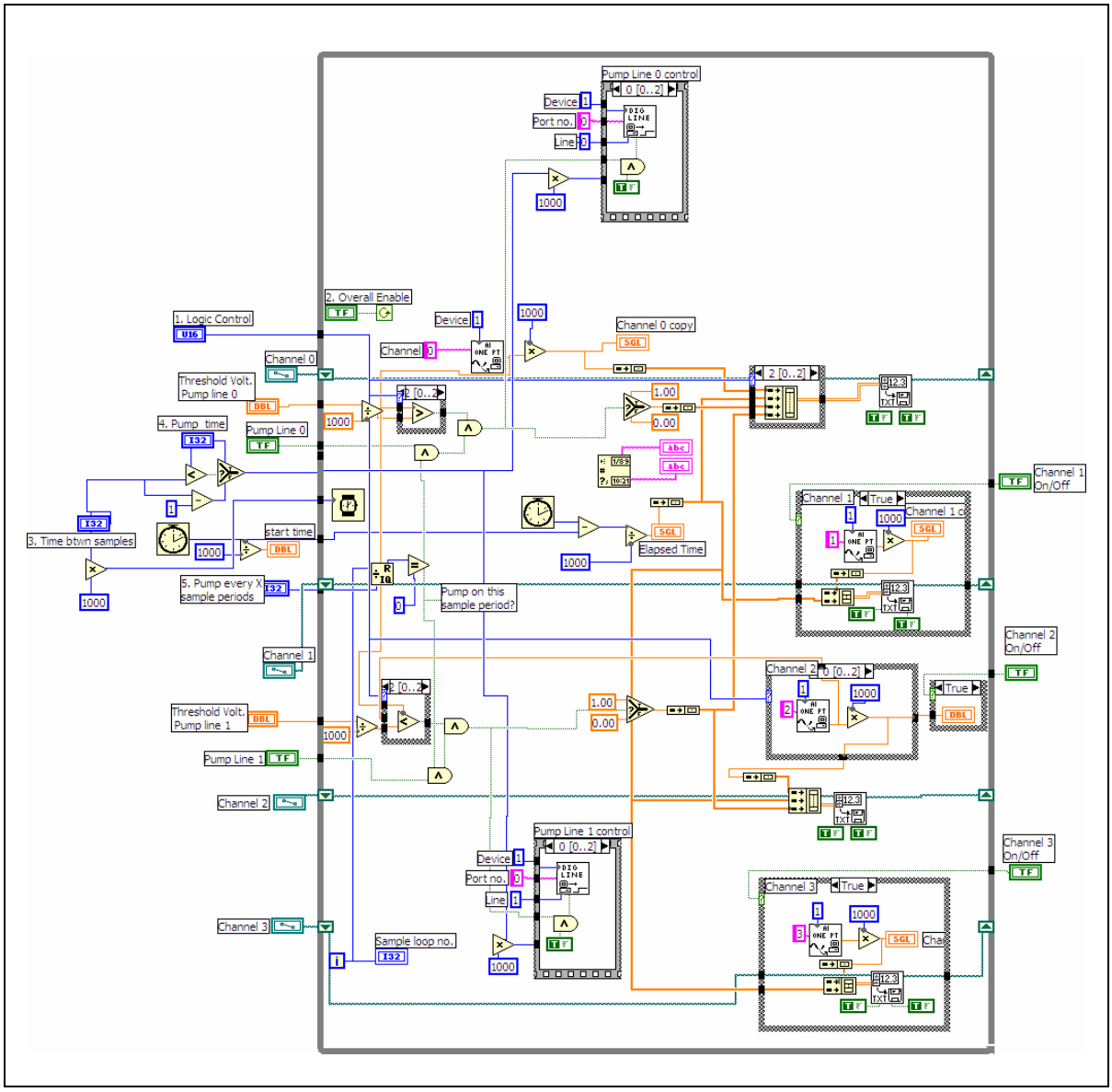

Figure A. 1. Labview data acquisition program wiring diagram.

APPENDIX B. STELLA SIMULATION MINIMODELS

B.1 Minimodel 1: Microbial Degradation with one limiting reservoir

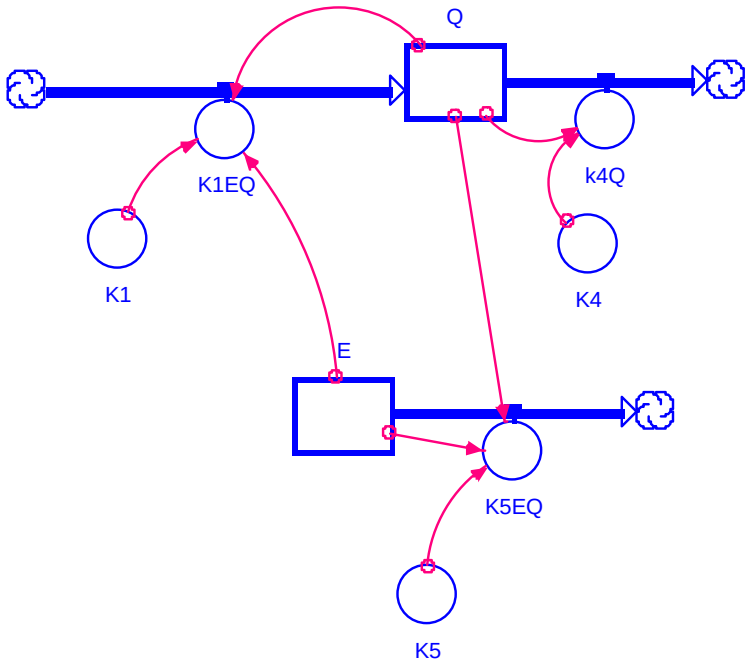

Figure B. 1. STELLA graphical construction of Minimodel 1: a simple microbial degradation microcosm with initial organic matter stock.

```
E(t) = E(t - dt) + (- K5EQ) * dt

INIT E = 100
OUTFLOWS:
K5EQ = K5*E*Q

Q(t) = Q(t - dt) + (K1EQ - k4Q) * dt
INIT Q = 0.05
INFLOWS:
K1EQ = K1*E*Q
OUTFLOWS:
k4Q = K4*Q
K1 = 0.1
K4 = 0.5
K5 = 0.1
```

Figure B. 2. STELLA code for Minimodel 1.

B.2 Minimodel 2: Microbial Degradation with two limiting reservoirs

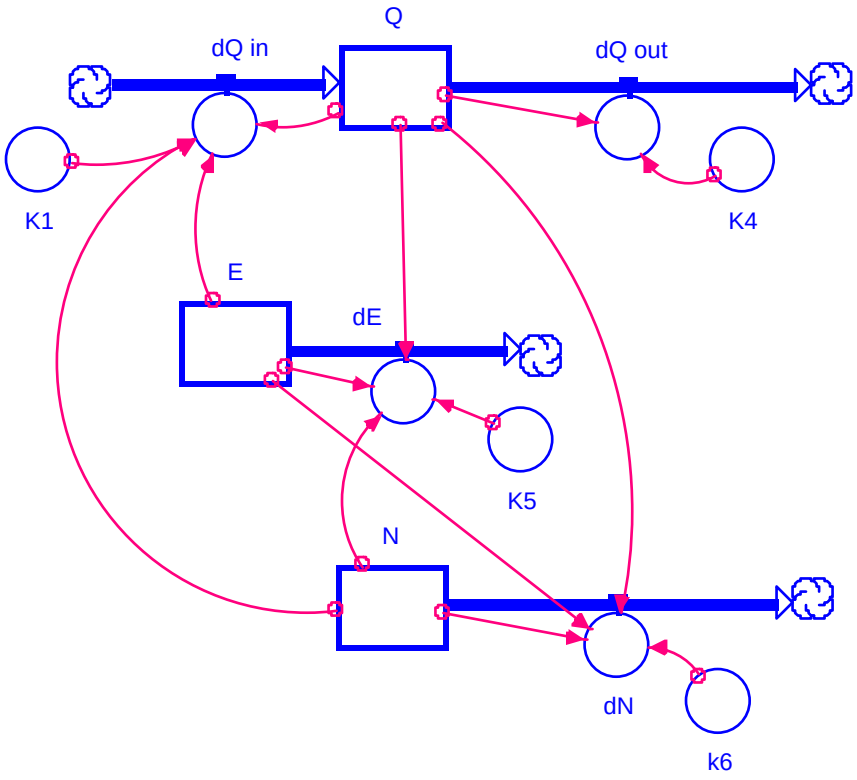

Figure B. 3. STELLA graphical construction of Minimodel 2: a microbial degradation microcosm with an initial organic matter stock (E) and an initial electron acceptor stock (N) controlling the availability of E to the consumer population Q.

```
E(t) = E(t - dt) + (- dE) * dt
INIT E = 100
OUTFLOWS:
dE = K5*E*N*Q

N(t) = N(t - dt) + (- dN) * dt
INIT N = 200
OUTFLOWS:
dN = k6*E*N*Q

Q(t) = Q(t - dt) + (dQ_in - dQ_out) * dt
INIT Q = 0.01
INFLOWS:
dQ_in = K1*E*N*Q
OUTFLOWS:
dQ_out = K4*Q

K1 = 0.001
K4 = 0.5
K5 = 0.1
K6 = 0.2
```

Figure B. 4. STELLA code for Minimodel 2.

B.3 Minimodel 3: Microbial Degradation with control over organic inputs

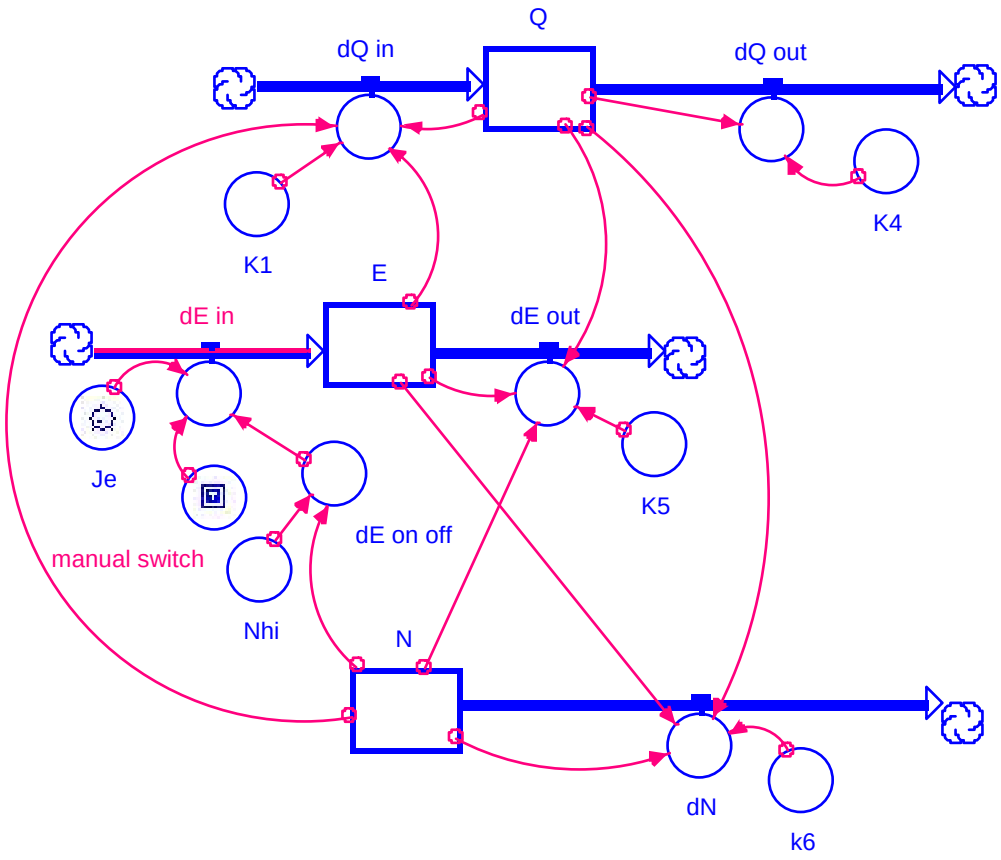

Figure B. 5. STELLA graphical construction of Minimodel 3: a soil microbial decomposition microcosm with an initial organic matter stock (E), an initial electron acceptor stock (N), and a control feedback loop controlling the input of organic matter (J_E) from outside the system based upon the sensed value of N. A manual switch is included to allow switching from Minimodel 3 simulation to Minimodel 2 simulation.

```
E(t) = E(t - dt) + (dE_in - dE_out) * dt
INIT E = 100
INFLOWS:
dE_in = Je*dE_on_off*manual_switch
OUTFLOWS:
dE_out = K5*E*N*Q

N(t) = N(t - dt) + (- dN) * dt
INIT N = 200
OUTFLOWS:
dN = k6*E*N*Q

Q(t) = Q(t - dt) + (dQ_in - dQ_out) * dt
INIT Q = 0.01
INFLOWS:
dQ_in = K1*E*N*Q
OUTFLOWS:
dQ_out = K4*Q

dE_on_off = if N>Nhi then 1 else 0
Je = 100

K1 = 0.001
K4 = 0.5
K5 = 0.1
K6 = 0.2

manual_switch = 1
Nhi = 2
```

Figure B. 6. STELLA code for Minimodel 3.

B.4 Minimodel 4: Microbial Degradation over all limiting inputs

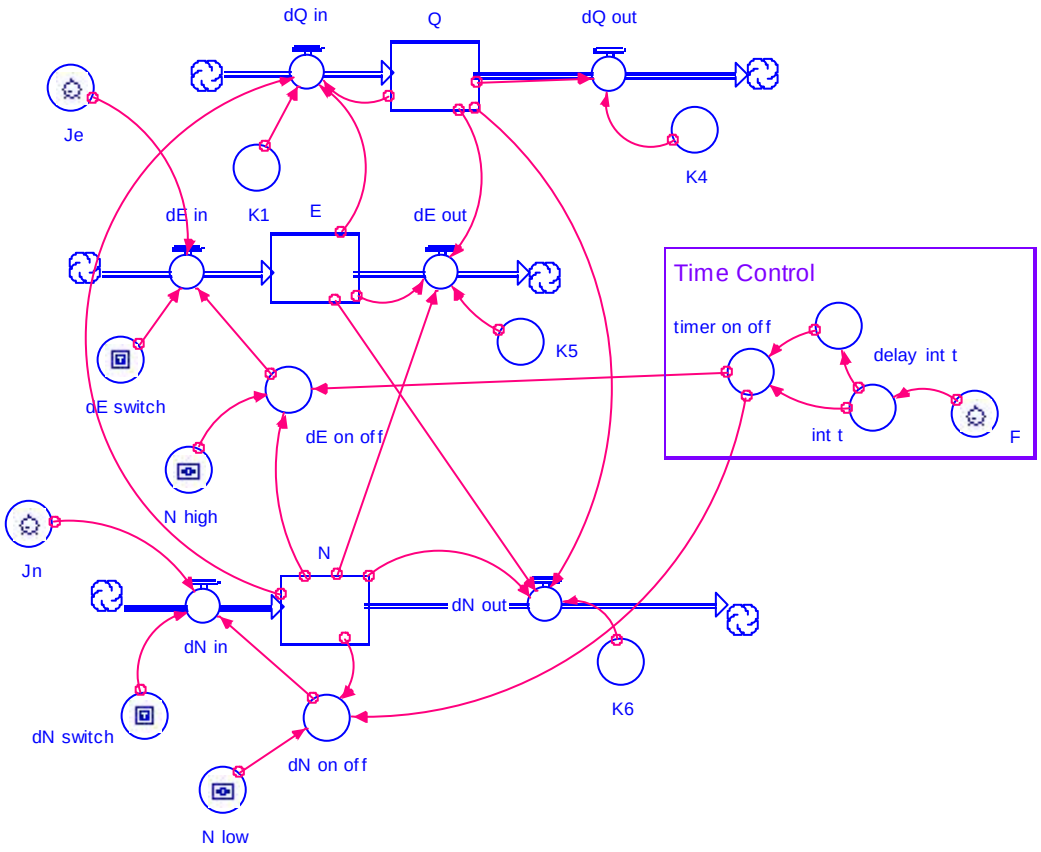

Figure B. 7. STELLA graphical construction of Minimodel 4: a soil microbial decomposition microcosm with an initial organic matter stock (E), an initial electron acceptor stock (N), and control feedback loops controlling the input of organic matter (J_E) and electron acceptor (J_N) from outside the system based upon the sensed value of N. The sector labeled "Time control" is a subprogram that allows pump events to occur at discrete time periods rather than continuously, as in previous models.

```
E(t) = E(t - dt) + (dE_in - dE_out) * dt
INIT E = 100
INFLOWS:
dE_in = Je*dE_on_off*dE_switch
OUTFLOWS:
dE_out = K5*E*N*Q

N(t) = N(t - dt) + (dN_in - dN_out) * dt
INIT N = 200
INFLOWS:
dN_in = Jn*dN_on_off*dN_switch
OUTFLOWS:
dN_out = K6*E*N*Q

Q(t) = Q(t - dt) + (dQ_in - dQ_out) * dt
INIT Q = 0.01
INFLOWS:
dQ_in = K1*E*N*Q
OUTFLOWS:
dQ_out = K4*Q

delay_int_t = delay (int_t, dt)
dE_switch = 1
dE_on_off = if N>N_high then 1*timer_on_off else 0
dN_switch = 1
dN_on_off = if N<N_low then 1*timer_on_off else 0
F = 2
int_t = int (TIME*F)

Je = 20
Jn = 100
K1 = 0.001
K4 = 0.5
K5 = 0.1
K6 = 0.2
N_high = 50
N_low = 50

timer_on_off = if int_t>delay_int_t then 1 else 0
```

Figure B. 8. STELLA code for Minimodel 4.

B.5 User Control Panel

The complexity of Minimodel 4, with its seven required inputs from the user, necessitates a graphical user panel for ease in use. Using the STELLA graphical interface design pad, a user interface was designed for ease in manipulation of the user input parameters for the control system (Figure B. 9). An explanation of the parameter controls is as follows:

- **dE switch** is a virtual switch that turns organic matter addition on or off; on is the up position;
- **dN switch** is a virtual switch that turns electron acceptor addition on or off; on is the up position;
- **Je** is a virtual dial that sets the organic matter supply rate at a value between 0 and 200 units per time step;
- **Jn** is a virtual dial that sets the electron acceptor supply rate at a value between 0 and 1000 units per time step;
- **F** is a virtual dial that sets the frequency at which the electron acceptor is measured by external sensing equipment and the control algorithm (whether or not to add organic matter or electron acceptor) is invoked; F may vary between 1 and 25 events per time step;
- **Nhigh** is a virtual slider that sets the upper threshold value of the sensed N above which organic matter (JE) is added;
- **Nlow** is a virtual slider that sets the lower threshold value of the sensed N below which electron acceptor (JN) is added.

The parameters available here for manipulation reflect those parameters that can be manipulated in the physical microcosm experiments, i.e., those parameters set by the human operator at the start of an experiment. Using these virtual controls, the user of the model may manipulate the parameters at will for various trials of the model as results are explored.

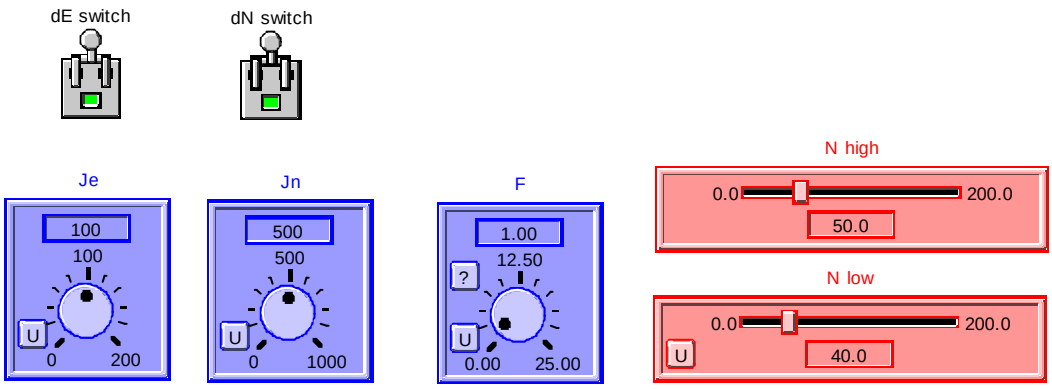

Figure B. 9. User control panel for STELLA Minimodel 4.

APPENDIX C. DERIVATION AND TESTING OF EQUATION FOR PROPOSED STATISTICAL MODEL

C.1 Derivation of General Equation Form

The derivation of a general equation that reflects the redox potential over time in a closed soil microcosm is started from the equation given by Patrick et al. (1996), itself based on the Nernst equation, that describes the theoretical redox potential for any reduction-oxidation pair:

$$Eh = E^{o} - \frac{RT}{nF}\ln\frac{(Rd)}{(Ox)} + \frac{mRT}{nF}\ln H^{+} \quad \text{(C.1)}$$

where E^0 is the standard potential for the reduction half-cell under consideration, R is the ideal gas constant (8.31 J K^{-1} mol^{-1}), T is the absolute temperature (in Kelvins), F is the Faraday constant (9.65 x 10^4 C mol^{-1}), n is the number of electrons exchanged in the half-cell reaction, m is the number of protons exchanged in the half-cell reaction, and *Rd* and *Ox* represent the aqueous concentrations of the individual reduced or oxidized component of the half-cell reaction. If the total mixed redox potential *Eh* in a solution is the weighted average of all the redox pairs present (Bohn 1971), then it may be represented that the total redox potential measured at the electrode is proportional to the sum of the redox potentials of the individual redox pairs:

$$Eh_{total} \propto \sum_i Eh_i = \sum_i [E_i^0 - \frac{RT}{n_i F}\ln\frac{(Rd_i)}{(Ox_i)} + \frac{m_i RT}{n_i F}\ln H^{+}] \qquad \text{(C.2)}$$

If a constant pH is assumed, the last term in equation (C.2) is a constant over time for each redox pair *i*. Likewise, the standard potential E^0 is a constant for each redox pair *i*. Thus, simplifying,

$$\sum_i Eh_i = \sum_i \left[C_i - \frac{A}{n_i} \ln \frac{(Rd_i)}{(Ox_i)} \right] \qquad \text{(C.3)}$$

where C_i is a constant and $A = RT/F$. To arrive at an equation that describes the change in redox potential over time, it is assumed that the reduced and oxidized components may themselves be described as functions of time; that is:

$$Eh(t) \propto \sum_i \left[C_i - \frac{A}{n_i} \ln \frac{(Rd_i(t))}{(Ox_i(t))} \right] \qquad \text{(C.4)}$$

Specifically, it is assumed that the oxidized component, which is being consumed in the microbially-mediated reduction half-reaction that accompanies the oxidation of organic matter, may be described by a first-order degradation reaction:

$$Ox_i(t) = Ox_i^0 e^{-k_i t} \qquad \text{(C.5)}$$

where Ox_i^0 is the concentration of the oxidized component at time 0 and k_i is the first-order reaction rate constant. Because the reduced component of the redox pair is one of the products of the reduction half-reaction, the concentration of the reduced component over time is related to the oxidized component as such:

$$Rd_i(t) = Rd_i^0 + (Ox_i^0 - Ox_i^0 e^{-k_i t}) \qquad \text{(C.6)}$$

where Rd_i^0 is the concentration of the reduced component at time 0. Inserting these back into equation (C.4) yields:

$$Eh(t) \propto \sum_i \left[C_i - \frac{A}{n_i} \ln \left(\frac{\left(Rd_i^0 + Ox_i^0 - Ox_i^0 e^{-k_i t} \right)}{\left(Ox_i^0 e^{-k_i t} \right)} \right) \right] \qquad \text{(C.7)}$$

This can be simplified to the following:

$$Eh(t) \propto \sum_i \left[C_i - \frac{A}{n_i} \ln\left(\frac{\left(Rd_i^0 + Ox_i^0\right)}{\left(Ox_i^0\right)} e^{k_i t} - 1 \right) \right] \quad \text{(C.8)}$$

Noting again that *C* and *A* are constants, and noting the rules of arithmetic for logarithms, equation (C.8) becomes the following:

$$Eh(t) \propto C - A \ln\left[\prod_i \left(B_i e^{k_i t} - 1 \right)^{1/n_i} \right] \quad \text{(C.9)}$$

where

$$B_i = \frac{Rd_i^0 + Ox_i^0}{Ox_i^0} \quad \text{(C.10).}$$

Equations (C.9) and (C.10) are the general equations used to represent the redox potential over time, further developed into a specific form for regression analyses with the data presented in this research.

C.2 Derivation of the Specific Equation Form

The general equation for redox potential as a function of time (equation C.9) was developed further using specific information regarding wetland soils. It is assumed here that five major reduction reactions (oxygen, nitrate, manganese, iron, and carbon dioxide) dominate the overall redox potential in freshwater wetland soils. It is assumed further that the rate of reaction of each of these reduction reactions is proportional to the Gibbs free energy available for the support of metabolism, given as

$$\Delta G_f^0 = -RT \ln K \quad \text{(C.11)}$$

where R is the universal gas law constant, T is the absolute temperature, and K is the equilibrium constant for the reduction reaction (Bartlett and James 1993). Using 8.31 J $K^{-1}mol^{-1}$ for R and 298K for T, equation (C.11) simplifies to

$$\Delta G_f^0 = -1.364 \log K \quad \text{(C.12)}$$

The values for the equilibrium constant for reduction half-reactions pertinent to soil, water, and microbial systems have been determined empirically and are tabulated in the literature (Bartlett and James 1993). Using these values, the Gibbs free energy was calculated for each of the five major reduction reactions selected here (Table C. 1).

Table C. 1. Equilibrium constant, Gibbs free energy, and normalized Gibbs free energy for select reduction half-reactions focused on in this research.

Primary Reduction half-reaction	log K	ΔG_f° (J mol^{-1})	Normalized rate
$O_2 + 4H^+ + 4e^- \rightarrow 2H_2O$	20.8	-28.4	0.99
$NO_3^- + 6H^+ + 5e^- \rightarrow ½\ N_2 + 3H_2O$	21.1	-28.8	1
$MnO_2 + 4H^+ + 2e- \rightarrow Mn^{2+} + 2H_2O$	20.8	-28.4	0.99
$Fe(OH)_3 + 3H^+ + e^- \rightarrow Fe^{2+} + 3\ H_2O$	15.8	-21.6	0.75
$CO_2 + 8H^+ + 8e^- \rightarrow CH_4 + 2\ H_2O$	2.9	-3.96	0.14

The values for the normalized rate, representing the ratio of the values of the Gibbs free energy for each of the reduction half-reactions to the nitrate reduction half-reaction, were then used as the ratios of the first-order reaction rate constants in equation (C.9). Expanding equation (C.9) to incorporate the five primary reduction half reactions, and using the simplifying assumption that all B_i are approximately the same value B yields the following:

$$Eh(t) \propto C - A\ln\left[\left(Be^{k_1 t} - 1\right)^{1/n_1}\left(Be^{k_2 t} - 1\right)^{1/n_2}\left(Be^{k_3 t} - 1\right)^{1/n_3}\left(Be^{k_4 t} - 1\right)^{1/n_4}\left(Be^{k_5 t} - 1\right)^{1/n_5}\right] \quad \text{(C.13)}$$

where

$$k_1 = 0.99k \qquad n_1 = 4$$
$$k_2 = k \qquad n_2 = 5$$
$$k_3 = 0.99k \qquad n_3 = 2$$
$$k_4 = 0.75k \qquad n_4 = 1$$
$$k_5 = 0.14k \qquad n_5 = 8$$

It is equation (C.13) that was used as a model in a non-linear regression analysis.

C.3 Preliminary regression analysis

The model proposed in equation (C.13) was calibrated using the method of subjective optimization, which is often used to calibrate complex models. In subjective optimization, the model coefficients are changed subjectively based upon changes to a comparison between the measured and predicted values of one or more criterion variables (McCuen 1993). The procedure for subjectively optimizing the model followed here is as follows. First, criterion variables for evaluating the goodness-of-fit of the predicted values from the model to the measured values were selected. Initial values for the model parameters (*B, C,* and *k*) were assumed, and the predicted values for redox potential for each time step was calculated. The criterion variables comparing the measured and predicted values were calculated. Changes were made to the value of one of the parameters, and the model predicted values were calculated again, This process was repeated until the values for the criterion variables were optimized.

The criterion variables selected to determine the goodness of fit for the model were the coefficient of determination R^2 (Kvalseth 1985), the ratio of S_e/S_y (McCuen 1993), and the sum of the residuals Σe_i (McCuen 1984). The coefficient of determination R^2 equals the percentage of variance in the measured variable that is explained by the

predicted variable. Its square root, R, is the correlation coefficient, an index of the degree of linear association between the measured and predicted values (McCuen 1984). The coefficient of determination is given by the following expression (McCuen 1984):

$$R^2 = \frac{\sum (y_p - y_{mean})^2}{\sum (y - y_{mean})^2} \quad \text{(C.14)}$$

where

y = measured data,

y_p = predicted data,

y_{mean} = mean of measured data.

As the ratio of the explained variation to the total variation, an R^2 with a value of 1 indicates that the model has a perfect fit to the measured data, whereas a value of 0 represents no association between the predicted and measured data.

The ratio of the standard deviation of the errors to the standard deviation of the measured data (y), S_e/S_y, was also used to evaluate the models (McCuen 1984). This ratio is the percent of variation that is not explained by the model and is calculated from the coefficient of determination:

$$\frac{S_e}{S_y} = \sqrt{(1 - R^2)} \quad \text{(C.15)}$$

where

S_e = standard deviation of the errors,

S_y = standard deviation of the measured data (y),

R^2 = coefficient of determination.

Because it is a function of R^2, the ratio S_e/S_y represents the ratio of the unexplained variation to the total variation: a value of 0 indicates the model has a perfect fit, whereas a value of 1 indicates a poor fit.

The residual, e_i, is the difference between the measured and predicted values at any point *i* (McCuen 1984) and is defined by

$$e_i = y_{p,i} - y_i \quad \text{(C.16)}$$

where

$y_{p,i}$ = the *i*th predicted value

y_i = the *i*th measured value.

The sum of the residuals indicates bias in the predicted values from the model as compared to the measured values. A positive value for the sum of the residuals indicates overprediction, a negative value indicates underprediction, and a zero value indicates no overall bias.

C.4 Subjective Optimization results

The equations for the proposed model (C.13) and the goodness of fit criterion variables (C.14 to C.16) were programmed into a Microsoft Excel spreadsheet. The method of subjective optimization was used to calibrate the model to measured redox data from select experiment and control units from the carbon addition trials described in this research. Whereas three model parameters (*B*, *C*, and *k*) were available for manipulation in the subjective optimization, the process was streamlined by assuming a value of 1.01 for the parameter *B* for all calibration attempts.

Preliminary results of the model calibration to eight separate data sets are presented in Table C. 1. Values for R^2 ranged from 0.068 to 0.996. Values for the ratio S_e/S_y ranges from 0.378 to 0.965. Values for the sum of the residuals Σe_i were all less than or equal to 3.00.

Table C. 1. Preliminary results for model calibration to various sets of measured redox potential over time. Results were obtained via subjective optimization of the model parameters *C* and *k*, with B = 1.01.

Trial	C	K	R^2	S_e/S_y	Σe_i
1-01	-160.2	0.0284	0.648	0.593	1.210
1-02	21.2	0.0585	0.857	0.378	0.347
5-01	191.4	0.03	0.132	0.932	3.00
5-02	212.9	0.016	0.857	0.378	2.47
7-01	77.7	-0.00023	0.142	0.926	2.346
7-02	253.8	0.290	0.850	0.3873	0.366
8-01	64.9	0.00284	0.996	0.0608	0.768
8-02	36.8	0.085	0.068	0.965	1.215

These results show that the model is in need of further development to better explain the variation observed in the measured data. When the measured data follows a smoothly declining curve over time, as in Trial 8-01, the model adequately predicts the decline in redox potential with high correlation (R^2 = 0.996) and low residuals (Σe_i =0.768). The extent to which the model predicts the measured data in these circumstances is most fully appreciated by plotting both the measured and predicted values of redox potential over time on the same axis (Figure C. 1). However, in other circumstances, the model does not adequately predict the measured data. For example, for Trial 8-02 (R^2=0.068), the model overpredicts for low values of time and underpredicts for high

values of time (Figure C. 2). Further refinement of this method can come from manipulation of the third model parameter *B* in addition to the other two, and also from the implementation of analytical or numerical model optimization methods via computational programming (McCuen 1993).

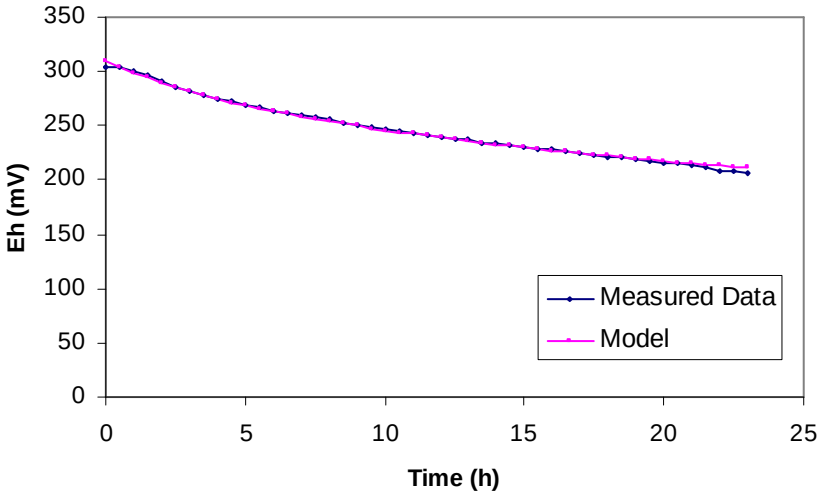

Figure C. 1. Measured and predicted values for redox potential over time. Measured values are from experiment Trial 8-01. The coefficient of determination R^2 is 0.996.

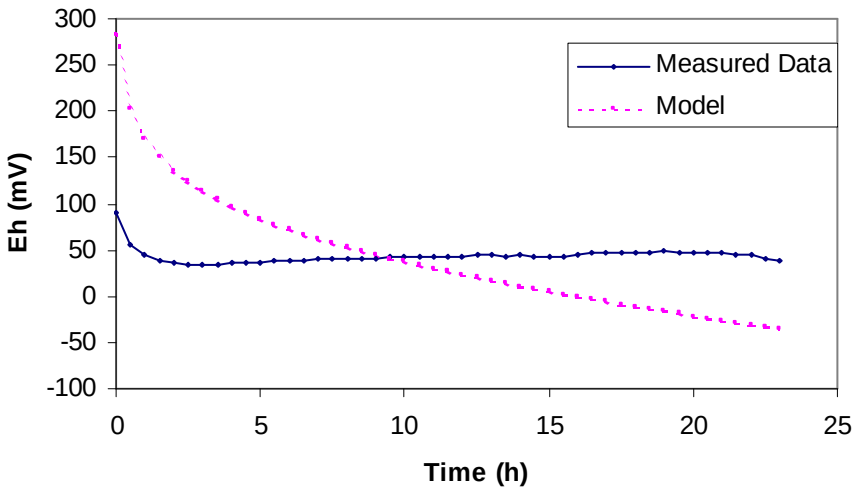

Figure C. 2. Measured and predicted values for redox potential over time. Measured values are from experiment Trial 8-02. The coefficient of determination R^2 is 0.068.

APPENDIX D. EXPERIMENTAL PROTOCOLS

D.1 Redox Probe Calibration

D.1.1 Probe Cleaning

The platinum electrodes used for measuring redox potential were periodically cleaned to remove organic buildup that might affect the probe calibration. Cleaning was performed using a procedure outlined in Patrick, et al. (1996). A paste was made using commercial scouring powder (Ajax), and a test-tube brush was used to scrub the exposed platinum on the electrode with the paste. The paste residue was then rinsed under ordinary tap water, and then the platinum tip was further rinsed under a stream of distilled water. To ensure complete rinsing, the probe tips were submerged in a large beaker of distilled water and allowed to soak over night with a stir-bar continuously mixing the contents of the beaker.

D.1.2 Calibration Solution Composition

Following cleaning, the electrodes were calibrated using a pH-buffered, quinhydrone solution, mixed as directed in Patrick, et al (1996). For this solution, 30 mL of pH-buffered solution (one each of pH 4 and pH 7) was placed in a 50-mL flask. Approximately 0.05 g (±0.002 g) of quinhydrone ($C_{12}H_{10}O$) was measured on a balance and placed into each flask. The contents were stirred vigorously for 10 seconds, allowed to sit for 15 minutes, and stirred again.

D.1.3 Probe Calibration

Calibration of the platinum electrodes followed the procedure outlined in Patrick, et al. (1996). The electrode to be tested was connected to the data acquisition computer and it's tip was placed in the calibration solution. The calomel reference electrode was placed into the solution as well, and the data acquisition system was activated with a sampling period of 10 seconds. The readings were observed for at least 5 minutes to ensure the reading stabilized. While the sampling was occurring, the temperature of the calibration solution was measured with a mercury thermometer. If the reading did not stabilize after 5 minutes, the probe was not used and set aside for further cleaning. If the reading did stabilize, the final reading after 5 minutes was compared to the expected calibration values given by Patrick, et al. (1996) and shown in Table D.1. If the probe differed from the expected calibration value by more than ±5 mV, the probe was not used and set aside for further cleaning. A probe within ±5 mV of expected values was assumed to be calibrated and was used in the experiments.

Table D.1. Expected calibration values for platinum redox electrodes in buffered quinhydrone solution (Patrick, et al., 1996).

Temperature	Calibration Solution	
	pH 4	pH 7
293 K (20°C)	223 mV	47 mV
298 K (25°C)	218 mV	41 mV

D.2 Nutrient Reservoir Mixing

D.2.1 Carbon Solution

Carbon reservoirs were mixed by calculating the molecular weight of the compound being used and mixing it with the appropriate volume of distilled water. For the acetate solution, the molecular weight of sodium acetate (CH_3COONa) was calculated to be 82.03 g/mol. Thus, to make the 2.0 M sodium acetate solution typically used in most of the experiments, 82.03 g (±0.1 g) of sodium acetate was measured on a digital balance and added to 500 mL of distilled water that had been measured with a graduated cylinder and placed into a beaker. A magnetic stir-bar was placed in the solution and used to mix the reservoir until all the solid sodium acetate had visibly dissolved.

D.2.2 Nitrate Solution

Nitrate reservoirs were mixed by calculating the molecular weight of the compound being used and mixing it with the appropriate volume of distilled water. For the nitrate solution, the molecular weight of potassium nitrate (KNO_3) was calculated to be 101.1 g/mol. Thus, to make the 1.0 M potassium nitrate solution typically used in most of the experiments, 50.55 g (±0.1 g) of potassium nitrate was measured on a digital balance and added to 500 mL of distilled water that had been measured with a graduated cylinder and placed into a beaker. A magnetic stir-bar was placed in the solution and used to mix the reservoir until all the solid sodium acetate had visibly dissolved.

D.3 Salt Bridge Construction

Salt bridges were constructed to provide ionic continuity between multiple redox probes in multiple microcosms and a common calomel reference probe. The general procedure (Warner Instruments, 1999) was used for constructing all the salt bridges.

D.3.1 KCl Reservoir Mixing

A 1.0 M reservoir of KCl solution was used to make the KCl agar and act as a central common reservoir in which the calomel probe was inserted. For the KCl solution, the molecular weight of potassium chloride (KCl) was calculated to be 74.6 g/mol. Thus, to make the 1.0 M KCl solution, 74.6 g (±0.1 g) of KCl was measured on a digital balance and added to 1.0 L of distilled water that had been measured with a graduated cylinder and placed into a beaker. A magnetic stir-bar was placed in the solution and used to mix the reservoir until all the solid sodium acetate had visibly dissolved.

D.3.2 Salt Bridge Manufacture

The salt brides were constructed using the procedure outlined in Warner Instruments (1999). The salt bridges were constructed in the lab using disposable 1.0-mL plastic pipettes attached end-to-end with 0.25 m of 1/8” diameter vinyl tubing. An ionic agar solution was prepared using 3 g of agar in 100 mL of 1.0 M KCl solution. The solution was heated on a hot plate until the agar dissolved, at which point a suction pump was used to draw the liquid agar into the length of the salt bridge tubing. The bridges were allowed to cool, and then tested for continuity by taking sample redox potential measurements in the buffered quinhydrone solutions prepared for probe calibration.

REFERENCES

Adey, W.H., C. Luckett, and K. Jensen. 1993. Phosphorus removal from natural waters using controlled algal production. *Restoration Ecology* 1: 29-39.

Al-Ghusain, I.A., J. Huang, O.J. Hao, and B.S. Lim. 1994. Using pH as a real-time control parameter for wastewater treatment and sludge digestion processes. *Water Science and Technology* 30 (4), 159-168.

American Heritage. 1985. *The American Heritage Dictionary*, Second College Edition. Houghton Mifflin Co., Boston, Massachussets.

Armstrong, N.E., and H.T. Odum. 1964. Photoelectric ecosystem. *Science* 143(3603): pp. 256-258.

Austin, W.E., and J.H. Huddleston. 1999. Viability of permanently installed platinum redox electrodes. *Soil Sci. Soc. Am. J.* 63:1757-1762.

Bartlett, R.J. and B.R. James. 1993. Redox chemistry of soils. *Advances in Agronomy* 50: 151-208.

Beyers, R.J. 1974. *Report of Savannah River Laboratory*. University of Georgia, Aiken, SC.

Beyers, R.J., and H.T. Odum. 1993. *Ecological Microcosms*. New York: Springer-Verlag.

Bohn, H.L. 1971. Redox potentials. *Soil Science* 112(1): 39-45.

Boling, R.H., and J.A. Van Sickle. 1975. Control theory in ecosystem management. In: *Ecosystem Analysis and Prediction: Proceedings of a SIAM-SIMS Conference held at Alta, Utah, July 1-5, 1974.* S. Levin, ed. pp. 219-229. Society for Industrial and Applied Mathematics, Philadelphia, Pennsylvania.

Bond, D.R., D.E. Holmes, L.M. Tender, and D.R. Lovley. 2002. Electrode-reducing microorganisms that harvest energy from marine sediments. *Science* 295: 483-485.

Brock, T.D. 1966. *Principles of Microbial Ecology*. Prentice-Hall, Inc., Englewood Cliffs, New Jersey.

Brock, T.D., M.T. Madigan, J.M. Martinko, and J. Parker. 1994. *Biology of Microorganisms*, Seventh Edition. Prentice Hall, Englewood Cliffs, New Jersey.

Calow, P. 1976. *Biological Machines: A Cybernetic Approach to Life*. Edward Arnold Publishers, Ltd., London.

Clark, O.G., R. Kok, and R. Lacroix. 1999. Mind and autonomy in engineered biosystems. *Engineering Applications of Artificial Intelligence* 12(3): 389-399.

Clark, O.G., and R. Kok. 1998. Engineering of highly autonomous biosystems: review of the relevant literature. *International Journal of Intelligent Systems* 13(8): 749-783.

DeAngelis, D.L., Post, W.M., Travis, C.C. 1986. *Positive Feedback in Natural Systems*. Springer-Verlag, New York City, New York.

Duffield, C. 1976. *Geothermal Technoecosystems and Water Cycles in Arid Lands*. Arid Lands Resource Information Paper No. 8. University of Arizona Office of Arid Lands Studies, Tucson, Arizona.

Fogg, G.E. 1975. *Algal Cultures and Phytoplankton Ecology*. University of Wisconsin Press, Madison, Wisconsin.

Ginot, V., M.G. Holleberg, M. Vuillot, and R. Billard. 1987. A recorder for physiochemical and meteorological parameters in fish ponds. pp. 137-141. In: J.G. Balchen (ed.), *Automation and Data Processing in Aquaculture*. International Federation of Automatic Controls (IFAC) Proceedings Series, Vol. 9, Pergamon Press, New York.

Goudie, A. 1984. *The Human Impact: Man's Role in Environmental Change*. MIT Press, Cambridge, Massachussetts.

Hannon, B. 1986. Ecosystem control theory. *Journal of Theoretical Biology* 121:417-437.

Hannon, B., and J. Bentsman. 1991. Control theory in the study of ecosystems: a summary review. pp. 240-260. In: *Theoretical Studies of Ecosystems: The Network Perspective*. Higashi, M., Burns, T.P., eds. Cambridge University Press, Cambridge, U.K.

Hannon, B. and M. Ruth. 1997. *Modeling Dynamic Biological Systems*. Springer-Verlag, New York City, New York.

Hunter, K.S., Y. Wang, and P. Van Cappellen. 1998. Kinetic modeling of microbially-driven redox chemistry of subsurface environments: coupling transport, microbial metabolism, and geochemistry. *Journal of Hydrology* 209: 53-80.

Issacs, S., T. Mah, and S.K. Maneshin. 1998. Automatic monitoring of denitrification rates and capacities in activated sludge processes using fluorescence or redox potential. *Water Science and Technology* 37(12): 121-129.

Ives-Halperin, J. and P. Kangas. 2000. Design analysis of a recirculating living machine for domestic wastewater treatment. *7th International Conference on Wetland Systems for Water Pollution Control*. International Water Association, Orlando, Florida, pp. 547-555.

Johnson, A.T. 1999. *Biological Process Engineering.* John Wiley and Sons, Inc., New York.

Jorgensen, S.E. 1989. Changes of redox potential in aquatic ecosystems. pp. 341-355. In *Ecological Engineering: An Introduction to Ecotechnology*. W.J. Mitsch and S.E. Jorgensen, ed., John Wiley and Sons, Inc., New York.

Kadlec, R.H., and R.L. Knight. 1996. *Treatment Wetlands*. CRC Press, Boca Raton, Florida.

Kangas, P.C. 2004. *Ecological Engineering: Principles and Practice*. Lewis Publishers, CRC Press, Inc., Boca Raton, Florida.

Kim, H., and O. Hao. 2001. pH and oxidation-reduction potential control strategy for optimization of nitrogen removal in an alternating aerobic-anoxic system. *Water Environment Research* 73(1): 95-102.

Kitching, R.L. 1983. *Systems Ecology: An Introduction to Ecological Modeling.* University of Queensland Press, St. Lucia, Queensland.

Kludze, H.K., and R.D. DeLaune. 1996. Soil redox intensity effects on oxygen exchange and growth of cattail and sawgrass. *Soil Sci. Soc. Am. Journal* 60: 616-621.

Koch, F.A., and W.K. Oldham. 1985. Oxidation-reduction potential—A tool for monitoring, control and optimization of biological nutrient removal systems. *Water Science and Technology* 17: 259-281.

Kvalseth, T.O. 1985. Cautionary note about R^2. *The American Statistician* 39(4 pt. 1): 279-285.

Latimer, W.M. 1952. *The Oxidation States of the Elements and Their Potentials in Aqueous Solutions*. Prentice Hall, Inc., New York.

Lowes, A.L., and C.C. Blackwell. 1975. Applications of modern control theory to ecological systems. In: *Ecosystem Analysis and Prediction: Proceedings of a SIAM-SIMS Conference held at Alta, Utah, July 1-5, 1974.* S. Levin, ed. pp. 299-305. Society for Industrial and Applied Mathematics, Philadelphia, Pennsylvania.

Margalef, R. 1968. *Perspectives in Ecological Theory*. University of Chicago Press, Chicago, Illinois.

McCuen, R.H. 1993. *Microcomputer Applications in Statistical Hydrology*. Prentice Hall, Englewood Cliffs, New Jersey.

McCuen, R.H. 1984. *Statistical Methods for Engineers*. Prentice Hall, Englewood Cliffs, New Jersey.

Mitsch, W.J., and J.G. Gosselink. 1993. *Wetlands*. Van Nostrand Reinhold, New York.

Myers, J. and L.B. Clark. 1944. Culture conditions and the development of the photosynthetic mechanism. II. An apparatus for the continuous culture of Chlorella. *Journal of General Physiology* 28:103-112.

National Instruments. 1993. *AT-MIO-16X User Manual*. National Instruments Corp., Austin, TX.

National Instruments. 1996. *LabVIEW: Data Acquisition VI Reference Manual for Windows*. National Instruments Corp., Austin, TX.

Odum, E.P. 1989. *Ecology and Our Endangered Life Support Systems*. Sinauer Associates, Inc., Sunderland, Massachusetts.

Odum, H.T. 1971. *Environment, Power and Society*. John Wiley and Sons, Inc., New York.

Odum, H.T. 1993. *Ecological and General Systems: An Introduction to Systems Ecology*. 2nd Edition. University Press of Colorado, Niwot, CO.

OECD. 1981. Simulation test--Aerobic sewage treatment: Coupled units test. *OECD Guideline for Testing of Chemicals*, no. 303A. Organization for Economic Cooperation and Development, Paris.

Parrot, L., and R. Kok. 2001. A generic, individual-based approach to modeling higher trophic levels in simulation of terrestrial ecosystems. *Ecological Modeling* 154: 151-178.

Patrick, W.H. 1966. Apparatus for controlling the oxidation-reduction potential of waterlogged soils. *Nature* 212(5067): 1278-1279.

Patrick, W.H., and R. Wyatt. 1964. Soil nitrogen loss as a result of alternate submergence and drying. *Soil Science Society of America Proceedings* 28:647-653.

Patrick, W.H., B.G. Williams, and J.T. Moraghan. 1973. A simple system for controlling redox potential and pH in soil suspensions. *Soil Science Society of America Proceedings* 37(2): 331-332.

Patrick, W.H. and R.D. Delaune. 1977. Chemical and biological redox systems affecting nutrient availability in the coastal wetlands. In *Geoscience and Man*, vol. 18. H.J. Walker, ed. Louisiana State University, Baton Rouge, Louisiana.

Patrick, W.H., R.P. Gambrell, and S.P. Faulkner. 1996. Redox measurements of soils. *Methods of Soil Analysis. Part 3. Chemical Methods*. Soil Science Society of America Book Series No. 5. Madison, Wisconsin.

Patten, B.C., and E.P. Odum. 1981. The cybernetic nature of ecosystems. *American Naturalist* 118: 886-895.

Petersen, J.E. 2001. Adding artificial feedback to a simple aquatic ecosystem: the cybernetic nature of ecosystems revisited. *Oikos* 94: 533-547.

Petersen, J.E. 1998. *Scale and energy input in the dynamics of experimental estuarine ecosystems*. Thesis (Ph.D.). University of Maryland, College Park, Md.

Phillips, C.L., and R.D. Harbor. 2000. *Feedback Control Systems*. Prentice Hall, Inc., New York.

Reimers, C. E., L.M. Tender, S. Fertig, and W. Wang. 2001. Harvesting energy from the marine sediment-water interface. *Environmental Science and Technology*, vol. 35, pp. 192-195.

Taub, F. 1974. Closed ecological systems. *Annual Review of Ecology and Systematics* 5:139-160.

Teal, J.M. 1991. Contributions of marshes and saltmarshes to ecological engineering. pp. 55-62. In: *Ecological Engineering for Wastewater Treatment*. C. Etnier and B. Guterstam (eds.). Bokskogen, Gothenburg, Sweden.

Todd, J., and B. Josephson. 1996. The design of living technologies for waste treatment. *Ecological Engineering* 6: 109-136.

Vepraskas, M.J. and S.P. Faulkner. 2001. Redox chemistry of hydric soils. pp. 85-135. In: Vepraskas, M.J. and S.P. Faulkner (eds.). *Wetland Soils: Genesis, Hydrology, Landscapes, and Classification*. CRC Press, Boca Raton, Florida.

Warner Instruments. 1999. A procedure for the formation of agar salt bridges. Internet publication. Salt Bridge Formation Rev. 9.1.99. Found at website: http://www.warnerinstrument.com/pdf/whitepapers/agar_bridges.pdf.

Weiner, N. 1948. *Cybernetics.* Wiley Inc., New York.

Wilkinson, S. 2000. “Gastrobots”—Benefits and challenges of microbial fuel cells in food powered robot applications. *Autonomous Robots* 9: 99-111.

Zabel, B., P. Hawes, H. Stuart, and B.D.V. Marino. 1999. Construction and engineering of a created environment: Overview of the Biosphere 2 closed system. pp. 43-64. In: Odum, H.T., and B.D.V. Marino (eds.). *Biosphere 2: Research Past and Present*. Elsevier Science, B.V.